

**Autologous Cell-based Human Meniscus Tissue Engineering**

by

Yan Liang

A thesis submitted in partial fulfillment of the requirements for the degree of

Doctor of Philosophy

in

Experimental Surgery

Department of Surgery

University of Alberta

© Yan Liang, 2020

## **Abstract**

The knee menisci are a pair of weight-bearing fibrocartilaginous tissues between the femoral condyles and tibial plateau. They are essential for mechanical load distribution and transmission, lubrication, and stability of the knee joint [1, 2]. Meniscus injury is a risk factor for the onset of knee osteoarthritis (OA) [3, 4], which is characterized as a progressive degenerative disease resulting in cartilage breakdown. The avascular nature of the inner meniscus regions limits their intrinsic healing capacity and early intervention is required after injury to prevent OA. The long-term clinical outcomes after partial meniscectomy for inner meniscus injuries are poor [3]. Cell-based meniscus tissue engineering by (re)-differentiating autologous cells towards an inner meniscus-like extracellular matrix (IM-ECM)-forming phenotype is an emerging strategy to repair or replace damaged tissues. Human meniscus fibrochondrocytes (MFCs) and mesenchymal stem cells (MSCs) can be isolated from surgical debris and through synovial fluid using minimally invasive techniques, respectively. Even though studies using these cell sources showed promising results regarding meniscus-like ECM formation *in vitro* and in animal studies, tissue engineering variables are being investigated to optimize the outcomes prior to clinical implantation.

The studies in this thesis focused on investigating cell isolation and expansion conditions, inductive stimuli for IM-ECM formation, and phenotype stability of *in vitro* preformed IM-ECM in human MFC and synovial fluid-derived MSC (SF-MSC)-based

meniscus tissue engineering.

For human MFCs, the first experiment aimed to identify the population doublings (PDs) of TGF- $\beta$ 1 and FGF-2 (T1F2)-expanded MFCs to retain their chondrogenic redifferentiation capacity under normoxia (21% O<sub>2</sub>) and hypoxia (3% O<sub>2</sub>) using an *in vitro* cell pellet model. The data demonstrated that MFCs with PDs of up to 10 can undergo chondrogenic redifferentiation. The IM-ECM formation was most pronounced in MFCs with PDs ranging from 2.5 to 3.3 under hypoxia. Moreover, the MFCs did not undergo osteogenic differentiation. A subsequent study was performed to investigate whether human meniscus-derived decellularized matrix (DCM) can re-differentiate T1F2-expanded MFCs to form IM-ECM under hypoxia (3% O<sub>2</sub>). The DCM supported IM-ECM formation only with an exogenous chondrogenic factor. A third experiment was performed to investigate the effects of oxygen levels, transient TGF- $\beta$ 3 supplementation (3 weeks), and long-term culture with TGF- $\beta$ 3 (8 weeks) on IM-ECM production by MFCs within a type I/III collagen scaffold. The study also assessed the behavior of the engineered IM-ECM after subcutaneous implantation in nude mice. The results showed that the constructs expressed genes and proteins associated with IM-ECM, especially in hypoxia. Long-term culture (8 weeks) led to superior IM-ECM compared to 3 weeks, but only with TGF- $\beta$ 3 in hypoxia. The IM-ECM formed after 3 weeks' hypoxic chondrogenic culture was better retained compared to normoxia and became vascularized without calcification after 5 weeks' implantation in nude mice.

For human SF-MSCs, the first experiment was to investigate whether TGF- $\beta$ 3, insulin-like growth factor 1 (IGF-1), and human meniscus-derived (DCM) can induce differentiation of SFMSCs towards an MFC phenotype under hypoxia (3% O<sub>2</sub>). In pellets, combined TGF $\beta$ 3 and IGF-1 synergistically enhanced IM-ECM formation compared to growth factors alone. In DCM, the combination of TGF- $\beta$ 3 and IGF1 induced IM-ECM production and upregulated aggrecan, collagens I and II expression compared to DCM alone. The differentiated SF-MSCs also showed little expression of hypertrophic differentiation marker type X collagen. A subsequent experiment was performed to assess whether hypoxic (2% O<sub>2</sub>) compared to normoxic (21% O<sub>2</sub>) chondrogenic culture can drive SF-MSCs to produce meniscus-like ECM rich with angiogenesis-promoting factors VEGF and SDF-1 within a type I collagen scaffold *in vitro*. The angiogenic potential of SF-MSCs and the stability of the generated ECM regarding calcification were tested using a subcutaneous nude mouse model. IM-ECM formation and production of VEGF by SF-MSCs was enhanced by HYP *in vitro*. IM-ECM from both oxygen tensions underwent vascularization and did not calcify in the nude mice.

In summary, the experiments in this thesis showed that enough MFCs with the capacity to form IM-ECM can be obtained through growth factor supplementation. Hypoxic preculture of both cell sources promote a chondrogenic phenotype to form IM-ECM rather than osteogenic differentiation both *in vitro* and *in vivo*. Moreover, this work

showed that precultured ECM allowed vascularization at the ectopic sites, which showed promise to enhance the repairing potential of avascular meniscus injuries.

## **Preface**

This thesis is an original work by Yan Liang. The research project, of which this thesis is a part, received research ethics approval from the University of Alberta's Research Ethics Board. The Health Research Ethics Board-Biomedical Panel provided ethical approval for the experimental use of human cells and tissue, under study Id, Pro00018778 and Study Title: "Regeneration of nasal and articular cartilage utilizing chondrocytes and mesenchymal stem cells". The Animal Care and Use Committee provided ethical approval for the experimental use of animals, Project Name "Tissue engineering: stability of cellular phenotype in animal models", No. AUP00001363

Chapter 2 has been published in part as: Yan Liang, Enaam Idrees, Stephen H. J. Andrews, Kirillos Labib, Alexander Szojka, Melanie Kunze, Andrea D. Burbank, Aillette Mulet-Sierra, Nadr M. Jomha, and Adetola B. Adesida, "Plasticity of Human Meniscus Fibrochondrocytes: A Study on Effects of Mitotic Divisions and Oxygen Tension," *Scientific Reports* 2017, volume 7, issue 1, pages 12148. YL performed the experiments, analyzed the data and wrote the manuscript. EI, MK, AM, SA, AS, and ABA were involved in data analysis. NJ procured meniscus specimens. SA, AS, AB, NJ, ABA were involved in manuscript writing. KL provided data for selection of growth factors. Study was conceived and supervised by ABA. Manuscript was finalized by ABA.

Chapter 3 has been published in part as: Yan Liang, Alexander R.A. Szojka, Enaam Idrees, Melanie Kunze, Aillette Mulet-Sierra, and Adetola B. Adesida, "Re-differentiation

of human meniscus fibrochondrocytes differs in three-dimensional cell aggregates and decellularized human meniscus matrix scaffolds,” *Annals of Biomedical Engineering* 2019. YL conducted the experiments and was responsible for data acquisition, analysis, and bulk of manuscript writing. AS was involved in data analysis and manuscript writing. EI, MK and AMS were involved in immunofluorescence, gene expression analysis, and cell culture. ABA conceived the study, supervised the study, performed data analysis, manuscript writing, and was responsible for final review of the manuscript

Chapter 5 has been published in part as: Yan Liang, Enaam Idrees, Alexander Szojka, Stephen Andrews, Melanie Kunze, Aillette Mulet-Sierra, Nadr Jomha, and Adetola B. Adesida, “Chondrogenic Differentiation of Synovial Fluid Mesenchymal Stem Cells on Human Meniscus-Derived Decellularized Matrix Requires Exogenous Growth Factors,” *Acta Biomaterialia* 2018, volume 80, pages 131-143. YL performed experiments, acquired data and was responsible for manuscript writing. EI, AMS, and MK were involved in immunofluorescence, flow cytometry, and gene expression assays analysis. SA and AS were involved in manuscript writing and data analysis. NJ was responsible for synovial fluid aspirate procurement and was involved in manuscript writing. ABA conceived the study, supervised the study, performed data analysis and was responsible for the writing of the final manuscript.

Chapter 4 has been submitted for publication in part as: Yan Liang, Alexander R.A. Szojka, Lynn B. Williams, Enaam Idrees, Xiaoyi Lan, Melanie Kunze, Aillette Mulet-

Sierra, Mark F. Sommerfeldt, Nadr M. Jomha, Adetola B. Adesida, “Hypoxic pre-culture of human meniscus fibrochondrocytes promotes non-calcifying vascularized matrix at ectopic sites in nude mice”. YL conducted the experiments and was responsible for data acquisition, analysis, and manuscript writing. LBW was responsible for animal surgery, EI, XL, MK and AMS were involved in immunofluorescence, gene expression analysis, and cell culture, AS was involved in data analysis and manuscript writing. MS and NMJ were involved in tissue procurement and manuscript review and writing. ABA conceived the study, supervised the study, performed data analysis including PCA, and was responsible for final review of the manuscript.

Chapter 6 has been submitted for publication in part as: Yan Liang, Clayton Molter, Alexander R.A. Szojka, Enaam Idrees, Lynn Williams, Melanie Kunze, Aillette Mulet-Sierra, Nadr M. Jomha, and Adetola B. Adesida, “Chondrogenically differentiated human synovial fluid-derived mesenchymal stem cells yield a vascularized and calcification-resistant matrix in immunodeficient mouse model”. YL conducted the experiments and was responsible for data acquisition, analysis, and manuscript writing. EI, MK and AMS were involved in immunofluorescence, gene expression analysis, and cell culture. LBW was responsible for anesthetic and surgical care of study animals. CWM and AS were involved in data collection and manuscript writing. NMJ was responsible for procurement of synovial fluid and manuscript review. ABA conceived the study. Study plans were designed by YL and ABA. ABA supervised the study and was responsible for final

review of the manuscript.

## **Dedication**

This thesis is dedicated to my wife, Mengxia Tan; my son, Junting Liang; my parents, Shaoqiong Zheng and Huaye Liang; and my mother-in-law, Yinsu Yu.

## **Acknowledgements**

Of all the parts of my thesis, I find the acknowledgments to be the most difficult to write. This is because I am so grateful and indebted to many people who have helped me along the way.

Foremost, I want to express my deep and sincere gratitude to my supervisor Dr. Adetola Adesida for introducing me to the world of tissue engineering and providing guidance and support during this process. Your motivation, vision, enthusiasm, and immense knowledge have inspired me. Thank you for your patience when I began my research, a time when I had difficulty understanding the English language in the lab and made many mistakes. Thank you for the encouragement to submit abstracts and attend local and international conferences. Thank you for all the time you spent with me to discuss set ups of experiments, to analyze and interpret data, and to review and submit my manuscripts. Thank you for all the support for my family that allowed my wife to visit me from China and start our family with baby Junting.

I would like to thank my advisory committee members: Drs. Nadr Jomha and Hasan Uludag, and my examiners: Drs. Fred Berry, Andrew Simmonds, and Fackson Mwale for their thoughtful input and insightful and challenging questions during meetings and examinations.

I would like to thank: Aillette Mulet-Sierra, Melanie Kunze, Enaam Idrees, Alexander Szojka, Dr. Troy Bornes, Dr. Stephen Andrews, Michelle Lan, Clayton Molter,

Colleen Moore, Esra Erkut, Dr. Matthew Anderson-Baron, Brayden Lyons, Dr. Hoda Atef, Dr. Rita De Cássia Marqueti Durigan, Dr. Gabriel Ochube, Dr. Leila Laouar, Dr. Kezhou Wu, Joshua Hahn, Dr. Leiah Luoma, Kirollos Labib, Karamveer Lalh, Samia Rahman, Victoria Goncalves, Austyn Roelofs, Dr. Ryan Chee, Tracey Zawalusky, and many others for all the help.

I would like to acknowledge Canadian Institutes of Health Research, Li Ka Shing Foundation, Alberta Cancer Foundation, Canada Foundation for Innovation, University Hospital Foundation, Edmonton Orthopaedic Research Committee, Edmonton Civic Employees Charitable Assistance Fund, Graduate Student Association, and Faculty of Graduate Studies and Research for all the funding support. I also would like to acknowledge the in-kind donation of type I collagen matrix from Integra LifeSciences Corp., USA and type I/III collagen matrix from Geistlich Pharma AG, Switzerland for our research.

# Table of Contents

Chapter 1 Introduction .....	1
1.1 Thesis overview .....	1
1.2 Anatomy .....	2
1.2.1 Embryology and development .....	3
1.2.2 Gross anatomy .....	4
1.2.3 Vascular supply .....	5
1.2.4 Biochemical composition.....	6
1.2.5 Cell types .....	10
1.3 Meniscus tears.....	10
1.3.1 Vertical longitudinal tear .....	11
1.3.2 Bucket-handle tears.....	11
1.3.3 Horizontal tears .....	11
1.3.4 Radial tears.....	12
1.3.5 Oblique tears .....	13
1.3.6 Complex tears .....	13
1.4 Treatment for meniscus tears .....	13
1.4.1 Meniscus repair .....	13
1.4.2 Meniscal allograft transplantation.....	16
1.4.3 Meniscectomy .....	19
1.5 Cell based meniscus tissue engineering: an emerging strategy .....	20
1.5.1 Meniscus fibrochondrocytes .....	20

1.5.2 Mesenchymal stem cells (MSCs).....	24
1.5.2.1 Types of meniscus tears and defects in preclinical studies using MSCs ..	25
1.5.2.2 Bone marrow derived MSCs (BMSCs) .....	26
1.5.2.3 Synovial membrane-derived mesenchymal stem cells (SMSCs) .....	29
1.5.2.4 Adipose tissue derived MSCs (ASCs) .....	31
1.5.2.5 Meniscus derived MSCs (MMSCs).....	32
1.5.2.6 Synovial fluid derived MSCs (SFMSCs).....	33
1.6 Clinical studies using MSCs .....	35
1.7 Thesis development and objectives .....	37
Chapter 2 Plasticity of human meniscus fibrochondrocytes: a study on effects of mitotic divisions and oxygen tension.....	41
2.1 Introduction.....	42
2.2 Methods .....	45
2.2.1 Ethics statement .....	45
2.2.2 Isolation and expansion of human meniscus fibrochondrocytes (MFCs).....	45
2.2.3 Mitotic effects on MFC chondrogenic differentiation potential .....	47
2.2.4 Mitotic effects on MFC adipogenic differentiation potential .....	48
2.2.5 Mitotic effects on MFC osteogenic differentiation potential.....	49
2.2.6 Histology for MFC chondrogenesis.....	50
2.2.7 Biochemical analysis for MFC chondrogenesis .....	50
2.2.8 Immunofluorescence for MFC chondrogenesis.....	50
2.2.9 Gene expression analysis of MFC trilineage differentiation .....	51

2.2.10 Statistical analysis .....	53
2.3 Result .....	54
2.3.1 Cell yield and expansion .....	54
2.3.2 Wet weights .....	55
2.3.3 Biochemical analysis .....	57
2.3.4 Safranin-O staining .....	58
2.3.5 Immunofluorescence .....	60
2.3.6 Gene expression analysis .....	64
2.3.6.1 Chondrogenesis.....	64
2.3.6.2 Adipogenic and osteogenic differentiation (gene expression and histological) analysis .....	67
2.4 Discussion.....	71
2.5 Conclusion .....	80
Chapter 3 Re-differentiation of human meniscus fibrochondrocytes differs in three- dimensional cell aggregates and decellularized human meniscus matrix scaffolds .....	82
3.1 Introduction.....	83
3.2 Methods: .....	85
3.2.1 Ethics statement .....	85
3.2.2 Isolation and expansion of human meniscus fibrochondrocytes .....	85
3.2.3 Human meniscus derived-decellularized matrix preparation.....	86
3.2.4 The culture of cell pellets and cell-seeded meniscus-derived DCM constructs .....	87

3.2.5 Analysis of chondrogenic differentiation of MFCs.....	87
3.2.6 Data presentation and statistical analysis.....	89
3.3 Results.....	90
3.3.1 Biochemical content (DNA, GAG, GAG/DNA) .....	90
3.3.2 Gross morphology and scanning electron microscopy .....	93
3.3.3 Safranin-O/fast green staining and immunofluorescence .....	96
3.3.4 mRNA gene expression.....	100
3.4 Discussion.....	104
3.5 Conclusion .....	110
Chapter 4 Hypoxic pre-culture of human meniscus fibrochondrocytes promotes non- calcifying vascularized matrix at ectopic sites in nude mice.....	111
4.1 Introduction.....	112
4.2 Methods .....	114
4.2.1 Ethic statements .....	114
4.2.2 Human meniscus fibrochondrocyte (hMFC) isolation and expansion.....	115
4.2.3 Culture of hMFCs on Chondro-Gide scaffolds.....	116
4.2.4 Experimental conditions .....	117
4.2.4.1 <i>In vitro</i> culture model.....	117
4.2.4.2 <i>In vivo</i> ectopic subcutaneous implantation in nude mouse (SNM) model .....	117
4.2.5 Statistical analysis and principal component analysis (PCA).....	120
4.3 Results.....	121

4.3.1 Cell yield and proliferation rates during monolayer expansion.....	121
4.3.2 Biochemical GAG/DNA quantification.....	122
4.3.3 Gross morphology and histology.....	125
4.3.3.1 Gross morphology.....	125
4.3.3.2 Safranin-O staining.....	126
4.3.3.3 Immunofluorescence for type I and II collagen.....	127
4.3.4 Blood vessel invasion and calcium deposition.....	129
4.3.5 Gene expression.....	131
4.3.5.1 Fibrochondrogenic differentiation-related genes.....	131
4.3.5.2 Other hypoxia responsive genes.....	132
4.3.5.3 TGF- $\beta$ isoform genes.....	133
4.3.5.4 Hypertrophic differentiation-related genes.....	134
4.3.6 Principal component analysis.....	137
4.4 Discussion.....	140
4.5 Conclusions.....	147
Chapter 5 Chondrogenic differentiation of synovial fluid mesenchymal stem cells on human meniscus-derived decellularized matrix requires exogenous growth factors .....	148
5.1 Introduction.....	149
5.2 Methods.....	152
5.2.1 Ethics statement.....	152
5.2.2 Isolation and culture of synovial fluid-derived mesenchymal stem cells (SF- MSCs).....	152

5.2.3 Colony-forming unit fibroblastic (Cfu-f) assay .....	154
5.2.4 Flow cytometry analysis .....	154
5.2.5 Decellularized meniscus-derived matrix scaffold preparation.....	156
5.2.6 Cell aggregate (pellet) culture.....	158
5.2.7 Decellularized matrix scaffold seeding and construct culture .....	158
5.2.8 Scanning electron microscopy (SEM) analysis .....	159
5.2.9 Analysis for fibrochondrogenic differentiation of SF-MSCs.....	160
5.2.10 Statistical analysis .....	161
5.3 Results.....	162
5.3.1 SF-MSCs isolation and expansion culture.....	162
5.3.2 Expression of MSC surface markers on SF-MSCs.....	164
5.3.3 Biochemical analysis of GAG and DNA content.....	165
5.3.4 Safranin-O staining and scanning electron microscopy.....	166
5.3.5 Immunofluorescence .....	170
5.3.6 ECM gene expression .....	173
5.4 Discussion.....	176
5.5 Conclusions.....	183
Chapter 6 Chondrogenically differentiated human synovial fluid-derived mesenchymal stem cells yield a vascularized and calcification-resistant matrix in immunodeficient mouse model .....	185
6.1 Introduction.....	186
6.2 Methods .....	188

6.2.1 Ethics statement .....	188
6.2.2 Isolation and monolayer expansion culture of human synovial fluid-derived mesenchymal stem cells (hSF-MSCs) .....	188
6.2.3 Type I collagen scaffold seeding and experimental conditions.....	189
6.2.4 Assessment of inner meniscus-like extracellular matrix (IM-ECM) formation .....	190
6.2.5 Immunofluorescence (IF).....	192
6.2.6 Enzyme-linked immunosorbent assay (ELISA) .....	193
6.2.7 Statistical analysis .....	193
6.3 Results.....	194
6.3.1 Isolation and monolayer expansion culture of hSF-MSCs under hypoxia (HYP) <i>in vitro</i> .....	194
6.3.2 Analysis of inner meniscus-like extracellular matrix (IM-ECM) formation under HYP and NRX.....	196
6.3.2.1 Biochemical analysis of glycosaminoglycan (GAG) and DNA content.	196
6.3.2.2 Gross morphology and Safranin-O Staining.....	197
6.3.2.3 Immunofluorescence (IF) analysis of ECM molecules .....	200
6.3.3 Alizarin Red S staining for calcium deposition .....	202
6.3.4 Analysis of angiogenic potential of pre-formed constructs .....	204
6.3.4.1 ELISA and immunofluorescence analysis of VEGF and SDF-1 .....	204
6.3.4.2 IF analysis of CD31 for vascular invasion <i>in vivo</i> .....	207
6.3.5 <i>In vitro</i> gene expression analysis .....	208
6.4 Discussion.....	211

6.5 Conclusions.....	217
Chapter 7 General discussion and conclusions.....	218
7.1 General discussion .....	218
7.2 Conclusions.....	228
References.....	230

## **List of Tables**

**Table 2-1:** Primer sequences used in quantitative polymerase chain reaction analysis

**Table 3-1:** Meniscus tissue donor details. PD: population doublings

**Table 3-2:** Primer sequences

**Table 4-1:** Meniscus tissue donor information

**Table 4-2:** Primer sequences

**Table 5-1:** Synovial fluid donor information

**Table 5-2:** Antibodies used to characterize SF-MSCs

**Table 5-3:** Primer sequences for quantitative polymerase chain reaction analysis

**Table 6-1:** Synovial fluid donor information

**Table 6-2:** Primer sequences

**Table 6-3:** Quantification of SDF-1 $\alpha$  and VEGF by ELISA

## List of Figures

**Figure 1-1:** Outline of the study

**Figure 2-1:** Isolation/expansion of meniscus fibrochondrocytes (MFCs) with TGF $\beta$ 1 and FGF-2 (T1F2) for four passages under normoxia (NRX).

**Figure 2-2:** Biochemical analysis of pellets derived from T1F2-expanded MFCs of four passages after 21 days chondrogenic stimulation under NRX or HYP (n=6).

**Figure 2-3:** Safranin-O staining analysis for proteoglycan deposition in pellets derived from T1F2-expanded MFCs of four passages after 21 days chondrogenic stimulation under NRX or HYP from one representative donor (male, 20 years old).

**Figure 2-4:** Immunofluorescence analysis of collagen I and collagen II in pellets derived from T1F2-expanded MFCs of four passages after 21 days chondrogenic stimulation under NRX or HYP from one representative donor (male, 20 years old).

**Figure 2-5:** Immunofluorescence analysis of hypertrophic marker collagen X in pellets derived from T1F2-expanded MFCs of four passages after 21 days chondrogenic stimulation under NRX or HYP from one representative donor (male, 20 years old).

**Figure 2-6:** (A) Real-time PCR analysis of cDNA of T1F2-expanded MFCs in monolayer culture at the end of each passage prior to pellet culture (n=4). ), (B) Real-time PCR analysis of cDNA of pellets derived from T1F2-expanded MFCs of four passages after chondrogenic stimulation for 21 days under NRX and HYP (n=4).

**Figure 2-7:** (A) Real-time PCR analysis of cDNA of T1F2-expanded MFCs of three

passages with or without adipogenic and osteogenic induction under NRX and HYP (n=4) and the fold changes of relative mRNA expression levels of adipogenic/osteogenic markers. (B) Oil Red O/Alizarin Red S staining analysis for lipid droplet and bone matrix deposition in T1F2-expanded MFCs from 3 passages after adipogenic and osteogenic stimulation under NRX and HYP from one representative donor (male, 20 years old).

**Figure 3-1:** Glycosaminoglycan (GAG) matrix and DNA contents in meniscus fibrochondrocyte (MFC)-based tissues after 21-days' culture in either pellets or meniscus-derived decellularized matrix (DCM) with and without supplementation of 10 ng/mL TGF- $\beta$ 3.

**Figure 3-2:** Assessment of growth medium turnover after 21-days' culture in medium under HYP using a 24-well plate.

**Figure 3-3:** Gross morphology of empty DCM scaffold after freeze-drying.

**Figure 3-4:** Scanning electron micrographs of meniscus fibrochondrocyte (MFC)-based tissues after 21-days culture in meniscus-derived decellularized matrix (DCM) with and without supplementation of 10 ng/mL TGF- $\beta$ 3.

**Figure 3-5:** Safranin-O staining and immunofluorescence of meniscus extracellular matrix (ECM) molecules of meniscus fibrochondrocyte (MFC)-based tissues after 21 days' culture in either pellets or meniscus-derived decellularized matrix (DCM) with and without supplementation of 10 ng/mL TGF- $\beta$ 3.

**Figure 3-6:** Relative expression of chondrogenic differentiation-related genes in

meniscus fibrochondrocyte (MFC)-based tissues after 21-days' culture in either pellets or meniscus-derived decellularized matrix (DCM) with and without supplementation of 10 ng/mL TGF- $\beta$ 3.

**Figure 3-7:** Relative expression of hypertrophy-associated genes in meniscus fibrochondrocyte (MFC)-based tissues after 21-days' culture in either pellets or meniscus-derived decellularized matrix (DCM) with and without supplementation of 10 ng/mL TGF- $\beta$ 3.

**Figure 4-1:** Monolayer *in vitro* cell expansion with TGF- $\beta$ 1 and FGF-2 (T1F2) under normoxia (NRX, 21% O<sub>2</sub>). (A) Cell morphologies of primary human meniscus fibrochondrocytes (hMFCs) in passage 0 (P0); (B, C) expanded hMFCs in P2 after liquid nitrogen storage; (D) Cumulative population doublings at the end of P1 and P2; E) population doublings per day during P1/P2.

**Figure 4-2:** Glycosaminoglycan (GAG) matrix and DNA contents in hMFCs-based constructs cultured *in vitro*. GAG (A), DNA (B), and GAG/DNA (C) *in vitro*. T3: TGF- $\beta$ 3, D: dexamethasone, A: ascorbic acid 2-phosphate, and P: L-proline (T3DAP). 3wks indicated pre-chondrogenic culture with T3DAP for three weeks, 8wks indicated after three weeks' prechondrogenic culture, the culture medium was switched to DAP or with continuous T3DAP for additional five weeks. The symbols indicating significant differences ( $p < 0.05$ ) are defined as 1) between oxygen tensions (NRX vs HYP): T3DAP/3wks (#), T3DAP/8wks (\*) and DAP/8wks (¥); 2) within NRX: T3DAP/3wks vs

T3DAP/8wks (a), T3DAP/3wks vs DAP/8wks (b), T3DAP/8wks vs DAP/8wks (c); 3) within HYP: T3DAP/3wks vs T3DAP/8wks (d), T3DAP/3wks vs DAP/8wks (e), T3DAP/8wks vs DAP/8wks (f). These symbols are also applied to the following gene expression analysis.

**Figure 4-3:** Gross morphology, Safranin-O staining, and immunofluorescence (IF) of type I/II collagen of hMFCs-based constructs cultured in vitro. DAPI staining (in blue) for cell nuclei is superimposed in IF images. The series of images labeled as A1-G1 represent gross morphology. The series of images labeled as A2-G2, A3-G3 represent the whole images and zoom in images of Safranin-O staining, respectively. The series of images labeled as A4-G4 represent IF images. Scale bar are presented in the last images of each row.

**Figure 4-4:** Gross morphology, Safranin-O staining, and immunofluorescence (IF) of type I/II collagen of hMFCs-based constructs after implantation. DAPI staining (in blue) for cell nuclei is superimposed in IF images. The series of images labeled as A1-D1 and A2-E2 represent gross morphology. The series of images labeled as A3-G3, A4-G4 represent the whole images and zoom in images of Safranin-O staining, respectively. The series of images labeled as A4-G4 represent IF images. Scale bar are presented in each row.

**Figure 4-5:** Safranin-O staining, and immunofluorescence (IF) of type II collagen, CD31 and Alizarin Red S staining of hMFCs-based constructs after implantation. DAPI staining

(in blue) for cell nuclei is superimposed in IF images only for CD31. The series of images labeled as A1-3 represent Safranin-O staining. The series of images labeled as B1-3 represent IF for type II collagen. The series of images labeled as C1-3, D1-3 and E1-3 represent DAPI, CD31 (green) and combined images. The series of images labeled as F1-3 and G represent Alizarin Red S staining for hMFCs constructs and human bone marrow mesenchymal stem cells (hBMSCs) constructs, respectively.

**Figure 4-6:** Relative gene expression of hMFCs-based constructs in vitro.

Fibrochondrogenic differentiation-related genes: (A) Aggrecan (ACAN); B) Type I collagen (COL1A2); (C) Type II collagen (COL2A1); and (D) SRY-box transcription factor 9 (SOX9). Other hypoxic response-related genes: (E) HIF-1 $\alpha$ ; (F) HIF-2 $\alpha$ ; (G) VEGF. TGF- $\beta$  isoform genes: (H) TGF- $\beta$ 1; I) TGF- $\beta$ 2; J) TGF- $\beta$ 3. Hypertrophic differentiation-related genes: (K) type X collagen (COL10A1); L) MMP-13. Values are presented as  $2^{\Delta\text{Ct}}$ , where  $\Delta\text{Ct}$  is the difference in Ct values of the average of three house-keeping genes and the gene of interest. Each donor has 2 biological replicates. The symbols indicating significant differences ( $p < 0.05$ ) are defined as 1) between oxygen tensions (NRX vs HYP): T3DAP/3wks (#), T3DAP/8wks (\*) and DAP/8wks (¥); 2) within NRX: T3DAP/3wks vs T3DAP/8wks (a), T3DAP/3wks vs DAP/8wks (b), T3DAP/8wks vs DAP/8wks (c); 3) within HYP: T3DAP/3wks vs T3DAP/8wks (d), T3DAP/3wks vs DAP/8wks (e), T3DAP/8wks vs DAP/8wks (f).

**Figure 4-7:** Relative gene expression of hMFCs-based constructs in vitro.

Fibrochondrogenic differentiation-related genes: (A) Chondromodulin-1 (CHM-1); (B) Frizzled related protein (FRZB); and (C) Gremlin 1 (GREM1). Values are presented as  $2\Delta Ct$ , where  $\Delta Ct$  is the difference in Ct values of the average of three house-keeping genes and the gene of interest. Each donor has 2 biological replicates. The symbols indicating significant differences ( $p < 0.05$ ) are defined as 1) between oxygen tensions (NRX vs HYP): T3DAP/3wks (#), T3DAP/8wks (\*) and DAP/8wks (¥); 2) within NRX: T3DAP/3wks vs T3DAP/8wks (a), T3DAP/3wks vs DAP/8wks (b), T3DAP/8wks vs DAP/8wks (c); 3) within HYP: T3DAP/3wks vs T3DAP/8wks (d), T3DAP/3wks vs DAP/8wks (e), T3DAP/8wks vs DAP/8wks (f).

**Figure 4-8:** A varimax rotated plot of a two-component solution of principal component analysis of measured variables. Measured variables are: ACAN, COL2A1, SOX9, HIF-1 $\alpha$ , HIF-2 $\alpha$ , TGF $\beta$ 1, TGF $\beta$ 2, TGF $\beta$ 3, VEGF, COL10A1, CHM-1, GREM1, FRZB, GAG, DNA and GAG/DNA. Principal component 1 (PC1) is on the x-axis and principal component 2 (PC2) is on the y-axis. The position of each variable on the plot indicates the degree to which it loads on the two different principal components.

**Figure 5-1:** Method diagram of fabrication of decellularized matrix (DCM) scaffold from human native meniscus (n=1, male, 46 years old).

**Figure 5-2:** Colony-forming unit fibroblastic (Cfu-f) assay of human synovial fluid mesenchymal stem cells (SF-MSCs) at the end of P0 expanded with FGF-2 (5 ng/mL) under hypoxia (HYP, 3% O<sub>2</sub>) (n=4).

**Figure 5-3:** Flow cytometry analysis of cell surface markers on P2 SF-MSCs after culture with FGF-2 (5 ng/mL) under HYP from one donor (male, 36 years old).

**Figure 5-4:** Biochemical analysis of pellets derived from SF-MSCs (n=4) after 21 days of *in vitro* culture in the presence of serum-free medium containing IGF-1, TGF $\beta$ 3 or the combination under HYP.

**Figure 5-5:** Safranin-O staining analysis for proteoglycan deposition in pellets derived from SF-MSCs (A) and DCM scaffolds seeded with SF-MSCs (B) after 21 days of *in vitro* culture under HYP; Scanning electronic microscope (SEM) for the morphology of SF-MSCs and DCM scaffold (C), (D: higher magnification) after 21 days of culture under HYP.

**Figure 5-6:** Scanning Electron Microscopy image of an empty decellularized matrix (DCM) scaffold from human native meniscus (n=1, male, 46 years old).

**Figure 5-7:** Indirect immunofluorescence analysis of aggrecan, collagen I and collagen II in pellets derived from SF-MSCs (A) and empty DCM scaffold or DCM scaffolds seeded with SF-MSCs (B) after 21 days of *in vitro* culture under HYP.

**Figure 5-8:** Indirect immunofluorescence analysis of hypertrophic marker collagen X in pellets derived from SF-MSCs (A) and empty DCM scaffold or DCM scaffolds seeded with SF-MSCs (B) after 21 days of *in vitro* culture under HYP.

**Figure 5-9:** Real-time PCR analysis of cDNA of pellets derived from SF-MSCs (A-E) and DCM scaffolds seeded with SF-MSCs (F-J) after 21 days of *in vitro* culture under

HYP, in the presence (+) and absence (-) of growth factors.

**Figure 6-1:** Colony-forming unit fibroblastic (Cfu-f) assay of human synovial fluid mesenchymal stem cells (hSF-MSCs) expanded with FGF-2 (5 ng/mL) under hypoxia (n=5). (A/B) Colony formation for two age-representative donors (17y/58y); (C/D) Morphology of expanded cells at the end of P0 and P2 as visualized under a light microscope; (E/F) Colony morphology of adherent cells from donor 1 as visualized by crystal violet staining on the colony edge and center. Scale bar: (B): 4 mm; (D): 100  $\mu$ m; (F): 200  $\mu$ m.

**Figure 6-2:** Biochemical analysis of hSF-MSCs-seeded constructs after 2 weeks of in vitro chondrogenic culture under normoxia (NRX) and hypoxia (HYP). (A) GAG content; (B) DNA content; and (C) GAG content normalized by total DNA content. \* indicates significant differences ( $p < 0.05$ ) between NRX and HYP groups, and ns indicates non-significant results. Donor 4 was deemed to be an outlier in this analysis because of its abnormally low DNA content measurement for the normoxia group, leading to a large skew in the GAG/DNA distribution. Error bars and p-values were calculated with the remaining four donors. Parenthesized values show the unadjusted p-values and each colour represent different donor (n=5).

**Figure 6-3:** Gross morphologies and Safranin-O staining analysis for proteoglycan deposition in hSF-MSCs-seeded constructs following different culture conditions and oxygen tensions. The series of images labeled as A1-4 and B1-4 represent 2 weeks of in

vitro chondrogenic cultured with TGF- $\beta$ 3 (T3/2wks in vitro) in NRX or HYP; images labeled as C1-4 and D1-4 represent 5 weeks of additional in vitro culture under NRX or HYP in DMEM with 10% FBS (DMEM/7wks in vitro); images labeled as E1-E4 and F1-F4 represent 5 weeks of additional in vivo implantation at a subcutaneous ectopic site using a nude SCID mouse model (Implantation/7wks), where NRX and HYP indicate the oxygen tensions from which the implanted constructs were sourced; images labeled as H1-2 represent subcutaneous implantation of chondrogenically-induced SF-MSC-seeded constructs before harvest. This analysis was completed on Donor 1 (17 years old male, meniscus tear) and Donor 2 (53 years old, osteoarthritis). Empty collagen scaffolds were either cultured in vitro (G1 and G3) or implanted in vivo (G2 and G4) as controls. Scale bar: (G2): 2 mm; (G4): 100  $\mu$ m.

**Figure 6-4:** Immunofluorescent analysis of type I and II collagen I in hSF-MSCs-seeded constructs in groups of T3/2wks in vitro and Implantation/7wks under NRX and HYP. Donor 1 and Donor 2 were used as representative samples. Analyses were also performed on constructs without primary antibody to characterize non-specific binding and empty scaffold controls in vitro and in vivo. Images labeled as A1-6 and E1-6 represent DAPI 4',6-diamidino-2-phenylindole for cells (blue); images labeled as B1-6 and F1-6 represent Alexa Fluor 594 for type I collagen (red); images labeled as C1-6 and G1-6 represent Alexa Fluor 488 for type II Collagen (Green); images labeled as D1-6 and H1-6 represent the overlap images of DAPI, type I and II collagen. Scale bar (H6): 200  $\mu$ m.

**Figure 6-5:** Alizarin Red S staining of hSF-MSCs-seeded constructs to assess calcium deposition in implantation/7wks (images E1-2 and F1-2). The groups of T3/2wks in vitro (images A1-2 and B1-2), DMEM/7wks in vitro (images C1-2 and D1-2) and empty collagen scaffold in vivo (image B3) were served as a negative control. Human BM-MSCs-derived matrix on the same collagen scaffold was implanted for 5 weeks as a positive control (image A3). Orange-red staining indicates calcium deposition. Scale bar: 200  $\mu\text{m}$ .

**Figure 6-6:** Analysis of angiogenic factors: VEGF and SDF-1 in hSF-MSC-seeded constructs by immunofluorescence in donor 1 and 2. SDF-1 and VEGF immunofluorescence was performed in TGF- $\beta$ 3/2wks in vitro group and implanted/7wks of the same donors where NRX and HYP indicate the preculture oxygen tensions from which the implanted constructs were sourced. Analyses were also performed on constructs without primary antibody to characterize non-specific binding and empty scaffold controls in vitro and in vivo. Images labeled as A1-6 and F1-6 represent DAPI for cells (blue); images labeled as B1-6 and G1-6 represent Alexa Fluor 594 for SDF-1 $\alpha$  (red); images labeled as C1-6 and H1-6 represent Alexa Fluor 488 for VEGF-A (Green); images labeled as D1-6 and I1-6 represent the overlap images of DAPI and SDF-1 $\alpha$ ; images labeled as E1-6 and J1-6 represent the overlap images of DAPI and VEGF-A. Scale bar: 200  $\mu\text{m}$ .

**Figure 6-7:** Immunofluorescence analysis of CD31 for blood vessel invasion in hSF-

MSCs-seeded constructs of implantation/7wks of donor 1 and donor 2. Analysis was also performed in empty collagen scaffold *in vivo*. No fluorescence was observed on primary antibody controls or on *in vitro* scaffolds and were therefore omitted. Images labeled as A1-3 and E1-3 represent DAPI for cells (blue); images labeled as B1-3 and F1-2 represent Alexa Fluor 488 for CD31 (Green); images labeled as C1-3 and G1-2 the zoom images of the interior matrix regions; images labeled as D1-3 and H1-2 represent the overlap images of DAPI and CD31. Scale bar: 1mm.

**Figure 6-8:** Real-time PCR analysis of gene expression levels of hSF-MSCs-seeded constructs in TGF- $\beta$ 3/2wks *in vitro* under NRX and HYP (n=5). Each gene expression level was normalized to the mean expression levels of 3 housekeeping genes:  *$\beta$ -actin*, *RPL13A* and *YWHAZ*. A-E represent inner meniscus matrix-related genes and F-K represent hypoxia and angiogenesis-related genes. \* indicates significant differences ( $p < 0.05$ ) between NRX and HYP groups, and ns indicates non-significant results.

## **List of Abbreviations**

OA: osteoarthritis

ECM: extracellular matrix

MFCs: meniscus fibrochondrocytes

MSCs: mesenchymal stem cells

BMSCs: bone marrow derived mesenchymal stem cells

GAG: glycosaminoglycan

GF: growth factor

PGA: polyglycolic acid,

PLGA: poly (lactic-co-glycolic acid

HGF: hepatocyte growth factor

CMI: collagen meniscus implant

PHBV: poly-3-hydroxybutyrate-co-3-hydroxyvalerate)

PLDLA/PCL-T: poly (L-co-D, L-lactic acid)/poly(caprolactone-triol)

SMSCs: synovial membrane derived mesenchymal stem cells

GFP: green fluorescent protein

SEM: scanning electronic microscopy

ACL: anterior cruciate ligament

EGFP: enhanced green fluorescent protein

AC: articular cartilage

P3. passage 3

PBS: phosphate buffered saline

Ihh: indian hedgehog

PTHrP: parathyroid hormone-like hormone

BMP2, bone morphogenetic protein 2

HA, Hyaff®-11

PRP: platelet-rich plasma

ASCs: adipose tissue derived mesenchymal stem cells

IFP: infrapatellar fat pad

IFPMSCs: infrapatellar fat pad derived mesenchymal stem cells

MMSCs: meniscus derived mesenchymal stem cells

SFMSCs: synovial fluid derived mesenchymal stem cells

RA: rheumatoid arthritis

HYP: hypoxia

NRX: normoxia

PD: population doublings

TE: tissue engineering

EDTA: ethylenediaminetetraacetic acid

DMEM: Dulbecco's modified Eagle's medium

FBS: fetal bovine serum

HEPES: 4-(2-Hydroxyethyl) piperazine-1-ethanesulfonic acid

DAPI: 4',6-diamidino-2-phenylindole

LPL: lipoprotein lipase

PPAR $\gamma$ : peroxisome proliferator-activated receptor gamma

RUNX2: runt-related transcription factor 2

OCN: osteocalcin

ALPL: alkaline phosphatase

DCM: decellularized matrix

RCF: relative centrifugal force

EtO: ethylene oxide

SEM: scanning electron microscopy

qRT-PCR: quantitative real time polymerase chain reaction

MMP-13: matrix metalloproteinase-13

BSP: bone sialoprotein

TE: tissue engineering

IM-ECM: inner meniscus-like extracellular matrix

hMFCs: human meniscus fibrochondrocytes

SNM: subcutaneous nude mouse

SFM: serum free medium

YWHAZ: tyrosine 3-monooxygenase/tryptophan 5-monooxygenase activation protein

zeta

RPL13A: ribosomal Protein L13a

CHM-1: chondromodulin-1

GREM1: gremlin1

FRZB: frizzled-related protein

SD: standard deviation

ANOVA: analysis of variance

PCA: principal component analysis

KMO: Kaiser-Meyer-Olkin

IF: immunofluorescence

PC: principal component

hACs: human articular cartilage

SF: synovial fluid

$\alpha$ -MEM: alpha minimum essential medium

MNCs: mononucleated cells

DVT: deep vein thrombosis

CFU: colony-forming unit fibroblastic

PSG: penicillin-streptomycin-glutamine

HMDS: hexamethyldisilane

# Chapter 1 Introduction

## 1.1 Thesis overview

Meniscus injury was reported to have an annual incidence of 66-70 per 10,000 people [5]. The intrinsic avascular nature of the inner two-thirds of the meniscus hinders its ability to heal after injuries [6, 7], of which majority end up with the surgical removal of damaged tissues. However, the mechanical and biochemical changes within the knee joint after meniscectomy, such as increased contact stress, are proved to be associated with the onset of osteoarthritis (OA) [3]. In 2011, OA affected 13% (1 in 8) Canadians and expected to increase to 25% in 30 years. The cumulative economic burden of OA from 2011-2015 for Canada was estimated to be \$195 million [8].

Autologous cell based meniscus tissue engineering to produce meniscus-like extracellular matrix (ECM) holds great promise for the repair or regeneration of the damaged meniscus tissues [9]. Adult meniscus fibrochondrocytes (MFCs) from surgical discard meniscus tissues and mesenchymal stem cells (MSCs) from bone marrow, synovium, adipose tissue and synovial fluid has been harvested by different enzymatic digestion and plastic-adherent methods [9-12]. Application of growth factors or oxygen tensions has been applied during 2 or 3-dimensional cell expansion to regulate cellular proliferation and post-chondrogenic differentiation capacity [11, 13-18]. 3-Dimensional environment such as cell pellet and porous scaffold have been frequently used to support and guide the ECM formation and tissue development *in vitro*. Biochemical, histological,

and mRNA expression analysis usually showed the formation of meniscus-like ECM molecules *in vitro*. A number of preclinical studies using different transplantation protocols such as intraarticular cell injection and implantation of cell-seeded constructs have been performed in animals [19]. Several clinical human studies have been reported only using MSCs for meniscus repair [20]. However only one randomized, double-blinded and control study using human bone marrow MSCs (BMSCs) has been carried out in 55 patients after partial meniscectomy [21]. Long-term evaluation is yet to be performed even though positive results were reported in both animal and human studies. More importantly, there are no consensus on cell sources, isolation and expansion condition, biomaterial sources, inductive stimuli to differentiate the cells towards a chondrogenic phenotype and implantation protocols.

This thesis aims to provide better understanding of the capacity of different cell types to synthesis meniscus-like ECM, through investigation of isolation and expansion conditions as well as culture environments favoring fibrochondrogenic differentiation. The thesis will begin with an introduction to meniscus anatomy and physiology, meniscus tears and treatment, followed by a review of literature on the use of MFCs and MSCs in meniscus tissue engineering. The subsequent chapters will investigate the meniscus tissue engineering variables using both *in vitro* and *in vivo* models.

## **1.2 Anatomy**

### **1.2.1 Embryology and development**

The meniscus originates from the middle layer of mesenchyme condensations around the articular capsule. At the 8th week, which represents the end of embryonic phase, the knee joint is similar to that of adults, with the menisci clearly identified in cellular form [22].

Another study aimed at investigating the development of meniscus during late fetal and postnatal periods showed that from the 14th week to 34th week of gestation, the meniscus consisted of dense fibroblast with the intercellular matrix becoming relatively

collagenous and the percentage of nucleus-to-cytoplasm decreasing. The arrangement of the collagenous fiber bundles within the meniscus became more organized. In the cross section, the fibers were mainly presented in circumferential direction while the rest were in radial pattern. At this stage, blood vessels can be seen throughout the entire meniscus.

Between the age of three and nine months after birth, the meniscus begin to change in size and shape to adapt to the growth of the epiphyses and the change of contact surface of distal femur and proximal tibia. The nucleus-to-cytoplasm ratio of meniscal cell continue to reduce, and the quantity of collagen increased. Blood vessels could be identified mainly in peripheral and intermediate one-thirds while some blood vessels could still be seen in the inner one-third region occasionally. From nine to eleven years, the shape of the menisci resembled that of adults. But blood vessels decreased comparing with previous stages while in adults, the blood vessels was only limited to the outer one-third of menisci [23]. However, although numerous histological alterations happened, the

area of the tibial plateau covered by the medial and lateral meniscus remained almost unchanged during all stages. To be specific, the medial menisci covered 51-74% surface of the medial plateau while 75-93% surface of the lateral plateau were covered by lateral menisci [24].

### **1.2.2 Gross anatomy**

The menisci of the knee joint are two pair of C-shaped or O-shaped fibrocartilage between the femoral condyles and tibial plateau in medial and lateral sides [25], which transmit ~ 50% of the load across the knee [26]. In cross section, the menisci are wedge-shaped structures. They are about 35mm in diameter [27]. The peripheral region of the menisci is convex and connected to the knee joint capsule and the margin of the inside region is concave, thin and unbounded [28]. The menisci are fixed to the subchondral bone of the tibial plateau by meniscal horns and to the femur through the ligaments of Humphrey (the anterior meniscal-femoral ligament) and Wrisberg (the posterior meniscal-femoral ligament). The menisci are connected to the patella by patellomeniscal ligaments [25]. For example, the medial meniscus appears C-shaped and its anterior horn is narrower than the posterior horn. Meanwhile the antero-posterior dimension is larger than the medio-lateral dimension [24, 28]. In addition, the locations vary for the attachment of the anterior horn of medial meniscus, but mostly firmly to the intercondylar site of the tibial plateau while the posterior horn attaches the tibial in front of the embedded location of posterior cruciate ligament (PCL). The outer edges fuses with the

knee joint capsule and is attached to the upper tibia via the coronary ligament [28]. As for the lateral meniscus, it appears O-shaped with more uniformity in width and circumference. Its anterior horn has an interconnection with that of medial meniscus by the transverse ligament and posterior horn is attached to PCL and medial femoral condyle by the menisconfemoral ligaments of Wrisberg and Humphrey. Because the medial meniscus is firmly attached to the knee joint capsule and medial collateral ligament, when comparing with the lateral meniscus, the medial meniscus is much less flexible. In fact, the lateral meniscus is not attached to the lateral collateral ligament and the tendon of the popliteus muscle will separate the posterior horn of the lateral menisci from the knee joint capsule [25].

### **1.2.3 Vascular supply**

By using the technique of immuno-histochemical detection, the blood vessels in 20 human menisci ranging from 22 weeks of gestation to 80 years were investigated [29]. Results showed that around 22 weeks of gestation, vessels can only be recognized in the outer third of the menisci. At the time of birth, vessels could be seen throughout the entire menisci while at the stage of 2 years old, a vascular region could be detected along the margin of inner area of the menisci. In addition, the insertional ligaments were present with good blood supply, but not fibrocartilage within the inserting structure. The cause of the development of an avascular region within the menisci can be attributed to the increasing pressure which acts on the knee joint [29]. Another study showed that the

majority of blood supplied to the medial and lateral menisci was from the lateral, medial and middle genicular arteries [7]. The branch vessels from these arteries would form a perimeniscal capillary plexus inside the synovial and capsular tissues, which gave blood supply to the peripheral edge of the menisci with radial branches extended towards the center of the joint [7]. Three zones were formed by the perimeniscal capillary plexus regarding different distributions of the blood vessels in adult. The blood vessels mainly penetrated into peripheral 10-30% of the medial meniscus or 10-25% of the lateral menisci and this area is called the red zone [26]. As for the middle third region, only a limited blood supply can be identified and is called the red/white zone. The inner third region of the menisci is called white zone which mainly depend on the nourishment from the synovial fluid or mechanical motion with no blood supply [30]. Besides, the anterior and posterior horns of both medial and lateral were found to be in good blood supply [7, 31, 32]. The lack of blood supply to the inner region of menisci is the primary cause of non-healing properties of the meniscus [33].

#### **1.2.4 Biochemical composition**

Four distinct types of substances, namely water, fibrillar components, proteoglycans, and adhesion glycoproteins, consist of the extracellular matrix (ECM) of the meniscus.

Normal meniscus has been showed to contain 72% water, 0.12% DNA, 22% collagen, and 0.8% glycosaminoglycan matrix [34]. The percentage of these substance varies according to the age, species and location in the meniscus [35].

Collagen and elastin are the two main classes of fibrillar components of the meniscus. While many studies have been carried out on the property of collagen, only a few knowledge of the elastin is reported [34]. The quantities of different types of collagen vary according to the region of the menisci. Five different types of collagen, namely type I, II, III, V, and VI, occupy 60-70% of the dry weight [36]. In bovine meniscus, type I collagen was more than 90% of the total collagen and type III accounted for less than 10%. Type II and V only occupied 1-2% [37]. A further study focusing on the distribution of the collagen of the bovine medial and lateral meniscus was carried out [38]. In this study, by using the methods of differential salt precipitation, cyanogen bromide-peptide analysis and SDS gel electrophoresis, people found that the proportion of collagen in the outer two-thirds of the menisci was 80% of which 17% was pepsin soluble. Most of these collagens were type I while less than 1% amount of type III, V collagen was detected. Regarding the inner one-third of the menisci, collagen made up 70% of the tissue by dry weight, of which 60% was type II collagen and 40% is type I collagen [38]. Except for the collagen, mature and immature elastin fibers has been detected in extremely low proportion (<0.6% of dry weight) in the adult meniscus [35].

As for the orientation of the collagen fibers, an early study using polarized light microscopy demonstrated that most of the collagen fibers orientate circumferentially within meniscus with some radially orientated fibers located in the intermediate region of the meniscus or on the meniscus surface [39]. Another study also confirmed these results

and found that the orientation of the collagen fibers is similar among dogs, pigs and human meniscus. Furthermore, no differences could be detected between medial and lateral menisci [40]. More details have been shown under scanning electron microscopy as three different layers of the meniscus can be seen clearly, namely superficial, lamellar and deep which is covered by the synovium. A network structure consisted of thin fibrils which were randomly oriented could be seen in the superficial layer. Under the superficial layer, the fibrils also oriented without clear direction, except for the fibrils locating in the outer region of the anterior and posterior horns which oriented radially. In the deep layer, the majority of the fibrils were arranged in a circular direction with some radial fibrils inserted among these circumferentially oriented fibers which was also termed as tie fibers [41].

Proteoglycans are highly glycosylated proteins that contain sulfated polysaccharides, (glycosaminoglycans, GAG) are the major components [34]. The heavily anionic GAG can collect counter-ions and water molecules within tissues, which determine the physical and biological characteristics of hydration and resistance to compressional forces. GAG can be divided into three types: chondroitin sulfate/dermatan sulfate, heparan sulfate/heparin, and keratan sulfate. The main components of GAGs found in normal human meniscus are chondroitin 6-sulphate (40%), chondroitin 4-sulphate (10-20%), dermatan sulphate (20-30%) , and keratan sulphate (15%) [34]. The meniscus contain approximately 8-fold less GAG than that of articular cartilage in dogs [42]. Two primary

types of proteoglycans can be found in meniscus. One is aggrecan which presents the large proteoglycan whereas the other are biglycan and decorin belonging to the major small leucine-rich proteoglycans [43]. In a study aimed to determine the ability of meniscus to synthesis proteoglycan, cells from outer one-third and inner two-thirds of the human medial meniscus were cultured in a monolayer [44]. They found that human meniscus cells from inner two-third possessed a greater ability to synthesize proteoglycans than cells from the outer one-third regardless of age [44]. Similar characteristics of proteoglycan synthesis was also found in the inner two-thirds of medial meniscus from sheep and the lateral meniscus produced more proteoglycan than the medial meniscus [45]. As for the small proteoglycans, research has been done in pigs to investigate their distribution. Biglycan was found to be concentrated in the inner one-third of the pig meniscus. Its role in the inner meniscus may be protecting cells during compressional forces. On the other hand, decorin may participate in organizing the direction of collagen fibril as they were found to be concentrated in the outer one-third of the porcine meniscus [43].

The main function of adhesion glycoproteins may be to connect the matrix components with cells. Three primary types of adhesion glycoproteins have been identified in human meniscus: type VI collagen, fibronectin, and thrombospondin. However, further investigation is needed to determine their exact function in human meniscus [36, 46, 47].

### **1.2.5 Cell types**

In rabbit meniscus, four primary morphologically distinguishable types of cells have been identified in the meniscus [48]. In the outer two-thirds (the vascular region) of the meniscus, two types of cells are present. At the outer edge of this region, cells have stellate shape because of the numerous long thin cytoplasmic projections which have branches to connect with the adjacent extracellular matrix. In the deeper and less vascular region of the outer two-thirds, cells generally possess one or two projections and these projections join the cells into sheets which are arranged in rows. In the inner one-third (the avascular region) of the meniscus, cells display a round morphology without projections. No clear orientation of these cells can be seen. In the superficial region of the meniscus, cells with a fusiform morphology are present. No prominent cytoplasmic projections can be detected [48]. For human meniscus, three different types of human meniscus cells has been characterized at the beginning of monolayer culture; elongated fibroblast-like cells, polygonal cells, and small round chondrocyte-like cells [12].

### **1.3 Meniscus tears**

Although many efforts have been made to classify meniscal tears, however there is no consensus within the orthopaedic community with regards to this question. In most cases, the tears are classified according to morphology under the observation of arthroscopy or the vertical depth of the tear as full-thickness or partial thickness [24, 49, 50]. For now, meniscal tears are divided into six primary types, namely vertical longitudinal, bucket-

handle, horizontal, radial, oblique, and complex tears [26] .

### **1.3.1 Vertical longitudinal tear**

A vertical longitudinal tear is defined as tears occurring between collagen fibrils which is parallel to the long axis of the meniscus and perpendicular to the tibial plateau with the tear equidistant from the peripheral edge of the meniscus [51].

### **1.3.2 Bucket-handle tears**

The term bucket handle originates from the appearance of the tear, in which the inner displaced fragment of the meniscus resembles a handle, and the peripheral non-displaced portion has the appearance of a bucket. This type of tear is a vertical or oblique tear with longitudinal extension toward the anterior horn in which the inner fragment is frequently displaced toward the antero-condylar notch with resultant mechanical locking of the knee joint [52]. The entire meniscus is often involved in bucket-handle tears and other portions of the meniscus, such as isolated anterior horn and posterior horn involvement or the posterior horn and body of the meniscus can happen in some cases [53]. A frequency of 26.6% of meniscal bucket-handle tears has been reported and 76% of these tears occurred in the medial meniscus which are often associated with anterior cruciate ligament (ACL) ruptures [54].

### **1.3.3 Horizontal tears**

A horizontal tear usually spreads parallel to the tibial plateau and divides the meniscus into upper and lower sections [51].

### **1.3.4 Radial tears**

A radial tear orients both perpendicular to the long circumferential axis of the meniscus and to the tibial plateau [51, 55]. As the tear goes through the cross-section of the circumferentially oriented collagen fibrils, it can divide the meniscus into two separate pieces or leave a large portion of meniscus attached to the tibia at one end, which leads to the meniscus being incapable of bearing radial oriented force [55]. In an arthroscopy study [56], an incidence of 14% of radial tear was found in 200 knees. When using the truncation or abnormal morphology as criteria for Magnetic resonance (MR) imaging examination, 68% sensitivity (19 of the 28 radial tears ) was demonstrated while additional criteria of increased signal in the area of abnormal morphology on fat-saturated T2-weighted or proton density weighted sequences was added, better results of sensitivity (89%, 25 of the 28 radial tears) was present. Another study also demonstrated similar incidence of 15% (29/196) of radial tears in 196 consecutive patients. MR examinations were also performed basing on four signs for MR detection, namely truncated triangle, cleft, marching cleft, and ghost meniscus signs, which also showed a 89% sensitivity of the radial tears [57]. Different parts of the medial and lateral meniscus were present with distinct incidences of radial tear. The incidences for the posterior horns of medial and lateral meniscus were 53%, 26%, respectively and only 5% of the radial tear occurred in the anterior horn and 16% happened in the body of the lateral meniscus [57].

### **1.3.5 Oblique tears**

An oblique tear is like radial tears that starts from the inner portions of the meniscus, but tilt inwards. It was reported that oblique and longitudinal tears comprised 81% of the meniscus tears [58].

### **1.3.6 Complex tears**

A complex tear is composed of two or more tear configurations which are not easily categorized into a specific type of tear. It is usually unrepairable and partial meniscectomy is required [51].

## **1.4 Treatment for meniscus tears**

### **1.4.1 Meniscus repair**

The type of meniscal tear and its relative blood supply determine the choices of surgical meniscus repairs, which are aimed at restoring the meniscus to its native state. Three zones exist within the meniscus, which mainly determine the healing capacity of the meniscus. Healing capacity is excellent in the red zone while it is good in the red/white zone. The avascular zone, also called white zone, poses the most difficult challenge to be repaired [59]. A study in dogs has shown that the lesions caused by complete transverse sectioning of the peripheral 25% of the meniscus could be completely repaired by fibrovascular scar while the lesion in the avascular region failed to heal [6]. Generally, non-degenerated, vertical longitudinal tears which are less than 3 cm in length and appear inside the peripheral region of the meniscus tend to repair. But tear morphologies such as

flaps, cleavage, and radial tears are usually unable to be repaired other than resection [60]. In addition, the age of patient can affect the healing capacity of the meniscus. Usually patients in young ages are reported to have improved healing results [61].

Various methods have been used to repair meniscus tears: suturing [61], trephination [62], introduction of a fibrin clot [63], platelet rich plasma (PRP) [64], and abrasion therapy [60]. With the use of arthroscopic, several techniques were used: inside-out, outside-in technique [61] and all-inside suturing devices [65, 66].

Trephination is a method attempting to build vascular channel from the vascular region of the meniscus to the tears in the avascular region [62]. Arnoczky *et al.*[6] reported that complete healing of tears in avascular portion of the meniscus by fibrovascular scar if these tears were connected to the peripheral synovial vasculature through a vascular channel. Using the similar principle, Zhong *et al.*[62] created blood supply to the injured avascular area of meniscus by need-like trephine in dogs. They found that all injuries were partly or completely healed. Furthermore, when treated with arthroscopic trephination plus suturing, more than 90% patients fully recovered without symptoms of meniscal tears while suturing alone led to 25% clinical failure rates.

Fibrin clots, which may contain platelet-derived growth factor and fibronectin, can act as a chemotactic and mitogenic stimulus for reparative cells and provide a scaffold for the repairing process in the avascular region of meniscus [67]. The fibrin clots were injected into meniscus tears in dog knees and the defects were filled with fibrous

connective tissue which may originate from the synovial membrane and the adjacent meniscal tissue. In another study, Henning *et al* [63] used exogenous fibrin clot alone or combined with fascia sheath to fill the meniscus tears in human. They reported that 64% of patients were healed, 24% incompletely healed and 12% failed.

Platelet-rich plasma (PRP) is approximately more than 3- to 8-fold in platelet concentration compared with that of whole blood [64]. It can be obtained from venous blood by centrifugation easily [68]. When activated, the platelets release of growth factors from the alpha and dense granules located in the platelet cytoplasm which initiate a healing cascade leading to cellular chemotaxis, angiogenesis, collagen matrix synthesis, and cell proliferation [64]. Tumian and Johnstone [69] reported that platelet derived growth factor-AB (PDGF-AB) can promote meniscus regeneration in inner (avascular), middle, and outer (vascular) zones. The meniscus cells from the avascular portion of meniscus can proliferate and form new matrix when stimulated by PDGF-AB. Other findings suggest that PRP facilitates the repair of meniscal defects is reported by Ishida *et al* [70]. They observed that meniscus cells cultured with PRP have greater mRNA expression of biglycan and decorin. As for the *in vivo* study, PRP were released in the 1.5-mm-diameter full-thickness defects created in the avascular region of rabbit meniscus by a gelatin hydrogel drug delivery system. Histological findings revealed that better meniscal repair in rabbits treated with PRP relative to rabbits received platelet-poor plasma or gelatin hydrogel only [70].

Introducing reparative cells to the tears of meniscus by a vascularized synovial flap also promotes the healing process in the avascular region [71]. Ghadially *et al.* [71] used suture to repair the bucket-handle tears in the avascular region of meniscus in sheep and no healing was achieved after six months. But by suturing a free flap of synovium to the site of injury, formation of cartilaginous tissue was presented in the tears. These tissues resembled a morphology between hyaline cartilage and fibrocartilage. In another study, free fraps of synovium were inserted into the longitudinal tears in the medial meniscus of 35 dogs and sutured. 11 of 35 with free synovium were healed with fibrous tissue while none of the control group were healed [72].

The various repairing methods of the meniscus have their limitations. The strength of scar resulting from different repairing methods has been studied in standardized longitudinal tears in the red/white zone of rabbit medial meniscus [73]. Three groups received different treatments: no therapy, suture, and fibrin glue, were performed in this study. After 6 weeks, the scar had recovered 19% (no therapy), 26% (suture), and 42.5% (fibrin glue) of strength compared to the intact healthy controls. In addition, a secondary tissue weakness was found in the peri-scar area.

#### **1.4.2 Meniscal allograft transplantation**

The first free meniscus transplants in clinical use were performed by Milachowski *et al.* [74]. They transplanted lyophilized or deep-frozen allogenic menisci in 22 patients that were followed-up for 14 months. Using arthroscopy, they found that both two types of

transplanted menisci showed some shrinkage after 8 months. But generally, the outcomes of the deep-frozen menisci were better than lyophilized menisci. Since then, great efforts to transplant or to replace a meniscus have been made in experimental and clinical studies [75]. It has become the treatment for the symptomatic post-meniscectomy patients without osteoarthritis and may have a potential chondroprotective effect [24, 76].

Four types of allogeneic transplants are available including fresh, frozen, lyophilized, and cryopreserved which are usually obtained from cadaveric donors [26]. Fresh tissue is beneficial for transplantation as the extracellular matrix may be disrupted after a long-termed preservation. Its application in clinical use is limited by storage and source.

Another problem associated with fresh tissue is the immunogenicity. Deep-frozen tissue is much easier to store, but when stored in a frozen environment, the process of freezing would kill the fibrochondrocytes within the tissue. A study has shown that deep-frozen technique not only kills all the fibrochondrocytes, but also denatures the histocompatibility antigenic activity [77]. But it can preserve the collagen framework, leaving the allograft as a scaffold. Comparing with the deep-frozen technique, cryopreservation of the allografts can leave 10-30% of the fibrochondrocytes viable.

Additionally, the measurement of proteoglycan concentration and water content has been carried out in transplanted allografts preserved by cryopreservation [78]. As a result, the water content of the cryopreserved group increased 12%-24% whereas proteoglycan concentration decreased up to 56% when compared to native tissues. As for lyophilized

menisci, water within the allograft is removed by lyophilization and donor cells lose their vitality [26, 75]. More shrinkage and degeneration were detected by second-look arthroscopy in clinical use [79] and now this technique has been abandoned.

Regarding the indications to meniscal allograft transplantation, current literatures have not yet come to an agreement. But two most commonly used clinical indications have been described in a review: (i) young patients (<50 years of age) with a symptomatic, meniscus-deficient compartment in a stable joint, without malalignment and with only minor chondral lesion (no more than grade 3 according to the International Cartilage Research Society (ICRS) score); and (ii) patients with an ACL-deficient knee which sustained a medial meniscectomy. In the second group of patients, meniscal transplantation is performed together with ACL reconstruction as it grants an improved stability compared to that obtained with ACL reconstruction alone. A third indication may be used in clinical practice: prophylactic transplantation in the young age of patients underwent totally meniscectomy with a desire to have sportive life style [80].

A meta-analysis, analyzing 39 all English-Language clinical trials with more than 6 months' clinical, radiological and/or histological follow-up subjects, demonstrated that meniscus allografts as an encouraging and long-lasting therapy for specific-selected patients who had developed early degenerative changes after meniscectomy [81]. It is reported about 75-90% of patients experienced fair to excellent functional results using pain scales and functional activity questionnaires after meniscus allografts

transplantation. Based on the finding of radiological examinations and MRI analysis, a number of patients did not develop further cartilage degeneration though joint space narrowing can be detected in some cases. In addition, second-look arthroscopy findings indicate that most of the patients had good integration of the allograft to the rim of the meniscus and tearing and shrinkage can be presented in some patients.

Allogenic meniscus transplantation is contraindicated in patients with advance chondral degeneration according to the International Cartilage Repair Society (ICRS) classification system. For example, if osteophyte formation or femoral condyle flattening is presented preoperatively, the outcomes of meniscal transplantation may be disappointed. Other contraindications are obesity, skeletal immaturity, instability of the knee joint, synovial disease, inflammatory arthritis and previous joint infection [81].

### **1.4.3 Meniscectomy**

Total meniscectomy was the one of the most popular orthopaedic treatment methods, because the meniscus was considered to be functionless and the removal of a ruptured meniscus seemed to have satisfactory results [24, 82, 83]. In a study by Perey, *et al* [83], 70% of 33 patients who underwent meniscectomy of medial meniscus after 30 years had excellent working capacity and 15% had good results. But the degenerative effects of such operations have been discovered [84]. For example, Fairbank, *et al* [85] examined X-ray films in 107 patients and found three types of changes in the knee joint after meniscectomy, including ridge formation, narrowing of the joint space, and flattening of

the femoral condyle. It is suggested that these degenerative changes usually result from the loss of the mechanical function of meniscus that can increase contact area and decrease contact stress between tibia and femur [86]. These understandings promoted the development of partial meniscectomy which is intended to save as much meniscus as possible [84]. Compared to total meniscectomy, partial meniscectomy leads to less severe degenerative outcomes, with 88% to 95% patients demonstrating good to excellent outcomes [87] and the degree of arthritic changes in partial meniscectomy have a close association with the amount of meniscus removed [88]. However, the degenerative changes of the knee joint were still observed after the partial meniscectomy.

### **1.5 Cell based meniscus tissue engineering: an emerging strategy**

Although positive results were reported using different treatments, meniscectomy still represent a major treatment for meniscus injuries to date [89]. Current evidences suggest that cell-based tissue engineering strategies in combination of growth factors and scaffolds to regenerate meniscus-like ECM may offer a promising option for the repair or replacement of damaged meniscus to restore normal knee function. In the following sections, several cell sources that have been demonstrated the potential for meniscus tissue engineering were reviewed.

#### **1.5.1 Meniscus fibrochondrocytes**

Since several different terms such as fibroblast, meniscus cells, fibrochondrocytes and chondrocytes have been used to described cells isolated from meniscus, the following

content in this thesis will use meniscus fibrochondrocytes (MFCs) to avoid confusion.

The ability of animal MFCs (rabbit) to proliferate and synthesis matrix in primary monolayer culture were first revealed by Webber, *et al* [90]. For human MFCs, the inner two-thirds of human meniscus cells were shown to have a better chondrogenic phenotype in terms of proteoglycans and type II collagen production when compared with outer one-third in monolayer culture [44, 91].

The surgical debris of meniscus are considered a potential tissue source of MFCs for meniscus tissue engineering [92]. The attempts to form meniscus-like ECM using human MFCs have been reported using monolayer [44], micromass [93], pellet [11, 94], and scaffold [92, 95] model. However, the insufficient cell number of MFCs that can be isolated from the surgical discarded tissue is a limitation, which usually requires monolayer expansion. Monolayer expansion of human MFCs has been shown to lose its extracellular matrix-forming phenotype regarding production of proteoglycan and type II collagen [12, 44, 96].

Several studies have been reported by researchers to improve cell proliferation rates and yield as well as meniscus-like ECM formation. Adesida, *et al* [11] expanded human MFCs with or without fibroblast growth factor 2 (FGF2) in monolayer culture. The expanded cells in passage 2 were prepared for following three-dimensional cell aggregate cultures under normoxia (20% O<sub>2</sub> or hypoxia (5% O<sub>2</sub>)). They found that the supplementation of FGF2 significantly increased human MFCs proliferation. The

production of type II collagen and glycosaminoglycan were further enhanced by low oxygen tensions using a cell pellets model. However, supplementation of TGF $\beta$ 1, FGF2 and PDGF-bb during human MFCs expansion did not result in meniscus-like matrix formation using a scaffold model even though the proliferation rate was significantly higher compared to no growth factor group [94]. Further studies were done to examine the regenerated ability of inner and outer meniscal cells from patients with osteoarthritic disease seeded on type I collagen scaffolds under hypoxic and normoxic condition, respectively by Adesida, *et al* [14]. Unlike the native meniscus that outer one-third of meniscus contains larger amount of type I collagen while inner two-third produce higher levels of type II collagen, outer meniscal cells produced higher level of type II collagen under normoxia whereas inner meniscal cells produced elevated amount of type I collagen [96], indicating that more investigation should be done to establish appropriate culture conditions for meniscus tissue engineering.

When human primary MFCs were co-cultured with human passaged bone marrow-derived mesenchymal stem cells (BMSCs), enhanced meniscus-like ECM formation was observed using a small-scale cell pellet model [97-99]. Furthermore, the human primary MFCs from the outer portion of meniscus were more potent to suppress the hypertrophic differentiation of BMSCs [98]. The use of human primary MFCs and passaged MSCs in the co-culture system may thus also have promise to solve the limited cell sources issue for meniscus tissue engineering. Even though the optimal ratios of human MFCs and

MSCs remains unknown, studies have identified that a relatively low ratio of MFCs/BMSCs, specifically 1:3, to reproducibly enhance ECM formation. More importantly, the non-expanded primary MFCs can maintain the ECM-forming phenotype expressed *in vivo* as a guide to differentiate MSCs towards a MFC phenotype [100].

The *in vivo* performance of animal and human-derived MFCs has been tested in nude mouse (subcutaneous [101-104] or meniscus tears [105]), rat (partially meniscectomy [106]), rabbit (partially [107] or total meniscectomy[108, 109]). Bovine calf meniscus derived MFCs showed the capacity to form meniscus-like ECM when seeded a 3D PGA scaffold after subcutaneous implantation in nude mouse [101]. Further study showed that the expanded bovine calf MFCs can be enriched with angiogenic factor and formed vascularized meniscus-like ECM in the same subcutaneous environment [102]. However, no meniscus-like ECM can be formed subcutaneously in the nude mouse using human MFCs was also reported [94].

In rabbit with total meniscectomy, the implanted allogenic MFCs-seeded PGA-PLGA after 36 weeks showed regeneration of meniscus-like tissues [108]. However, the structure of the matrix, content of the collagen and mechanical properties were all different from the native meniscus. The degeneration of articular cartilage was also observed even though it was less in cell-seeded group compared to scaffold only. In large animal model (sheep) with partially meniscectomy, enhanced vascularization, scaffold remodeling and matrix formation was reported after implantation of autologous MFCs-

seeded CMI constructs [110]. However, the destruction of the implanted constructs (reduced sizes and complete loss of the constructs) and degeneration of articular cartilage was observed. Only one study reported no signs of articular cartilage disruption after implantation of MFCs-seeded PLDLA/PCL-T constructs in rabbit with total meniscectomy after 24 weeks [111].

### **1.5.2 Mesenchymal stem cells (MSCs)**

MSCs isolated from bone marrow, synovial membrane, adipose tissue and meniscus are frequently used for meniscus tissue engineering. The minimal criteria [112] for MSCs are defined by International Society for Cellular Therapy as 1) able to adhere to plastic, 2) expression of certain cell surface markers and 3) able to differentiate into osteoblast, adipocytes and chondroblast *in vitro*. However, one of the challenges in meniscus tissue engineering using MSCs may be that there are no unique positive or negative markers to identify and isolate MSCs. Even though there are minimum criteria for defining MSCs mentioned above, these are not enough to uniquely identify MSCs nor to distinguish their sub-populations to achieve consistent results between donors and research groups. The reported cell surface markers are not only shared by MSCs, but also other cell types [113, 114]. The initial expression of surface markers on MSCs was reported to change during *in vitro* expansion [115, 116] and may not be associated with the differential potentials of MSCs [116]. Subpopulations of MSCs within the same tissue may express different surface markers, demonstrating different levels of chondrogenic potential [117, 118].

MSCs can also be isolated from non-plastic adherent methods and demonstrated enhanced proliferation and differentiation potential than plastic adherent MSCs [119]. The MSCs isolated from the same or different tissue sources thus may contain various subpopulations, which with unique phenotypes and whose specific stable markers need to be identified. This may assist with isolation and characterization of their unique differentiation potentials.

Another challenge may be how to differentiate the isolated MSCs towards a desired chondrogenic phenotype. The *in vitro* chondrogenic phenotype induced by growth factors does not necessarily correspond to demonstrated performance *in vitro*, as SM-MSC [120] and BM-MSC [121]-derived cartilaginous tissue *in vitro* failed to maintain a stable chondrogenic phenotype and underwent calcification, respectively when implanted *in vivo*. More investigation needs to perform regarding the isolation, expansion and differentiation of MSCs.

The following paragraphs will summarize the findings using MSCs from different sources both *in vitro* and *in vivo* for meniscus tissue engineering.

#### **1.5.2.1 Types of meniscus tears and defects in preclinical studies using MSCs**

The surgical-induced meniscus tears include longitudinal tears in dog [122], rabbit [123-125], pig [126]; oblique tears in pig [127] and radial tears in sheep [128]. The surgical-induced defects include cylindrical defects made by punch in rabbit [129, 130], rat [131], pig [132]; partially meniscectomy in goat [133], rabbit [134], rat [135], sheep [136], pig

[137] and horse [138]; total meniscectomy in rabbit [139, 140]. The meniscus tears that received cell transplantation were all reported to be better heal compared to cell-free controls. On the other hand, most of the studies reported enhanced regeneration of meniscus defects after cell transplantation. However, Mizuno, *et al.* reported similar regenerated meniscus-like tissue in the cylindrical meniscus defects (1 mm in diameter) between injection of SMSCs and PBS after 12 weeks in rat. Port, *et al.* reported less regeneration of avascular medial meniscus defects (6 mm long and 1.5 mm thick) after implantation of BMSCs (with fibrin clot and suture) compared to suture with fibrin clot in goat [133]. In contrast, fibrin clot with bone marrow derived nucleated cells were reported to promote regeneration of cylindrical meniscus defects (1.5 mm in diameter) in rabbit [129]. In the rabbit with partially meniscectomy, implanted BMSCs seeded with type I collagen promoted meniscus regeneration in the rabbit model [141]. However, blood vessel invasion and hypertrophic differentiation of BMSCs to form bone within the newly formed matrix was also reported in this study.

#### **1.5.2.2 Bone marrow derived MSCs (BMSCs)**

A number of studies have investigated the potential roles of BMSCs in meniscus tissue engineering. The formation of meniscus-like ECM of BMSCs *in vitro* has been reported in pellet model [97-99], hydrogels [142] and polyethylene glycol diacrylate scaffold [143] mixed with meniscus-derived ECM, seeded onto scaffold derived from meniscus ECM [142-145], PCL (poly( $\epsilon$ -caprolactone)) [95, 146-150], PU (polyurethane) [151],

CMI (collagen meniscus implant) [152]. The quantity and quality of the BMSCs-derived ECM were reported to be modulated by several factors: growth factors [16, 17], native meniscus derived ECM [142, 143], mechanical stimulation [147, 151, 152], low oxygen tensions [15] and co-culture with MFCs [98, 99]. The hypertrophic differentiation of BMSCs to form bone matrix *in vivo* after chondrogenic differentiation is undesired for meniscus tissue engineering [121]. The hypertrophic differentiation of human BMSCs was reported to be suppressed when coculture of human MFCs [98] or chondrogenic culture under low oxygen tension [15].

Compared to donor matched bovine calf MFCs, BMSCs were reported to produce greater amount of meniscus-like ECM on a PCL scaffold, but with similar mechanical properties [146]. The same group later showed that no differences of ECM formation were found between donor match human MFCs and BMSCs in a pellet model. However, human MFCs produced more ECM with better mechanical properties compared to BMSCs using the PCL scaffold. Another study showed that the bovine MFCs produce larger and more organized fibers similar to native meniscus compared to bovine BMSCs [153]. For other factors like the effects of mechanical loading on meniscus ECM formation, Baker *et al.* [147] showed that dynamic tensile loading enhanced total collagen content production and tensile properties of bovine BMSCs seeded PCL constructs compared to non-loading group; even though no differences were observed in proteoglycan production. However, Nerurkar, *et al.* [150] showed that dynamic culture

significantly decreased GAG production of bovine calf BMSCs and did not improve tensile compared to non-loading group

Animal studies have shown that the direction injection of autologous BMSCs improved healing of meniscus injuries in dogs [122], pig [127], horse [154]. The injection of human BMSCs was also reported to enhanced regeneration of meniscus after partially meniscectomy in rat [135, 155]. In meniscus tears of sheep, the beneficial effects of injection of autologous BMSC on meniscus regeneration were case-dependent [128] even though the macroscopic and histological scores were better in the injection group. It should be noted that the injection of BMSCs with PBS resulted in type X collagen deposition and calcification of the regenerated meniscus tissues in nude rats [155]

The implantation of BMSC-seeded hyaluronan/gelatin constructs that received prechondrogenic culture for 2 weeks showed good integration with remaining native meniscus tissue and filled the defects with meniscus-like tissue contains type II collagen compared to cell free scaffold in a rabbit model [134]. Similar study also showed that preculture of BMSCs on hyaluronan/gelatin scaffold promote the repair of longitudinal meniscus tears in rabbits [123]. Another study using meniscus injury model in rats showed that pre-culture allogenic BMSC on allogenic meniscus-derived scaffold promoted ECM formation after 8 weeks implantation. Moreover, less degeneration of the articular cartilage in the knee joint that received cell-seeded constructs than scaffold only group [156]. In contrast, implantation of non-precultured BMSCs-seeded

hyaluronan/gelatin constructs showed better integration than precultured group (TGF- $\beta$ 1/2weeks) in a meniscus punch defects in rabbits after 12 weeks [123]. The capacity for undifferentiated BMSCs or precultured BMSCs to repair and regenerated the meniscus seemed to be dependent on the type and location of defects. A recent report also showed that autologous bone marrow concentrate seeded onto the Hyaff<sup>®</sup>-11 scaffold was more beneficial to promote meniscus regeneration compared to BMSCs-seeded constructs in the sheep model [136]. Another study showed bone marrow concentrate with suture promoted the healing of meniscus tears in rabbit [124]

In rat and rabbit, studies have shown that the injected BMSCs [155, 157] can mobilize to the meniscus injured sites and potentially promote meniscus healing by generating ECM or differentiating into meniscus cells. However, free bodies of scar tissue were observed in the knee joint after 4 weeks injection in one study [157]. The number of injected BMSCs seemed to influence the repair of the tissue as the mobilization of BMSCs were observed at meniscus injury sites using  $1 \times 10^7$  instead of  $1 \times 10^6$  cells [157]. Another study showed that injected human BMSCs adhere to defect sites and enhanced the regeneration of rat meniscus by the upregulation of type II collagen expression by Indian hedgehog pathway [135].

### **1.5.2.3 Synovial membrane-derived mesenchymal stem cells (SMSCs)**

*In vitro* studies showed that SMSCs had higher proliferation rates, colony-forming potential and chondrogenic differentiation capacity compared to BMSCs [158-161]. Co-

culture of porcine [162], rat [163] and human [164] SMSCs with meniscus fibrochondrocytes (MFCs) resulted in enhanced matrix formation, which are demonstrated by enhanced production of glycosaminoglycan and collagen.

Animal studies showed that injection of SMSCs can also adhere to meniscus tears or defects induced by punch and meniscectomy, which promote meniscus healing and regeneration by differentiating into meniscus cells in rats, rabbits, and pigs [126, 131, 159, 165]. On the other hand, a study has shown that implantation of cell aggregates of SMSCs better promoted the meniscus regeneration compared to the injection of same number of cells [166]. This study also showed that SMSCs can be better maintained in the form of aggregate than suspension.

In large animal model (miniature pig), SMSCs derived scaffold-free cell/matrix construct seemed to promote meniscus regeneration after meniscectomy and protect the articular cartilage compared to untreated group [132]. However, no proteoglycan deposition based on safranin-O staining can be detected in the repaired tissues. Multiple injection of SMSCs (3 times, two weeks interval, follow-up for 16 weeks) to regenerate dissected meniscus were also reported in pig model (Mexican hairless pig) [137]. The regenerated matrix was safranin-O positive and contained type I/II collagen, which was more than that in the no-cell injected group. In miniature pig with longitudinal meniscus tears, injected SMSCs promote healing of the tissue with better tensile strength than no-cells group [126]. The combination of SMSCs with autologous Achilles tendon grafts and

PCL scaffold (no pre-chondrogenic culture) was also reported to promote meniscus regeneration [167]. In an aged primate model which is more genetically close to human, implantation of autologous SMSCs derived cell pellets improved regeneration of meniscus and delay the degeneration of articular cartilage compared to untreated group [168].

#### **1.5.2.4 Adipose tissue derived MSCs (ASCs)**

There are studies showing that MSCs can be isolated from adipose tissue and with a focus on articular cartilage repair and regeneration [169]. An *in vitro* study showed that the MSCs isolated from extraarticular adipose tissue did not share a similar gene expression profile as those isolated from intraarticular tissue [170]. Mechanical stimulation (tension strain) has been shown to promote fibrogenic differentiation (production of type I collagen and version) of ASC (from liposuction adipose tissue) [171]. Another MSCs population isolated from infrapatellar fat pad (IFP) was also tested and showed promising results. Human IFPMSCs were shown to produce meniscus-like tissue with higher mechanical properties and cell distribution than MFCs, BMSCs and SMSCs [172]. The phenotype of the porcine IFPMSCs was shown to be modulated by hydrogels functionalized by porcine meniscus-derived ECM [173]. Inner meniscus ECM promoted a more chondrogenic phenotype of IFPMSCs than the outer meniscus ECM in this study. Adesida *et al.* [174] showed that co-culture of human IFPMSCs with MFCs can significantly enhanced ECM formation. When cultured under simulated microgravity,

the enhanced production of ECM is accompanied with hypertrophic differentiation.

Human IFPMSCs-seeded hydrogel preloaded with TGF $\beta$ 3 also promoted healing of bovine radial meniscus tears in an *in vitro* explant model [175].

ASCs promoted healing and regeneration of longitudinal meniscus tears and meniscus defects induced by partially meniscectomy in rabbit [125, 176]. The implanted ASCs were shown to differentiate into MFCs in the repaired tissues [125, 176]. The application of ASCs-seeded polymeric constructs was tested in the total meniscectomy model (rabbit). However, the quantity and quality of the regenerated tissue were inferior to articular chondrocytes (AC) or ASCs/ACs-seeded constructs after 6 months' implantation [177]. In large animal model horse, autologous ASCs-seed collagen constructs promote similar regeneration of meniscus defects compared to BMSCs [138]. However, no preclinical studies have used the IFPMSCs.

#### **1.5.2.5 Meniscus derived MSCs (MMSCs)**

Currently, the MSCs or progenitor cells isolated from meniscus has been reported and showed promising results for meniscus tissue engineering. *In vitro* studies showed human MMSCs are multipotential and have surface markers typical of MSCs [170]. The *in vitro* monolayer culture human MMSCs from passage 0 shared similar gene expression profiles of the MSCs isolated from intraarticular tissues: synovial membrane, anterior cruciate ligament and articular chondrocytes, not the extraarticular tissue like muscle, bone marrow and adipose tissues. CD34 and CD146 positive MMSCs isolated from the

vascular region of human fetal menisci showed enhanced multipotential differentiation capacity than those isolated from the inner regions [105]. Human MMSCs had higher clonogenicity and expressed higher mRNA levels of type II collagen than BMSC and SMSCs [106]. Ding, *et al* [104] further demonstrated the superiority of MMSCs compared to BMSCs for meniscus repair by showing that rabbit MMSCs had higher chondrogenic capacity while BMSCs are more towards an osteogenic phenotype *in vitro* and after subcutaneous implantation in the nude rat. Better healing of a rabbit meniscus defects (1 mm in diameter) *ex vivo* after direct seeding of MMSCs compared to BMSCs.

An *in vivo* study has shown that human fetal MMSCs promote healing of meniscus tears in nude rats by adhering to the tear sites [105]. In rabbit model with partially meniscectomy, the injection of allogenic expanded MMSCs promote meniscus regeneration and protected the articular cartilage and the joint spaces after 12 weeks [107]. The same group further showed that the migration of injected human MMSCs to promote meniscus regeneration in a rat model (partially meniscectomy) is mediated by SDF-1/CXCR4 axis [106]. The injected human MMSCs also seemed to reduce the degeneration of articular cartilage at 12 weeks.

#### **1.5.2.6 Synovial fluid derived MSCs (SFMSCs)**

SFMSCs isolated from the knee joint may be another promising cell source for meniscus tissue engineering. Studies have shown that the SFMSCs existed in the human synovial fluid of knee joint suffered of rheumatoid arthritis (RA), osteoarthritis (OA), intraarticular

ligament and meniscus injury [178-181], suggesting the possible responsive roles in the injury and degeneration of knee joint. These SFMSCs were shown to be clonogenic and multipotent with the expression of cell surface marker like BMSCs [178]. However, other studies showed that their phenotype were more similar to SMSCs than BMSC [180, 181].

The advantage of SFMSCs was their commitment for the chondrogenic differentiation. Bovine and equine SFMSCs exhibited more consistent chondrogenesis [179, 182], but less osteogenic differentiation than donor-matched BMSCs [179]. Ando *et al.* [183] showed that porcine SFMSCs showed similar chondrogenic differentiation capacity to SMSCs but better than BMSCs. More importantly, SFMSCs had least osteogenic potential compared to SMSCs and BMSCs. Lee *et al.* [184] showed that the proliferation rates of porcine SF-MSC in P2 were higher than BMSCs after 14 days monolayer culture. Similar results of higher chondrogenic but less osteogenic potential of SFMSCs than BMSCs was reported in this study. When compared to IFPMSCs, human donor matched SFMSCs proliferated less but with similar chondrogenic and less osteogenic potential [185]. It should be noted that the medical condition of the knee joint where the synovial fluid from was shown to influence the chondrogenic differentiation of SFMSCs [186]. The human SFMSCs isolated from healthy knee joint (cadavers) can undergo sufficient chondrogenesis without the micro-mass culture condition while SFMSCs from OA knee joint required this step. The supplementation of growth factor FGF2 (500 ng/mL) during the monolayer expansion of equine SFMSCs was also shown

to promote proliferation rates [187]. However, the post-expansion chondrogenesis of SFMSC was not enhanced in this study. On the other hand, the effect of low oxygen tensions during chondrogenic differentiation of human SFMSCs was tested [188]. Even though low oxygen tension (5% O<sub>2</sub>) can significantly increase the chondrogenic-related gene expressions, the synthesis of matrix was not enhanced in a collagen scaffold model after 28 days culture *in vitro*.

Only one *in vivo* study in rabbit with radial meniscus tears showed that the magnesium may recruited the endogenous stem cells from the synovial fluid and promote the meniscus healing [189].

## **1.6 Clinical studies using MSCs**

Several studies have been performed and showed the potential application of MSCs for the meniscus regeneration in human knee joint. MSCs isolated from bone marrow [21, 190, 191], synovial membrane [192], and adipose tissue [193, 194] were tested.

Most of the studies used intra-articular injection as a deliver method of MSCs except one study using implanted MSCs-seeded type I collagen constructs for healing of the meniscus tears. Injection of BMSCs was performed in 2 studies. Centeno *et al.* [190] injected autologous BMSCs in 1 patient with multiple knee injuries. Decreased knee pain, improved knee motions with increased meniscus volume under MRI was reported after 24 weeks. However, dexamethasone was also injected after application of BMSCs in this study. Vangsness *et al.* [21] injected allogenic BMSCs in 55 patients after partially

meniscectomy within 7-10 days. Only 3 out of 35 patients showed an increased volume greater than 15% after 2 years while no patients in the control group reached this criterion. This study showed the significant pain reduction in patients with osteoarthritis changes at the time of injection compared to non-injected groups. Safety of using MSCs in the human knee joint was proved regarding the adverse effects and ectopic tissue formation in this study. Autologous BMSCs seeded type I collagen constructs was implanted in 5 patients with medial avascular meniscus tears by Whitehouse *et al.*[191]. No meniscus displacement, signal of tears decreased over time and improved knee functional scores were reported in 3 patients after 2 years while the constructs failed in 2 patients.

Injection of autologous ASCs isolate from abdominal adipose tissues were reported in two studies [193, 194]. Pak *et al.*[193] first injected a mixture of ASCs, platelet-rich plasma (PRP), hyaluronic acid (HA) and dexamethasone in the 2 patients with knee pain and reduced sizes of meniscus due to osteoarthritis. Then the patients received 4 more injection of PRP, HA and dexamethasone weekly. Improvement of knee pain, motion and significant increase of meniscus thickness under MRI were reported after 12 weeks compared to previous multiple injection of HA and dexamethasone without the use of ASCs. Pak *et al.* [194] further injected the mixture of ASCs, PRP and HA into the knee joint of 1 patient with meniscus tears. The patient received the 4 more injections of PRP and HA with dexamethasone used in the third injection. Improved of symptoms and

complete absences of meniscus tears under MRI was reported.

A case report (5 patients) using the injection of autologous SMSCs onto the repaired meniscus with complex degenerative tears showed improved clinical scores after 2 years. The meniscus tears were not distinguishable under MRI. Human serum was used in this study during *in vitro* expansion of SMSCs while other study mentioned above used animal serum. However, no control groups without injection of SMSCs and a second examination using arthroscopy were included in this study.

### **1.7 Thesis development and objectives**

Due to the unique biochemical composition, conformation and vascular distribution of meniscus, the healing capacities are limited, and current treatment methods results in various outcomes. Meniscus tissue engineering studies have provided the possibilities to improve the healing or regeneration process and the properties of engineered tissue resemble native tissue. Human MFCs and SFMSCs seems to be more promising in producing meniscus-like ECM formation without hypertrophic differentiation tendency compared to other cell sources. However, majority of these studies are in experimental stages and no clinical studies have been performed using these two cell types. Further studies to optimize the formation and development of meniscus-like ECM are needed prior to clinical translation.

In this thesis, several *in vitro* and *in vivo* experiments were performed to:

1. Chapter 2:

- a) identify the appropriate population doublings of human MFCs expanded using TGF- $\beta$ 1 and FGF-2 (T1F2) that can retain the functional meniscus-like ECM-forming capacity
- b) investigate the effect of oxygen tensions ((normoxia 21% O<sub>2</sub>, hypoxia 3% O<sub>2</sub>) matrix-forming phenotype of T1F2-expanded MFCs during chondrogenic culture
- c) investigate the osteogenic and adipogenic differentiation potential of T1F2 expanded MFCs under different oxygen tensions.

## 2. Chapter 3:

- a) evaluate the capacity of human T1F2-expanded MFCs to attach, populate, and re-differentiate upon human meniscus-derived DCM in both a non-chondrogenic and chondrogenic environment (TGF- $\beta$ 3)
- b) evaluate the capacity or potential of human meniscus-derived DCM to induce chondrogenesis of human MFCs without hypertrophic differentiation in growth factor-free conditions under hypoxia

## 3. Chapter 4:

- a) determine the effects of transient and continuous exposure to TGF- $\beta$ 3 supplementation under HYP and NRX over a long-term *in vitro* culture period on meniscus-like ECM formation of human MFCs on a clinically approved and commercially available collagen scaffold
- b) assess *in vivo* behavior within the subcutaneous nude mouse model after 3-weeks of *in vitro* pre-culture with TGF- $\beta$ 3 supplementation under HYP and NRX regarding

degradation, hypertrophic differentiation, calcification, and vascularization.

4. Chapter 5:

a) investigate whether human meniscus DCM has the capacity to induce differentiation of synovial fluid-derived mesenchymal stem cells (SFMSCs) towards an MFC phenotype.

b) investigate the potential roles of transforming growth factor beta-3 (TGF- $\beta$ 3) and insulin-like growth factor 1 (IGF-1) in the differentiation of SFMSCs towards an MFC phenotype

5. Chapter 6:

a) investigate the effects of HYP (2% O<sub>2</sub>) relative to normoxia (NRX, ~20% O<sub>2</sub>) during pre-culture of hSF-MSCs in porous collagen scaffolds on IM-ECM formation and accumulation of angiogenic factors VEGF and SDF-1

b) investigate the *in vivo* stability in terms of ECM maintenance and calcification as well as the vascularization tendencies of SFMSC-based IM-ECM in the subcutaneous nude mouse model after HYP and NRX pre-culture

## Outline of the Study

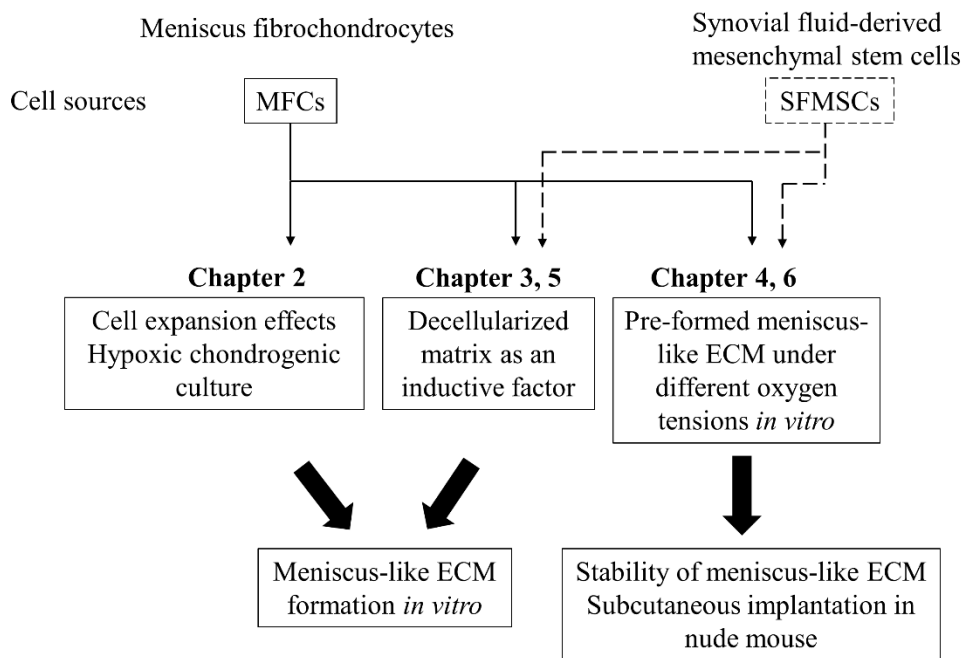


**Figure 1-1:** Outline of the study

## **Chapter 2 Plasticity of human meniscus fibrochondrocytes: a study on effects of mitotic divisions and oxygen tension**

**Yan Liang, Enaam Idrees, Stephen H. J. Andrews, Kirolos Labib, Alexander Szojka, Melanie Kunze, Andrea D. Burbank, Aillette Mulet-Sierra, Nadr M. Jomha, and Adetola B. Adesida**

This chapter has been published in part in Scientific Reports:

Yan Liang, Enaam Idrees, Stephen H. J. Andrews, Kirolos Labib, Alexander Szojka, Melanie Kunze, Andrea D. Burbank, Aillette Mulet-Sierra, Nadr M. Jomha, and Adetola B. Adesida: **Plasticity of Human Meniscus Fibrochondrocytes: A Study on Effects of Mitotic Divisions and Oxygen Tension.** *Scientific Reports* 2017, 7(1): 12148

## 2.1 Introduction

Musculoskeletal diseases including osteoarthritis (OA) comprise an increasing proportion of the global burden of disease; in 2015, they were estimated to account for 6.7% of the global disability-adjusted life years, making them the fourth greatest burden on the health of the world's population (third in developed countries) [195]. It is estimated that the cumulative economic burden of OA in Canada from 2010 to 2015 was \$195 billion and annual costs are expected to rise in the future [8].

Symptomatic OA of the knee affects over 10% of adults over the age of 60 [196].

Injury to the knee menisci is a significant risk factor in the development of knee OA [197]. The knee menisci are load-bearing fibrocartilages positioned between the articular surfaces of the femoral condyle and tibial plateau. The menisci are integral to joint homeostasis by decreasing contact stresses [198], increasing stability [199] and aiding joint lubrication [200]. These complex functions are facilitated by the extracellular matrix (ECM), which is produced and maintained by a heterogenous population of cells in the menisci, the predominance of which are referred to as meniscus fibrochondrocytes (MFCs) [201]. This family of ECM molecules include an abundance of type I collagen throughout the meniscus, with substantial amounts of type II collagen and aggrecan in the avascular region [202-204]. The inner two-thirds of meniscus are colloquially termed the “white zone” because that area is avascular, receiving nutrients mainly by diffusion [6, 7]. The avascular nature of this region combined with the severe loading within the knee

joint inhibits its ability to repair. Current treatments for damaged avascular menisci have poor long-term outcomes with limited reduction in the incidence of OA progression[205].

Due to the unsatisfactory outcomes of current treatments, cell-based tissue engineering (TE) strategies have been an area of interest for meniscus repair or replacement [206]. Meniscus TE aims to recreate meniscus-like tissue to replace damaged tissues after injury and restore normal function. Cell source is an important consideration for meniscus TE. The cell sources may include MFCs, articular chondrocytes, and precursor cells such as mesenchymal stem cells (MSCs). Previous research predominantly focused on articular chondrocytes [94, 207] and MSCs derived from bone marrow [208], synovium [209], and adipose tissue [210]. However, current work focuses on MFCs as a preferred cell source for two main reasons. First, they are derived from native meniscus tissue and are conditioned to synthesize the functional ECM of meniscus [201]. Second, when compared to the most commonly-used bone marrow-derived MSCs, MFCs were reported to have better fibrochondrogenic differentiation potential [104, 106] and form thicker collagen fibres and orientations resembling native meniscus [153]. MFCs were also demonstrated to have less tendency to form bone precursors through hypertrophic differentiation *in vitro* [106] and calcify *in vivo* [121]. However, acquiring sufficient numbers of MFCs from surgically removed tissues to develop a TE meniscus replacement remains a major challenge. MFCs reside in a dense ECM *in situ* and account for only about 0.1-0.12% of the wet weight of normal

meniscus [211]. Limited cell numbers are available to be isolated from meniscus tissue after partial meniscectomy, necessitating *in vitro* monolayer cell expansion [12].

However, MFCs were found to dedifferentiate and lose their matrix-forming phenotype after serial cell passaging [12, 96, 212, 213]. Increased population doublings (PD) of MFCs resulted in significant downregulation of mRNA expression levels of type II collagen and aggrecan, with an increased gene expression of type I collagen [96, 212]. Expanded MFCs were also shown to display trilineage differentiation plasticity [104].

The combination of transforming growth factor  $\beta$ 1 (TGF $\beta$ 1) and fibroblast growth factor-2 (FGF-2) for cell expansion has been shown to promote proliferation rates of periosteal cells [214] and human articular chondrocytes [215, 216]. Furthermore, after expansion in TGF $\beta$ 1 and FGF-2 both periosteal cells and articular chondrocytes demonstrated enhanced chondrogenic differentiation and restoration of the matrix-forming capacity, respectively. Moreover, oxygen tension was shown to improve matrix-forming phenotype of expanded MFCs especially after expansion with FGF-2 [14]. Our previous work [11] has shown that the hypoxia (5% O<sub>2</sub>) could also be beneficial for MFC proliferation and upregulation of the expression of collagen II and aggrecan in expanded MFCs with the use of FGF-2. However, little is known about the effect of combined TGF $\beta$ 1 and FGF-2 (T1F2) on MFC proliferation and subsequent redifferentiation capacity under different oxygen tensions.

To this end, our objectives were to characterize the maximal population doublings

(PD) for T1F2-expanded MFCs while retaining their functional matrix-forming capacity.

The effect of oxygen tension (normoxia 21% O<sub>2</sub>, hypoxia 3% O<sub>2</sub>) on chondrogenic differentiation and matrix-forming phenotype of T1F2-expanded MFCs was also tested.

We also characterized the adipogenic and osteogenic differentiation potential of these T1F2-expanded MFCs.

## **2.2 Methods**

### **2.2.1 Ethics statement**

Experimental methods and tissue collection were with the approval of and in accordance the University of Alberta's Health Research Ethics Board- Biomedical Panel (Study ID: Pro00018778). Ethics Board waived the need for written informed consent of patients, as specimens used in the study were intended for discard in the normal course of the surgical procedure. Extensive precautions were taken to preserve the privacy of the participants donating specimens.

### **2.2.2 Isolation and expansion of human meniscus fibrochondrocytes (MFCs)**

Fresh meniscus specimens were obtained from six male patients undergoing partial meniscectomy for acute traumatic injuries (ages 20-37, mean age  $28 \pm 6$  years). Wet weights of meniscus tissue were recorded before collagenase mediated digestion for MFC isolation. MFCs were released via treatment with trypsin-EDTA (0.05% w/v; Corning, Mediatech Inc. VA, USA) at 37°C for 1 hour followed by 22 hours at 37°C in type II collagenase (0.15% w/v; 300 U/mg solid; Worthington, NJ, USA) in a high glucose

Dulbecco's modified Eagle's medium (DMEM; 4.5 mg/mL D-Glucose) supplemented with 5% v/v fetal bovine serum (FBS) (all from Sigma-Aldrich Co., MO, USA). The cell suspension obtained after digestion was passed through a 100  $\mu$ m nylon-mesh filter (Falcon, BD Bioscience, NJ, USA). Isolated cells were plated at  $10^4$  cells/cm<sup>2</sup> and cultured in a standard medium: high glucose DMEM supplemented with 10% FBS (Sigma-Aldrich), 100 U/mL penicillin, 100  $\mu$ g/mL streptomycin, 2 mM L-glutamine, and 10mM 4-(2-hydroxyethyl)-1-piperazineethanesulfonic acid (HEPES) (Sigma-Aldrich) (all others from Life Technologies, ON, Canada) for 48 hours under normal oxygen tension (~21% O<sub>2</sub>; 5% CO<sub>2</sub>/95% air) at 37°C in a humidified incubator. After 48 hours (passage 0), non-adherent cells were aspirate and adherent primary cells were detached with trypsin-EDTA (0.05% w/v). Thereafter the number of viable MFCs were counted using a haemocytometer after trypan blue staining. MFCs were plated at  $10^4$  cells/cm<sup>2</sup> and cultured in the standard medium described above supplemented with FGF-2 (5 ng/mL; Neuromics, MN, USA, Catalog#: PR80001) and TGF $\beta$ 1 (1 ng/mL; ProSpec, NJ, USA, Catalog#: cyt-716) under normal oxygen tension (21% O<sub>2</sub>) at 37°C in a humidified incubator, as previously described [11, 14]. When cells were 80-85% confluent, first-passage (P1) cells were detached with trypsin-EDTA and culture was continued at  $10^4$  cells/cm<sup>2</sup> to produce second passage (P2), third passage (P3) and fourth passage (P4) cells. MFCs at the end of each passage were counted and population doublings during exponential growth phase were calculated as  $\log_2(N/N_0)$ , where  $N_0$  is the number of cells

plated at the beginning of a passage and N is the number of cells counted at the end of a passage [217].

### **2.2.3 Mitotic effects on MFC chondrogenic differentiation potential**

Chondrogenic differentiation was performed by using a three-dimensional cell pellet culture model. At the end of each passage,  $5 \times 10^5$  of MFCs were centrifuged at 1500 rpm for 5 minutes to make pellets in 1.5 mL sterile conical microtubes with removable screw-type lids (Bio Basic Inc, Ontario, Canada). For each condition (i.e. for each passage, oxygen tension, and donor) six identical pellets were set up to provide two technical replicates for biochemical, histological and gene expression analysis. The pellets were then cultured in 0.5 mL of serum-free chondrogenic medium consisting of high glucose DMEM (Sigma-Aldrich) containing 100 units/mL penicillin, 100  $\mu\text{g/mL}$  streptomycin, 2 mM L-glutamine, 10 mM HEPES (Sigma-Aldrich) (all others from Life Technologies), ITS+1 premix (Corning, Discovery Labware, Inc., MA, USA), 10 ng/mL transforming growth factor  $\beta 3$  (TGF $\beta 3$ ; ProSpec, NJ, USA, Catalog#: cyt-113), 100 nM dexamethasone, 365  $\mu\text{g/mL}$  ascorbic acid 2-phosphate, 125  $\mu\text{g/mL}$  human serum albumin and 40  $\mu\text{g/mL}$  L-proline (all from Sigma-Aldrich) under normal oxygen (NRX; 21% O<sub>2</sub>) or low oxygen tension (HYP; 3%) at 37°C in a humidified incubator with 5% CO<sub>2</sub> for 21 days, as previously described [13, 15]. Conical microtube lids were loosened to allow gas exchange during culture. At the same time,  $5 \times 10^5$  cells were suspended in 1 mL of Trizol (Life Technologies) as a control for monolayer culture gene expression. Medium changes

were performed twice per week in a normoxic environment and the pellets cultured in hypoxic conditions thus had a brief exposure to normoxic conditions (<5 minutes per media change). At the end of each culture stage, the wet weights of cell pellets were recorded and the pellets were assessed biochemically for glycosaminoglycan (GAG) and DNA content, histologically and immunofluorescence for cartilage-specific matrix proteins and by real time quantitative reverse transcription polymerase chain reaction (qRT-PCR) for gene expression analysis.

#### **2.2.4 Mitotic effects on MFC adipogenic differentiation potential**

At the end of P1, P2, and P3, adipogenesis was performed by plating  $5 \times 10^3$  MFCs/cm<sup>2</sup> from 4 donors in a six-well plate (Falcon, BD, NJ, USA) as previously described, [13] with three technical replicates for the induction group for each condition. Initially, MFCs were cultured in 3 mL of the standard medium supplemented with FGF-2 (5 ng/mL) and TGF $\beta$ 1 (1 ng/mL) until confluent in each well under NRX. Adipogenesis was then induced in hypoxic or normoxic conditions for three days by adding 3 mL of the standard medium supplemented with 1  $\mu$ M dexamethasone, 0.5 mL ITS+1, 100  $\mu$ M indomethacin, and 500  $\mu$ M isobutyl-1-methylxanthine (IBMX; Sigma-Aldrich) and then by culturing the cells in 3 mL of the standard medium supplemented with 0.5 mL ITS+1 for one day. This induction-culture cycle was repeated four times. Then, cells were cultured in 3 mL of the standard medium supplemented with 0.5 mL of ITS+1 only for another 7 days. At the end of 23 days' culture, the culture medium was removed and cells were collected by adding

1 mL of Trizol per well followed by total RNA extraction for gene expression by qRT-PCR analysis or fixed with 2 mL of 10% w/v buffered formalin (Anachemia Canada Co, QC, Canada) for 3 minutes, then stained with 3 mL of 0.3% w/v Oil Red O (Sigma-Aldrich) per well for 1 hour at room temperature. After Oil Red O was removed and the cells were washed with distilled water three times, the staining was examined immediately by taking pictures using an Eclipse Ti-S microscope (Nikon Canada, ON, Canada).

### **2.2.5 Mitotic effects on MFC osteogenic differentiation potential**

At the end of P1, P2, and P3, osteogenesis was performed by plating  $5 \times 10^3$  MFCs/cm<sup>2</sup> from 4 donors in a six-well plate (Falcon, BD, NJ, USA) as previously described, [13] with three technical replicates for the induction group for each condition. Briefly, MFCs were cultured in 3 mL of osteogenic medium consisting of the standard medium supplemented with 100  $\mu$ M ascorbic acid 2-phosphate, 10 nM dexamethasone, and 10 mM beta ( $\beta$ )-glycerophosphate (all from Sigma-Aldrich) for 21 days with medium changed twice per week. After 21 days' culture, culture medium was removed and cells were collected by adding 1 mL of Trizol per well, followed by total RNA extraction for gene expression by qRT-PCR analysis or fixed with 2 mL of 10% w/v buffered formalin for 10 minutes and stained with 1 mL of 1% w/v Alizarin Red S (Sigma Aldrich) (pH = 4.2) for 30 minutes at room temperature followed by washing with distilled water for 1 hour on an orbital shaker. The staining was examined immediately by taking pictures

using an Eclipse Ti-S microscope or preserved in 70% v/v glycerol (Fisher Scientific, NH, USA) at 4°C.

### **2.2.6 Histology for MFC chondrogenesis**

After 21 days of chondrogenic culture, pellets were removed from medium, fixed overnight in 10% v/v neutral buffered formalin at 4°C, dehydrated by serially-dipping into ethanol baths of increasing concentration and embedded in paraffin wax. 5 µm thick sections were cut and stained with 0.01% (w/v) Safranin-O and counterstained with 0.02% (w/v) fast green (Sigma-Aldrich) to reveal proteoglycan matrix deposition as described previously[14].

### **2.2.7 Biochemical analysis for MFC chondrogenesis**

After 21 days of chondrogenic culture, pellets were rinsed in 500 µL of phosphate buffered saline (Sigma-Aldrich) to remove residual medium and were then digested in 250 µL of proteinase K (1 mg/mL in 50 mM Tris with 1 mM EDTA, 1 mM iodoacetamide, and 10 mg/mL pepstatin A; all from Sigma-Aldrich) overnight at 57°C. The GAG content was measured spectrophotometrically after 1,9-dimethylmethylene blue binding using chondroitin sulfate as standard (Sigma-Aldrich) [218]. The DNA content was determined using the CyQuant cell proliferation assay Kit (Invitrogen, ON, Canada) with supplied bacteriophage λ DNA as standard.

### **2.2.8 Immunofluorescence for MFC chondrogenesis**

5 µm thick paraffin-embedded pellets were deparaffinized, rehydrated, and then treated

with protease XXV (AP-9006-005, Thermo Scientific) and hyaluronidase (H6254, Sigma-Aldrich). Sections were then incubated with primary antibody: rabbit anti-collagen I (CL50111AP-1, Cedarlane, ON, Canada), mouse anti-collagen II (II-II6B3, Developmental Studies Hybridoma Bank, IA, USA) using a 1:200 dilution and rabbit anti-collagen X (58632, Abcam, UK) using 1:100 dilution at 4°C overnight, followed by incubation with a goat anti-rabbit IgG (H&L Alexa Fluor 594, Abcam, UK) with a 1:200 dilution for collagen I, X and goat anti-mouse IgG (H&L Alexa Fluor 488, Abcam) with a 1:200 dilution for collagen II. Sections were then stained with DAPI (4', 6-diamidino-2-phenylindole, Cedarlane) and mounted with Glycerol and PBS (1:1 ratio). Immunofluorescence was visualized by an Eclipse Ti-S microscope (Nikon Canada, Mississauga, Canada).

### **2.2.9 Gene expression analysis of MFC trilineage differentiation**

Total RNA was extracted from cell suspensions for adipogenesis, osteogenesis, and monolayer controls as well as cell pellets after grinding with Molecular Grinding Resin (G-Biosciences, MO, USA) for chondrogenesis using Trizol (Life Technologies). To reduce changes of gene expression levels, cell suspensions and pellets were transferred into Trizol immediately when harvesting. Total RNA (100 ng) in a 40 µL reaction was reverse transcribed to cDNA by GoScript reverse transcriptase using 1 µg of oligo(Dt) primers (all from Promega Corporation, WI, USA). Reverse-transcription quantitative polymerase chain reaction was performed in a DNA Engine Opticon I Continuous

Fluorescence Detection System (Bio-RAD, CA, USA) using hot start Taq and SYBR Green detection (Eurogentec North America Inc, San Diego, CA, USA). Primers sequences were obtained from previously published work and purchased from Invitrogen (Table 2-1). mRNA expression levels for each primer set were normalized to the expression level of  $\beta$ -actin using the  $2^{-\text{ct}}$  method [219].

**Table 2-1:** Primer sequences used in quantitative polymerase chain reaction analysis

Genes	Forward	Reverse	GenBank accession
$\beta$ -actin ( <i>ACTB</i> )	AAGCCACCCAC TTCTCTCTAA	AATGCTATCACCTCC CCTGTGT	NM_00110 1.4
Aggrecan ( <i>ACAN</i> )	AGGGCGAGTGGA ATGATGTT	GGTGGCTGTGCCCTT TTAC	M55172
Collagen I ( <i>COL1A2</i> )	TTGCCCAAAGTTG TCCTCTTC T	AGCTTCTGTGGAACC ATG GAA	NM_00008 9
Collagen II ( <i>COL2A1</i> )	CTGCAAAATAAA ATCTCGGTGTT CT	GGGCATTTGACTCAC ACCAGT	NM_03315 0
Collagen X ( <i>COL10A1</i> )	GAAGTTATAATTT ACACTGAGGGTTT CAAA	GAGGCACAGCTTAA AAGTTTTAAACA	X60382
SRY-Box 9 ( <i>SOX9</i> )	GACTTCCGCGAC GTGGAC	GTTGGGCGGCAGGT ACTG	Z46629
Lipoprotein Lipase ( <i>LPL</i> )	TGTGGATGTGTAA ATGGAGCTTGT	CACATACAGTTAGCA CCACACATTTATAA	NM_00023 7
Alkaline phosphatase ( <i>ALPL</i> )	CCTGGCAGGGCT CACACT	AAACAGGAGAGTCG CTTCAGAGA	NM_00047 8
Peroxisome proliferative activated receptor, gamma ( <i>PPAR<math>\gamma</math></i> )	AAGCTGCTCCAG AAAATGACAGA	CGTCTTCTTGATCAC CTGCAGTA	NM_13871 2
Osteocalcin ( <i>OCN</i> )	AATCCGACTGTG ACGAGTTG	CCTAGACCGGGCCGT AGAAG	NM_19917 3
Runt related transcription factor 2 ( <i>RUNX2/CBFA1</i> )	GGAGTGGACGAG GCAAGAGTTT	AGCTTCTGTCTGTGC CTTCTGG	NM_00102 4630

### 2.2.10 Statistical analysis

Data are presented as mean  $\pm$  standard deviation. Statistical analyses were performed by SPSS version 23 (IBM, NY, USA) and Excel 2016 (Microsoft, WA, USA). Normality of data was assessed with Shapiro Wilk test. Levene's test was used to assess the equality of variance for variables before multiple comparisons. For cases with equal variances, different passage groups were compared using one-way analysis of variance (ANOVA)

with Tukey's multiple comparison *post hoc* tests within the same oxygen tension; otherwise a Kruskal-Wallis one-way ANOVA with pairwise comparisons was applied. For comparison between two oxygen tensions within the same passage, a Student's *t*-test was used. Significance was considered when  $p < 0.05$ . Pearson's correlation coefficient was determined to assess linear correlation between two variables.

## 2.3 Result

### 2.3.1 Cell yield and expansion

Meniscus tissues were obtained from 6 male donors (age: 20-37 years) undergoing partial meniscectomy for acute traumatic injury. Mean wet weight ( $\pm$  SD) of the meniscus tissue pre-digestion was  $2.70 \pm 0.87$  g and mean viable cell yield ( $\pm$  SD) after 48 hours of post collagenase isolation culture was  $3.14 \pm 1.46$  million cells/g of wet meniscus tissue.

Isolated MFCs were cultured in monolayer with T1F2 under normal oxygen tension (21% O<sub>2</sub>). The cell morphologies were elongated fibroblast-like and small round-shaped chondrocyte-like during these 48 hours. After one week of monolayer culture with T1F2, the morphology of the cells became universally elongated and spindle-like. Mean population doublings (PD) per day ( $\pm$  SD) was  $0.49 \pm 0.07$  at P1,  $0.42 \pm 0.04$  at P2,  $0.49 \pm 0.06$  at P3, decreasing to  $0.32 \pm 0.04$  at P4. While P1-P3 were not significantly different from each other, P4 was significantly lower than each of the previous three passages (P1-P3 vs. P4 all  $p < 0.05$ ) (Fig.2-1A). The mean cumulative PD in monolayer culture ( $\pm$  SD) increased from  $2.91 \pm 0.41$  at P1,  $6.30 \pm 0.57$  at P2,  $9.76 \pm 0.96$  at P3, and  $12.89 \pm 0.81$  at

P4 (Fig.2-1B).

### 2.3.2 Wet weights

At the end of each passage,  $5 \times 10^5$  MFCs were centrifuged into pellets for culture in a defined serum-free chondrogenic media containing TGF $\beta$ 3. After 21 days of culture in normoxia (NRX, 21% O<sub>2</sub>) and hypoxia (HYP, 3% O<sub>2</sub>), wet weights of pellets were recorded as an indicator of ECM production (Fig.2-1C). HYP resulted in increased wet weights when compared to NRX within each passage. While this difference was not significant in P1 ( $p=0.145$ ), it increased and became significant in P2 ( $p=0.009$ ), P3 ( $p=0.006$ ) and P4 ( $p=0.037$ ). The effect of passaging on wet weight was variable. A significant decrease was observed between P1 and P3 or P2 and P3 in both NRX and HYP ( $p<0.05$ ). However, this difference was not significant between P1 and P4 or P2 and P4 for both conditions ( $p>0.05$ ). There was a moderate-to-weak, but significant negative correlation (HYP:  $R^2 = 0.34$ , adjusted  $p<0.05$ , NRX:  $R^2 = 0.26$ , adjusted  $p<0.05$ ) between wet weight and donor age when all passages were grouped. Interestingly, the correlation between age and wet weight when each passage was analyzed separately was stronger but not significant as passage increased for both HYP and NRX (i.e. HYP, P1:  $R^2 = 0.20$ , P2:  $R^2 = 0.35$ , P3:  $R^2 = 0.56$ , P4:  $R^2 = 0.69$ ).

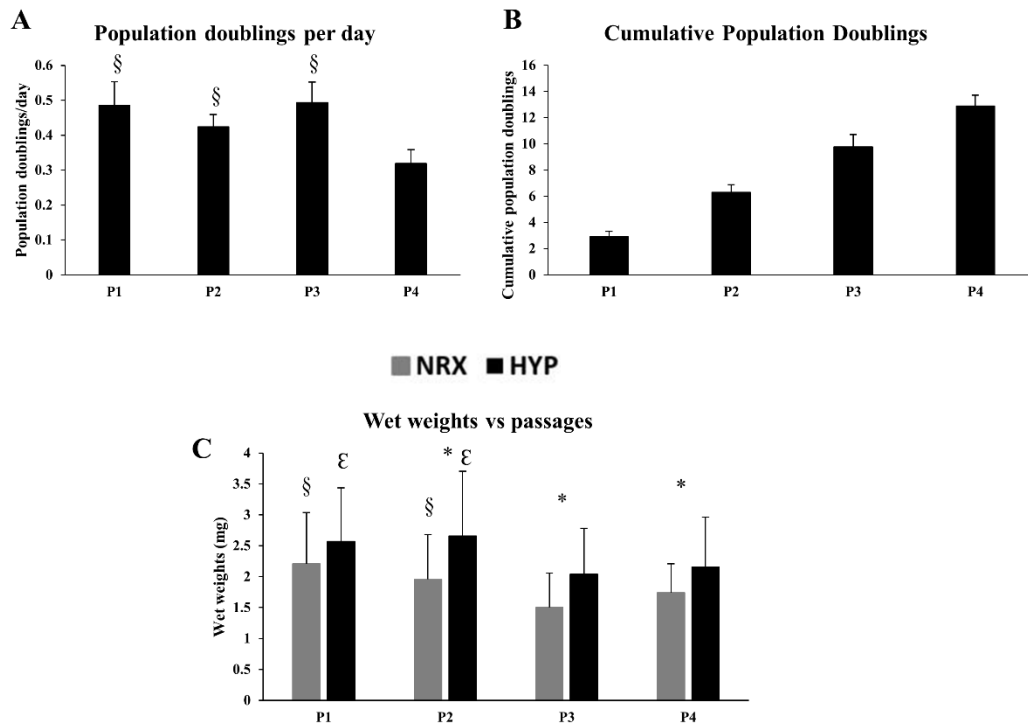


**Figure 2-1:** Isolation/expansion of meniscus fibrochondrocytes (MFCs) with TGF $\beta$ 1 and FGF-2 (T1F2) for four passages under normoxia (NRX). (A) Population doublings per day (n=6). Statistical analysis is presented as follows: § significance between P1-P3 and P4 in NRX ( $p < 0.05$ ). P: passage; (B) Cumulative population doublings at each passage during expansion of MFCs (n=6). (C) Wet weights of pellets derived from T1F2-expanded MFCs of four passages after 21 days chondrogenic stimulation under normoxia or hypoxia (HYP) (n=6). Statistical analysis is presented as: §significance between P1/P2 and P3 in NRX,  $\epsilon$  significance between P1/P2 and P3 in HYP, \* significance between NRX and HYP within the same passage ( $p < 0.05$ ). Data all presented as mean  $\pm$  standard deviation.

### 2.3.3 Biochemical analysis

Biochemical analysis was performed to assess the glycosaminoglycan (GAG) and DNA contents in pellets after 21 days of culture in chondrogenic medium under NRX and HYP. GAG content was dramatically higher in P1 relative to subsequent passages in both oxygen tensions (Fig.2-2A). It decreased significantly between P1 and P2-P4; with GAG content at P1 approximately double that of P2 ( $p=0.004$  NRX,  $p=0.013$  HYP) and highly significant when compared to P3 and P4 (all  $p<0.001$ ). A significant decrease was also observed between P2 and P4 in HYP only ( $p=0.04$ ). No other significant differences were observed in GAG content between passages. When GAG content was normalized to cellular DNA content (GAG/DNA), it followed the same trend (Fig.2-2C). GAG/DNA decreased significantly between P1 and P2-P4 in both oxygen tensions; P1 was almost double when compared to P2 ( $p<0.001$  NRX,  $p=0.0001$  HYP), P3 ( $p=0.001$  NRX,  $p<0.001$  HYP) and P4 (NRX/HYP, all  $p<0.001$ ). There were no significant differences in GAG/DNA between P2-P4 under both oxygen tensions. Although there was a significant difference in DNA content in P2 compared to P4 in HYP, no other significant differences were found in DNA content within passages between oxygen tensions or between passages (Fig.2-2B). No significant differences were found in GAG content or GAG/DNA between oxygen tensions within the same passage (Fig.2-2A, C).

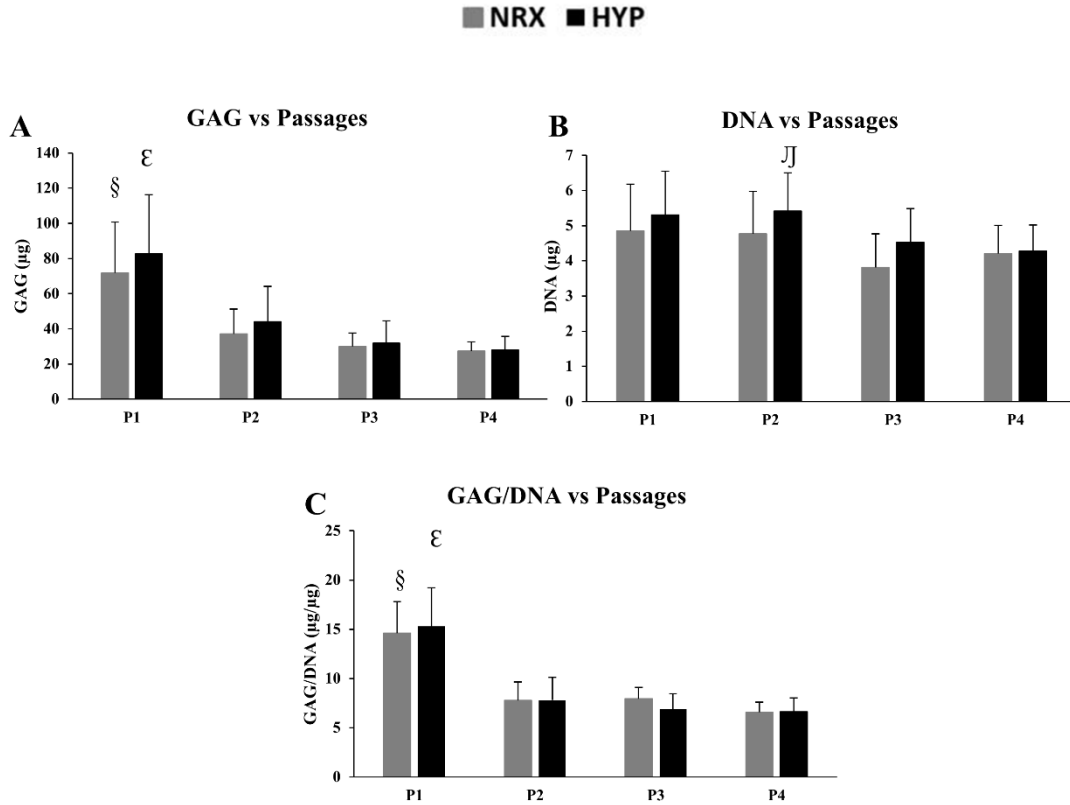


**Figure 2-2:** Biochemical analysis of pellets derived from T1F2-expanded MFCs of four passages after 21 days chondrogenic stimulation under NRX or HYP (n=6). (A) GAG content, (B) DNA content and (C) GAG/DNA in pellets. Statistical analysis is presented as follows: §significance between P1 and P2-P4 in NRX,  $\epsilon$  significance between P1 and P2-P4 in HYP,  $^{JJ}$  significance between P2 and P4 in HYP ( $p < 0.05$ ). Data all presented as mean  $\pm$  standard deviation.

### 2.3.4 Safranin-O staining

After 21 days of culture in chondrogenic media, pellets from 4 passages were embedded, cut and stained with Safranin-O for proteoglycan deposition (pink/red staining). One representative donor (male, age 20) is presented in figures below. In both oxygen

tensions, Safranin-O positive proteoglycan (pink staining) was most intense in P1, sharply decreasing in P2, and gradually decreasing to faint staining in P4. Chondrocyte-like (i.e. rounded) cells were in the lacunae-like structures in P1, but became progressively interspersed with fibroblast-like (i.e. elongated) cells from P2-P4 with loss of lacunae (Fig.2-3).

Within P1 and P2, no qualitative differences were observed between oxygen tensions (Fig.2-3A, B vs E, F). However, it appears HYP resulted in qualitatively more Safranin-O staining in P3 and P4 (Fig.2-3G, H vs C, D). More chondrocyte-like cells in P3 were observed in HYP compared to NRX. Additionally, although pellets were cut to approximately the same depths, pellet diameter was qualitatively larger in HYP compared to NRX within the same passage, which is consistent with the differences in wet weights between oxygen tensions (Fig.2-1C). Although proteoglycan production in HYP appeared to be retained in P3-P4 as compared to NRX qualitatively (pink staining under Safranin-O), quantitative analysis did not show significant differences to support this observation (Total GAG and GAG/DNA; Fig.2-2A, C).

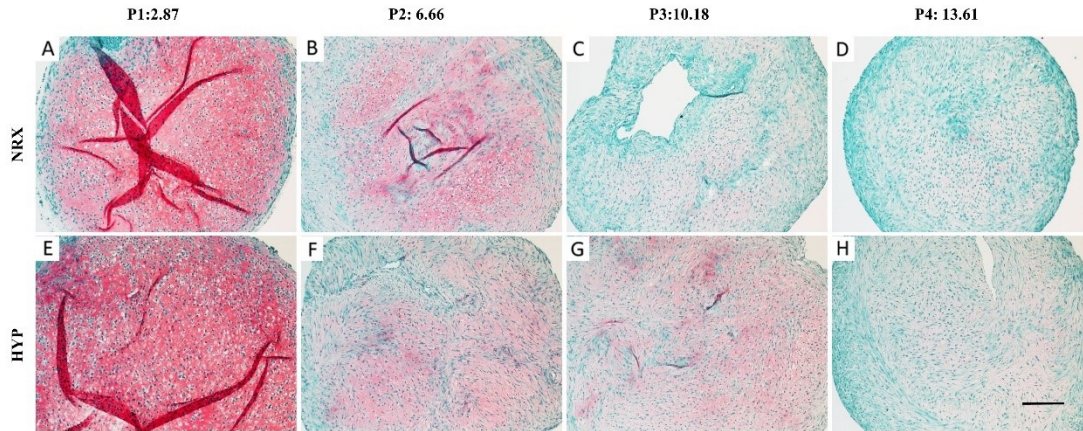


**Figure 2-3:** Safranin-O staining analysis for proteoglycan deposition in pellets derived from T1F2-expanded MFCs of four passages after 21 days chondrogenic stimulation under NRX or HYP from one representative donor (male, 20 years old). (A-D) Pellets cultured under NRX, (E-H) Pellets cultured under HYP. The top panel of numbers indicate population doublings of each passage. Scale bar: 200  $\mu$ m

### 2.3.5 Immunofluorescence

Indirect immunofluorescence was performed to detect cells (DAPI), extracellular matrix components using primary antibodies to collagen I and collagen II (Fig.2-4) and the hypertrophic chondrogenic differentiation marker, collagen X (Fig.2-5).

Chondrogenically differentiated pellets ( $2.5 \times 10^5$ ) of human bone marrow derived-mesenchymal stem cells (hBM-MSCs) under NRX served as a positive control for collagen X. Qualitatively, MFCs visualized via DAPI were evenly distributed throughout the pellets across all passages under both oxygen tensions. Collagen I was homogeneously distributed across passages. In contrast, collagen II immunofluorescence

was most intense in P1 and then decreased in P2 in both oxygen tensions. Type II collagen immunofluorescence was only positive in HYP at P3 with ~ 10PDs but negative at P4 with ~ 13PDs with negligible presence in P3-P4 in both oxygen tensions. Collagen II immunofluorescence results corresponded well with Safranin-O staining for proteoglycan content. Negligible deposition of collagen X was observed by immunofluorescence in pellets derived from T1F2-expanded MFCs when compared to the pellets derived from hBM-MSCs (Fig.2-5). Only punctate pericellular fluorescence was observed in MFC pellets compared to the diffuse fibrillar signal from the positive control hBM-MSC pellets.

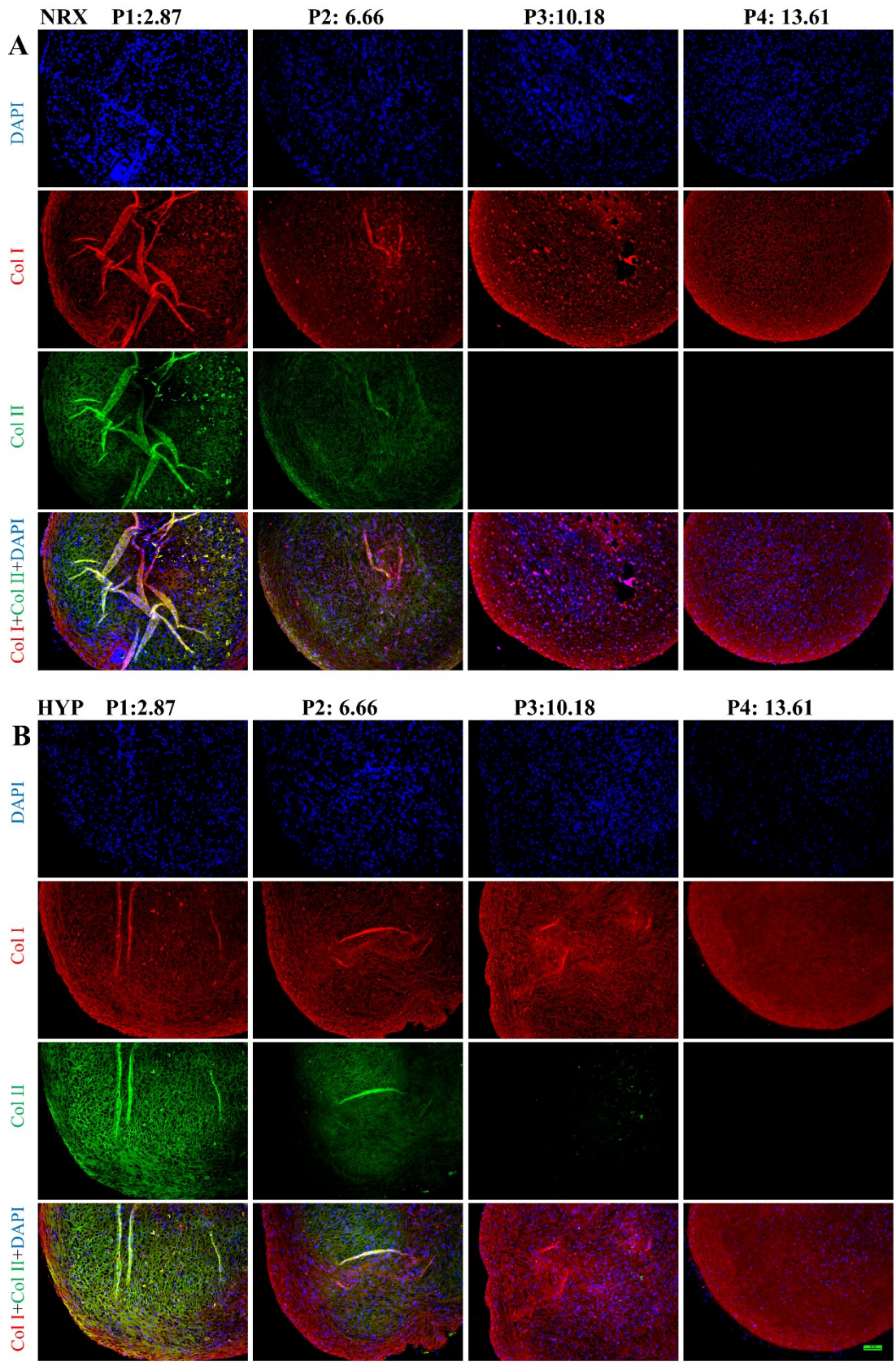


**Figure 2-4:** Immunofluorescence analysis of collagen I and collagen II in pellets derived from T1F2-expanded MFCs of four passages after 21 days chondrogenic stimulation under NRX or HYP from one representative donor (male, 20 years old). Blue (DAPI): cells, Red (Texas Red): collagen I, Green (FITC): collagen II. (A) Pellets cultured under NRX, (B) Pellets cultured under HYP from four passages. Scale bar: 100  $\mu$ m

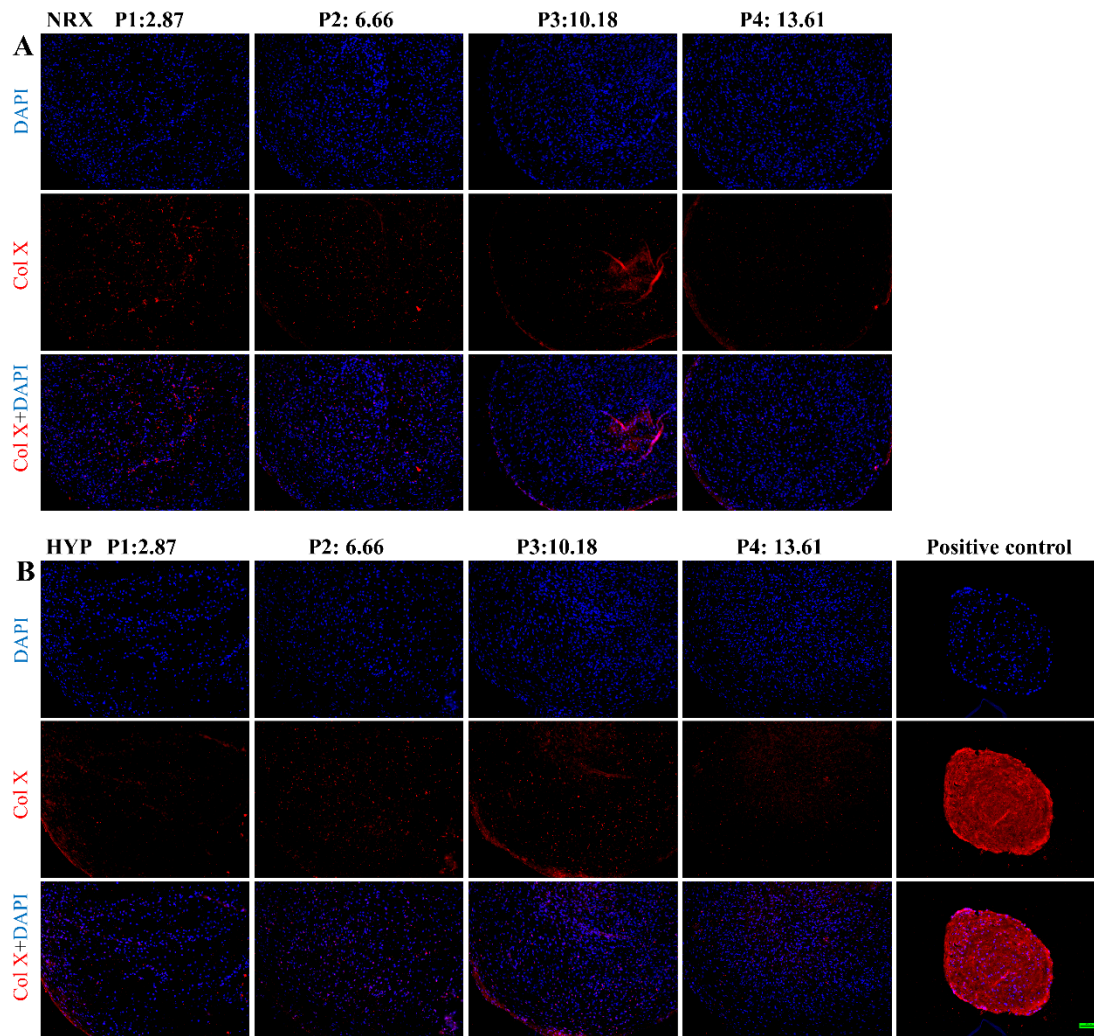


**Figure 2-5:** Immunofluorescence analysis of hypertrophic marker collagen X in pellets derived from T1F2-expanded MFCs of four passages after 21 days chondrogenic

stimulation under NRX or HYP from one representative donor (male, 20 years old). Blue (DAPI): cells, Red (Texas Red): collagen X. (A) Pellets cultured under NRX, (B) Pellets cultured under HYP from four passages. Positive control: pellets from human bone marrow-derived mesenchymal stem cells cultured with the same chondrogenic medium under normoxic condition. Scale bar: 100  $\mu$ m.

### 2.3.6 Gene expression analysis

#### 2.3.6.1 Chondrogenesis

To further characterize the ECM generated in pellets, gene expression was assessed by qRT-PCR after 21 days of chondrogenic culture under NRX or HYP. Additionally, similar gene expression analysis was conducted for monolayer cultured MFCs prior to centrifugation into pellets. The mean relative gene expression levels of aggrecan (*ACAN*), collagen I (*COL1A2*), collagen II (*COL2A1*), collagen X (*COL10A1*) and *SOX9* is presented in Fig.2-6. In monolayer cultured MFCs with T1F2 (Fig.2-6A), the overall trend for *ACAN* and *COL1A2* tended to decrease after P2 and *COL2A1* seemed to decrease from P1. The increased PD had no significant effects on gene expression levels of *ACAN*, *COL1A2*, *COL2A1* and *SOX9*. The relative gene expression level of *COL10A1* had a significant decrease in monolayer cultured MFCs from P1 to P3 ( $p=0.009$ ) and P1 to P4 ( $p=0.014$ ) although the relative levels were low.

In pellets (Fig.2-6B), the relative gene expression level of *COL1A2* was not affected by increased PD or different oxygen tensions, which remained stable with no significant

changes. Although relative gene expression levels of *ACAN*, *COL2A1* and *COL10A1* in pellets tended to decrease over passages, this change was not significant from P1-P2 in either oxygen tension. *ACAN* decreased significantly after serial passaging in HYP (P1 to P3  $p=0.008$ , P1 to P4  $p=0.02$ ; P2 to P3  $p=0.046$ ) while no significant changes were observed in NRX. *COL2A1* decreased significantly in pellets after serial passaging in both oxygen tensions (P1 to P3 and P1 to P4; P2 to P3 and P2 to P4, all  $p<0.05$ ). Gene expression levels of *SOX9* followed the same decreasing trend as *COL2A1*, but no significant difference was found between different passages. Gene expression levels of the hypertrophic marker *COL10A1* in pellets decreased significantly after serial passaging in both oxygen tensions (P1 to P4,  $p=0.048$  NRX/ $p=0.001$  HYP) with low relative expression levels.

Within the same passage, HYP tended to stimulate higher relative gene expression levels of *ACAN*, *COL1A2*, *COL2A1* and *SOX9* in pellets when compared to NRX (Fig.2-6B). However, this trend was not significantly different in relative gene expression level of *COL1A2*. The relative gene expression level of *ACAN* was significantly higher in HYP than NRX of P2 (3.31-fold,  $p=0.018$ ) and P4 (3.07-fold,  $p=0.01$ ) while HYP stimulated a higher relative gene expression level of *COL2A1* in P1 (4.03-fold, approaching significance:  $p=0.07$ ), P2 (6.17-fold,  $p=0.029$ ) and P4 (8.91 fold:  $p=0.085$ ). The only significantly higher relative gene expression level for *SOX9* was found in P2 in HYP compared to NRX (2.60 fold,  $p=0.014$ ). In contrast, NRX tended to upregulate the

relative gene expression level of *COL10A1* compared to HYP except for P2. It was 1.68-fold higher in P3 (approaching significance:  $p=0.067$ ) and 3.68-fold in P4 ( $p=0.032$ ) in NRX compared to HYP.

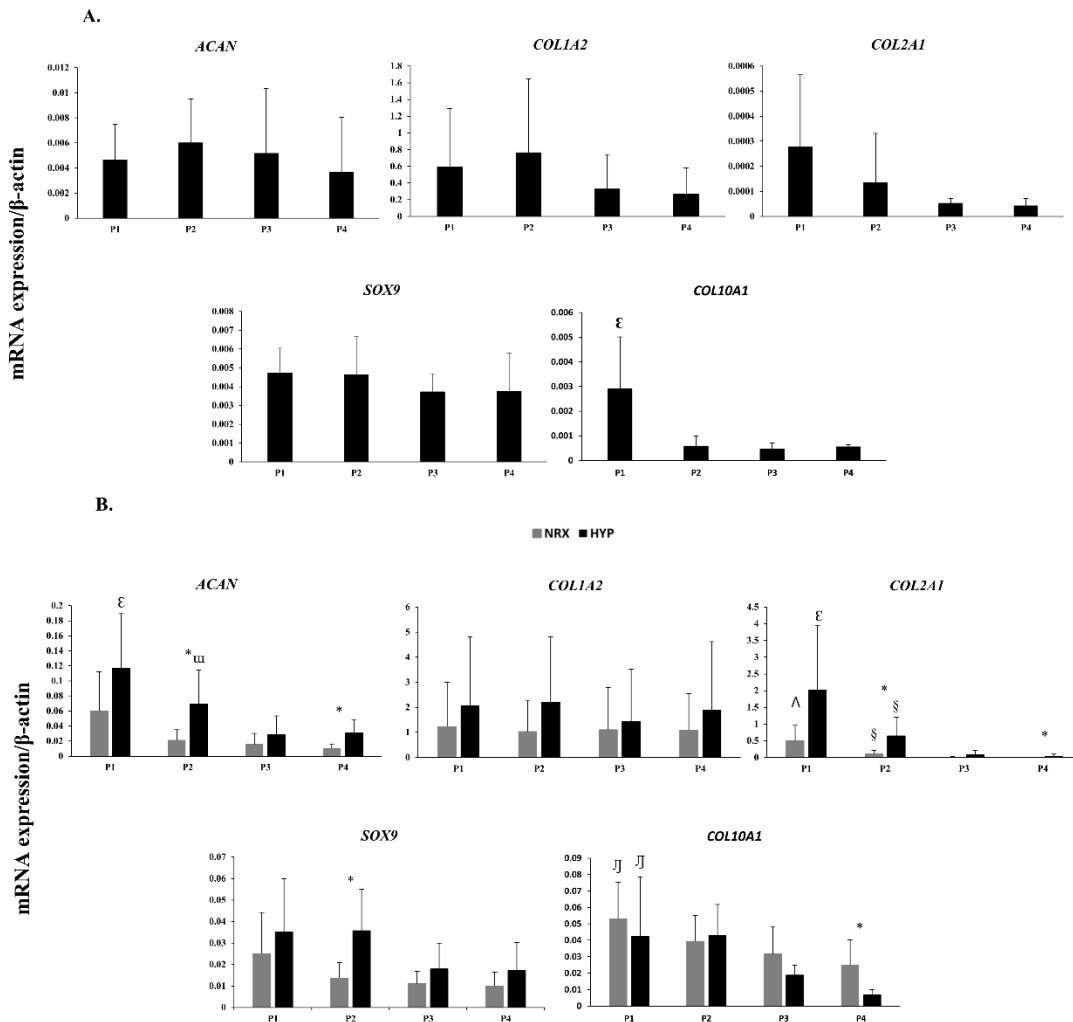


**Figure 2-6:** (A) Real-time PCR analysis of cDNA of T1F2-expanded MFCs in monolayer culture at the end of each passage prior to pellet culture (n=4).  $\epsilon$  significance between P1 and P3/P4 ( $p<0.05$ ), (B) Real-time PCR analysis of cDNA of pellets derived from T1F2-expanded MFCs of four passages after chondrogenic stimulation for 21 days

under NRX and HYP (n=4).  $\epsilon$  significance between P1 and P3/P4 in HYP,  $\omega$  significance between P2 and P3,  $\Lambda$  significance between P1 and P3/P4 in NRX,  $\xi$  significance between P2 and P3/P4 in both oxygen tensions,  $\text{JJ}$  significance between P1 and P4 in both oxygen tensions, \* significance between oxygen tensions within the same passage ( $p < 0.05$ ). Data all presented as mean  $\pm$  standard deviation.

### **2.3.6.2 Adipogenic and osteogenic differentiation (gene expression and histological) analysis**

To further characterize the adipogenic and osteogenic capacity of T1F2-expanded MFC, the fold changes of relative gene expression levels in adipogenic and osteogenic groups were compared against control groups (without adipogenic and osteogenic induction media) within the same oxygen tension and passage, e.g. P1 (NRX) induction vs P1 (NRX) control (Fig.2-7A). For adipogenic differentiation, the relative gene expression levels of lipoprotein lipase (*LPL*) and peroxisome proliferator-activated receptor gamma (*PPAR $\gamma$* ) were upregulated compared to control cells without induction (i.e. fold change > 1) (Fig.2-7A). Within passages, the relative gene expression levels tended to be higher in MFCs cultured under HYP for *LPL* and *PPAR $\gamma$* , corresponding with histological findings (not shown). In P2, the fold changes of gene expression levels of *LPL* were significantly higher in HYP compared to NRX ( $p=0.035$ ), while the fold changes of relative gene expression levels of *PPAR $\gamma$*  were significantly higher in P2 ( $p=0.047$ ) under HYP and P3 ( $p=0.0026$ ) under NRX. The fold change of relative gene expression levels appeared to

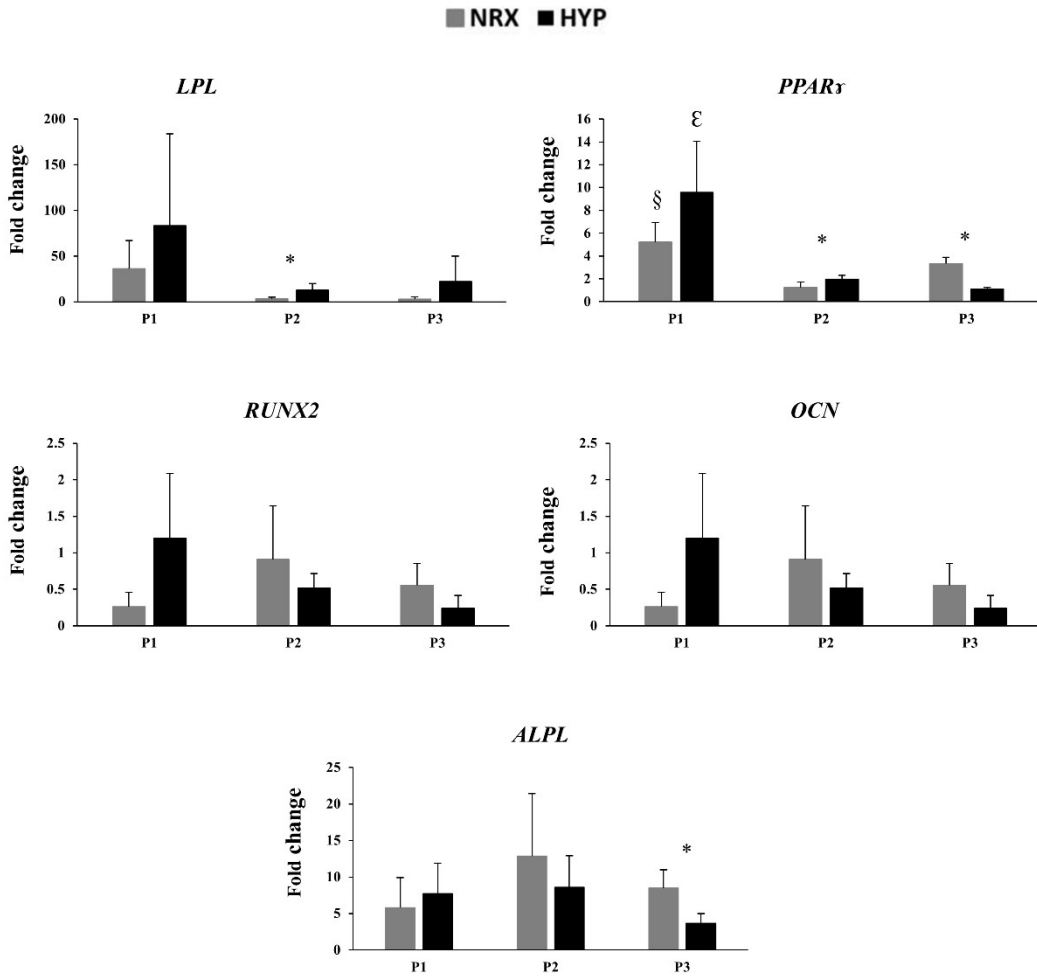
be highest in T1F2-expanded MFCs from P1 in both oxygen tensions which is consistent with the Oil Red O staining. No significant difference was found in fold change of relative gene expression levels of *LPL* between passages while in *PPAR $\gamma$* , it was significantly higher in P1 compared to P2 (NRX,  $p=0.003$ ) and P1 compared to P3 (HYP,  $p=0.002$ ).

For osteogenic differentiation, the relative gene expression levels of the osteogenic markers, runt-related transcription factor 2 (*RUNX2*) and osteocalcin (*OCN*) were not upregulated compared to control cells without induction (i.e. fold change < 1). However, the relative gene expression levels of alkaline phosphatase (*ALPL*) were upregulated for all passages and oxygen conditions compared to control cells (i.e. fold change > 1). Significant differences were only found between NRX and HYP in P3 ( $p < 0.05$ ) for *ALPL*. These gene expression results are consistent with the histological findings that showed no positive staining of Alizarin Red S in osteogenically induced T1F2-expanded MFCs.

T1F2-expanded MFCs from P1, P2 and P3 underwent adipogenic and osteogenic culture for 23 days and 21 days, respectively under HYP and NRX. The same representative donor as above (male, age 20) is presented in Figure 2-7B. Oil Red O and Alizarin Red S staining were performed to assess the formation of lipid droplets and bone matrix. All 3 passages stained positively with Oil Red O indicating adipogenic induction (Fig.2-7B). In both oxygen tensions, the number of lipid droplets seemed to be highest in

P1. In P1, HYP induced more lipid droplet formation than NRX, and this trend continued in P2-P3. While lipid droplets sharply decreased after P1 in NRX, HYP retained some adipogenic differentiation capacity of T1F2-expanded MFCs. In contrast to chondrogenic and adipogenic differentiation, no Alizarin Red S staining was observed in all three passages (Fig.2-7B).

A.



B.

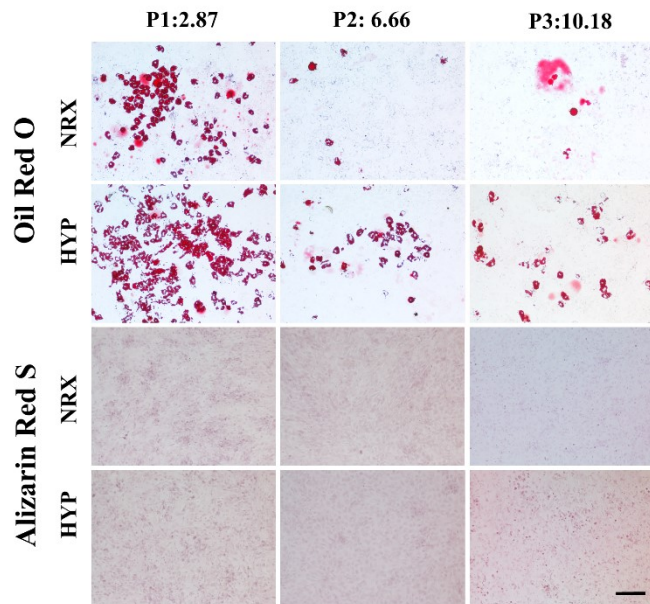


**Figure 2-7:** (A) Real-time PCR analysis of cDNA of T1F2-expanded MFCs of three passages with or without adipogenic and osteogenic induction under NRX and HYP (n=4) and the fold changes of relative mRNA expression levels of adipogenic/osteogenic markers. Fold changes were calculated as ratio of NRX (induction)/NRX (control), HYP (induction)/HYP (control) within the same passage. \* significance between NRX and HYP within the same passage, § significance between P1 and P2 in NRX, <sup>ε</sup> significance between P1 and P3 in HYP, ( $p < 0.05$ ). All mRNA expression levels were relative to  $\beta$ -actin. Data all presented as mean  $\pm$  standard deviation. (B) Oil Red O/Alizarin Red S staining analysis for lipid droplet and bone matrix deposition in T1F2-expanded MFCs from 3 passages after adipogenic and osteogenic stimulation under NRX and HYP from one representative donor (male, 20 years old). The top panel of numbers indicate population doublings of each passage. Scale bar: 200  $\mu$ m

## 2.4 Discussion

In cell-based meniscus tissue engineering strategies, a major challenge is the low cell yield from typical partial meniscectomy biopsies. When expanded during monolayer culture to increase cell numbers, the matrix-forming capacity of MFCs has been shown to decrease significantly from primary MFCs [212, 220] with a morphology change to fibroblast-like cells, a process referred to as dedifferentiation [12]. The primary goals of this study were to: 1) investigate the proliferation rates and subsequent chondrogenic differentiation of TGF $\beta$ 1 and FGF-2 (T1F2)-expanded MFCs under normal oxygen (21%

O<sub>2</sub>) or low oxygen tension (3%); 2) identify the number of population doublings (PD) these cells can undergo while still maintaining the capacity to form meniscus-like extracellular matrix; 3) to characterize the plasticity of these cells in terms of multilineage differentiation in chondrogenesis, adipogenesis and osteogenesis.

Growth factor supplementation during monolayer cell expansion has a profound effect on matrix-forming phenotype of expanded cells from a variety of sources [11, 94]. The capacity of FGF-2 to enhance MSC [16, 17] and articular chondrocyte [221, 222] proliferation rates and subsequent chondrogenic differentiation has been well demonstrated. FGF-2 can also upregulate the synthesis of collagen II and aggrecan in MFCs from osteoarthritic human knee joints [11]. Another important growth factor, TGFβ1, can also enhance the proliferation of articular chondrocytes [223] and periosteal cells [214]. When TGFβ1 and FGF-2 were used in combination, they had a synergistic effect on both proliferation and chondrogenic differentiation of chondrocytes in human articular cartilage explants [224]. However, when these two growth factors were combined with PDGF-BB during monolayer expansion of MFCs, proliferation rates increased but without any beneficial effects on matrix production [94].

Here, we examined the effect of T1F2 on proliferation and restoration of chondrogenic re-differentiation capacity of MFCs. MFCs proliferated well in T1F2 supplemented medium;  $7.5 \pm 1.3$  days were required for the MFCs to reach 80-85% confluence in monolayer culture. PD per day was similar in P1, P2 and P3 and then

decreased significantly at P4 (Fig.2-1A). When compared to our previous study, MFCs in P4 divided faster in T1F2 medium than in control-expanded MFCs without growth factors ( $0.32 \pm 0.04$  vs.  $0.14 \pm 0.03$  doublings/day) or FGF-2-expanded MFCs ( $0.22 \pm 0.04$  doublings/day) in P1 [11]. Contrary to previous studies [96, 212, 220], gene expression of ECM molecules were not statistically different between passages to approximately 13 populations doublings in monolayer cultured cells (Fig.2-6A): no significant decreases of collagen II and aggrecan or increase of collagen I gene expression in monolayer cultured cells were observed. While this result suggests that T1F2 may maintain the gene expression profile of normal human MFCs in monolayer expansion, the gene expression profile of aggrecan and type II collagen suggests a decline albeit not statistically significant. Other possible explanations for this unexpected finding may be differences in sources of MFCs and expansion conditions compared to published literature. For example, MFCs were isolated from young bovine (1-2 weeks) meniscus[212, 220] and human meniscus (54-79 years) [96] obtained from osteoarthritic knee joints with either no growth factors or FGF-2 alone added to the expansion medium.

During chondrogenic stimulation, T1F2-expanded MFCs showed a chondrogenic response in the pellet model when compared to monolayer MFCs regardless of the PD (Fig.2-6). The response was much greater in P1 MFCs with a PD of  $2.9 \pm 0.4$ . We observed that T1F2-expanded MFCs in P1 expressed a superior functional matrix-

forming phenotype than those with a higher PD in both normoxic and hypoxic conditions. Biochemical analysis showed that total GAG content and GAG content normalized to DNA was approximately two times higher in P1 pellets than pellets with PD range of  $6.3 \pm 0.6$  (P2) to  $12.9 \pm 0.8$  (P4) (Fig.2-2A, C). These results were consistent with Jakob *et al.* who found that T1F2-expanded articular chondrocytes regained their chondrocytic phenotype under proper stimulation [216]. Further, Safranin-O staining for proteoglycan deposition verified the dramatic decrease in chondrogenic capacity from P1 to P2 (Fig.2-3). Interestingly, relative gene expression levels of chondrogenic markers aggrecan and collagen II in pellets showed no significant decreases from P1 to P2 (Fig.2-6B), but immunofluorescence analysis for collagen II deposition revealed a substantial qualitative decrease from P1 to P2 (Fig.2-4). This may be due to the relatively late time-point selected for the gene expression analysis (21 days of chondrogenic differentiation). A time course study investigating gene expression and matrix changes during chondrogenic differentiation of the T1F2-expanded MFCs could be performed in the future to optimize culture times. In contrast, T1F2-expanded MFCs from P3 ( $9.8 \pm 1$  PD) and P4 ( $12.9 \pm 0.8$  PD) showed qualitative differences in the deposition of collagen I between oxygen tensions. Hypoxia cultured T1F2 expanded MFCs were positive for type II collagen, albeit with reduced intensity. Normoxia cultured T1F2 expanded MFCs were negative for type II collagen. These findings are consistent with the Safranin-O staining intensity in P3 and P4. This indicates that T1F2-expanded MFCs with  $\sim 10$  PDs may be appropriate

for tissue engineering of the avascular inner meniscus which exists in a more hypoxic microenvironment than its vascularized outer counterpart.

To date, no studies have assessed the effect of oxygen tension on matrix-forming capacity of T1F2-expanded MFCs derived from normal human menisci. Oxygen tension in the knee joint is hypoxic [225, 226]; thus, several studies have investigated the effect of oxygen tension on chondrogenic differentiation of expanded MFCs. Adesida *et al.* showed that hypoxic conditions (5% O<sub>2</sub>) enhanced matrix-forming capacity of MFCs from OA knee joints [11] and several others have demonstrated the positive effects of low oxygen tension on chondrogenic differentiation of BM-MSCs [227, 228]. In our study, HYP (3% O<sub>2</sub>) enhanced the expression of aggrecan (*ACAN*) and collagen II (*COL2A1*) when compared to NRX (21% O<sub>2</sub>) in T1F2-expanded MFCs derived from non-arthritic knee joints (Fig.2-6B). HYP culture stimulated a more intense Safranin-O staining in P3 and P4 (Fig.2-3). This finding was consistent with the wet weight results (Fig.2-1C), albeit with no significant difference in total GAG contents relative to NRX cultured pellets (Fig.2-2A). It is probable that the total collagen content of the pellets differs between NRX and HYP; HYP has been reported to increase collagen content [229] and collagen has been reported to hold water [230]. Taken together, chondrogenic culture under hypoxic conditions resulted in a more robust chondrogenic differentiation of T1F2-expanded MFCs, which may improve their clinical applicability for avascular meniscus tissue engineering.

In our study, adipogenic differentiation of human T1F2-expanded MFCs was observed under both hypoxic and normoxic conditions (Fig.2-7B). T1F2-expanded MFCs derived from P1 exhibited superior adipogenic capacity under hypoxic conditions. Increased PD resulted in decreased staining for lipid droplets in both oxygen tensions, and adipogenic differentiation was benefited by hypoxic conditions in all three passages. In contrast, no osteogenesis was induced under either oxygen tension, demonstrated by the absence of Alizarin Red staining for deposition of calcium (Fig.2-7B). This was consistent with Mauck *et.al.* who demonstrated minimal deposition of bone matrix in bovine MFCs from the inner region of the meniscus. However, that study did demonstrate substantial osteogenic differentiation in cells obtained from the outer portion of the meniscus tissue [231]. Since the meniscus tissues in our study were obtained from partial meniscectomy, most of the tissues are likely to be from the inner, avascular region of meniscus. Gross observation of the meniscus tissues obtained also suggested that they were removed from the inner meniscus. The outer meniscus regions possess a spontaneous healing capacity, which may not only be due to sufficient blood supply but due to the presence of perivascular derived stem cells [232]. The absence of osteogenesis in our study may also be related to MFC phenotype after expansion in T1F2. Previous studies have shown that expanded MFCs from the whole meniscus of humans [106, 233] or animals [104, 107, 234] have similar surface markers to MSCs and have multipotent differentiation capacity, including osteogenesis. However, the cells from those studies

were expanded without growth factor supplementation which may have been a factor in the lack of osteogenesis observed in our study. Moreover, it is well known that the meniscus contains a heterogeneous cell population, which varies from inner to outer regions, [48, 201] and by using the whole tissue the population of cells would be quite different. Recently, however, Fu *et al.* have shown that expanded human MFCs from the inner region did exhibit osteogenic differentiation, but again no growth factors were used during cell expansion [235]. This identifies that the use of T1F2 in inner meniscus cells may inhibit their capacity to undergo osteogenic differentiation but this requires further examination to gain mechanistic insight. Collagen X (*COL10A1*) is a marker of hypertrophic differentiation of MSCs and has been correlated with bone formation after chondrogenic stimulation both *in vitro* and *in vivo* [121]. It was notable that negligible deposition of collagen X was observed in all pellets from T1F2-expanded human MFCs when compared to human BM-MSCs (Fig.2-5). This lack of collagen X supports the findings of limited osteogenic potential in these expanded MFCs. Low relative gene expression levels of collagen X were demonstrated in pellets derived from T1F2-expanded MFCs and no significant differences were found between oxygen tensions (Fig.2-6B). This is in contrast to other studies which have shown that hypoxic conditions can suppress hypertrophic differentiation of MSCs [15, 228]. These results suggest that the T1F2-expanded MFCs may be a promising cell source for meniscus repair with a potentially stable chondrocytic phenotype without the tendency of hypertrophic

differentiation *in vitro*. While a study comparing cell sources using matched donors may be of interest in determining their relative advantages for meniscus repair, the difficulty in obtaining multiple tissues from healthy donors for this purpose may be prohibitive.

Further study will be required to investigate the phenotypic stability of T1F2-expanded MFCs *in vivo* to ensure they do not undergo hypertrophic differentiation and calcification, as well as adipogenesis.

To determine the cell density of surgically-removed meniscus tissue, viable primary cell yield per gram wet weight of meniscus tissue was calculated. MFC physiology changes in meniscus tissue in osteoarthritic knee joints [236]. For this reason, tissues in this study were obtained only from partial meniscectomy patients suffering from acute injuries to limit the effects of chronic injury on cell biology. A limitation of this study was that we did not have detailed information regarding the severity of damage to donor tissues and the precise portion of the meniscus they were taken from. However, in general partial meniscectomy removes the irreparable inner avascular regions, which would have influenced the phenotypes of the initial cell population. Donor age is another variable which has been demonstrated to be relevant for cell yield from articular cartilage [237]. In this study, we did not find significant age effects on cell yield; however, it should be noted that all donors were relatively young (20-37) and otherwise healthy. As a future study, it may be of interest to compare the cell yield and tissue quality formed by MFCs derived from patients from a wider age range. The average cell yield per gram of

meniscus tissue in this study was lower than that previously shown in human articular cartilage in donors between 20-40 years old [237] ( $3.14 \pm 1.46 \times 10^6$  cells/g vs  $7.9 \times 10^6$  cells/g). These results have a significant clinical implication. Based on the fact that the volume of human medial and lateral meniscus is approximately  $4.50 \text{ cm}^3$  and  $4.95 \text{ cm}^3$  respectively [238], and the potentially optimal cell seeding density of a scaffold for meniscus tissue engineering is  $5 \times 10^6 \text{ cm}^3$  [239], a total of 22.5-25 million cells would be required to generate an entire human medial or lateral meniscus. Damaged meniscus tissue could be partially removed arthroscopically and used to isolate autologous MFCs. These could be expanded with T1F2 and seeded on scaffolds that mimic the natural meniscus environment. *In vitro* strategies to recapitulate the different regions of the meniscus could then be employed, such as using growth factor-releasing scaffolds [240] and mechanical conditioning under hypoxia to generate tissue with meniscus-like composition and mechanical properties before implantation. We note that substantial work is needed to ensure the new tissues restore normal meniscus function in protecting the articular cartilage to prevent early onset osteoarthritis *in vivo*. In our study, T1F2-expanded MFCs with approximately 3.3 PD retained the best matrix-forming capacity without hypertrophic differentiation. After 3 PD, i.e.  $8 \times$  the mean number of primary MFCs ( $3.14 \pm 1.46$  million/g) in monolayer expansion, approximately 25 million MFCs can be obtained from 1 g of meniscus tissue. If a meniscus biopsy has an insufficient cell yield and higher numbers of MFCs are needed, expansion can be continued to P2 (PD:

~7, i.e. 128 x the number of primary MFCs) while retaining the capacity for proteoglycan and collagen II production, albeit in reduced quantities relative to P1. This may be clinically relevant for meniscus repair for older patients or particularly small meniscus biopsies less than 1g.

## **2.5 Conclusion**

In this study, we have characterized the proliferation rates and chondrogenic capacity of TGF $\beta$ 1 and FGF-2 (T1F2)-expanded meniscus fibrochondrocytes (MFCs) under normoxic and hypoxic conditions. We found that MFCs expanded up to 10 doublings have the capacity to express the extracellular matrix (ECM)-forming phenotype especially under hypoxic conditions which is consistent with their natural microenvironment with the knee joint[241]. MFCs in the range of 2.9+0.4 PDs synthesized the most glycosaminoglycans and the highest Safranin-O positive ECM. For the first time, we demonstrated that the T1F2 expansion strategy may produce enough cells possessing an ECM-forming phenotype to repair a meniscus defect from a small tissue biopsy within a relatively brief period of time based on the human meniscus volume and the optimal seeding density for a type I collagen scaffold. Hypoxia was shown to be advantageous for chondrogenic culture, resulting in improved ECM quality and relevant gene expression profiles of MFCs at low PDs. Furthermore, we have demonstrated that hypertrophic and osteogenic tendencies are virtually absent for MFCs expanded with T1F2, although they show adipogenic capacity. Overall, this highlights the

potential use of T1F2-expanded MFCs from the inner meniscus in combination with hypoxic culture conditions to produce robust tissue engineered meniscus-like ECM. Further investigation will be required to evaluate the phenotypic stability of this cell source *in vivo* and to build grafts of clinically relevant size on three dimensional scaffolds.

**Chapter 3 Re-differentiation of human meniscus fibrochondrocytes differs in three-dimensional cell aggregates and decellularized human meniscus matrix scaffolds**

**Yan Liang, Alexander R.A. Szojka, Enaam Idrees, Melanie Kunze, Aillette Mulet-Sierra, and Adetola B. Adesida**

This chapter has been published in part in *Annals of Biomedical Engineering*:

Yan Liang, Alexander R.A. Szojka, Enaam Idrees, Melanie Kunze, Aillette Mulet-Sierra, and Adetola B. Adesida: **Re-differentiation of human meniscus fibrochondrocytes differs in three-dimensional cell aggregates and decellularized human meniscus matrix scaffolds**. *Annals of Biomedical Engineering* 2019

### 3.1 Introduction

The menisci are a pair of weight-bearing fibrocartilaginous tissues in the knee joint. They increase contact area for load transmission and provide lubrication to support smooth joint motion [2, 242]. The inner portion of the menisci may not heal after injury due to their avascular nature; partial tissue removal by surgery may be performed but this may not reduce the risk for early development of osteoarthritis [243]. The biomechanically functional extracellular matrix (ECM) of inner meniscus consists mostly of types I and II collagen [244], and proteoglycan (predominantly aggrecan) [245]. The ECM is produced and maintained by a heterogenous population of cells known collectively as meniscus fibrochondrocytes (MFCs) [12].

MFCs are known to lose their ECM-forming phenotype during *in vitro* cell expansion with decreased expression of aggrecan and type II collagen [12]. However, we found that MFCs expanded with simultaneous transforming growth factor- $\beta_1$  (TGF- $\beta_1$ ) and fibroblast growth factor-2 (FGF-2) (T1F2) re-expressed an inner meniscus-like ECM-forming phenotype in a small-scale pellet model following chondrogenic induction even after approximately 10 population doublings (1000-fold expansion) [246]. However, the ECM-forming phenotype of T1F2-expanded MFCs needs to be investigated using a scaffold model if large-scale constructs are to be used to repair and replace injured meniscus tissues.

The ECM is an important regulator of cell behavior in a variety of tissues [247]. The

use of meniscus-derived decellularized ECM (DCM) as a scaffold to provide biological cues inducing cellular differentiation has become an area of interest [248]. Animal meniscus-derived DCM has been tested using human and animal MSCs [142, 143, 249, 250]. Furthermore, ovine and canine meniscus-derived DCM has been shown to support attachment, infiltration, and proliferation of autologous MFCs, although differentiation requires further investigation [250, 251]. One promising study found that increasing concentrations of porcine meniscus-derived DCM could enhance differentiation of rabbit MFCs at the gene expression level on hybrid polycaprolactone/meniscus-derived DCM scaffolds, suggesting the potential for inner meniscus-like ECM formation [252].

Sadmann *et al.* described the preparation of human meniscus-derived DCM, though its effects on human MFCs were not investigated [253]. In the absence of growth factor supplementation, porcine articular cartilage and meniscus-derived DCM were respectively shown to induce chondrogenic differentiation of human MSCs and re-differentiation of rabbit chondrocytes, implying the presence of sequestered bioactive factors [249, 254]. Thus, the combination of human meniscus DCM with human MFCs may be of considerable interest. We previously prepared human meniscus-derived DCM scaffolds using physical homogenization methods. These supported the chondrogenic differentiation of human knee joint synovial fluid derived-MSCs (SF-MSCs), but only with supplementation of chondrogenic growth factor TGF- $\beta$ 3 [255]; however, their effects on human T1F2-expanded MFCs remained to be investigated.

In this study, our first objective was to evaluate the capacity of human MFCs to attach, populate, and re-differentiate upon human meniscus-derived DCM in both a non-chondrogenic and chondrogenic environment (TGF- $\beta$ 3). We used cell pellets with TGF- $\beta$ 3 supplementation as a positive model comparison. Our second objective was to evaluate the capacity or potential of human meniscus-derived DCM to induce chondrogenesis of human MFCs without hypertrophic differentiation in growth factor-free conditions under hypoxia. We used cell pellets without TGF- $\beta$ 3 supplementation as a negative control.

## **3.2 Methods:**

### **3.2.1 Ethics statement**

Experimental methods and tissue collections were performed with the approval of and in accordance with the University of Alberta's Health Research Ethics Board- Biomedical Panel (Study ID: Pro00018778). Ethics Board waived the need for written informed consent of patients, as specimens used in the study were intended for discard in the normal course of the surgical procedure. Extensive precautions were taken to preserve the privacy of the participants donating specimens.

### **3.2.2 Isolation and expansion of human meniscus fibrochondrocytes**

We obtained human meniscus tissues (n=3, all male) from partial meniscectomy procedures for acute meniscus injuries (See Table 3-1: Donors 1-3). We isolated meniscus fibrochondrocytes (MFCs) by collagenase digestion and expanded them with combined

TGF- $\beta$ 1 (1 ng/mL) and FGF-2 (5 ng/mL) *in vitro* in monolayer, a process expected to result in the de-differentiation of MFCs [12], under normoxia (5% CO<sub>2</sub>, 95% humidified air) as previously described [246]. We passaged MFCs at a 1:2 ratio until passage 2 (P2) before experimental use. We calculated population doublings as  $\log_2(N_f/N_i)$  that  $N_f$  and  $N_i$  are respectively the final and initial expansion cell numbers.

**Table 3-1:** Meniscus tissue donor details. PD: population doublings.

Identifier	Tissue use	Age	Sex	Meniscus	PD
Donor 1:M34_A	MFC source	34	Male	Medial	3.7
Donor 2:M34_B	MFC source	34	Male	Medial	3.5
Donor 3:M21	MFC source	21	Male	Lateral	2.9
Donor 1:M72	DCM preparation	72	Male	All four	N/A

### 3.2.3 Human meniscus derived-decellularized matrix preparation

We obtained human lateral and medial meniscus tissues one-day post-mortem from the Comprehensive Tissue Centre in Edmonton, Alberta (See Table 3-1: Donor 4). We observed no macroscopic signs of degenerative changes to the menisci. We prepared meniscus-derived decellularized matrix (DCM) as previously described with one change: after we collected the meniscus slurry by centrifugation at 300 relative centrifugal force (RCF), we collected the supernatant and centrifugated it at 600 RCF to generate more slurry that we then mixed into the rest [255]. The reason for this was to help capture possible inductive factors from the suspended meniscus slurry. After we freeze-dried the tissue in 1 mL aliquots within 1.5 mL screw-cap cryotubes, we manually sectioned them

into 1.8-2 mm thick discs that we then cored using a 6-mm diameter biopsy punch to produce scaffolds. We later sterilized these scaffolds by ethylene oxide (EtO) as previously described [254, 256].

### **3.2.4 The culture of cell pellets and cell-seeded meniscus-derived DCM constructs**

At the end of P2, we set up two culture models using the expanded MFCs: we spun  $5 \times 10^5$  cells into high-density cell pellets or seeded them onto the meniscus-derived DCM scaffolds ( $8.8\text{-}9.8 \times 10^6$  MFCs/cm<sup>3</sup>) as previously described [255]. We cultured each cell pellet and allogeneic cell-seeded DCM construct respectively in 0.5 mL and 1 mL of a defined serum-free chondrogenic medium with 10 ng/mL (+TGF- $\beta$ 3) or without (-TGF- $\beta$ 3) supplementation for three weeks. We used hypoxic (HYP, 3% O<sub>2</sub>) incubator conditions as they have been shown to enhance the ECM-forming capacity of human MFCs with chondrogenic stimulation [11, 242, 246]. The cell pellets and DCM constructs experienced about 5 to 10 minutes of exposure to atmospheric O<sub>2</sub> levels each time we changed the medium twice a week.

### **3.2.5 Analysis of chondrogenic differentiation of MFCs**

After 3 weeks of culture, we harvested the pellets and cell-seeded DCM constructs for the analysis of ECM formation. We performed scanning electron microscopy (SEM) to assess MFC infiltration into the DCM and the surface morphology of MFCs and their newly-formed ECM. To assess chondrogenic differentiation, we carried out biochemical

assays for glycosaminoglycan (GAG) and DNA quantification, Safranin-O staining for sulfated proteoglycan deposition, immunofluorescence for ECM-related components: aggrecan, types I, II, and X collagen, and quantitative polymerase chain reaction (qRT-PCR) of chondrogenic and hypertrophic-associated genes. We performed all methods as previously described [246, 255], except for type II collagen immunofluorescence. The type II collagen immunofluorescence was performed on different sections of the same constructs from type I collagen. Briefly, paraffin sections of 5  $\mu\text{m}$  were deparaffined and rehydrated. After antigen retrieval using protease XXV and hyaluronidase, the sections were incubated with the primary antibody: mouse anti-collagen II (II-II6B3, Developmental Studies Hybridoma Bank, IA, USA) using a 1: 200 dilution overnight at 4°C. Then they were incubated with goat anti-mouse IgG biotinylated secondary antibody (ab97021, Abcam, Cambridge, MA) using a 1: 200 dilution for 45 minutes, followed by incubation with streptavidin-Alexa 488 (cat#S32354, ThermoFisher, Waltham, MA) for 45 minutes. After that, the sections were stained with DAPI and immunofluorescence was visualized using an Eclipse TI-S microscope (Nikon Canada). We present primer sequences in Table 3-2.

**Table 3-2: Primer sequences**

Genes	Forward	Reverse	GenBank accession
$\beta$ -actin ( <i>ACTB</i> )	AAGCCACCCCACTT CTCTCTAA	AATGCTATCACCTCC CCTGTGT	NM_00110 1.4
Beta-2 microglobulin ( <i>B2M</i> )	TGCTGTCTCCATGT TTGATGTATCT	TCTCTGCTCCCCACC TCTAAGT	NM_00404 8.3
Tyrosine 3 Monooxygenase/Tryptophan 5-Monooxygenase Activation Protein Zeta ( <i>YWHAZ</i> )	TCTGTCTTGTCCACC AACCATTCTT	TCATGCGGCCTTTTT CCA	NM_00340 6.3
Aggrecan ( <i>ACAN</i> )	AGGGCGAGTGGAA TGATGTT	GGTGGCTGTGCCCTT TTTAC	NM_00113 5.3
Collagen I ( <i>COL1A2</i> )	GCTACCCAACCTTGC CTTCATG	GCAGTGGTAGGTGAT GTTCTGAGA	NM_00008 9.3
Collagen II ( <i>COL2A1</i> )	CTGCAAATAAAAT CTCGGTGTTCT	GGGCATTTGACTCAC ACCAGT	NM_00184 4.5
SRY-Box 9 ( <i>SOX9</i> )	CTTTGGTTTGTGTT CGTGTTTTG	AGAGAAAGAAAAAG GGAAAGGTAAGTTT	NM_00034 6.3
Collagen X ( <i>COL10A1</i> )	GAAGTTATAATTTA CACTGAGGGTTTCA AA	GAGGCACAGCTTAA AAGTTTTAAACA	NM_00049 3.3
Matrix metalloproteinase-13 ( <i>MMP-13</i> )	CATCCAAAAACGC CAGACAA	CGGAGACTGGTAATG GCATCA	NM_00242 7.4
Runt related transcription factor 2 ( <i>RUNX2/CBFA1</i> )	GGAGTGGACGAGG CAAGAGTTT	AGCTTCTGTCTGTGC CTTCTGG	NM_00102 4630.4
Alkaline phosphatase ( <i>ALPL</i> )	CCTGGCAGGGCTC ACACT	AAACAGGAGAGTCG CTTCAGAGA	NM_00047 8.6
Bone sialoprotein ( <i>BSP</i> )	GCGAAGCAGAAGT GGATGAAA	TGCCTCTGTGCTGTT GGTACTG	NM_00496 7.4

### 3.2.6 Data presentation and statistical analysis

We present all quantitative data donor-by-donor to show variability and aid in assessing differences between conditions. We carried out statistical analysis as previously described [242]. Briefly, we applied two-way ANOVA with the model (pellet vs. meniscus-derived

DCM) and TGF- $\beta$ 3 supplementation treated as within-subjects factors in SPSS version 24 (IBM, USA). We first tested the interaction term between model and TGF- $\beta$ 3 for significance ( $p < 0.05$ ); in this case, we carried out paired t-tests between 1. pellet/-TGF- $\beta$ 3 vs. pellet/+TGF- $\beta$ 3, 2. DCM/-TGF- $\beta$ 3 vs. DCM/+TGF- $\beta$ 3, 3. pellet/-TGF- $\beta$ 3 vs. DCM/-TGF- $\beta$ 3, and 4. pellet/+TGF- $\beta$ 3 vs. DCM/+TGF- $\beta$ 3. In cases where the interaction was not significant, we evaluated the pooled main effects for significance. The type I error rate for statistical significance for each test applied within individual metrics (e.g. wet weight) was maintained at  $P < 0.05$  (no adjustments). We interpreted P-values from 0.05 to 0.1 as weak evidence and did not attempt to interpret P-values greater than 0.1. Specific quantitative results should be interpreted knowing that statistical power was limiting ( $n=3$  MFC donors); in certain cases, taking the whole of evidence from the study may be more useful to discern the main trends.

### **3.3 Results**

#### **3.3.1 Biochemical content (DNA, GAG, GAG/DNA)**

The empty meniscus-derived DCM contained 0.08  $\mu$ g of DNA (Fig.3-1A: Cell-free, DCM Model), which when normalized to dry weight was 19 ng/mg, below a guideline of 50 ng/mg from a previous report regarding successful decellularization of tissues [257]. TGF- $\beta$ 3 stimulation during the 3-week culture period led to a consistent trend of higher DNA content compared to the growth factor-free conditions, with a significant 2.1-fold increase within the DCM model that appeared larger than the 1.3-fold increase within the

pellet model. Culture in the DCM model also led to a consistent trend of higher DNA content relative to the pellet model.

We first normalized GAG content in the MFC-seeded DCM groups by subtracting the residual GAG content found in a non-cell-seeded DCM (Fig.3-1B: Cell-free, DCM Model) after 3-weeks of incubation in the medium. Thus, the GAG values represent newly synthesized GAG matrix within the DCM model groups for comparison to the pellet model, which naturally did not have any appreciable GAG content at the time of the set up of the experiment. There was no obvious growth media turnover as assessed by color change in the non-cell-seeded DCM (Fig.3-2), further confirming the absence of any viable cells within the DCM scaffolds.

There was a consistent trend of increased GAG content in DCM seeded with MFCs in the presence of TGF- $\beta$ 3 (Fig.3-1B), indicating that the DCM appeared to support chondrogenic re-differentiation of the seeded dedifferentiated MFCs. However, within the no TGF- $\beta$ 3 group (i.e. -TGF- $\beta$ 3 groups), we measured marginal GAG content beyond what was present in the non-cell-seeded DCM, with two of three donors showing a decline in GAG content relative to the pellet model.

In terms of GAG content (synthesis) normalized to DNA, there was weak evidence for a negative effect of the DCM relative to the pellet model and a positive TGF- $\beta$ 3 effect pooled across culture models (Fig.3-1C). Even with TGF- $\beta$ 3 supplementation, the GAG/DNA content on the DCM was relatively low. Taken together with the GAG and

DNA results, this appeared to indicate that the DCM favored MFC proliferation and relatively less synthesis of inner meniscus-like ECM to the pellet model by the end of the 3-week culture period.

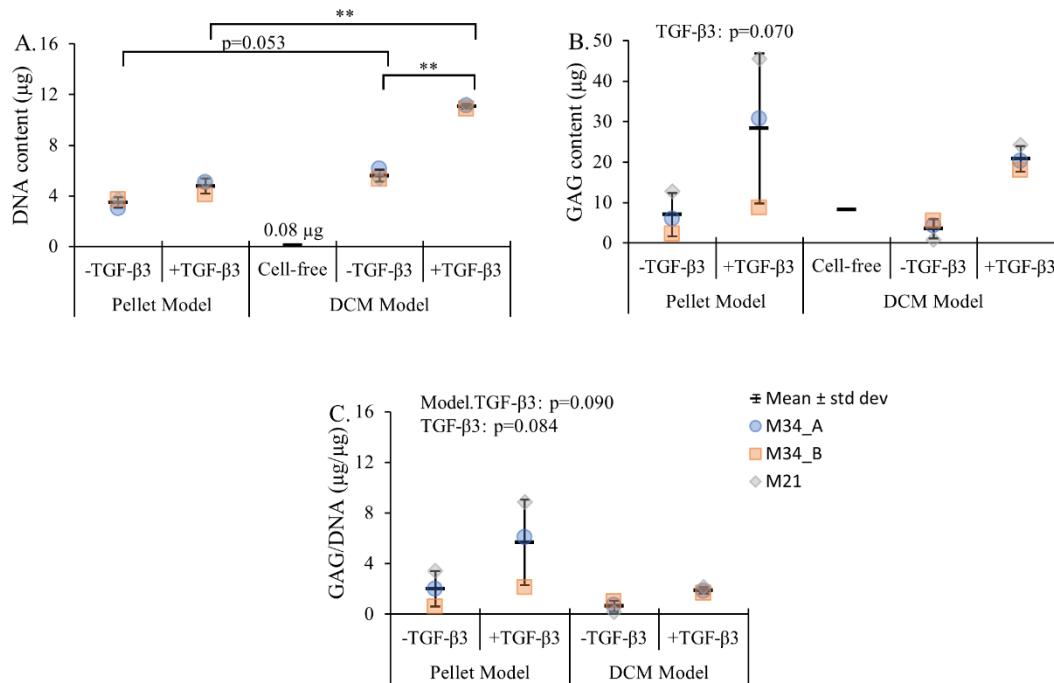


**Figure 3-1:** Glycosaminoglycan (GAG) matrix and DNA contents in meniscus fibrochondrocyte (MFC)-based tissues after 21-days' culture in either pellets or meniscus-derived decellularized matrix (DCM) with and without supplementation of 10 ng/mL TGF-β3. A) DNA; B) GAG; and C) GAG/DNA data. The GAG content in the DCM model had the values of the empty/cell-free DCM subtracted such that they reflect the contribution of MFCs for comparison to the pellet model and thus contained more GAG than the empty DCM. Each data point represents the average of 1 or 2 biological replicates. P-values are derived from two-way within-subjects ANOVA. P-values greater

than 0.1 were suppressed. \*\*:  $p < 0.01$ .

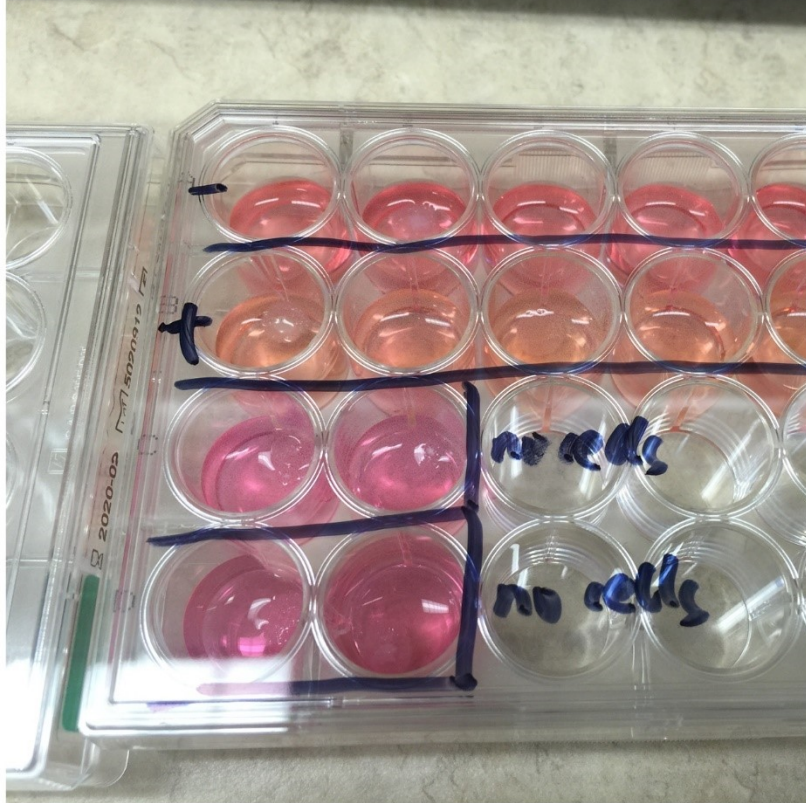


**Figure 3-2:** Assessment of growth medium turnover after 21-days' culture in medium under HYP using a 24-well plate. “-” and “+” indicated the whole row of cell-seeded DCM constructs were cultured in serum-free medium without and with TGF- $\beta$ 3, respectively. “No cells” indicated two rows of empty DCM were cultured with the same medium without and with TGF- $\beta$ 3.

### 3.3.2 Gross morphology and scanning electron microscopy

In terms of gross morphology (Fig.3-3), the meniscus-derived matrix appeared white-

yellow and sponge-like as was previously observed [255]. During the 3-week culture period, we observed that DCM scaffolds seeded with allogeneic MFCs demonstrated some contraction in the radial direction, although we did not record the images and quantify contraction in this study. Under scanning electron microscopy (SEM), it was clear that the MFCs had formed a layer of tissue in both DCM/-TGF- $\beta$ 3 (Fig.3-4A) and DCM/+TGF- $\beta$ 3 (Fig.3-4B) groups on the cell-seeded surface but that much of the DCM had not been remodeled. This did not appear to be due to the DCM providing physical barriers to MFC migration, given that pores appeared interconnected and were on the order of 100  $\mu$ m, much larger than resident MFCs. Rather, this was perhaps a combined effect of the static seeding strategy used to initially populate the scaffold with MFCs and the static environment used to culture the constructs, which may have limited the tendency of MFCs to migrate outwards on the DCM material. Safranin-O staining (Fig.3-5), discussed below, revealed the presence of newly-formed ECM across the span of the DCM demonstrating partial MFC infiltration into the DCM. Rather, it seems more likely that the rate of new ECM synthesis was insufficient to completely fill up the DCM with newly-formed ECM during the 3-week culture period given the static seeding method used. While cells in both -TGF- $\beta$ 3 and +TGF- $\beta$ 3 groups were densely packed and flat-looking, they demonstrated differences in morphology: cells in the -TGF- $\beta$ 3 group appeared polygonal-shaped with smooth surfaces and were loosely-connected to one another (Fig. 3-4C/D), whereas cells in the +TGF- $\beta$ 3 group appeared spindle-like with

roughened surfaces and were tightly-integrated together (Fig.3-4D/F). Interestingly, prominent round nuclei could be observed only in the +TGF- $\beta$ 3 group (Fig.3-4F: white arrows and magnified insets).



**Figure 3-3:** Gross morphology of empty DCM scaffold after freeze-drying. Scale bar: 3-mm

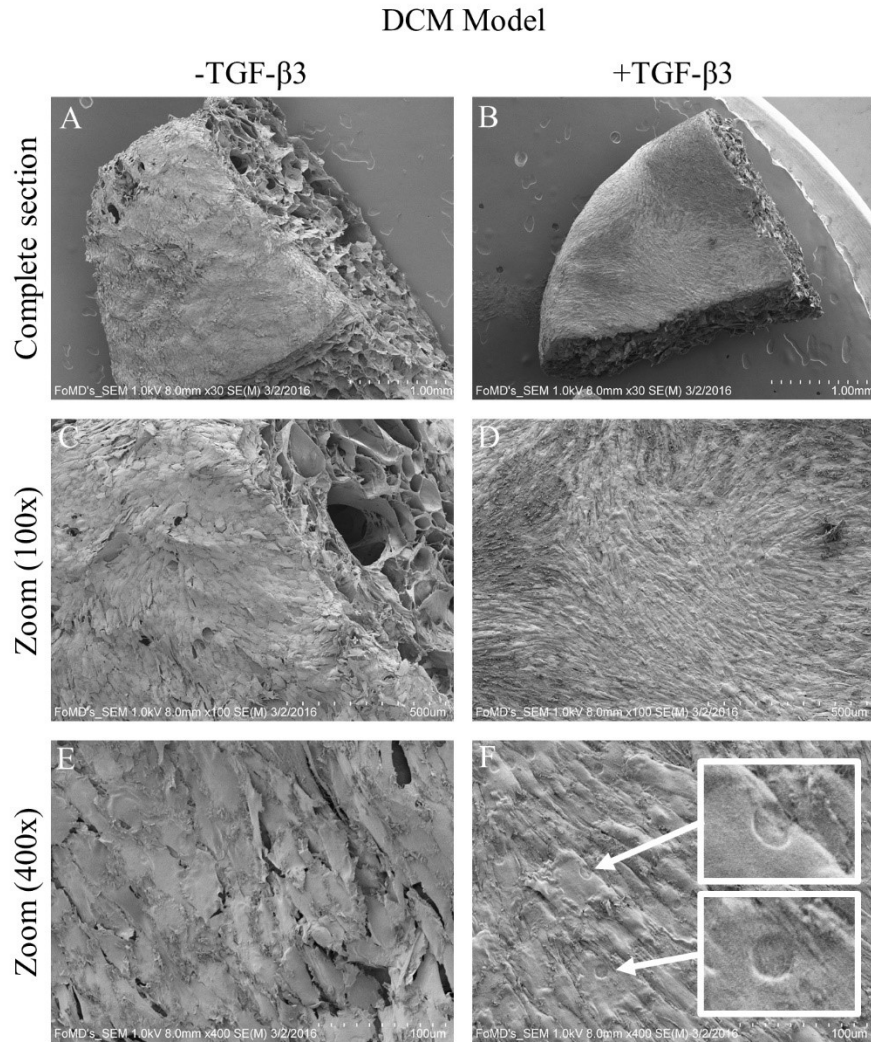


**Figure 3-4:** Scanning electron micrographs of meniscus fibrochondrocyte (MFC)-based tissues after 21-days culture in meniscus-derived decellularized matrix (DCM) with and without supplementation of 10 ng/mL TGF- $\beta$ 3. A, C & E represent micrographs derived from tissues after in vitro culture in the absence of TGF- $\beta$ 3, and B, D and F represent micrographs from tissues generated after in vitro in the presence of TGF- $\beta$ 3.

### 3.3.3 Safranin-O/fast green staining and immunofluorescence

In the pellet model, sulfated proteoglycans were abundant in the +TGF- $\beta$ 3 group based

on Safranin-O/Fast Green FCF staining (Fig. 3-5B1/B2). We also identified faint Safranin-O positive ECM in the -TGF- $\beta$ 3 group along with well-developed lacuna-like structures (Fig. 3-5A1/A2). Regardless of TGF- $\beta$ 3 supplementation, all pellets displayed a fibrous ring with Fast Green staining for collagen with elongated cells near the edge (Fig. 3-5A2/B2).

In the DCM model, the non-cell-seeded group showed the presence of large pores and Fast Green FCF-staining fibers but with no Safranin-O staining (Fig. 3-5C1/C2). These fibers could still be observed in both cell-seeded groups (Fig. 3-5D1/D2, Fig. 3-5E1/E2). As well, both cell-seeded groups (Fig. 3-5D1/D2, Fig. 3-5E1/E2) showed the presence of ECM that was much sparser than in the pellet model (Fig. 3-5A1, A2/B1, B2). While ECM was present in the DCM/-TGF- $\beta$ 3 group it did not stain for Safranin-O (Fig. 3-5D2). Safranin-O staining was observed in the DCM/+TGF- $\beta$ 3 group (Fig. 3-5E2) but it was less intense than in the pellet/+TGF- $\beta$ 3 group (Fig. 3-5B2). Moreover, the size of the DCM constructs was clearly much larger than the pellets. Together, these indicate that higher seeding densities or longer culture times may be necessary for the appreciable accumulation of newly synthesized matrix.

Immunofluorescence of collagens showed that the major collagen present in the meniscus-derived matrix was type I (Fig. 3-5C4) and absence of type II (Fig. 3-5C5). Immunofluorescence revealed obvious differences in DAPI staining density between the pellet and DCM model, reflecting the high-density of cells in the pellet model as

compared to the DCM. The non-cell-seeded DCM showed no DAPI staining (Fig. 3-5C3/C4/C5/C6), indicating the likely absence of DNA. Aggrecan was present in both pellet (Fig. 3-5A3/B3) and DCM (Fig. 3-5D3/E3) models, even in -TGF- $\beta$ 3 groups (Fig. 3-5A3/D3). In the pellet model, type I collagen was nearly ubiquitous regardless of TGF- $\beta$ 3 supplementation (Fig. 3-5A4/B4). Type II collagen was abundant in the +TGF- $\beta$ 3 group (Fig. 3-5B5) whereas traces were detected in the -TGF- $\beta$ 3 group (Fig. 3-5A5), corroborating the similarly faint Safranin-O staining observed in this group (Fig. 3-5A2). In the DCM model, the +TGF- $\beta$ 3 group showed regions of type I (Fig. 3-5E4) & II (Fig. 3-5E5) collagen-rich matrix interspaced with fibers of the DCM material. Type II collagen was absent in the DCM/-TGF- $\beta$ 3 group (Fig. 3-5D5). Together with Safranin-O and biochemical data, these results indicate that the human meniscus-derived DCM combined with TGF- $\beta$ 3 under hypoxia supported chondrogenic re-differentiation of human MFCs but not in the absence of TGF- $\beta$ 3 supplementation.

We also assessed the hypertrophy-induction capacity of the DCM, given that we prepared it from a donor of advanced age (72 years) whose joint tissues may have been osteoarthritic. While no traces of type X collagen were detected in the empty DCM (Fig. 3-5C6) and in the pellet/-TGF- $\beta$ 3 conditions (Fig. 3-5A6), collagen X was detected in both pellet (Fig. 3-5B6) and DCM (Fig. 3-5E6) models with TGF- $\beta$ 3 treatment (i.e. +TGF- $\beta$ 3 groups). However, it was surprising to observe collagen X fluorescence in the DCM/-TGF- $\beta$ 3 group (Fig. 3-5D6). This may point towards a synergistic interaction

between the MFCs and the DCM because collagen X was not expressed by MFCs alone in the pellet model nor was it detected in the empty DCM, but it was present when the two were combined even in the absence of TGF- $\beta$ 3.

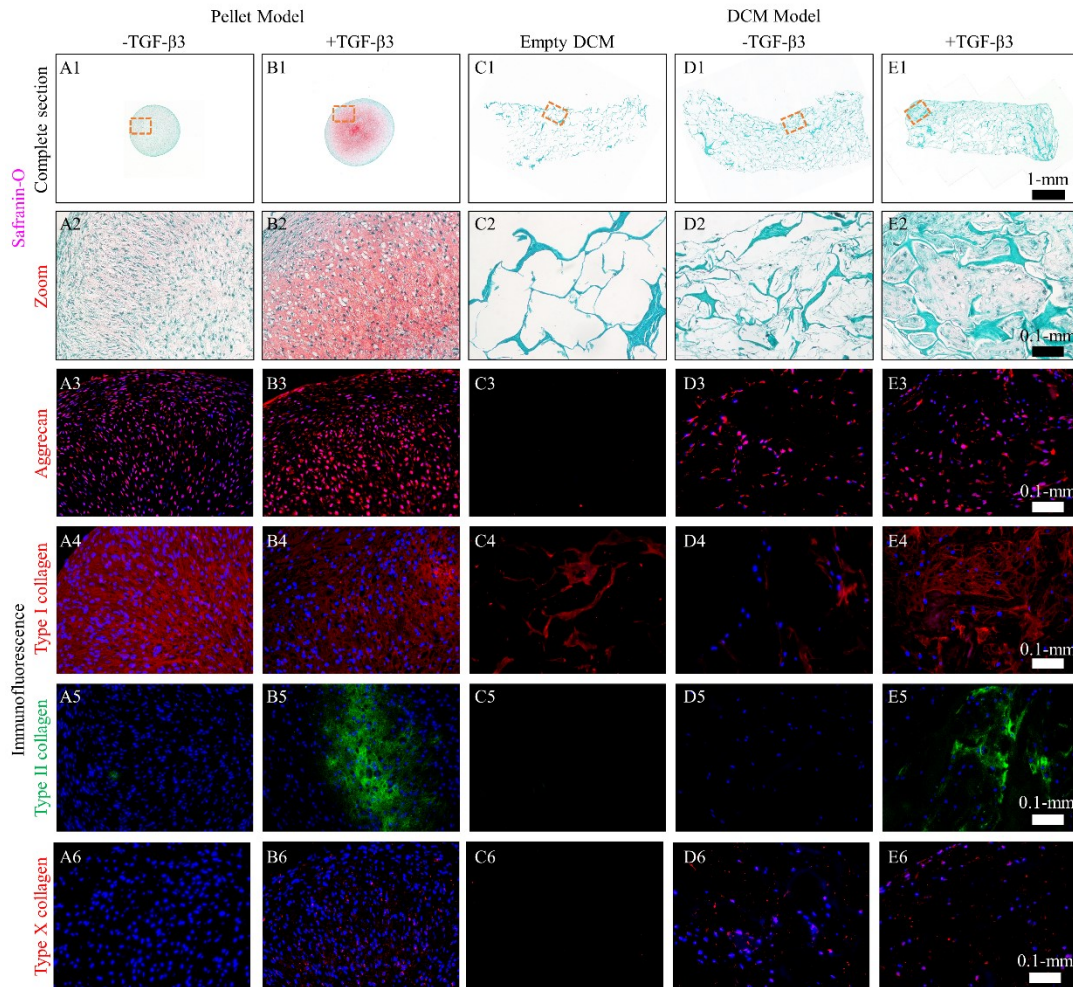


**Figure 3-5:** Safranin-O staining and immunofluorescence of meniscus extracellular matrix (ECM) molecules of meniscus fibrochondrocyte (MFC)-based tissues after 21 days' culture in either pellets or meniscus-derived decellularized matrix (DCM) with and without supplementation of 10 ng/mL TGF- $\beta$ 3. DAPI staining (in blue) for cell nuclei is superimposed in all images with the exception of the Safranin O stained images. The

series of images labeled as A1-A6, and B1-B6 represent micrographs derived from pellet cultures of MFC in the absence and presence of TGF- $\beta$ 3, respectively. The series of images labeled as C1-C6 represent micrographs of cell-free DCM scaffold after 21-days incubation in serum-free growth media. The series of images labeled as D1-D6, and E1-E6 represent micrographs derived from DCM cultures of MFC in the absence and presence of TGF- $\beta$ 3, respectively.

### 3.3.4 mRNA gene expression

We used qRT-PCR to measure the expression of a profile of chondrogenic (Fig.3-6) and hypertrophy/osteogenesis-associated (Fig.3-7) genes. Chondrogenic genes *ACAN* (aggrecan, Fig.3-6A), *COL2A1* (type II collagen, Fig.3-6B), and *SOX9* (Fig. 3-6D) all followed similar expression profiles, with a poor expression without TGF- $\beta$ 3 supplementation and elevated expression in response to TGF- $\beta$ 3. Expression of *ACAN* and *COL2A1* were minimal in the absence of TGF- $\beta$ 3 even on the DCM, further confirming the absence of chondrogenic bioactive factors. *ACAN* and *COL2A1* expression tended to be greatest in the DCM/+TGF- $\beta$ 3 condition. In the absence of TGF- $\beta$ 3, it appeared that expression of the chondrogenic genes mentioned above was elevated in the pellets relative to the DCM, which may reflect the rounded 3D environment of pellets versus the flattened morphology observed in the DCM model. As an example, *ACAN* expression relative to the pellet/-TGF- $\beta$ 3 condition was upregulated 20-fold and 98-fold in the pellet and DCM models with TGF- $\beta$ 3, respectively, whereas it

downregulated 2.7-fold in the DCM/-TGF- $\beta$ 3 ( $p=0.085$ ). Culture in the DCM significantly increased relative expression of *COL1A2* (Fig. 3-6C), which encodes part of the primary constituent of the meniscus. This may reflect the nature of the DCM scaffold being primarily type I collagen and the altered 3D environment of the cells. With regards to hypertrophy-associated genes (i.e. *COL10A1* and *MMP-13*; Fig. 3-7A/B) and osteogenic genes (i.e. *RUNX2*, *ALPL* and *BSP*; Fig. 3-7C/D/E), all tended to be upregulated by TGF- $\beta$ 3 supplementation. Comparing the no TGF- $\beta$ 3 (i.e.-TGF- $\beta$ 3) groups' expression of all hypertrophy-related genes except for *BSP* was elevated in the DCM relative to the pellet but generally lower than in +TGF- $\beta$ 3 groups. For example, *COL10A1* expression relative to the pellet model was upregulated in the DCM model by an average of 2.7-fold ( $p<0.05$ ), whereas it was increased in +TGF- $\beta$ 3 groups relative to -TGF- $\beta$ 3 groups by an average of 111-fold ( $p<0.05$ ).

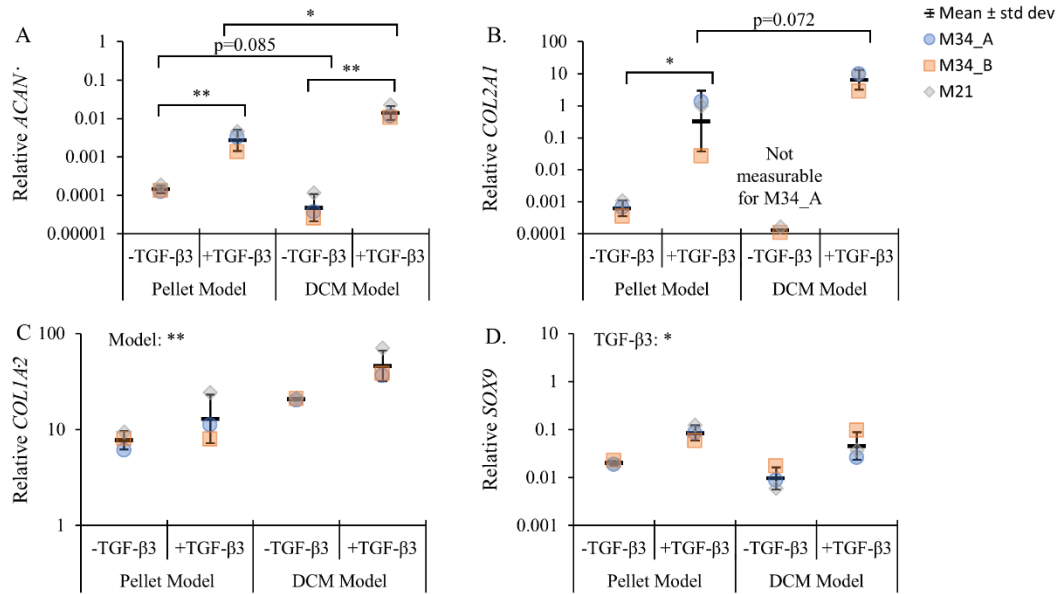


**Figure 3-6:** Relative expression of chondrogenic differentiation-related genes in meniscus fibrochondrocyte (MFC)-based tissues after 21-days' culture in either pellets or meniscus-derived decellularized matrix (DCM) with and without supplementation of 10 ng/mL TGF-β3. A) Aggrecan (*ACAN*); B) Type II collagen (*COL2A1*); C) Type I collagen (*COL1A2*); and D) *SOX9*. Values are presented as  $2^{\Delta C_t}$ , where  $\Delta C_t$  is the difference in  $C_t$  values of the average of three house-keeping genes and the gene of interest. Each data point represents the average of 1 or 2 biological replicates. P-values are derived from two-way within-subjects ANOVA using  $\Delta C_t$  values. P-values greater than 0.1 were suppressed. \*:  $p < 0.05$ , \*\*:  $p < 0.01$ .

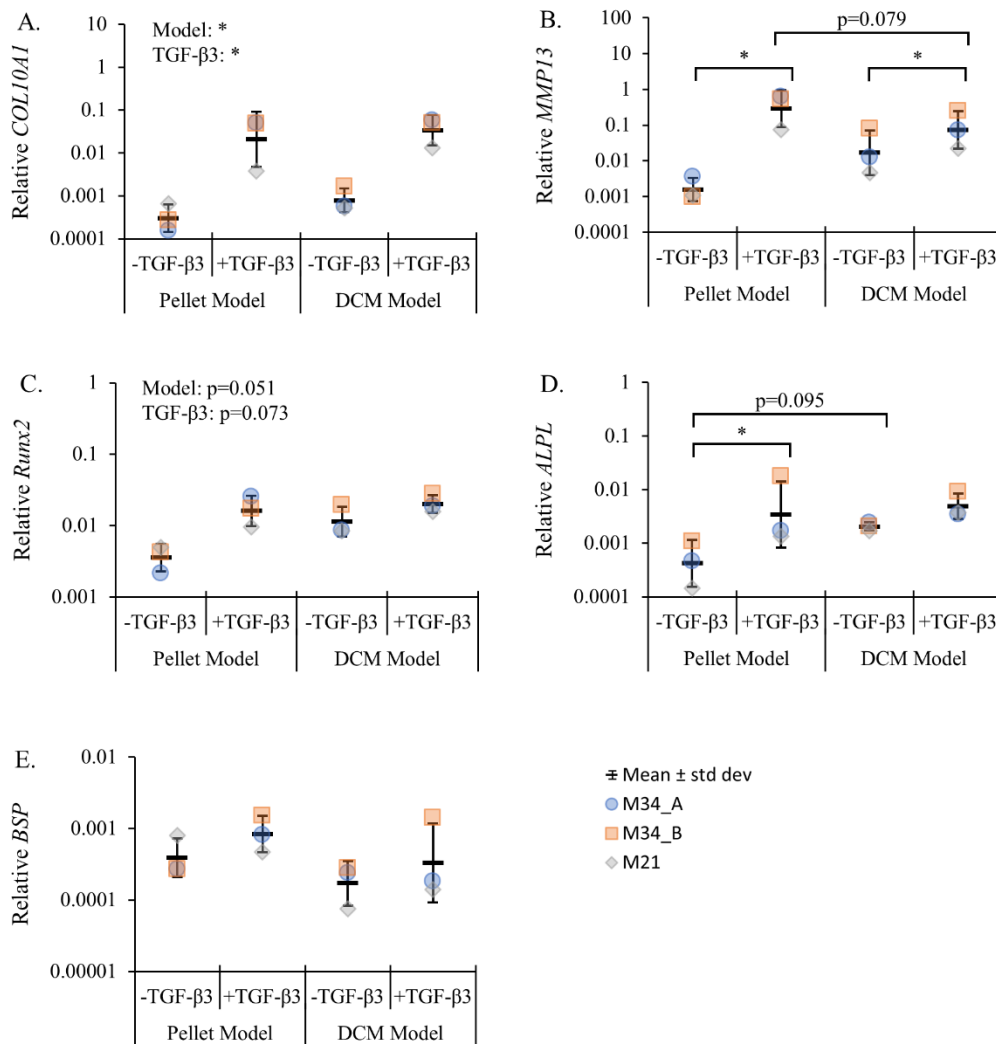


**Figure 3-7:** Relative expression of hypertrophy-associated genes in meniscus fibrochondrocyte (MFC)-based tissues after 21-days' culture in either pellets or meniscus-derived decellularized matrix (DCM) with and without supplementation of 10 ng/mL TGF-β3. A) Type X collagen (*COL10A1*); B) Matrix Metalloproteinase-13 (*MMP-13*); C) Runt related transcription factor 2 (*RUNX2/CBFA1*); D) Alkaline phosphatase (*ALPL*); and E) Bone sialoprotein (*BSP*). Values are presented as  $2^{\Delta C_t}$ , where  $\Delta C_t$  is the difference in  $C_t$  values of the average of three house-keeping genes and the gene of

interest. Each data point represents the average of 1 or 2 biological replicates. P-values are derived from two-way within-subjects ANOVA using  $\Delta C_t$  values. P-values greater than 0.1 were suppressed. \*:  $p < 0.05$ .

### 3.4 Discussion

In this study, we investigated whether human meniscus-derived decellularized matrix (DCM) scaffold had the capacity to re-differentiate and stimulate the inner-meniscus like extracellular matrix (ECM)-forming phenotype of *in vitro* expanded human meniscus fibrochondrocytes (MFCs). The investigation was implemented under low oxygen tension culture conditions (i.e. 3%O<sub>2</sub>) as a mimic of the low oxygen microenvironment of MFC within native menisci in synovial the knee joint [241], and as a reported pro-chondrogenic environmental factor [258]. Moreover, the study was performed both in the absence and presence of exogenously supplemented chondrogenic morphogen (i.e. TGF- $\beta$ 3). Furthermore, human MFCs have been reported to lose mRNA expression of functional inner meniscus-relevant matrix components; type II collagen and aggrecan, after *in vitro* monolayer expansion [12], we supplemented the monolayer expansion of our human MFCs in with TGF- $\beta$ 1 (1 ng/mL) and FGF-2 (5 ng/mL) under normoxia (NRX) which may maintain their ECM-forming response to chondrogenic stimulation [246]. The population doublings (PD: 2.91-3.66) of the human MFCs used in this study were within the range shown to generate the most inner meniscus-like ECM in the cell pellet model [246]. To the best of our knowledge, this is the first study showing that

human MFCs can attach, proliferate and undergo chondrogenic re-differentiation within a human meniscus-derived DCM. We observed the accumulation of inner meniscus-like matrix including aggrecan and types I & II collagen.

To assess the capacity of the meniscus-derived DCM to re-differentiate dedifferentiated MFC under hypoxic conditions, we compared it with the re-differentiation of the MFC in a cell aggregate pellet under chondrogenic stimulation mediated by TGF- $\beta$ 3. Based on the biochemical analysis (GAG and GAG/DNA), pure DCM did not facilitate chondrogenic re-differentiation of dedifferentiated MFC without TGF- $\beta$ 3 supplementation. However, DNA data showed that it did facilitate MFC proliferation relative to the cell pellet model and surprisingly a synergistic upregulation of collagen X at both the transcript and translation levels. Moreover, the upregulation of collagen X was concomitant with an increased transcriptional expression of *MMP-13*. The mechanism underlying the concomitant increase is unclear but appears to be consistent with the activation of the Indian hedgehog (Ihh) pathway. Activation of Ihh has been reported to promote chondrocyte hypertrophy (i.e. collagen X as a marker of chondrocyte hypertrophy) and *MMP-13* expression [259]. Our findings with regards to the enhanced proliferation of MFC on the DCM scaffold was consistent the findings of previous report that decellularized porcine meniscus supported the proliferation of human primary chondrocytes [249].

Even though we observed no difference in GAG accumulation between the DCM and

pellet models, much more intense Safranin-O positive matrix was observed in the pellet model and aggrecan immunofluorescence, indicating a higher concentration of sulfated proteoglycans. This is despite the two models having started with the same number of cells. The difference in staining intensity may be the product of several factors. First, the high density of cells in the pellet model favors the concentration of newly-synthesized matrix into a smaller space; this is evident by considering the Safranin-O section sizes in Fig. 3-5B2. Second, the proliferation we observed on the DCM would have led to increased nutritional demands, causing the volume of supplied medium to potentially limit the rate of ECM formation with chondrogenic stimulation [260]. Third, the cell pellet model, which mimics the condensation environment during embryonic chondrogenic differentiation, allows more direct cell-to-cell communication [261, 262].

Our previous study showed that  $5-10 \times 10^6$  BMSCs/cm<sup>3</sup> seeded on type I collagen scaffold promoted better chondrogenic differentiation compared to other seeding densities [263]. The seeding density of MFCs in the current study was about  $8.8-9.8 \times 10^6$  MFCs/cm<sup>3</sup>, which is within the optimal seeding density for BMSCs on a type I collagen scaffold [263]; however, different capacities of ECM formation regarding collagen and GAG between MFCs and MSCs have been reported [146, 153] indicating that the cell-seeding density of human MFCs on the DCM may need to be optimized. In addition to seeding density, another factor that affects the accumulation of ECM is the chondrogenic culture time, which led to the dramatic accumulation of GAG, collagen, and more intense

ECM staining [92, 146]. Longer time points are of interest for future investigation to see if MFCs can fully populate and fill meniscus-derived DCM with dense newly-formed ECM.

In our previous study with human synovial fluid-derived MSCs seeded upon a different human meniscus DCM treated with combined TGF- $\beta$ 3 and insulin-like growth factor 1 (IGF-1) but with otherwise similar culture conditions, we observed more intense Safranin-O staining and type II collagen than in the present study [255]. Furthermore, the cell morphology on the construct surface of SF-MSCs in the previous study displayed obvious differences to MFCs in the present study under scanning electron microscopy. Round-shaped human SF-MSCs resided upon the surface yet were separate from the newly-synthesized matrix, appearing to lay down collagen fibers [255]. In contrast, the MFCs in the present study were elongated, flat-shaped, and well-integrated into the newly-synthesized matrix. Cell shape may be related to the capacity of cells to go through chondrogenic differentiation; a previous report showed that limb bud MSCs underwent spontaneous chondrogenesis after being forced into a round shape by disruption of cytoskeleton using cytochalasin D [264].

We next investigated the bioactive effects of human meniscus DCM on MFCs without chondrogenic growth factors under hypoxia. The goal was to identify whether the native human meniscus DCM could drive the re-differentiation of dedifferentiated MFCs without growth factor supplementation, perhaps through the presence of sequestered

bioactive factors as was reported for bone and cartilage-derived DCM [254, 265]. Human MFCs cultured in the DCM without TGF- $\beta$ 3 produced an immature-looking matrix that did not stain for Safranin-O nor show the presence of type II collagen, which was corroborated at the gene expression level (Fig.3-6). This was consistent with our previous findings with human meniscus-derived DCM and human SF-MSCs. These are also consistent with previous studies that DCM extracted from porcine articular cartilage promoted robust chondrogenic differentiation of human BMSCs only with exogenous growth factors [142]. The absence of Safranin-O staining on the empty DCM may indicate the potential loss of growth-factor binding matrix proteins during the preparation protocol [266]. Previous studies preparing meniscus DCM showed loss of GAG but residual collagen regardless of the processing methods and species [267-269], which is consistent with our type I collagen immunofluorescence. Porcine meniscus-derived DCM generated by acid treatment was reported to retain most of the GAG and collagen content relative to the native tissue; this may explain the re-differentiation of human primary chondrocytes without growth factors observed in that study, although this could also be due to cell type [249].

It was interesting to find type X collagen immunofluorescence in the DCM with dedifferentiated MFCs in the absence of TGF- $\beta$ 3 but not in the pellet model. This was supported by an increased *COL10A1* transcript in the DCM model. Moreover, the expression of *COL10A1* was accompanied with upward trend in expression of other

hypertrophic and osteogenic genes in the DCM model relative to the pellet model without growth factors. These findings suggest the possible presence of hypertrophic and osteogenic factors in the human meniscus-derived DCM. An alternative explanation is that the observed collagen X expression by MFCs on the DCM may be the product of the scaffold-based, 3D culture environment rather than bioactivity inherent to the DCM. Further study incorporating a control using a known non- or minimally bioactive scaffold material may be necessary to rule out this alternative explanation.

We also applied low oxygen tension during chondrogenic culture since it has been shown to enhance ECM formation of human MFCs in the pellet model [11, 242, 246], and reduce hypertrophic differentiation of human bone marrow mesenchymal stem cells [15]. The finding of Safranin-O positive ECM with trace immunofluorescence of type II collagen in the cell pellet is consistent with previous report of 2% oxygen tension driving the chondrogenic differentiation of human BMSCs in pellet model [270]. However, this finding was inconsistent with our previous finding that hypoxia alone was not sufficient to drive the chondrogenic differentiation of human MFCs in the pellet model [242]. The inconsistency may be due to methodological differences in culture under hypoxic conditions and the use of a more sensitive biotinylated secondary antibody for collagen II detection in the present study. Our previous work was implemented under continuous hypoxic conditions whereas in the present study, the pellet and DCM constructs experienced 5-10 minutes reoxygenation during the medium change twice a

week.

Perhaps the most important limitation of this study is the physical method for DCM preparation. Our study results here, taken together with previous work showing the presence of inductive factors within meniscus DCM, may indicate that the DCM preparation resulted in a partial loss of bioactive factors contained within the meniscus matrix. Other methods for DCM preparation such as acid treatment [249] may have maintained these potential bioactive factors in the DCM preparation. Another potential limitation of the current study is the use of a single meniscus donor (a 72-year old male) for DCM preparation. Future work would be necessary to determine if the observed results for this meniscus DCM are consistent across multiple meniscus donors. Much work remains towards development of a meniscus implant based on a meniscus DCM; this will include evaluation of immunogenicity and potential tissue rejection as well as achieving suitable biomechanical properties for implant function within the knee.

### **3.5 Conclusion**

In summary, we found that the bioactivity of the decellularized matrix from human cadaver-derived meniscus on human MFC was to support chondrogenic differentiation and a relatively proliferative phenotype in the presence of exogenous TGF- $\beta$ 3. Moreover, the pure DCM did not induce chondrogenic re-differentiation of dedifferentiated human MFC.

**Chapter 4 Hypoxic pre-culture of human meniscus fibrochondrocytes promotes non-calcifying vascularized matrix at ectopic sites in nude mice**

**Yan Liang, Alexander R.A. Szojka, Lynn B. Williams, Enaam Idrees, Xiaoyi Lan, Melanie Kunze, Aillette Mulet-Sierra, Mark F. Sommerfeldt, Nadr M. Jomha, Adetola B. Adesida**

This chapter has been submitted for publication.

## 4.1 Introduction

The avascular inner meniscus is non-healing in adults. This presents a clinical challenge as inner meniscus tears are linked to the early development of osteoarthritis, even after minimally-invasive surgical intervention to remove damaged tissues [3]. A proposed strategy to address this problem is meniscus tissue engineering (TE). Meniscus TE may involve *in vitro* growth and subsequent implantation of functional inner meniscus-like ECM (IM-ECM) using autologous cells [9, 134].

Previously, we demonstrated a strategy to acquire large numbers of cells that produce IM-ECM under growth factor (TGF- $\beta$ 3) supplementation (Chapter 1) [246]. This involved the isolation of human meniscus fibrochondrocytes (hMFC) from partial meniscectomy biopsies followed by monolayer expansion with a two-growth factor combination of transforming growth factor- $\beta$ 1 (TGF- $\beta$ 1) and basic fibroblast growth factor (FGF-2) – abbreviated as T1F2.

Low oxygen (hypoxia (HYP)) compared to uncontrolled oxygen levels (i.e., near-atmospheric: normoxia (NRX)) during *in vitro* culture has consistently been shown to promote the synthesis of inner meniscus and cartilage-specific constituents, type II collagen and sulfated proteoglycans, by hMFCs under transforming growth factor- $\beta$ 3 (TGF- $\beta$ 3) supplementation within a cell pellet model [11, 242, 246]. However, this finding does not always extend to larger-scale three-dimensional (3D) scaffold models [14, 96]. To allow more time for such ECM accumulation and maturation, long-term

culture ( $\geq 6$ -weeks) periods have been used in the context of cartilage TE with animal cells [271, 272] and meniscus TE with hMFC [92] or animal MFCs [146], and also combined with HYP conditions for animal MFCs [273]. However, long-term culture under HYP has not been investigated for hMFC in the context of a 3D scaffold model. Another strategy to enhance IM-ECM may be transient TGF- $\beta$ 3 supplementation during scaffold-based culture [274, 275]. Such strategies, involving withdrawal of TGF- $\beta$ 3 supplementation after 2-weeks' culture, was previously shown to enhance the functional properties of bovine calf chondrocyte-based tissues compared to continuous supplementation of TGF- $\beta$ 3 using agarose as a 3D scaffold model [276]. However, this type of strategy has not yet been tested using MFCs, nor has it been combined with HYP. Our previous investigation with T1F2-expanded hMFCs in a cell pellet model showed that limited IM-ECM formation could occur without growth factor supplementation under HYP [277]. Together, these formed the basis of our speculation that strategies involving transient TGF- $\beta$ 3 supplementation may be promising to enhance IM-ECM synthesis by T1F2-expanded hMFC, especially under HYP.

*In vitro*-formed cartilaginous ECM and IM-ECM using human mesenchymal stem cells (hMSCs) [120, 121] and hMFC [94] respectively have been shown to undergo undesirable changes upon ectopic implantation in the commonly-used subcutaneous nude mouse (SNM) model. These changes include ECM degradation, blood vessel invasion, and hypertrophic differentiation with potential resulting calcification, all of which appear

to be interrelated processes and partially regulated by oxygen tension. For example, HYP *in vitro* culture has been shown to suppress hypertrophic differentiation of bone marrow-derived hMSCs [15] and promote expression of factors associated with angiogenesis such as VEGF and SDF-1 [278]. From a meniscus TE perspective, vascularization of an implant or the native inner meniscus may be a desirable outcome as it could lead to integration and healing of damaged avascular inner meniscus tissue [279]. However, the performance of IM-ECM-rich hMFC-based tissues within an *in vivo* microenvironment such as the SNM model and the potential contributions of HYP pre-culture have yet to be investigated. To this end, this study had the following objectives, using hMFCs on a clinically approved and commercially available collagen scaffold: 1) determine the effects of transient and continuous exposure to TGF- $\beta$ 3 supplementation under HYP and NRX over a long-term *in vitro* culture period on IM-ECM formation; 2) assess *in vivo* behavior within the SNM model after 3-weeks of *in vitro* pre-culture with TGF- $\beta$ 3 supplementation under HYP and NRX with regard to degradation, hypertrophic differentiation, calcification, and vascularization.

## **4.2 Methods**

### **4.2.1 Ethic statements**

The meniscus specimens were collected with the approval of the University of Alberta's Health Research Ethics Board- Biomedical Panel (Study ID: Pro00018778). Work involving research animals was conducted in accordance with protocols approved by the

University of Alberta Animal Care Committee (AUP00001363).

#### **4.2.2 Human meniscus fibrochondrocyte (hMFC) isolation and expansion**

Human meniscus specimens were obtained from 6 patients (5 male/1 female, ages: 28±4 years old (mean ± standard deviation (SD)), range: 21-34 years old) undergoing partial meniscectomy after acute meniscus injuries (see Table 4-1 -patient information). hMFC isolation was performed as previously described [246]. Briefly, hMFCs were released from the specimens by collagenase treatment. Isolated hMFCs were plated into standard tissue culture flasks and cultured using a standard high glucose DMEM supplemented with 10% (v/v) fetal bovine serum (“DMEM complete”) for 5 days under near-atmospheric oxygen tension (~20% O<sub>2</sub>; 5% CO<sub>2</sub>/95% air) at 37°C in a humidified incubator. Non-adherent cells were removed by aspiration during the medium change, and the number of viable hMFCs were counted after 5 days (passage 0, P0). hMFCs were reseeded into flasks at 10<sup>4</sup> cells/cm<sup>2</sup> and cultured in DMEM complete supplemented with FGF-2 (5 ng/mL) and TGF-β1 (1 ng/mL) (T1F2) in the same incubator (P1). Once cells reached 90-95% confluence, hMFCs from each donor were frozen separately into cryogenic vials (mean cell number (16.4±4.4)×10<sup>6</sup>) and banked in liquid nitrogen for less than one month. To set up experiments, one vial of hMFCs from each donor was thawed and cultured in the standard DMEM culture medium for 12 hours. The viable adherent cells were counted and reseeded at 10<sup>4</sup> cells/cm<sup>2</sup> under the same culture conditions using T1F2 to produce P2 cells for experimental use. The population doublings (PDs) of

hMFCs were calculated as  $\log_2(N/N_0)$ , where  $N_0$  is the number of cells plated at the beginning of a passage and  $N$  is the number of cells counted at the end of a passage [221]. Cumulative PDs were calculated as the sum of PDs from P1 and P2.

**Table 4-1:** Meniscus tissue donor information

<b>Identifier</b>	<b>Age</b>	<b>Aex</b>	<b>Meniscus</b>	<b>Implanted</b>
Donor 1	30	Male	Right knee medial	Yes
Donor 2	27	Male	Left knee medial	Yes
Donor 3	34	Female	Right knee medial	Yes
Donor 4	25	Male	Right knee medial	No
Donor 5	21	Male	Left knee lateral	No
Donor 6	31	Male	Right knee medial	No

### 4.2.3 Culture of hMFCs on Chondro-Gide scaffolds

T1F2-expanded hMFCs at the end of P2 were used for chondrogenic re-differentiation as previously described [14, 246]. A type I and III collagen membrane scaffold (Chondro-Gide, Geistlich Pharma, Wolhusen, Switzerland) served as a 3-dimensional structure for hMFC growth and extracellular matrix deposition. Discs of 6 mm diameter and 2 mm thickness were biopsy punched from the same lot of membrane scaffolds to control for lot to lot variability. hMFCs at  $5 \times 10^5$  per scaffold were seeded onto the porous side of each scaffold and then cultured in 1 mL of a defined serum-free chondrogenic medium with TGF- $\beta$ 3 (10 ng/mL). The cell-scaffold constructs were placed under either NRX or hypoxia (HYP; 3% O<sub>2</sub>) with 5% CO<sub>2</sub> at 37°C. Hypoxic culture was implemented in an Xvivo X3 incubator system (Biospherix, NY, USA). In previous studies from our lab,

media changes for both NRX and HYP took place at atmospheric conditions (21% O<sub>2</sub>, room temperature, pre-warmed media to 37°C in a water bath) for less than 5 minutes of exposure, with the medium change performed twice per week [246]. By using the Biospherix incubator system, we avoided this re-oxygenation limitation as the HYP conditions were maintained during media changes, and media was additionally equilibrated to HYP conditions for 2 h before use. Thus, our HYP samples experienced continuous low oxygen tension during the entirety of *in vitro* culture.

#### **4.2.4 Experimental conditions**

##### **4.2.4.1 *In vitro* culture model**

To examine the effects of transient exposure and continuous culture of TGF-β<sub>3</sub> on the IM-ECM of T1F2-expanded hMFC under different oxygen tensions, three experimental groups were set up: 1) 3 weeks' culture in the serum-free chondrogenic medium (SFM) with TGF-β<sub>3</sub> (*T3*), dexamethasone (*D*), ascorbic acid 2-phosphate (*A*) and L-proline (*P*) (T3DAP/3wks) (n=6); 2) similar to the first group except with five additional weeks' culture in SFM with T3DAP (T3DAP/8wks) (n=6); 3) Similar to the first group except with five additional weeks' culture in SFM in medium with DAP but with TGF-β<sub>3</sub> withdrawn for the later culture period (DAP/8wks) (n=3). All three of these groups were carried out in both oxygen tensions (six groups total).

##### **4.2.4.2 *In vivo* ectopic subcutaneous implantation in nude mouse (SNM) model**

To evaluate the *in vivo* behavior of the engineered meniscus ECM, especially with

regards to degradation, angiogenic potential, and hypertrophic differentiation with resultant calcification, the constructs derived from T3DAP/3wks in each oxygen tension were divided into two experimental groups: 1) five additional weeks' culture implanted subcutaneously in nude mice (Implantation/8wks) (n=3); 2) five additional weeks' culture in DMEM complete *in vitro* as a control (DMEM/8wks *in vitro*) (n=3).

The neo-matrix was implanted into the dorsal subcutem of athymic CD-1 nude mice (n=9, 7 weeks old, Charles River, Wilmington, USA) as previously described [280]. Four constructs for each condition (T3DAP/3wks in HYP and NRX) for n=3 hMFC donors were implanted into the backs of n=6 nude mice total plus 3 additional mice with one empty scaffold each. Four incisions (4-5 mm, 2 cranial and 2 caudal) were made on the skin of each mouse using sterile technique. Small subcutaneous pockets were bluntly dissected and immediately implanted with constructs. Incisions were closed with suture and cyanoacrylate tissue adhesive. No post-surgical complications were observed. After implantation for 5 weeks mice were euthanized by CO<sub>2</sub> inhalation and constructs were macroscopically dissected from murine subcutaneous tissues.

At the end of each culture period *in vitro* and *in vivo*, the gross morphologies of constructs were assessed using a stereo microscope (Stemi 2000-C, Zeiss, Oberkochen, Germany), followed by biochemical analysis for glycosaminoglycan (GAG) and DNA content, histology and immunofluorescence for cartilage-specific matrix proteins, angiogenic factors, calcium deposition, and blood vessel invasion, and by real-time

quantitative reverse transcription-polymerase chain reaction (qRT-PCR) for gene expression analysis (for primer information see Table 4-2). The methods were performed as previously described [280] except the gene expression levels were normalized to three housekeeping genes:  $\beta$ -actin, Ribosomal Protein L13a (*RPL13A*) and Tyrosine 3-Monooxygenase/Tryptophan 5-Monooxygenase Activation Protein Zeta (*YWHAZ*), using the  $2^{-\Delta\text{ct}}$  method [219].

**Table 4-2:** Primer sequences

<i>Genes</i>	<i>Forward</i>	<i>Reverse</i>	<i>GenBank accession</i>
$\beta$ -actin ( <i>ACTB</i> )	AAGCCACCCCACTTCTCTC TAA	AATGCTATCACCTCCCCTGT GT	NM_00110 1.4
Beta-2 microglobulin ( <i>B2M</i> )	TGCTGTCTCCAATGTTTGATG TATCT	TCTCTGCTCCCCACCTCTA AGT	NM_00404 8.3
Tyrosine 3 Monooxygenase/Tryptophan 5-Monooxygenase Activation Protein Zeta ( <i>YWHAZ</i> )	TCTGTCTTGTACCAACCAT TCTT	TCATGCGGCCTTTTTCCA	NM_00340 6.3
Aggrecan ( <i>ACAN</i> )	AGGGCGAGTGGAATGATGT T	GGTGGCTGTGCCCTTTTTA C	NM_00113 5.3
Collagen I ( <i>COL1A2</i> )	GCTACCCAACTTGCCTTCAT G	GCAGTGGTAGGTGATGTTC TGAGA	NM_00008 9.3
Collagen II ( <i>COL2A1</i> )	CTGCAAATAAAATCTCGG TGTTCT	GGGCATTTGACTCACACCA GT	NM_00184 4.5
SRY-Box 9 ( <i>SOX9</i> )	CTTTGGTTTGTGTTTCGTGTT TTG	AGAGAAAGAAAAAGGGAA AGGTAAGTTT	NM_00034 6.3
<i>HIF-1<math>\alpha</math></i>	GTAGTTGTGGAAGTTTATGC TAATATTGTGT	TCTTGTTTACAGTCTGCTC AAAATATCTT	NM_00153 0.4
<i>HIF-2<math>\alpha</math></i>	GGTGGCAGAACTTGAAGGG TTA	GGGCAACACACACAGGAA ATC	NM_00143 0.5

			(EPAS1)
<i>VEGF</i>	GCACGGTCCCTCTTGAA	CGGTGATTTAGCAGCAAGA AAA	NM_00117 1623.1
<i>TGF-β1</i>	GGGAAATTGAGGGCTTTCG	AGTGTGTTATCCCTGCTGT CACA	XM_01152 7242.2
<i>TGF-β2</i>	CGAGAGGAGCGACGAAGA GT	AGGGCGGCATGTCTATTTT G	NM_00113 5599.3
<i>TGF-β3</i>	CTGGCCCTGCTGAACTTTG	AAGGTGGTGCAAGTGGAC AGA	NM_00323 9.4
Collagen X ( <i>COL10A1</i> )	GAAGTTATAATTTACTACTGA GGGTTTCAAA	GAGGCACAGCTTAAAAGTT TTAAACA	NM_00049 3.3
Matrix metalloproteinase- 13 ( <i>MMP-13</i> )	CATCCAAAAACGCCAGACA A	CGGAGACTGGTAATGGCAT CA	NM_00242 7.4
Chondromodulin- 1 ( <i>CHM-1</i> )	GCGCAAGTGAAGGCTCGTA T	GTTTGGAGGAGATGCTCTG TTTG	NM_00701 5.3
Gremlin 1 ( <i>GREM1</i> )	CATGTGACGGAGCGCAAAT A	GCTTAAGCGGCTGGGTTTT	NM_01337 2.7
Frizzled-related protein ( <i>FRZB</i> )	GCATCCCCCTGTGCAAGT	GCAGGTGGTTGGGCATCTT A	NM_00146 3.4

#### 4.2.5 Statistical analysis and principal component analysis (PCA)

The quantitative data were presented as mean ± SD. Statistical analysis was performed as previously described [246]. Different culture conditions were compared using one-way analysis of variance (ANOVA) with Tukey's multiple comparison post hoc tests within the same oxygen tension. For comparison between the two oxygen tensions within the same passage, a Student's t-test was used. Significance was considered when  $p < 0.05$ . We used principal component analysis (PCA) to summarize all quantitative data. Individual measurements that fell below a Kaiser-Meyer-Olkin (KMO; measures for sampling adequacy) of 0.5 were excluded. We used SPSS version 25 to perform PCA.

## 4.3 Results

### 4.3.1 Cell yield and proliferation rates during monolayer expansion

The primary MFCs after collagenase digestion were heterogeneous with elongated fibroblast-like (orange arrow) and round-shaped chondrocyte-like (red arrow) morphologies (Fig. 4-1A). TGF $\beta$ 1/FGF2 (T1F2)-expanded hMFCs in P2 became mostly elongated and spindle-like with some round-shaped cells (Fig. 4-1C). Mean wet weights ( $\pm$  SD) of the meniscus tissues (n=6) were  $1.65 \pm 0.82$  g before collagenase digestion. The viable cell yields after 5 days' culture (passage 0, P0) post-digestion was  $7.94 \pm 2.79 \times 10^6$  cells, i.e.,  $5.41 \pm 1.41 \times 10^6$  per g tissue. After 6-8 days' culture with T1F2 in P1, the mean population doublings and population doublings per day were  $3.04 \pm 0.32$  and  $0.43 \pm 0.06$  (Fig. 4-1D/E), respectively. The percentage of viable adherent cells after thawing from liquid nitrogen and 12 h culture was  $52.2 \pm 12.5\%$  (not included). The population doublings per day in P2 were  $0.61 \pm 0.03$  (Fig. 4-1E), which was significantly higher than P1 ( $p < 0.001$ ). The cumulative population doublings for the hMFCs used to set up experiments were  $6.82 \pm 0.56$  (Fig. 4-1D).

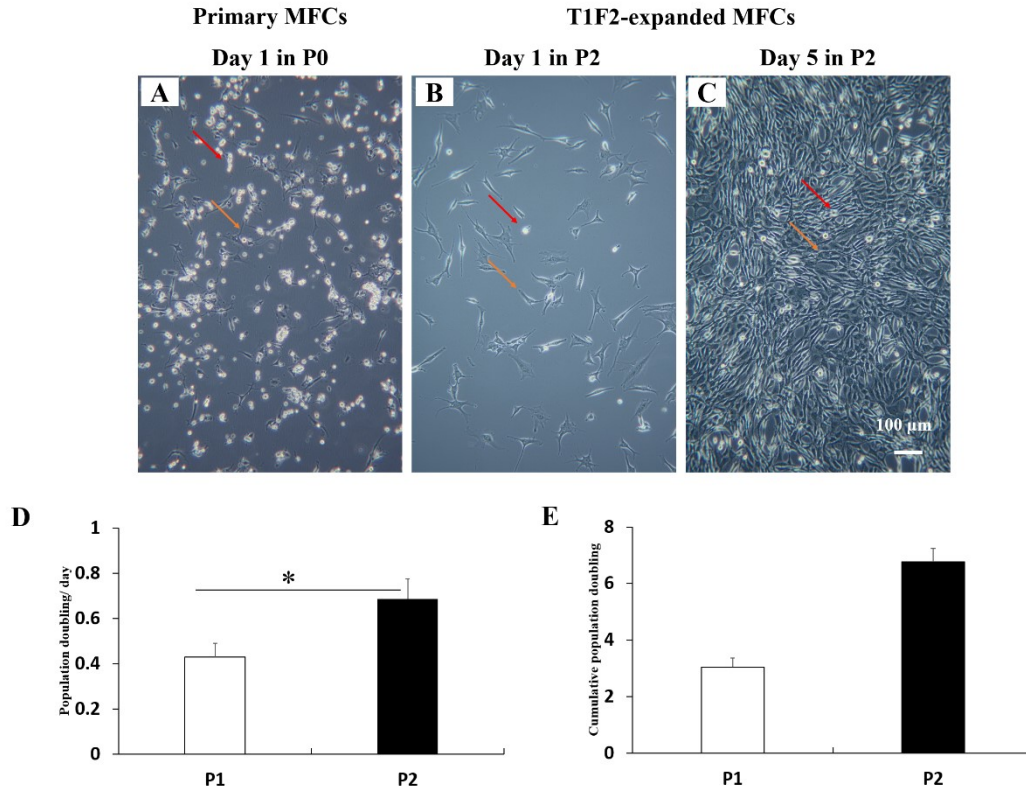


**Figure 4-1:** Monolayer *in vitro* cell expansion with TGF- $\beta$ 1 and FGF-2 (T1F2) under normoxia (NRX, 21% O<sub>2</sub>). (A) Cell morphologies of primary human meniscus fibrochondrocytes (hMFCs) in passage 0 (P0); (B, C) expanded hMFCs in P2 after liquid nitrogen storage; (D) Cumulative population doublings at the end of P1 and P2; (E) population doublings per day during P1/P2.

### 4.3.2 Biochemical GAG/DNA quantification

Biochemical analysis was performed to quantify the GAG and DNA contents after each *in vitro* culture stage (total 8 weeks). Within the HYP groups, there were no significant differences in GAG (Fig. 4-2A), DNA (Fig. 4-2B) or GAG/DNA (Fig. 4-2C) in comparing the transient exposure to TGF- $\beta$ 3 group (DAP/8wks) to the baseline group

T3DAP/3wks. In contrast, the continuous supplementation group with T3DAP for 8 weeks (T3DAP/8wks) resulted in significantly higher GAG content (T3DAP/8wks vs T3DAP/3wks,  $p<0.001$  and T3DAP/8wks vs DAP/8wks,  $p=0.013$ ), and GAG/DNA content (T3DAP/8wks vs T3DAP/3wks,  $p<0.001$  and T3DAP/8wks vs DAP/8wks,  $p=0.001$ ) than both T3DAP/3wks and DAP/8wks constructs. The DNA content was significantly higher in T3DAP/8wks relative to T3DAP/3wks ( $p=0.002$ ).

Within the NRX groups, the total GAG and GAG/DNA contents appeared to be lower in DAP/8wks constructs compared to T3DAP/3wks and T3DAP/8wks, but there were no significant differences. Moreover, there were no significant differences between the DNA contents of the groups.

Between oxygen tensions, HYP consistently had significantly upregulated the total GAG contents (T3DAP/8wks ( $p<0.001$ ) and DAP/8wks ( $p=0.002$ )) and GAG/DNA (T3DAP/3wks ( $p=0.018$ ), T3DAP/8wks ( $p<0.001$ ) and DAP/8wks ( $p=0.004$ )) relative to NRX in each culture condition except for total GAG in T3DAP/3wks group. In terms of DNA, there was significantly higher content in the T3DAP/8wks group under HYP compared to NRX ( $p=0.004$ ).

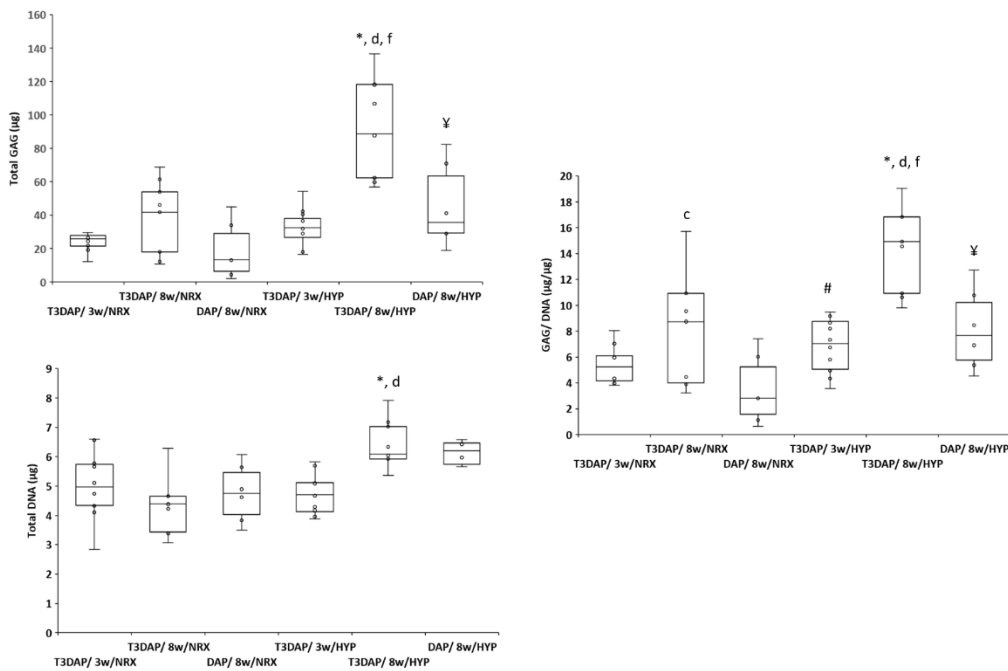


**Figure 4-2:** Glycosaminoglycan (GAG) matrix and DNA contents in hMFCs-based constructs cultured in vitro. GAG (A), DNA (B), and GAG/DNA (C) in vitro. T3: TGF- $\beta$ 3, D: dexamethasone, A: ascorbic acid 2-phosphate, and P: L-proline (T3DAP). 3wks indicated pre-chondrogenic culture with T3DAP for three weeks, 8wks indicated after three weeks' prechondrogenic culture, the culture medium was switched to DAP or with continuous T3DAP for additional five weeks. The symbols indicating significant differences ( $p < 0.05$ ) are defined as 1) between oxygen tensions (NRX vs HYP): T3DAP/3wks (#), T3DAP/8wks (\*) and DAP/8wks (¥); 2) within NRX: T3DAP/3wks vs T3DAP/8wks (a), T3DAP/3wks vs DAP/8wks (b), T3DAP/8wks vs DAP/8wks (c); 3) within HYP: T3DAP/3wks vs T3DAP/8wks (d), T3DAP/3wks vs DAP/8wks (e), T3DAP/8wks vs DAP/8wks (f). These symbols are also applied to the following gene

expression analysis.

### **4.3.3 Gross morphology and histology**

At the end of each culture condition, the constructs after culture *in vitro* and *in vivo* were washed with phosphate buffered saline and then the gross morphologies were captured micro photographically (Fig.4-3A/3A, B), followed by histochemical Safranin-O staining for sulfated proteoglycans (Fig.4-3B, C/4C, D) and immunofluorescently for type I and II collagens (Fig.4-3D/4E).

#### **4.3.3.1 Gross morphology**

In the *in vitro* culture model, all constructs seemed thicker, and the peripheral edges contracted towards the center of the cell-seeded side relative to the empty scaffolds (Fig.4-3A1). Under NRX, T3DAP/8wks (Fig.4-3D1) resulted in smaller sized constructs than the T3DAP/3wks experimental group (Fig.4-3B1). However, the transient exposure to TGF- $\beta$ 3 (DAP/8wks) (Fig.4-3F1) maintained similar-sized constructs relative to T3DAP/3wks (Fig. 4-3B1). There was less size variability in the HYP-culture constructs across the three culture conditions (Fig.4-3C1/E1/G1). Between NRX and HYP, the sizes of constructs under HYP were larger. This finding was coincident with a significantly higher total GAG and GAG/DNA content in the HYP groups.

In the *in vivo* culture model, the implanted constructs were surrounded by mouse blood vessels (Fig.4-4A1/B1/C1). No noticeable size difference was observed between NRX (Fig.4-4B1) and HYP (Fig.4C1) pre-cultured constructs, which were all smaller

than the empty scaffold (Fig.4-4A1) *in vivo*. The *in vitro* cultured control group in 10% (v/v) FBS under both oxygen tensions behaved like the implanted constructs in that the pre-formed matrix seemed to degrade (Fig.4-4D2/E2).

#### 4.3.3.2 Safranin-O staining

In the *in vitro* culture model (Figure.4-3), two different layers were shown in the empty scaffold (Fig.4-3A3): a compact layer (asterisk) and a porous layer (arrow) on which we seeded the hMFCs. In T3DAP/3wks group, Safranin-O positive matrix with chondrocyte-like cells in a round shape which resided in lacunae-like structures were observed in HYP (Fig.4-3C3). There were no Safranin-O positive matrix and lacunae-like structures in the NRX-cultured T3DAP/3wks group; instead, fibroblast-like cells were ubiquitous (Fig.4-3B3). During the additional five weeks' culture without TGF- $\beta$ 3 (DAP/8wks), the pre-formed ECM was maintained, especially under HYP (Fig.4-3G3) while NRX had only faint Safranin-O staining (Fig.4-3F3). In contrast, after continuous culture with T3 for the additional five weeks (T3DAP/8wks) under HYP, constructs showed more intense Safranin-O staining (Fig.4-3E3) compared to the groups with DAP/8wks (Fig.4-3G3). The NRX-cultured constructs in T3DAP/8wks exhibited faint Safranin-O staining (Fig.4-3D3), which seemed to be more intense than transient exposure to TGF- $\beta$ 3 (NRX DAP/8wks) (Fig.4-3F3) but was much less compared to T3DAP/8wks HYP (Fig.4-3E3).

In the *in vivo* model, the empty scaffold increased in size relative to before implantation perhaps as a consequence of mouse cell invasion (Fig.4-4A4). The HYP-

derived constructs retained some level of Safranin-O positive matrix in the central region (Fig.4-4C4, black arrows). In contrast, there was no Safranin-O positive matrix in the NRX-derived constructs (Fig.4-4B4), and the *in vitro* controls with DMEM complete regardless of oxygen tensions. (Fig.4-4D4/E4). All of the Safranin-O positive matrix constructs were consistent with GAG content and the gross morphologies.

#### 4.3.3.3 Immunofluorescence for type I and II collagen

In the *in vitro* culture model (Figure.4-3), DAPI was not detected in the empty scaffold (Fig.4-3A4). Type I collagen was observed in all constructs, and the fluorescence was least intense in the empty scaffold (Fig.4-3A4). The distribution of type II collagen seemed to match Safranin-O positive matrices. Type II collagen was detected in T3DAP/8wks under NRX (Fig.4-3D4) and all the HYP-cultured constructs. HYP maintained the detection of type II collagen (Fig.4-3G4) after transient exposure to TGF- $\beta$ 3 compared to NRX (Fig.4-3F4). The fluorescence was most pronounced in T3DAP/8wks in HYP (Fig.4-3E4).

In the *in vivo* culture model (Figure.4-4E), DAPI was detected in all the constructs, including the empty scaffold (Fig.4-4A5). Limited type I collagen could be observed in the empty scaffold while it was intense in both oxygen tension-derived constructs (Fig.4-4B5/C5). Type II collagen was partially retained in HYP pre-cultured constructs in this ectopic environment (Fig.4-4C5, white arrows). The pre-formed type I collagen became discontinuous and contracted, leaving some empty spots within the *in vitro* controls

(Fig.4-4D5/E5) while no type II collagen maintained.

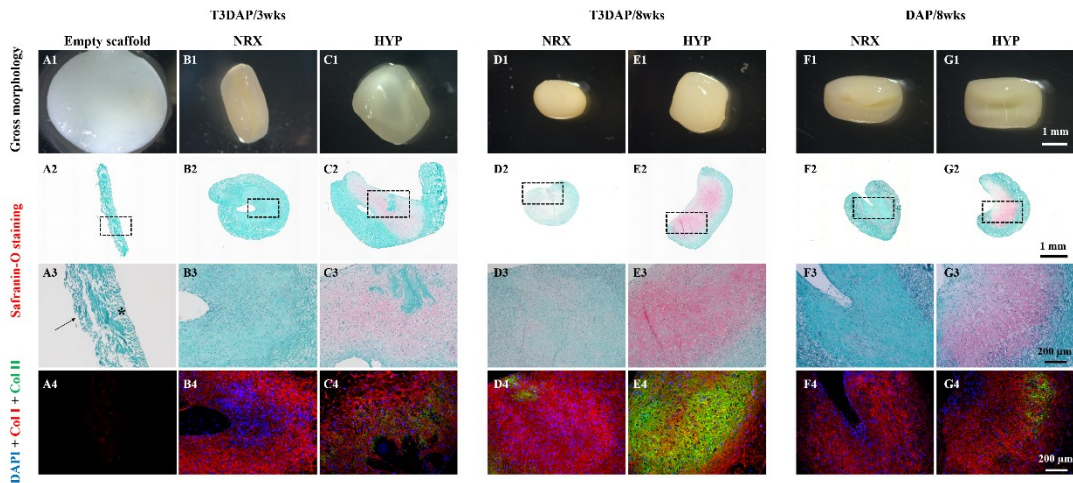


**Figure 4-3:** Gross morphology, Safranin-O staining, and immunofluorescence (IF) of type I/II collagen of hMFCs-based constructs cultured in vitro. DAPI staining (in blue) for cell nuclei is superimposed in IF images. The series of images labeled as A1-G1 represent gross morphology. The series of images labeled as A2-G2, A3-G3 represent the whole images and zoom in images of Safranin-O staining, respectively. The series of images labeled as A4-G4 represent IF images. Scale bar are presented in the last images of each row.

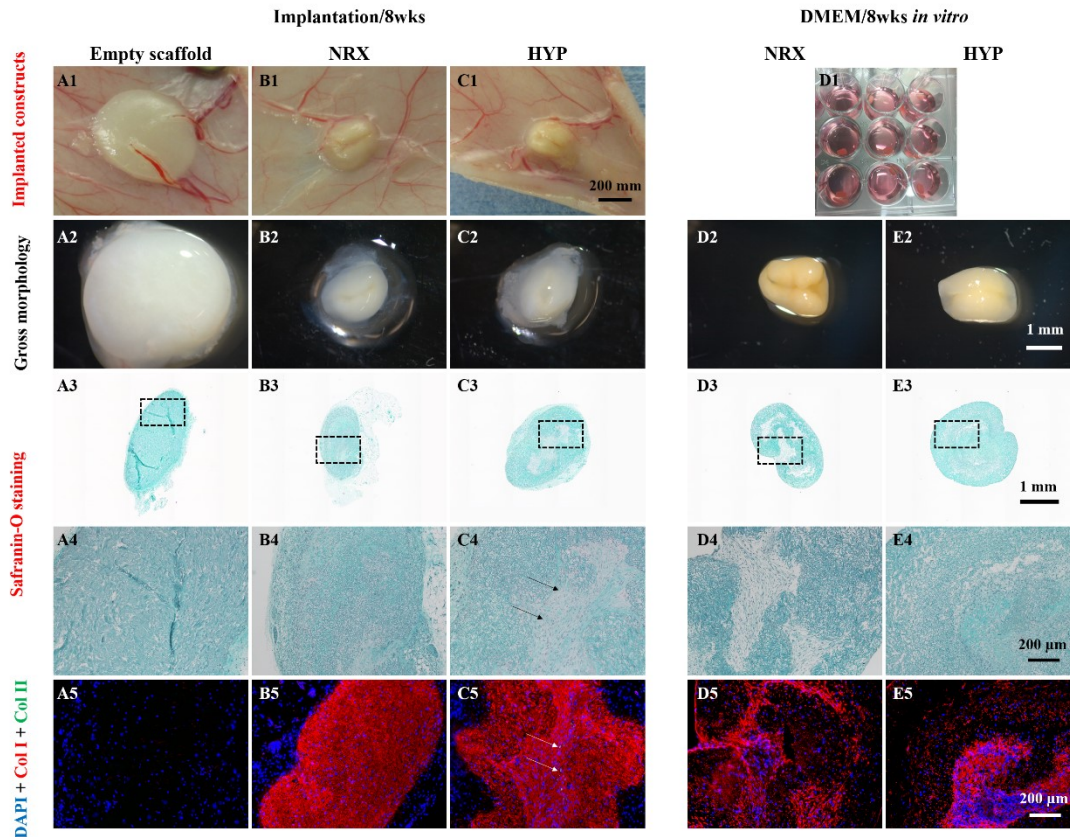


**Figure 4-4:** Gross morphology, Safranin-O staining, and immunofluorescence (IF) of type I/II collagen of hMFCs-based constructs after implantation. DAPI staining (in blue) for cell nuclei is superimposed in IF images. The series of images labeled as A1-D1 and A2-E2 represent gross morphology. The series of images labeled as A3-G3, A4-G4 represent the whole images and zoom in images of Safranin-O staining, respectively. The series of images labeled as A4-G4 represent IF images. Scale bar are presented in each row.

#### 4.3.4 Blood vessel invasion and calcium deposition

CD31 immunofluorescence and Alizarin red staining were performed for the implanted constructs to detect blood vessel invasion and calcium deposition in the ectopic

environment, respectively (Figure.4-5). Safranin-O staining (Fig.4-5A1-3) and type II collagen immunofluorescence (Fig.4-5B1-B2) from the analysis described above were used to provide positional information of the remaining matrix. Blood vessel invasion (Fig.4-5D1/D2/D3, white arrows) was observed in the middle of all constructs, regardless of higher *VEGF* gene expression (Fig.4-6G, see gene expression results described below) in the HYP-derived constructs compared to NRX. Vessels concentrated in the regions where Safranin-O positive proteoglycan (Fig.4-5A2, black arrows) and type II collagen (Fig.4-5B2, white arrows) remained in HYP-derived constructs. Matrix derived from human bone marrow mesenchymal stem cells seeded onto a type I collagen scaffold (pre-cultured with T3 for 3 weeks under HYP, then implanted subcutaneously for 5 weeks in nude mice) served as a positive control for alizarin red staining (Fig.4-5G). It stained intensively with Alizarin Red S (orange color) and confirmed the deposition of a bone matrix using the same nude mouse model. No positive staining was observed in any of the *in vivo* constructs of MFCs (Fig.4-5F1-2) from both oxygen tensions and the empty scaffold (Fig.4-5F3).

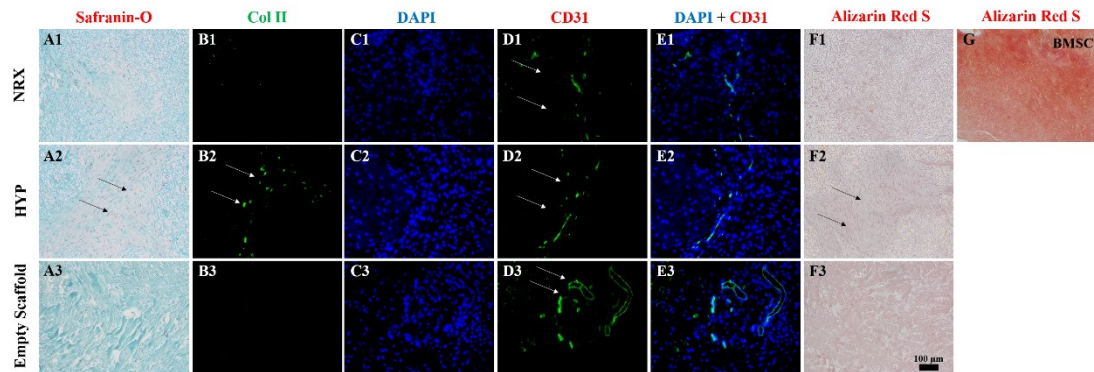


**Figure 4-5:** Safranin-O staining, and immunofluorescence (IF) of type II collagen, CD31 and Alizarin Red S staining of hMFCs-based constructs after implantation. DAPI staining (in blue) for cell nuclei is superimposed in IF images only for CD31. The series of images labeled as A1-3 represent Safranin-O staining. The series of images labeled as B1-3 represent IF for type II collagen. The series of images labeled as C1-3, D1-3 and E1-3 represent DAPI, CD31 (green) and combined images. The series of images labeled as F1-3 and G represent Alizarin Red S staining for hMFCs constructs and human bone marrow mesenchymal stem cells (hBMSCs) constructs, respectively.

### 4.3.5 Gene expression

Gene expression analysis (Fig.4-6/4-7) was performed only for the *in vitro* experiments, not including the constructs cultured in DMEM with 10% FBS (DMEM) *in vitro* and implanted *in vivo*.

#### 4.3.5.1 Fibrochondrogenic differentiation-related genes

For both oxygen tensions, the transient exposure to TGF- $\beta$ 3 (DAP/8wks) tended to result in decreased gene expression levels of *ACAN*, *COL2A1*, and *SOX9* compared to the

baseline (T3DAP/3wks), but no significant differences were found. As well, for both oxygen tensions continuous culture with T3 for additional 5 weeks (T3DAP/8wks) resulted in increased gene expression levels of *ACAN* and *COL2A1* compared to T3DAP/3wks and DAP/8wks with significant differences observed in *ACAN* (NRX, T3DAP/8wks vs T3DAP/3wks ( $p=0.012$ ) and vs DAP/8wks ( $p=0.003$ ), respectively), *COL2A1* (NRX, T3DAP/8wks vs T3DAP/3wks ( $p=0.002$ ) and vs DAP/8wks ( $p=0.001$ ), respectively and HYP, T3DAP/8wks vs T3DAP/3wks ( $p=0.026$ ) and vs DAP/8wks ( $p=0.001$ ), respectively). The gene expression level of *SOX9* was significantly upregulated in T3DAP/8wks compared to T3DAP/3wks ( $p=0.042$ ) and DAP/8wks ( $p=0.001$ ) in NRX while no significant differences were observed in HYP. No significant differences in *COL1A2* were found among any group.

Between NRX and HYP, the gene expression levels of ECM molecules: *ACAN* (T3DAP/3wks ( $p=0.002$ ), T3DAP/8wks ( $p=0.026$ ) and DAP/8wks ( $p=0.025$ )), *COL2A1* (T3DAP/3wks ( $p=0.002$ ) and T3DAP/8wks ( $p=0.041$ )), and chondrogenic regulator *SOX9* (T3DAP/3wks ( $p<0.001$ ), T3DAP/8wks ( $p=0.021$ ) and DAP/8wks ( $p=0.021$ )), were all significantly upregulated in HYP compared to NRX within conditions except for *COL2A1* in DAP/8wks and *COL1A2* in all culture groups. *COL1A2* tended to be more highly expressed in HYP, but there were no significant differences in any group.

#### **4.3.5.2 Other hypoxia responsive genes**

No significant differences in *HIF-1 $\alpha$*  gene expression were observed between any

condition. The gene expression levels of *HIF-2 $\alpha$*  were upregulated in DAP/8wks compared to T3DAP/3wks ( $p<0.001$ ) and T3DAP/8wks ( $p=0.038$ ) with significance observed in NRX only. The gene expression levels of the angiogenic factor *VEGF* seemed to be lower in DAP/8wks compared to T3DAP/3wks and T3DAP/8wks in both oxygen tensions with significant differences observed in NRX (DAP/8wks vs. T3DAP/3wks ( $p<0.001$ ) and vs. T3DAP/8wks ( $p=0.021$ ), respectively) and HYP (DAP/8wks vs. T3DAP/3wks ( $p=0.007$ )). As well, it was significantly lower in T3DAP/8wks compared to T3DAP/3wks within NRX ( $p=0.046$ ) for *VEGF*. Like the ECM genes, *HIF-2 $\alpha$*  (T3DAP/3wks ( $p=0.007$ ) and T3DAP/8wks ( $p=0.030$ )), and *VEGF* (T3DAP/3wks ( $p=0.001$ ), T3DAP/8wks ( $p=0.002$ ) and DAP/8wks ( $p=0.019$ )), were both significantly upregulated in HYP compared to NRX in all conditions except for *HIF-2 $\alpha$*  DAP/8wks.

#### 4.3.5.3 TGF- $\beta$ isoform genes

Gene expression levels of *TGF- $\beta$ 1* were significantly lower in DAP/8wks compared to the other groups within HYP (T3DAP/3wks ( $p=0.016$ ) and T3DAP/8wks ( $p<0.001$ )). *TGF- $\beta$ 2* had significantly more expression in T3DAP/8wks compared to T3DAP/3wks ( $p=0.030$ ) and still more expression in the transient exposure group DAP/8wks ( $p<0.001$ ) within NRX. Finally, *TGF- $\beta$ 3* had less expression in T3DAP/8wks and DAP/8wks compared to T3DAP/3wks within both oxygen tensions (NRX, T3DAP/3wks vs. T3DAP/8wks ( $p<0.001$ ) and vs. DAP/8wks ( $p<0.001$ ), respectively) and HYP,

T3DAP/3wks vs. T3DAP/8wks ( $p=0.001$ ) and vs DAP/8wks ( $p<0.001$ ), respectively).

There were significant increases of *TGF- $\beta$ 1* expression in HYP compared to NRX in T3DAP/3wks ( $p<0.001$ ) and T3DAP/8wks ( $p=0.018$ ). *TGF- $\beta$ 2* expression was significantly higher in HYP compared to NRX in T3DAP/3wks ( $p<0.001$ ) and T3DAP/8wks ( $p<0.001$ ) yet the trend was reversed in DAP/8wks ( $p=0.004$ ). Finally, *TGF- $\beta$ 3* expression was significantly higher in HYP than NRX at the early time point T3DAP/3wks ( $p=0.043$ ) but not at the later time point T3DAP/8wks, and was significantly higher in NRX than HYP in the DAP/8wks condition ( $p=0.016$ ).

#### **4.3.5.4 Hypertrophic differentiation-related genes**

In T3DAP/8wks, the gene expression levels of hypertrophic differentiation marker *COL10A1* were significantly upregulated compared to T3DAP/3wks (NRX,  $p<0.001$  and HYP,  $p<0.001$ ) and DAP/8wks (NRX,  $p=0.004$ ). The gene expression levels of antiangiogenic factor chondromodulin-1 (*CHM-1*) and two anti-hypertrophic differentiation genes (*FRZB* and *GREM1*) are shown in Fig.4-7. *CHM-1* were significantly upregulated in T3DAP/8wks compared to baseline T3DAP/3wks (NRX,  $p=0.032$  and HYP,  $p=0.023$ ) and DAP/8wks (NRX,  $p=0.030$  and HYP,  $p=0.035$ ) in both oxygen tensions (Fig.4-7A). *FRZB* was significantly upregulated in T3DAP/8wks compared to T3DAP/3wks in NRX ( $p=0.013$ ) and in DAP/8wks compared to T3DAP/3wks in HYP ( $p=0.006$ ) (Fig.4-7B). No significant differences of *GREM1* across groups within the same oxygen tensions (Fig.4-7C).

Between oxygen tensions, HYP suppressed gene expression levels of *COL10A1* in T3DAP/3wks ( $p=0.001$ ). HYP seemed to downregulate *MMP-13* (Fig.4-6L) in all groups, but with significant suppression in DAP/8wks ( $p=0.017$ ) (Fig.4-6L). HYP significantly upregulated *CHM-1* compared to NRX in T3DAP/3wks ( $p=0.010$ ) and T3DAP/8wks ( $p=0.028$ ). There were no significant differences observed between oxygen tensions in regard to the expression of *FRZB* in any groups (Fig.4-7B). HYP downregulated *GREM1* in T3DAP/3wks ( $p=0.009$ ) (Fig.4-7C).

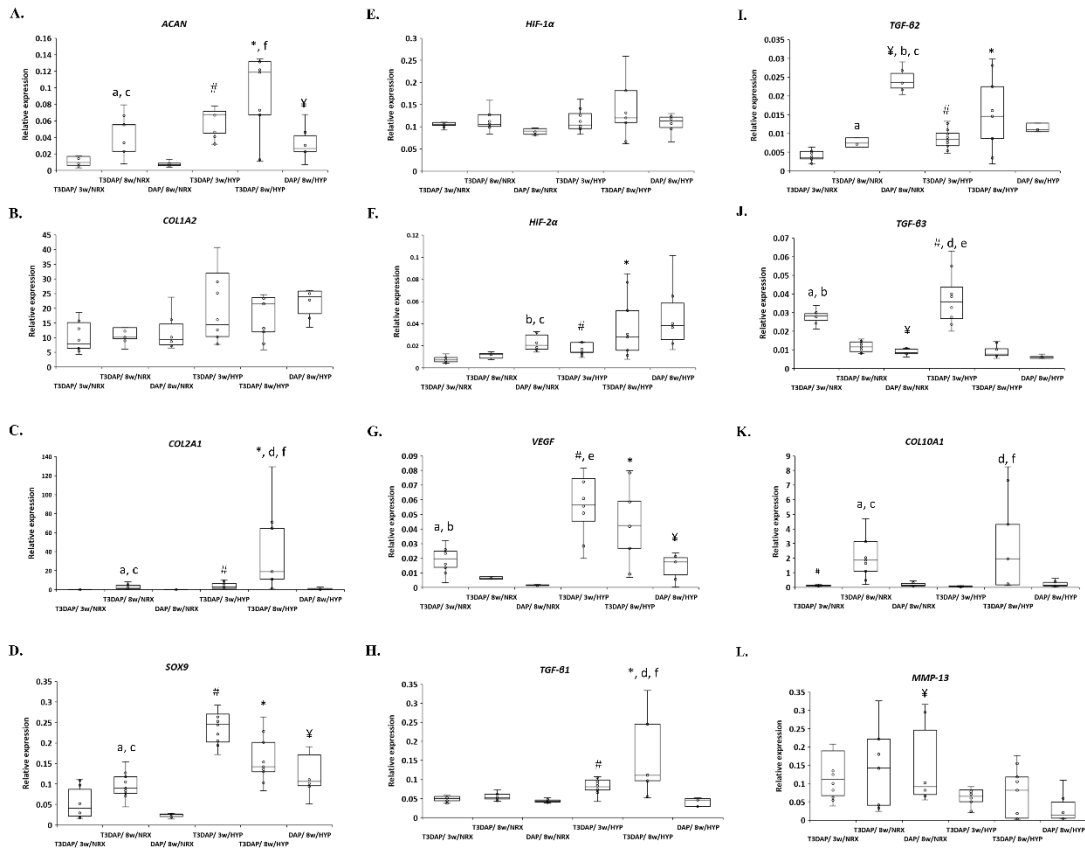


**Figure 4-6:** Relative gene expression of hMFCs-based constructs in vitro.

Fibrochondrogenic differentiation-related genes: (A) Aggrecan (ACAN); B) Type I

collagen (COL1A2); (C) Type II collagen (COL2A1); and (D) SRY-box transcription factor 9 (SOX9). Other hypoxic response-related genes: (E) HIF-1 $\alpha$ ; (F) HIF-2 $\alpha$ ; (G) VEGF. TGF- $\beta$  isoform genes: (H) TGF- $\beta$ 1; (I) TGF- $\beta$ 2; (J) TGF- $\beta$ 3. Hypertrophic differentiation-related genes: (K) type X collagen (COL10A1); (L) MMP-13. Values are presented as  $2^{\Delta Ct}$ , where  $\Delta Ct$  is the difference in Ct values of the average of three house-keeping genes and the gene of interest. Each donor has 2 biological replicates. The symbols indicating significant differences ( $p < 0.05$ ) are defined as 1) between oxygen tensions (NRX vs HYP): T3DAP/3wks (#), T3DAP/8wks (\*) and DAP/8wks (¥); 2) within NRX: T3DAP/3wks vs T3DAP/8wks (a), T3DAP/3wks vs DAP/8wks (b), T3DAP/8wks vs DAP/8wks (c); 3) within HYP: T3DAP/3wks vs T3DAP/8wks (d), T3DAP/3wks vs DAP/8wks (e), T3DAP/8wks vs DAP/8wks (f).

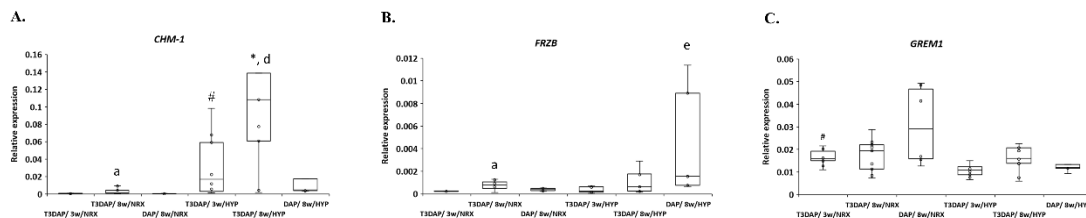


**Figure 4-7:** Relative gene expression of hMFCs-based constructs in vitro.

Fibrochondrogenic differentiation-related genes: (A) Chondromodulin-1 (CHM-1); (B) Frizzled related protein (FRZB); and (C) Gremlin 1 (GREM1). Values are presented as  $2^{\Delta Ct}$ , where  $\Delta Ct$  is the difference in Ct values of the average of three house-keeping genes and the gene of interest. Each donor has 2 biological replicates. The symbols indicating significant differences ( $p < 0.05$ ) are defined as 1) between oxygen tensions (NRX vs

HYP): T3DAP/3wks (#), T3DAP/8wks (\*) and DAP/8wks (¥); 2) within NRX:

T3DAP/3wks vs T3DAP/8wks (a), T3DAP/3wks vs DAP/8wks (b), T3DAP/8wks vs DAP/8wks (c); 3) within HYP: T3DAP/3wks vs T3DAP/8wks (d), T3DAP/3wks vs DAP/8wks (e), T3DAP/8wks vs DAP/8wks (f).

#### 4.3.6 Principal component analysis

PCA was used to summarize quantitative data and determine salient relationships between the quantifiable variables. On initial PCA of all pooled data, a five-component solution was permuted with each component having eigenvalues  $>1$ , and collectively accounted for 83% of the entire quantitative data. The KMO measure of sampling adequacy was 0.62. On close inspection of the five-component solution, it became apparent that multiple measured variables, including *ACAN*, *GAG*, *DNA*, *COL1A2*, *MMP13*, and *CHMI*, loaded equally on any two or three of the five principal component (PC) solution. To that end, we restricted the PCA to a two-component solution; PC1 and PC2. The KMO remained at 0.62. Eigenvalues for PC1 was 7.2 and that for PC2 was 2.9. PC1 and PC2 respectively accounted for 40% and 16% of the variances in the pooled data. *COL1A2* and *MMP13* loaded equally on PC1 and PC2. Thus, we removed these variables from the final PCA calculations with a two-component solution. The KMO reduced to 0.60. PC1 and PC2 respectively accounted for ~44% and ~17% of the total variances in the pooled data. Eigenvalues were ~ 7 and 2.6 for PC1 and PC2, respectively. PC1 correlated mostly strongly with *TGF $\beta$ 1* mediated hypertrophic

chondrogenesis (*ACAN*, *COL2A1*, *HIF1A*, *TGFβ1*, *TGFβ2*, *COL10A1*, *CHM-1*, GAG and GAG/DNA) and PC2 correlated most strongly with a chondrogenic pathway involving *TGFβ3*, *SOX9*, BMP signaling antagonist (*GREM1*), and the canonical wingless type MMTV integration site (WNT)/β-catenin signaling antagonist, *FRZB* (Table 3; Fig.4-8).

**Table 4-3: PCA Correlation Matrix**

Correlation matrix		
	PC1	PC2
<i>ACAN</i>	.883	-.346
<i>COL2A1</i>	.921	.136
<i>SOX9</i>	.411	-.717
<i>HIF1A</i>	.874	-.024
<i>HIF2A</i>	.714	-.029
<i>TGFB1</i>	.946	-.033
<i>TGFB2</i>	.512	.381
<i>TGFB3</i>	-.156	-.696
<i>VEGF</i>	.607	-.681
<i>COL10A1</i>	.484	.111
<i>CHMI</i>	.912	.110
<i>GREM1</i>	.057	.542
<i>FRZB</i>	.178	.425
<i>GAG</i>	.736	.360
<i>DNA</i>	.491	.479
<i>GAGDNA</i>	.676	.233

Extraction Method: Principal Component Analysis.

Rotation Method: Varimax with Kaiser Normalization.

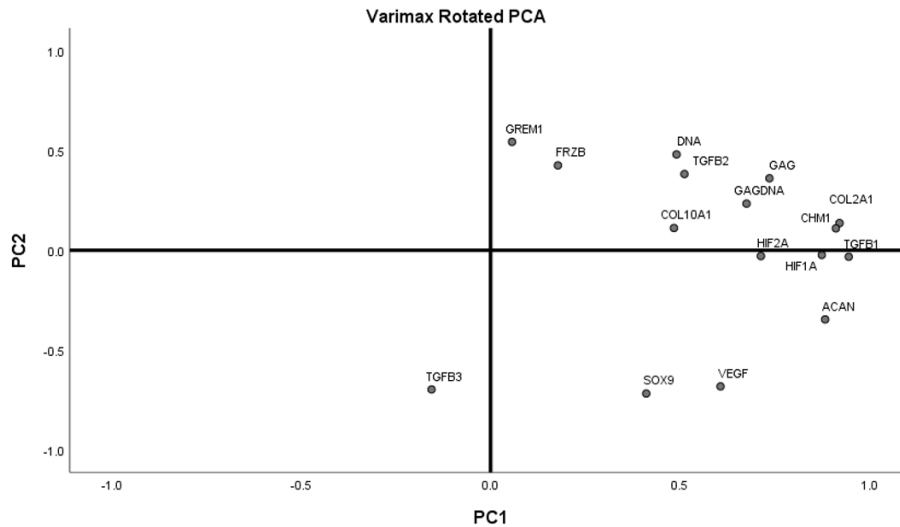


**Figure 4-8:** A varimax rotated plot of a two-component solution of principal component analysis of measured variables. Measured variables are: *ACAN*, *COL2A1*, *SOX9*, *HIF-1 $\alpha$* , *HIF-2 $\alpha$* , *TGF $\beta$ 1*, *TGF $\beta$ 2*, *TGF $\beta$ 3*, *VEGF*, *COL10A1*, *CHM-1*, *GREM1*, *FRZB*, *GAG*, DNA and GAG/DNA. Principal component 1 (PC1) is on the x-axis and principal component 2 (PC2) is on the y-axis. The position of each variable on the plot indicates the degree to which it loads on the two different principal components.

#### 4.4 Discussion

In this study, we demonstrated that the cartilaginous ECM formed *in vitro* by monolayer-expanded human meniscus fibrochondrocytes (hMFCs) on a clinically approved collagen membrane scaffold under hypoxic culture conditions in the presence of chondrogenic factors is amenable to vascularization without calcification *in vivo*.

The effects of T1F2 on hMFC proliferation rates in P1 before freezing were similar to our previous study [246]. However, the significantly higher proliferation rates noted in P2 post-freezing was a surprise [246], and in contrast to other studies where no difference in proliferation rates was observed between fresh and frozen adipose-derived stem cells and umbilical cord blood progenitor cells [281, 282].

Our *in vitro* results showed that superior inner meniscus-like ECM (IM-ECM) was formed on the scaffold by hMFCs under HYP compared to NRX in all culture conditions. These results were consistent with our previous studies using F2-expanded hMFC but from osteoarthritic joints[11], and T1F2-expanded hMFC from partial meniscectomies using the cell pellet model [242, 246]. However, previous results showed that NRX resulted in superior or similar ECM formation compared to HYP (3% O<sub>2</sub>) using a scaffold model [14, 96]. Several reasons may account for these inconsistent results. First, previous studies used hMFCs from osteoarthritic menisci. Secondly, FGF-2 was used during the expansion phase, and chondrogenic culture occurred all within the same oxygen tensions in the previous studies, unlike herein where hMFCs were expanded with T1F2 under NRX, then separated into either NRX or HYP groups for chondrogenic culture. Thirdly, the constructs in the previous studies experienced normoxia during media changes compared to continuous HYP during the chondrogenic culture in this study. Finally, the composition of the scaffold in the previous studies was type I collagen while the scaffold in this study comprised types I and III collagen. Different behaviors in terms of cell

distribution, cell morphologies, and the matrix formation of ovine meniscus cells between scaffolds have been reported [283]. Interestingly, pure type I collagen scaffold, and an hybrid scaffold with type II collagen have been compared but with human articular chondrocytes (hACs) [284]. However, the hACs failed to produce matrix within both scaffolds when cultured without growth factor supplementation *in vitro* under NRX. The gene expression levels of type II collagen were similar between scaffolds, but the cell numbers were significantly higher in the type I/III collagen scaffold. To this end, the potential role of type III collagen in regulating the ECM-forming capacity of hMFC needs further investigation.

The transient exposure to TGF- $\beta$ 3 for 3 weeks followed by 5 weeks' TGF- $\beta$ 3-free culture (DAP/8wks) did not appear to further enhance IM-ECM formation compared to the baseline (T3DAP/3wks) in either oxygen tension; instead, the pre-formed ECM appeared to be retained in terms of GAG and DNA contents, and type I and II collagen immuno-histochemical characteristics. In contrast, continuous culture with TGF- $\beta$ 3 for 8 weeks (T3DAP/8wks) resulted in enhanced IM-ECM under both oxygen tensions compared to the baseline and DAP/8wks. These results are in contrast to a previous study using bovine calf articular chondrocytes in agarose as a scaffold under serum-free normoxic conditions. In the study, transient exposure to TGF- $\beta$ 3 for 2 weeks significantly enhanced the accumulation of GAG matrix at the end of 8 weeks' relative to continuous culture with TGF- $\beta$ 3 [276]. However, in another involving the bovine calf articular

chondrocytes and agarose as a scaffold, there was no difference between transient and continuous culture with TGF- $\beta$ 3 under NRX in the context of GAG matrix content [274]. But the authors reported enhanced mechanical properties in the transient group.

Previous studies showed that hMFCs respond to hypoxia via HIF-1 $\alpha$  [10], and that TGF- $\beta$ 3 supplementation correlated with higher *HIF-1 $\alpha$*  mRNA in hMFC pellets [242]. Thus, we were curious if mRNA expression of *HIF-1 $\alpha$*  and other transcription factors related to the HYP response in cartilaginous tissue would increase over time with TGF- $\beta$ 3 supplementation (T3DAP/3wks vs. T3DAP/8wks) and if they would be maintained after TGF- $\beta$ 3 withdrawal [285]. It should be noted, however, that both *HIF-1 $\alpha$*  and *HIF-2 $\alpha$*  are both known to be constitutively expressed and are regulated at the protein level [286]; yet, higher gene expression could technically lead to more protein to potentiate the HYP response. We did not observe any time-dependent regulation of *HIF-1 $\alpha$* , though *HIF-2 $\alpha$*  increased significantly in T3DAP/8wks compared to T3DAP/3wks in NRX only. *HIF-1 $\alpha$*  also appeared to be maintained at the baseline level after 5 additional weeks without TGF- $\beta$ 3 supplementation (DAP/8wks), whereas the expression of *HIF-2 $\alpha$*  exceeded all other groups in DAP/8wks, reaching significance in NRX only. Previous studies found that HIF-2 $\alpha$ , not HIF-1 $\alpha$ , played an essential role in the synthesis of cartilaginous ECM in hACs (1% O<sub>2</sub>) [287], BM-MSCs (3% O<sub>2</sub>) [15] and infrapatellar fat pad mesenchymal stem cells (IFP-MSCs) (5% O<sub>2</sub>) [288]. The mRNA expression of *SOX9* did not correlate with the upregulated levels of *HIF-2 $\alpha$*  in DAP/8wks, and in T3DAP/8wks relative to

T3DAP/3wks in both oxygen tensions. This finding is in contrast with previous reports that HYP-enhanced production of ECM in hACs and IFP-MSCs was induced by a HIF-2 $\alpha$ -mediated upregulation of *SOX9* [287, 288]. To this end, the role of HIF-2 $\alpha$  in the enhancement and maintenance of IM-ECM may be independent of *SOX9*. However, our results cannot exclude the possibility that HIF-1 $\alpha$  and HIF-2 $\alpha$  act synergistically since both have different roles in response to HYP [289, 290]. For example, HIF-1 $\alpha$  has been reported to modulate *SOX9* which in turn increased the expression of *ACAN* and *COL2A1* [291].

The role of TGF- $\beta$  family members: *TGF- $\beta$ 1*, *TGF- $\beta$ 2*, and *TGF- $\beta$ 3* were investigated due to their importance in chondrogenesis [292]. Moreover, HYP has been shown to enhance TGF- $\beta$ 3-induced chondrogenic redifferentiation of hMFC [246]. Furthermore, a recent study showed that hypoxia (2% O<sub>2</sub>) alone can drive the spontaneous chondrogenesis of hBM-MSCs via the activation of the endogenous TGF- $\beta$  pathway [293]. However, we observed no clear trends in the expression of the three *TGF $\beta$*  isoforms. The increased IM-ECM observed in HYP relative to NRX in the T3DAP/3wks and T3DAP/8wks experimental groups seemed to be associated with a significant upregulation of *TGF- $\beta$ 1* and *TGF- $\beta$ 2*. A similar pattern was noted with *HIF-2 $\alpha$*  and *SOX9* expression. But the maintenance of IM-ECM was only observed in the HYP (DAP/8wks) experimental group at the removal of TGF- $\beta$ 3. Moreover, *TGF- $\beta$ 1* was significantly downregulated in HYP relative to NRX when TGF- $\beta$ 3 was removed. In

contrast, *TGF-β2* remained constant while *TGF-β3* was significantly downregulated in DAP/8wks compared to T3DAP/3wks.

The effects of HYP to suppress the expression of hypertrophic markers (*COL10A1* and *MMP13*) during *in vitro* chondrogenesis were consistent with previous results [15]. However, it was surprising that the expression of *COL10A1* was unchanged after TGFβ3 withdrawal regardless of oxygen tension.

The long-term chondrogenic culture (10 weeks) with TGF-β3 under NRX has been shown to enhance the maturation of ECM derived from bovine [146], and human [92] MFCs using an *in vitro* scaffold model. But there was no assessment of the hypertrophic potential. In this study, *COL10A1* expression increased significantly in long-term culture of T3DAP/8wks regardless of oxygen tension. This outcome was inconsistent with the findings of another study that showed *COL10A1* was not induced in hACs pellets after 42 days of *in vitro* chondrogenesis in the presence of TGF-β3[121]. To this end, it would seem like our T1F2-expanded hMFC behaved similarly to hBM-MSCs in that *COL10A1* expression increased with chondrogenic culture time [121, 294]. The reason for the disparity is unclear but may be associated with the pathophysiology of the osteoarthritic hACs used in the study [295], while the hMFC are non-osteoarthritic.

Pelttari *et al* have shown that the expression of *COL10A1* in hBM-MSCs after 3-7 weeks of chondrogenic differentiation correlated with a calcifying and vascularizing phenotype in the SNM model[121]. In contrast, despite the increased *COL10A1*

expression even in our long-term culture constructs, there was evidence of neovascularization but no calcification after ectopic implantation in SNM. Moreover, HYP-cultured constructs only exhibited superior ECM formation *in vitro* but also partially maintained ECM components like type II collagen and Safranin-O positive proteoglycan *in vivo* compared to NRX. Even though the hMFC cultured under HYP had increased *VEGF* expression, the level of blood vessel invasion seemed similar regardless of oxygen tension based CD31 IF.

The HYP-precultured constructs showed potential as a strategy to engineer IM-ECM that may be enriched with the angiogenic factor, VEGF, for the repair of avascular meniscus injuries given the upregulation of *VEGF in vitro* and subsequent vascularization of pre-cultured IM-ECM formed after 5 weeks' of implantation in the SNM model. However, it is noteworthy that even though VEGF is highly expressed in the avascular region of the meniscus after injury relative to controls in rabbits, there was no neovascularization [296]. Moreover, the direct application of free VEGF with VEGF-coated sutures in the avascular region was also not adequate to facilitate neovascularization in a sheep model [297]. The reason for the lack of neovascularization is unclear but may be concentration dependent, given that the eye cornea (an avascular tissue) underwent neovascularization after application of VEGF at ( $\geq 200$ ng) [298]. To the best of our knowledge, our study is the first demonstrating that hMFC precultured under HYP (3%) can promote neovascularization.

Our PCA revealed a two-component solution accounting for more than 56% of the variance in the obtained data. One component, PC1, favored a hypertrophic chondrogenic pathway with endogenous TGF- $\beta$ 1 and TGF- $\beta$ 2, and the other component correlated with a TGF- $\beta$ 3 mediated non-hypertrophic chondrogenesis via SOX9 upregulation and anti-hypertrophic mechanisms involvement.

#### **4.5 Conclusions**

In summary, our study describes two different strategies to maintain and promote IM-ECM formation by hMFC under HYP compared to commonly used 3 weeks' chondrogenic culture *in vitro*. Our *in vitro* results indicated that: 1) autologous hMFCs can be expanded up to ~113 fold in about two weeks cumulatively, and their IM-ECM-forming capacity under hypoxia was retained after short-term storage in liquid nitrogen; 2) Pre-formed IM-ECM can be maintained under HYP without exogenous growth factor supplementation, while longer chondrogenic culture with TGF- $\beta$ 3 under HYP can enhance its production at the expense of a more hypertrophic phenotype. Also, this study showed the feasibility for hMFC-derived IM-ECM to support neo-vascularization without ossification at the ectopic site, even though partial degradation of pre-formed IM-ECM was observed.

**Chapter 5 Chondrogenic differentiation of synovial fluid mesenchymal stem cells on human meniscus-derived decellularized matrix requires exogenous growth factors**

**Yan Liang, Enaam Idrees, Alexander Szojka, Stephen Andrews, Melanie Kunze, Aillette Mulet-Sierra, Nadr Jomha, and Adetola B. Adesida**

This chapter has been published in part in *Acta Biomaterialia*:

Yan Liang, Enaam Idrees, Alexander Szojka, Stephen Andrews, Melanie Kunze, Aillette Mulet-Sierra, Nadr Jomha, and Adetola B. Adesida: **Chondrogenic Differentiation of Synovial Fluid Mesenchymal Stem Cells on Human Meniscus-Derived Decellularized Matrix Requires Exogenous Growth Factors.** *Acta Biomaterialia* 2018, 80: 131-143

## 5.1 Introduction

The menisci are a pair of crescent-shaped fibrocartilages between the femoral condyle and tibial plateau that withstand compressive and tensile forces [299]. They are essential for mechanical load distribution and transmission, lubrication, and stability of the knee joint [2]. The biomechanical properties of the menisci are due to its extracellular matrix (ECM), which is composed primarily of collagens and proteoglycans. Collagen I is found throughout the entire meniscus while collagen II and aggrecan, a large proteoglycan, are found in the inner regions [300]. The avascular nature of the inner two-thirds of the tissue limits its potential for healing [6]. Injuries in the avascular portion are commonly treated by partial meniscectomy [3]. However, partial meniscectomy results in altered biomechanics of the knee joint and poses a major risk for the early onset of knee osteoarthritis [3]. To this end, alternative and novel strategies to repair avascular meniscus injuries are of significant interest in orthopaedic research and therapy. Cell-based tissue engineering and regenerative medicine strategies have been advocated as a potential approach to address this issue [9].

From a clinical and bioengineering perspective, autologous meniscus fibrochondrocytes (MFCs) isolated from a partial meniscectomized tissue specimen are the ideal cell source for engineering the meniscus as they are responsible for the synthesis of the ECM of the meniscus. However, isolated primary MFCs are limited in numbers and cell expansion protocols to increase numbers suffer from dedifferentiation and loss of

their functional ECM synthetic capacity [11]. Although an improved cell expansion protocol was recently reported to mitigate this limitation [301], readily accessible cell sources such as adult-derived mesenchymal stem cells (MSCs) remain promising as alternative cell sources[9]. These include MSCs from bone marrow MSCs (BM-MSCs) [99], synovial membrane MSCs (SM-MSCs) [209], and adipose MSCs (AD-MSCs) [210]. Increasing evidence has demonstrated that MSCs also exist in synovial fluid (SF-MSCs) of healthy human knee joint and their number increases under pathological conditions [180, 302], suggesting they may potentially have a reparative role in meniscus injuries [303]. When compared to BM-MSCs, SM-MSCs, and AD-MSCs, SF-MSCs have a decreased tendency to form bone [185, 304], and also have a better chondrogenic capacity compared to BM-MSCs [304]. However, specific factors that induce SF-MSCs differentiation towards a robust fibrochondrogenic phenotype are currently unknown.

Insulin-like growth factor 1 (IGF-1) and transforming growth factors  $\beta$  (TGF $\beta$ ) signaling were recently shown to be highly elevated during morphogenesis of mouse meniscus [305]. Furthermore, in mature menisci, the expression of insulin-like growth factor-1 (IGF-1) was shown to be upregulated after injury [306] and induction of IGF-1 enhanced repair of meniscus defects *in vivo* [307]. Since IGF-1 is known for enhancing matrix formation of articular chondrocytes [308] and TGF $\beta$  superfamily members can induce chondrogenic differentiation of SF-MSCs [180, 304], it is reasonable to propose that IGF-1 may be important in regulating the fibrochondrogenic differentiation of SF-

MSC.

Since the demonstration of demineralized bone matrix's capacity to induce ectopic bone formation [309], a growing body of evidence has similarly demonstrated that decellularized matrix (DCM) from native tissue has capacity to regulate stem cell differentiation in tissue engineering applications [247]. The sequestration of bio-inductive factors in DCM derived from porcine articular cartilage has been shown to drive the chondrogenic differentiation of human AD-MSCs without exogenous growth factors [254]. Similarly, supplementation of culture media with protein extracts derived from decellularized inner and outer bovine meniscus was shown to differentially differentiate human BM-MSCs without the addition of growth factors [310]. Moreover, bovine meniscus-derived DCM has also been demonstrated to upregulate gene expression levels of fibrochondrogenic markers in human BM-MSCs compared to DCM-free control under chondrogenic stimulation in 3-dimensional scaffold culture [142, 310]. Based on these studies, we speculate that human meniscus-derived ECM may provide meniscus-specific inductive factors such as TGF- $\beta_3$  and IGF-1 for fibrochondrogenic differentiation of human SF-MSCs.

The oxygen tension during isolation and expansion of MSCs has a significant impact on their matrix-forming phenotype. SF-MSCs reside in a hypoxic knee joint environment [226] and hypoxic conditions during cell isolation and expansion have been shown to enhance chondrogenic differentiation of BM-MSCs [15].

The objective of this study was to evaluate the effect of DCM derived from the human native meniscus, TGF- $\beta_3$  and IGF-1 on fibrochondrogenesis of human SF-MSCs for meniscus tissue engineering under hypoxic conditions (3% O<sub>2</sub>). We hypothesized that human meniscus-derived DCM would stimulate human SF-MSCs to produce ECM that resembles native meniscus under hypoxic conditions and these effects would be further enhanced by TGF- $\beta_3$  and IGF-1.

## **5.2 Methods**

### **5.2.1 Ethics statement**

Experimental methods and tissue collection were approved and in accordance with the University of Alberta's Health Research Ethics Board (HREB)- Biomedical Panel (Study IDs: Pro00018778 and Pro00001141). Ethics Board waived the need for written informed consent of patients where relevant, as specimens used in the study were either intended for discard in the normal course of the surgical procedure (i.e. study ID: Pro00018778) or were human cadaver tissue specimens from the Comprehensive Tissue Centre, Alberta Health Services, and approved for use within the limitations of human experimentation (i.e. study ID: Pro00001141). Extensive precautions were taken to preserve privacy of all donors.

### **5.2.2 Isolation and culture of synovial fluid-derived mesenchymal stem cells (SF-MSCs)**

Human synovial fluid (SF) aspirate was obtained (mean volume  $\pm$  SD of 13  $\pm$  9 mL) from

5 male donors (age 18-57 years). The non-identifiable donor information is summarized in Table 4-1. Briefly, SF aspirate was passed through a 100  $\mu\text{m}$  nylon mesh filter (Falcon, BD Bioscience, NJ, USA) after a 1:20 dilution with standard  $\alpha$ -MEM supplemented with 10% v/v fetal bovine serum (FBS), 100 mM 4-(2-hydroxyethyl)-1-piperazineethanesulfonic acid (HEPES), 1mM sodium pyruvate (all from Sigma-Aldrich Co., MO, USA), 100U/mL penicillin, 100  $\mu\text{g}/\text{mL}$  streptomycin and 0.29 mg/mL glutamine (PSG; Life Technologies, ON, Canada). Cells in the aspirate were isolated after centrifugation at 1500 rpm for 10 min and the number of mononucleated cells (MNCs) was determined after crystal violet nuclei staining on a hemocytometer. Isolated MNCs were plated at 1,000/cm<sup>2</sup> and cultured in standard  $\alpha$ -MEM as above but with 5 ng/mL of bFGF or FGF-2 (Neuromics, MN, USA, Catalog#: PR80001), to maintain the cells' chondrogenic potential [16] under hypoxia (HYP, 3% O<sub>2</sub>) at 37°C in a humidified incubator containing 5% CO<sub>2</sub>. Adherent nucleated cells (SF-MSCs) were expanded under HYP until passage 2 (P2) before experimental use. The time from seeding MNCs and reaching 80% confluence at P2 varied from 4 to 9 weeks.

**Table 5-1:** Synovial fluid donor information

Donor	Gender	Age, years	Medical history	Volume, mL
1	Male	36	Asthma, previous DVT	25
2	Male	29	Meniscus tear	20
3	Male	18	Osteochondral lesion	6
4	Male	57	Knee osteoarthritis	8
5	Male	32	Anterior cruciate ligament injury	5

DVT: deep vein thrombosis

### 5.2.3 Colony-forming unit fibroblastic (Cfu-f) assay

A colony-forming unit fibroblastic (Cfu-f) assay was performed as previously described to determine the clonogenic and population doubling characteristics of SF-MSCs [15]. Briefly, 2,500 MNCs from synovial fluid aspirates were plated in 100 mm sterile petri dishes in triplicated (Becton Dickinson, ON, Canada) and cultured under HYP. The media used was  $\alpha$ -MEM with FGF-2 as above. The duration of the Cfu-f assay for each donor (mean  $\pm$  SD of  $23.3 \pm 9.0$  days) was equivalent to the time required to reach 80% SF-MSCs confluence at P0 in the culture flasks prior to subsequent detachment and splitting to P1 for expansion. The number of cell colonies for each donor was recorded as well as their diameters.

### 5.2.4 Flow cytometry analysis

Flow cytometry was used to characterize the cell membrane surface markers of SF-MSCs derived from one donor (male, 36 years old) as previously described [15]. Monolayer cultured SF-MSCs at the end of P2 were analyzed using a FACScan flow cytometer

(Becton Dickinson). All primary monoclonal antibodies used herein were directly conjugated antibodies to fluorescein isothiocyanate (mAb-FITC) or to phycoerythrin (mAb-PE). Antibodies were either from BD Pharmingen or Invitrogen (see Table 4-2).

**Table 5-2:** Antibodies used to characterize SF-MSCs

Specificity	Isotype*	Cat.#/Fluorochrome	Source
CD13 (aminopeptidase-n)	mIgG1	sc-70529/PE	Santa Cruz Biotechnology
CD29	mIgG1	CD2901/FITC	Invitrogen
CD34	mIgG1	sc-19621/FITC	Santa Cruz Biotechnology
CD44 (Pgp-1, H-CAM, Ly 24)	mIgG2b	560977/FITC	BD Pharmingen
CD 45 (2B11)	mIgG1	Sc-20056/PE	Santa Cruz Biotechnology
CD49c ( $\alpha$ 3 integrin chain)	mIgG1	556025/PE	BD Pharmingen
CD49f ( $\alpha$ 6 integrin chain)	rIgG2a	555735/FITC	BD Pharmingen
CD73	mIgG1	550257/PE	BD Pharmingen
CD90 (Thy-1)	mIgG1	55596/PE	BD Pharmingen
CD 105 (endoglin)	mIgG1	sc-71043/PE	Santa Cruz Biotechnology
CD151 (PETA-3)	mIgG1	556057/PE	BD Pharmingen
CD184 (CXCR4)	mIgG2a	560937/PE- CyTM5	BD Pharmingen
Not specified (Isotype control)	mIgG1	sc-2855/FITC	Santa Cruz Biotechnology
Not specified (Isotype control)	mIgG1	sc-2866/PE	Santa Cruz Biotechnology

\*m, mouse; r, rat

### 5.2.5 Decellularized meniscus-derived matrix scaffold preparation

Human medial and lateral menisci were harvested from the left knee joint of a one-day

old cadaver (male, 46 years old) and processed the next day based on a published protocol [254]. Briefly, meniscus tissue was cut into small chips and suspended in PBS containing 1% (v/v) PSG. Meniscus slurry was collected after homogenization using a tissue homogenizer and the remaining small particles were removed using forceps. Meniscus slurry was then resuspended in sterile Milli-Q water, centrifuged, and collected. Thereafter, 1 mL of meniscus slurry aliquots were pipetted into cryogenic vials (Wheaton Science, NJ, USA), frozen overnight in -80 °C and then freeze-dried for ~17h. Porous meniscus extracellular matrix-derived scaffolds (6 mm (diameter) x 1.8-2.0 mm (thickness)) were cut using sterile scalpels and biopsy punches (Fig.4-1). The resulting scaffolds were sterilized with ethylene oxide before experimental use.

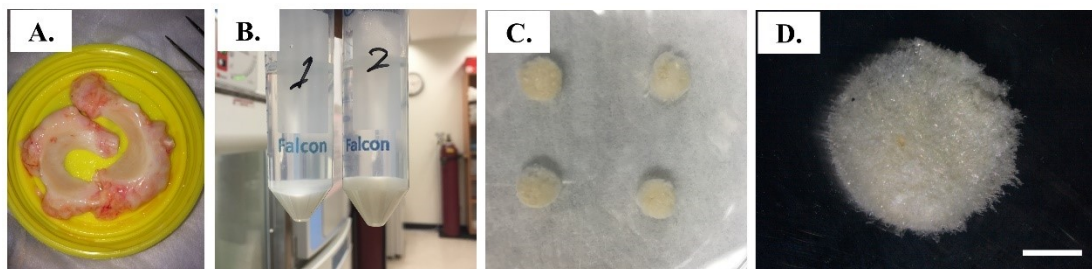


**Figure 5-1:** Method diagram of fabrication of decellularized matrix (DCM) scaffold from human native meniscus (n=1, male,46 years old). (A) gross morphology of the native meniscus tissue, (B) Collection of a slurry of meniscus matrix after centrifugation, (C) DCM scaffold after freeze-drying, (D) gross morphology of the DCM scaffold (6 mm (diameter) x ~ 1.8-2 mm (height)). Scale bar (white): 2 mm.

### **5.2.6 Cell aggregate (pellet) culture**

A three-dimensional cell pellet culture model was applied to test the effect of the individual growth factors on fibrochondrogenic differentiation of SF-MSCs as previously described [246]. At the end of P2,  $5 \times 10^5$  of SF-MSCs were centrifugated at 1500 rpm for 5 min to make pellets in 1.5 mL sterile conical microtubes (Bio Basic Inc, Ontario, Canada.). Thereafter, the pellets were cultured in 0.5 mL of a defined serum-free chondrogenic medium (SFM) composed of high glucose DMEM, HEPES (10 mM), PSG, dexamethasone (100 nM), ascorbic acid 2-phosphate (365  $\mu\text{g}/\text{mL}$ ), human serum albumin (125  $\mu\text{g}/\text{mL}$ ) and 40  $\mu\text{g}/\text{mL}$  L-proline all from Sigma-Aldrich), ITS+1 premix (Corning, Discovery Labware, Inc., MA, USA), TGF- $\beta_3$  (10 ng/ml; ProSpec, NJ, USA, Catalog#: cyt-113), IGF-1 (10 ng/mL; ProSpec, NJ, USA, Catalog#: cyt-216) or both growth factors under HYP at 37°C in a humidified incubator with 5% CO<sub>2</sub> for 21 days. Medium changes were performed twice per week.

### **5.2.7 Decellularized matrix scaffold seeding and construct culture**

To test the effect of the decellularized extracellular matrix (DCM) on the fibrochondrogenic differentiation of SF-MSCs, DCM scaffolds were placed in a 24-well low attachment plate (Sarsdedt AG & Co, Germany) and SF-MSCs from P2 were seeded per scaffold as previously described [13]. The scaffolds were pre-wet with SFM to promote cell attachment and infiltration.  $5 \times 10^5$  SF-MSCs were suspended in 20  $\mu\text{l}$  of pure SFM or SFM supplemented with TGF- $\beta_3$  and IGF-1, and then micro-pipetted onto

each scaffold. After cell seeding of one scaffold, it was placed immediately in  $-80^{\circ}\text{C}$  freezer as a day 0 control for the initial DNA content prior to scaffold culture. Scaffolds seeded with SF-MSCs and empty scaffolds were cultured in a static environment at  $37^{\circ}\text{C}$  under HYP and 5%  $\text{CO}_2$  with or without TGF- $\beta_3$  and IGF-1 for 21 days. Medium changes were performed twice per week.

### **5.2.8 Scanning electron microscopy (SEM) analysis**

The microarchitecture of the DCM scaffolds and the morphologies of SF-MSCs on the scaffolds were investigated via scanning electron microscopy (SEM). SEM was performed on SF-MSCs seeded scaffolds post 21 days of *in vitro* culture. Briefly, each scaffold was fixed with a pre-warmed fixative solution consisting of 2% (v/v) glutaraldehyde and 2.5% (v/v) paraformaldehyde overnight at  $4^{\circ}\text{C}$ . Scaffolds were then carefully cut into 4 pieces using scalpels. The scaffolds were washed with Milli-Q water 3 times for 2 min the next day. Then a second fixation process was performed using 2% (v/v) osmium tetroxide in Milli-Q water for 15 min, followed by washing the scaffolds in Milli-Q water, then fixing the scaffolds using 2% (w/v) tannic acid in Milli-Q water for 15 min. This step was repeated three times before stepwise dehydration using: 30%, 50%, 70%, 80%, 90%, 95% and 100% ethanol (% v/v) twice each for 5 min each followed by hexamethyldisilazane (HMDS) treatment (twice) for 5 min. The scaffolds were then air dried at room temperature overnight. The scaffold images were captured using a scanning electron microscopy (SEM) (Model S-4800, Hitachi, JA). The pore sizes of the DCM

were measured based on SEM images by ImageJ software (U.S. National Institutes of Health, Bethesda, Maryland, USA). All the reagents used were from Electron Microscope Science, PA, USA.

### **5.2.9 Analysis for fibrochondrogenic differentiation of SF-MSCs**

At the end of culture stage under HYP, pellets and scaffolds were assessed biochemically for glycosaminoglycan (GAG) and DNA content, histologically by Safranin-O staining and by immunofluorescence (IF) for characteristic meniscus matrix proteins (e.g. aggrecan, collagen I/II) and hypertrophic differentiation marker (collagen X) and by quantitative polymerase chain reaction (q-PCR) for gene expression analysis as previously described [246]. For aggrecan IF, paraffin sections of 5  $\mu\text{m}$  thick were treated with epitope retrieval solution (IW-1100, IHC) in a steamer (IHC-Tek™) after deparaffinization and rehydration. The sections were incubated with primary antibody: rabbit anti-aggrecan (36861, Abcam) using a 1:100 dilution in 4°C overnight followed by incubation with a goat anti-rabbit IgG (H&L Alexa Fluor 594, Abcam) with a 1:200 dilution. For gene expression analysis, primers sequences were either obtained from previously published work or newly designed using Primer Express software (ThermoFisher, ON, Canada) (Table 3). mRNA expression levels for each primer set were normalized to the geometric mean expression level of these housekeeping genes:  $\beta$ -actin, Ribosomal Protein L13a (*RPL13A*) and Tyrosine 3-Monooxygenase/Tryptophan 5-Monooxygenase Activation Protein Zeta (*YWHAZ*), using the  $2^{-\Delta\text{ct}}$  method [219].

**Table 5-3:** Primer sequences for quantitative polymerase chain reaction analysis

Gene	Primer sequences		GenBank accession or reference
$\beta$ -actin ( <i>ACTB</i> )	5'AAGCCACCCCACTTCTCTCTAA3'	Forward	NM_001110 1
	5'AATGCTATCACCTCCCCTGTGT3'	Reverse	
Aggrecan ( <i>ACAN</i> )	5'AGGGCGAGTGGAATGATGTT 3'	Forward	M55172
	5'GGTGGCTGTGCCCTTTTAC3'	Reverse	
Collagen I ( <i>COL1A2</i> )	5'TTGCCCAAAGTTGTCCTCTTC T3'	Forward	NM_000089
	5'AGC TTCTGTGGAACC ATG GAA3'	Reverse	
Collagen II ( <i>COL2A1</i> )	5' CTGCAAATAAAAATCTCGGTGTTCT3'	Forward	[15]
	5' GGCATTTGACTCACACCAGT3'	Reverse	
Collagen X ( <i>COL10A1</i> )	5'GAAGTTATAATTTACTGAGGGTTTCAA A3'	Forward	X60382
	5'GAGGCACAGCTTAAAAGTTTTAAACA3'	Reverse	
RPL13A	5'CCTGGAGGAGAAGAGGAAAGAGA3'	Forward	NM_001270 491.1
	5'TTGAGGACCTCTGTGTATTTGTCAA3'	Reverse	
SRY-Box 9 ( <i>SOX9</i> )	5'GACTTCCGCGACGTGGAC3'	Forward	Z46629
	5'GTTGGGCGGCAGGTACTG3'	Reverse	
<i>YWHAZ</i>	5'TCTGTCTTGTCACCAACCATTCTT3'	Forward	NM_003406
	5' TCAATGCGGCCTTTTCCA3'	Reverse	

### 5.2.10 Statistical analysis

Data represent the mean of four donors, excluding the donor used solely for flow cytometry characterization, each measured at least in independent duplicates or at most in triplicates  $\pm$  standard deviation in four experiments. Statistical analyses were performed

using SPSS (version 23; IBM Canada Ltd, ON, Canada) and Excel 2016 (Microsoft, WA, USA). Outliers were defined as values 1.5 interquartile ranges below the 1st quartile or above the 3rd quartile. Data were assessed for normality using the Shapiro-Wilk test. Levene's test was used to assess homogeneity of error variances. For cases with equal variances, distinct groups were compared using one-way analysis of variance (ANOVA) with Tukey's multiple comparison *post hoc* tests; otherwise, a Kruskal-Wallis one-way ANOVA with pairwise comparisons was applied. For comparison between the DCM scaffold with or without growth factors, a Student's *t*-test was used. Significance was considered when  $p < 0.05$ .

## **5.3 Results**

### **5.3.1 SF-MSCs isolation and expansion culture**

A colony forming unit fibroblastic (Cfu-f) assay was performed to assess the percentage of adherent SF-MSCs isolated from human synovial fluid (SF) cultured with basic fibroblast growth factor (FGF-2) under hypoxia (HYP, 3% O<sub>2</sub>) (Fig.5-2). All Petri dishes seeded with cells had colonies formed (n=4; Fig.5-2A). Cell morphology was visualized by staining with crystal violet. On the edge of the colonies, cells were loosely connected while cells in the center were highly compact. Cell morphology ranges from long-spindle shaped to polygonal-like (Fig.5-2B). The number and diameter of the cell colonies were recorded at the end of P0 when the corresponding expanded SF-MSCs in culture flasks were about 80-90% confluence ( $23.5 \pm 9.0$  days of culture). The mean number and

diameter of the cell colonies were  $36.6 \pm 24.7$  and  $1.2 \pm 0.2$  cm. Cfu-f efficiencies varied between donors with a mean efficiency of  $1.5 \pm 1.0\%$  (Fig.5-2C). The total number of colonies per mL of synovial fluid were  $4.2 \pm 2.4$ . All data in this study are presented as the mean  $\pm$  standard deviation (Fig.5-2D). Isolated SF-MSCs were at the same time cultured in monolayer with FGF-2 under HYP. Mean cumulative population doublings (PD) were  $11.6 \pm 0.6$  at the end of P1 and  $13.9 \pm 0.6$  in P2 (Fig.5-2D). The mean time between plating of SF-MSCs at P1 and reaching 85-90% confluence at the end of P2 was  $16.5 \pm 6.2$  days. PD per day was highest in P1 at  $0.6 \pm 0.2$  and then decreased in P2 at  $0.2 \pm 0.1$  (Fig.5-2D).

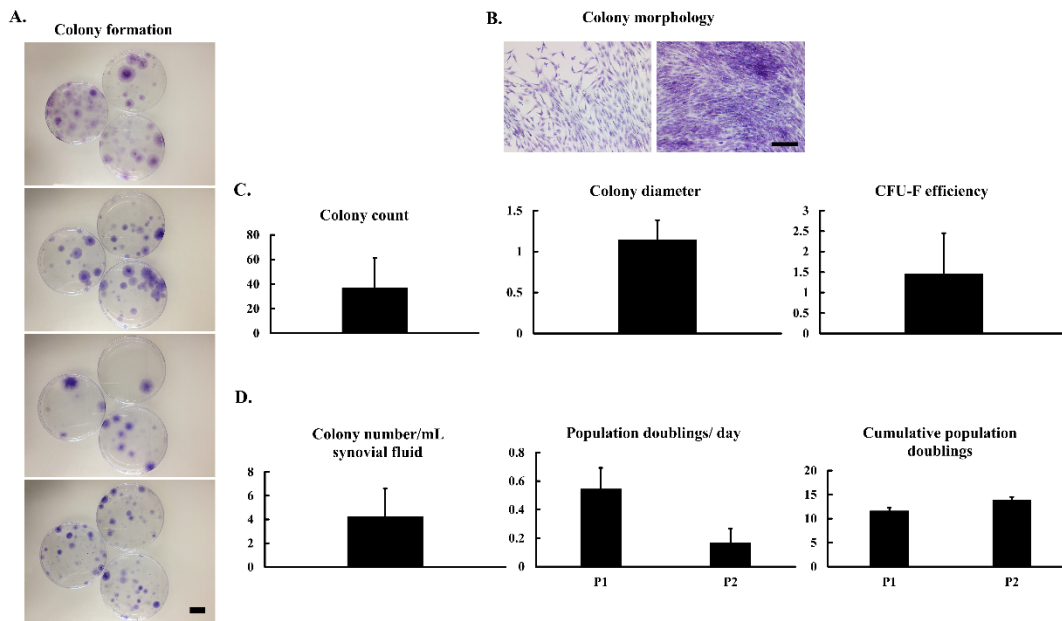


**Figure 5-2:** Colony-forming unit fibroblastic (Cfu-f) assay of human synovial fluid mesenchymal stem cells (SF-MSCs) at the end of P0 expanded with FGF-2 (5 ng/mL) under hypoxia (HYP, 3% O<sub>2</sub>) (n=4). (A) Colony formation of plastic-adherent SF-MSCs

and visualized by crystal violet staining, (B) morphology of the adherent cells, (C) colony count, colony diameter, and Cfu-f efficiency, (D) colony number per mL SF, population doublings per day and cumulative population doublings. D: donor, scale bar (A): 2 mm and (B): 200  $\mu\text{m}$ , all data presented as a mean  $\pm$  standard deviation.

### 5.3.2 Expression of MSC surface markers on SF-MSCs

To characterize the immunophenotype of isolated SF-MSCs, one donor (male, 36 years old) was analyzed for the cell surface molecule expression. SF-MSCs were positive for CD13, 29, 44, 49C, 73, 90, 105, 151 and negative for CD34, 45, 49f, 184 (Fig.5-3). The positive and negative immunophenotypic characteristics of the isolated SF-MSCs were consistent with MSC cell surface properties [112].

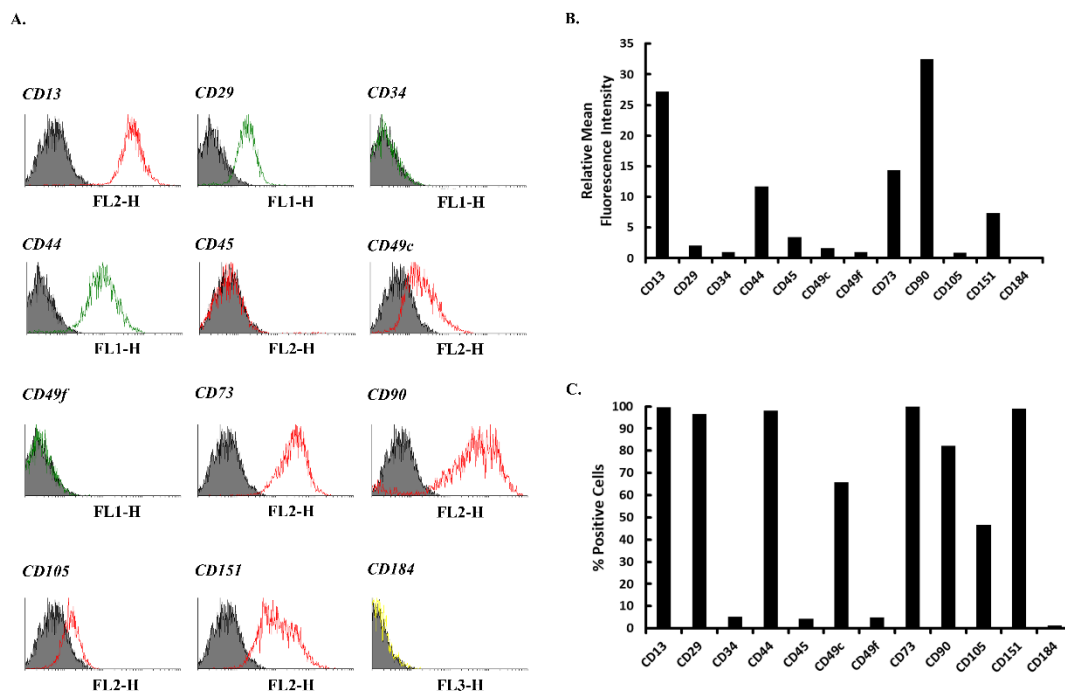


**Figure 5-3:** Flow cytometry analysis of cell surface markers on P2 SF-MSCs after

culture with FGF-2 (5 ng/mL) under HYP from one donor (male, 36 years old). (A) Fluorescence intensity histograms, (B) The fluorescence intensity of cell surface markers, (c) the percentage (%) of positive SF-MSCs

### 5.3.3 Biochemical analysis of GAG and DNA content

To assess the effect of DCM and growth factors on fibrochondrogenic differentiation potential of SF-MSCs *in vitro*, the biochemical analysis was performed on SF-MSCs in pellets (Fig.5-4A) and DCM scaffold model (Fig.5-4B) after 21 days of culture under HYP. In the pellet groups, no significant differences were found in DNA content. Pure TGF- $\beta_3$  (+TGF $\beta_3$ ) or the combination of TGF- $\beta_3$  /IGF-1 (+TGF $\beta_3$ /IGF-1) tended to stimulate more GAG production when compared to pure IGF-1 (+IGF-1) which was consistent with the Safranin-O staining results, though there was no statistical difference. The same trend was also observed when quantitative GAG production was normalized to DNA content (GAG/DNA) without significant difference (Fig.5-4A). In the DCM groups, the GAG content and GAG/DNA were significantly higher in +TGF $\beta_3$ /IGF-1 compared to the group without exogenous growth factors (-TGF $\beta_3$ /IGF-1) ( $p=0.04$  and  $p=0.01$ , respectively). +TGF $\beta_3$ /IGF-1 also tended to promote SF-MSCs proliferation after seeding on DCM when compared to day 0 control and -TGF $\beta_3$ /IGF-1, but no significant difference was found (Fig.5-4B). The GAG and DNA contents of an empty DCM scaffold were measured to provide a baseline value prior to seeding with SF-MSCs. While GAG was detected on the empty DCM with similar levels to the SF-MSC-seeded

DCM without growth factors, it was nearly acellular with very little DNA detected in comparison to the cell-seeded groups.

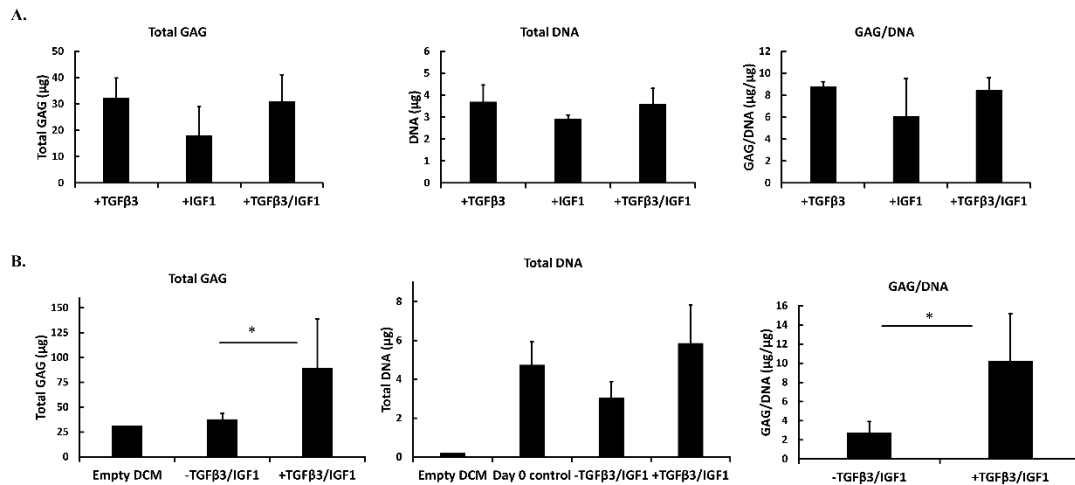


**Figure 5-4:** Biochemical analysis of pellets derived from SF-MSCs (n=4) after 21 days of *in vitro* culture in the presence of serum-free medium containing IGF-1, TGFβ3 or the combination under HYP. (A) GAG content, DNA content and GAG/DNA in pellets; Biochemical analysis of DCM scaffolds seeded with SF-MSCs (n=4) after 21 days of *in vitro* culture in serum-free medium with or without combined +TGFβ3/IGF-1 under HYP. (B) GAG content, DNA content and GAG/DNA in DCM scaffolds. + and - indicates with or without growth factors, \* indicates significant differences ( $p < 0.05$ ), data all presented as a mean  $\pm$  standard deviation.

### 5.3.4 Safranin-O staining and scanning electron microscopy

After 21 days of *in vitro* culture under HYP, pellets and DCM scaffolds were embedded in paraffin and then 5 μm thick sections were cut and stained with Safranin-O to visualize

the deposition of sulfated proteoglycan. The pellet results were consistent with the biochemistry analysis. Safranin-O positive staining occurred in both +TGF $\beta$ 3 and +TGF $\beta$ 3/IGF-1 while +IGF-1 was negative (Fig.5-5A). In the DCM groups, Safranin O positive ECM was abundant in +TGF $\beta$ 3/IGF-1 with chondrocyte-like cells residing within lacunae-like structures. However, although deposition of ECM was noted in -TGF $\beta$ 3/IGF-1, no Safranin-O staining was observed (Fig.5-5B).

Scaffolds were fixed with glutaraldehyde and paraformaldehyde and then processed with osmium tetroxide and tannic acid to visualize the microarchitecture and morphologies of the empty scaffold or SF-MSCs seeded on scaffolds after 21 days using SEM. The gross morphology of the empty scaffold appeared sponge-like; under SEM imaging it exhibited a 3-dimensional porous structure with collagen leaves/sheets after freeze-drying (Fig.5-5C). The pore sizes in the empty scaffold ranged widely from 32  $\mu$ m to 290  $\mu$ m based on the SEM image (Fig.5-6)

Under both conditions (i.e. -TGF $\beta$ 3/IGF-1 and + TGF $\beta$ 3/IGF-1), SF-MSCs adhered to and penetrated into the DCM scaffolds. The scaffold pores were filled with SF-MSCs and abundant extracellular matrix was synthesized. In -TGF $\beta$ 3/IGF-1, the scaffold structure was modified by closely-packed, flat-shaped, fibroblast-like SF-MSCs on the order of 50 $\mu$ m with microvilli (Fig.5-5C). Some round-shaped SF-MSCs were located on top of or between the fibroblastic-like SF-MSCs of around 2-5  $\mu$ m in diameter. Collagen-like fibers synthesized by the fibroblast-like cells branched out from their surfaces and

appeared to connect them together. In contrast, in +TGF $\beta$ 3/IGF-1 , the upper layer was covered in round-shaped chondrocyte-like SF-MSCs of around 1-7  $\mu$ m in diameter with microvilli. They appeared to form very long collagen-like fibers that integrated into the newly-formed extracellular matrix. Some of these cells were buried by the dense network of fibers. Beneath this upper layer, the matrix was extremely dense with some elongated cells on the order of 50-100  $\mu$ m. Higher magnification of SEM images for scaffold seeded with SF-MSCs is shown in Fig.5-5D.

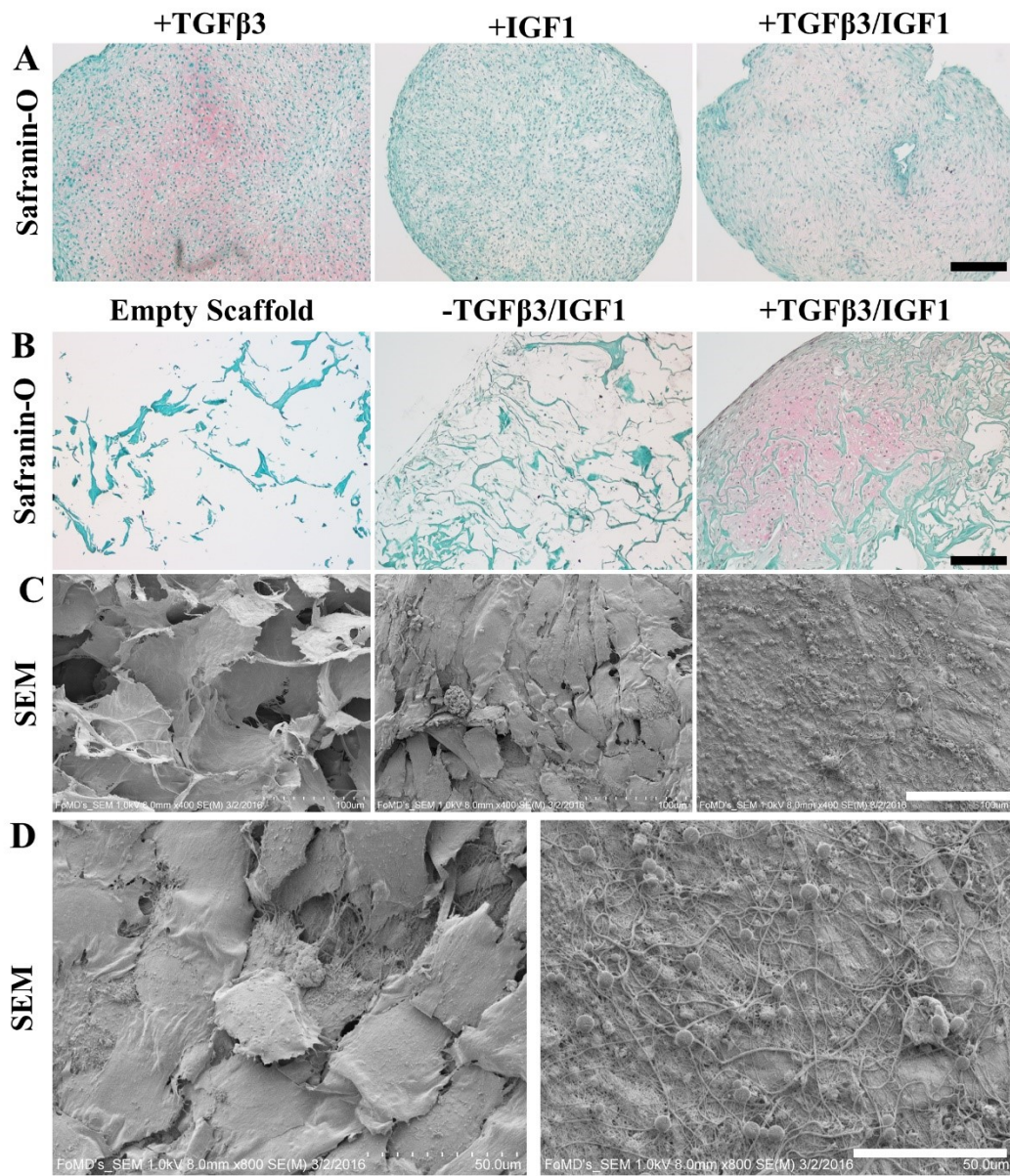


**Figure 5-5:** Safranin-O staining analysis for proteoglycan deposition in pellets derived from SF-MSCs (A) and DCM scaffolds seeded with SF-MSCs (B) after 21 days of *in vitro* culture under HYP; Scanning electronic microscope (SEM) for the morphology of SF-MSCs and DCM scaffold (C), (D: higher magnification) after 21 days of culture under HYP. + and - indicates with or without growth factors, scale bars in μm: (A &B)

200 (C) 100 (D) 50.

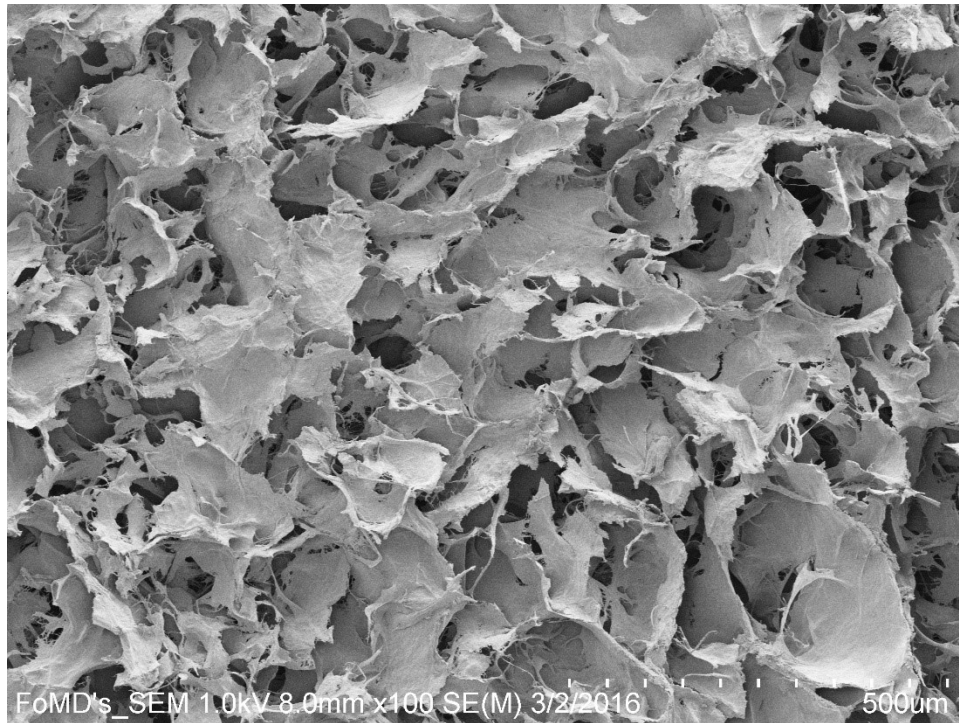


**Figure 5-6:** Scanning Electron Microscopy image of an empty decellularized matrix (DCM) scaffold from human native meniscus (n=1, male, 46 years old).

### 5.3.5 Immunofluorescence

After 21 days of *in vitro* culture in HYP, indirect immunofluorescence was performed to detect extracellular matrix components using a primary antibody to collagen I, collagen II, aggrecan (Fig. 5-7), the hypertrophic marker collagen X (Fig. 5-8) and cells (DAPI) in pellets and scaffolds. Pellets derived from human bone marrow mesenchymal stem cells (BM-MSCs) from a previous study served as a positive control for collagen X (Fig. 5-8). The first and fourth column of DAPI staining in Fig. 5-7 was done separately in aggrecan and collagen I/II immunofluorescence.

In the pellet groups, SF-MSCs visualized via DAPI were evenly distributed throughout the pellets in three conditions qualitatively (Fig. 5-7A). Aggrecan immunofluorescence was noticeable in both +TGF $\beta$ 3/IGF-1 and +TGF $\beta$ 3 while +IGF-1 did not induce deposition of aggrecan. Deposition of collagen I was homogenous across the three conditions. In contrast, collagen II deposition was most remarkable in +TGF $\beta$ 3/IGF-1 and then decreased in +TGF $\beta$ 3, with no collagen II deposition in +IGF-1. Both aggrecan and collagen II fluorescence corresponds well with safranin O staining for GAG content (Fig.5-5A). Negligible deposition of collagen X was observed in +IGF-1 when compared to the positive control BM-MSC pellet (Fig. 5-8A). For +TGF $\beta$ 3/IGF-1 and +TGF $\beta$ 3, punctate immunofluorescence signal was observed compared to the diffuse signal in the BM-MSC pellet (Fig.5-8A). In the DCM groups, no DAPI staining was observed in the empty scaffold after the decellularization process (Fig.5-8B). Most of the empty scaffold components were collagen I with some collagen II and X (Fig.5-8B). The number of SF-MSCs in -TGF $\beta$ 3/IGF-1 was less than in +TGF $\beta$ 3/IGF-1, which was consistent with the DNA analysis. Immunofluorescence indicated collagen I deposition in both groups. In contrast, intense collagen II immunofluorescence was observed in +TGF $\beta$ 3/IGF-1 while no deposition of collagen II was detected in -TGF $\beta$ 3/IGF-1 (Fig.5-7B). No obvious differences in collagen X deposition were observed between the two groups and the fluorescence was much less pronounced relative to the positive control (Fig.5-8B).

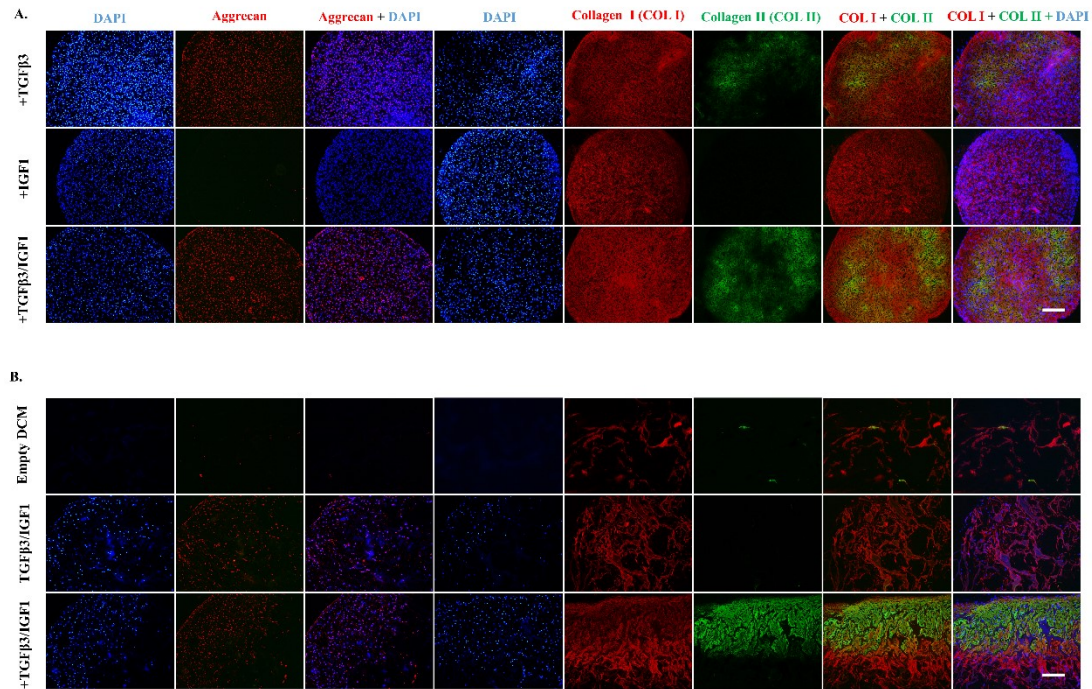


**Figure 5-7:** Indirect immunofluorescence analysis of aggrecan, collagen I and collagen II in pellets derived from SF-MSCs (A) and empty DCM scaffold or DCM scaffolds seeded with SF-MSCs (B) after 21 days of *in vitro* culture under HYP. Blue (DAPI: 4',6-diamidino-2-phenylindole.): cells, Red (Alexa Fluor 594): aggrecan and collagen I, Green (Alexa Fluor 488): collagen II. Aggrecan and collagen I/II was performed on separate slides and thus DAPI was presented for each. Scale bar (white): 200  $\mu$ m

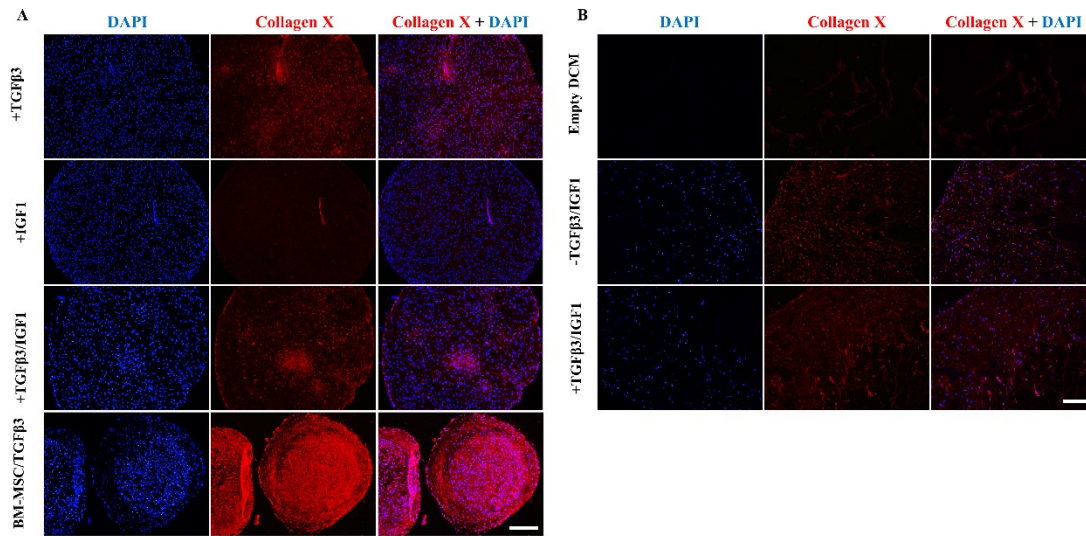


**Figure 5-8:** Indirect immunofluorescence analysis of hypertrophic marker collagen X in pellets derived from SF-MSCs (A) and empty DCM scaffold or DCM scaffolds seeded with SF-MSCs (B) after 21 days of *in vitro* culture under HYP. Blue (DAPI): cells, Red (Texas Red): collagen X. Positive control (A): pellets from human bone marrow-derived mesenchymal stem cells cultured with the same chondrogenic medium. Scale bar (white): 200  $\mu\text{m}$ .

### 5.3.6 ECM gene expression

Relative gene expression levels were assessed in SF-MSCs cultured in pellets and in DCM scaffolds by qPCR after 21 days of *in vitro* culture under hypoxic conditions to further characterize the newly-formed ECM. The mean relative gene expression levels of aggrecan (*ACAN*), collagen I (*COL1A2*), collagen II (*COL2A1*), *SOX9*, collagen X (*COL10A1*) are shown in Fig.5-9.

In the pellet groups, both +TGF $\beta$ 3 and +TGF $\beta$ 3/IGF-1 showed significant or nearly

significant mRNA gene upregulation compared to +IGF1 of ECM macromolecules *ACAN* ( $p=0.002$  and  $p=0.003$ , respectively), *COL1A2* ( $p=0.007$  and  $p=0.056$ ), and *COL2A1* ( $p=0.011$  and  $p=0.020$ ), hypertrophic differentiation marker *COL10A1* ( $p=0.04$  and  $p=0.21$ ), and chondrogenic regulator *SOX9* ( $p=0.012$  and  $p=0.008$ ) (Fig.5-9A-E). However, there was no significant difference between +TGF $\beta$ 3 and +TGF $\beta$ 3/IGF-1 for any gene measured (Fig.5-9A-E).

In the DCM scaffolds, the addition of +TGF $\beta$ 3/IGF-1 seemed to induce higher gene expression of *ACAN*, *COL1A2*, *COL2A1*, and *SOX9* relative to their expression in pure DCM scaffold with no growth factor treatment (-TGF $\beta$ 3/IGF-1). However, not all the inductions were statistically different: it was not significant for *ACAN* ( $p=0.09$ , Fig. 5-9F), it was significant for *COL1A2* and *SOX9* ( $p=0.04$ , Fig. 5-9G and  $p=0.03$ , Fig. 5-9J, respectively), and it was not significant for *COL2A1* and *COL10A1* ( $p=0.17$ , Fig. 5-9H and  $p=0.14$ , Fig.5-9I, respectively).

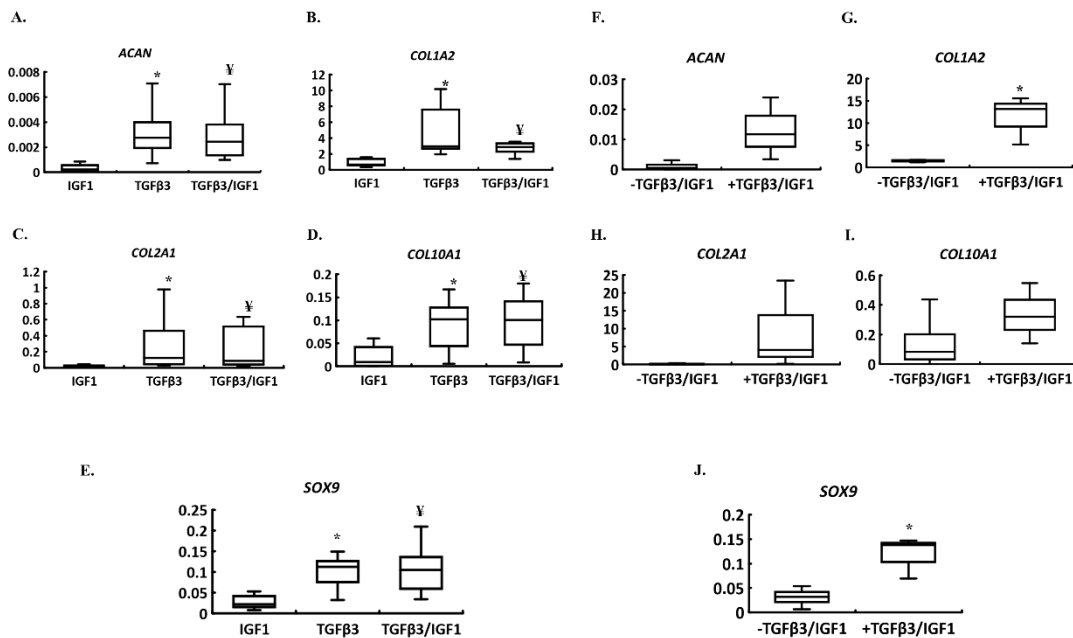


**Figure 5-9:** Real-time PCR analysis of cDNA of pellets derived from SF-MSCs (A-E) and DCM scaffolds seeded with SF-MSCs (F-J) after 21 days of *in vitro* culture under HYP, in the presence (+) and absence (-) of growth factors. \* and ‡ in pellets indicates significant differences ( $p < 0.05$ ) in IGF-1 vs. TGFβ3, and IGF-1 vs. TGFβ3/IGF1, respectively. \* in scaffolds indicates significant differences ( $p < 0.05$ ) between -TGFβ3/IGF-1 and +TGFβ3/IGF-1 group.

## 5.4 Discussion

SF-MSCs are a promising stem cell source for engineering cartilaginous tissues as a consequence of their reduced hypertrophic tendencies [185, 304]. However, the growth and chondrogenic differentiation of multiple MSCs is influenced by a variety of biochemical, microenvironmental and biomechanical factors; TGF $\beta$ s [292], oxygen tension [311], extracellular matrix (ECM) [247] and mechanical stimuli [312].

In this study, we asked the question: “can the ECM derived from human meniscus stimulate fibrochondrogenic differentiation of SF-MSCs *in vitro*?” Cheng *et al* had demonstrated that the native ECM of articular cartilage had the capacity to differentiate adipose-derived MSCs towards a chondrocyte phenotype with the capacity to synthesize cartilaginous matrix [254].

To address our question, we demonstrated the isolation and characterization of SF-MSCs. Our isolation and cell expansion protocol involved hypoxia (HYP, 3% O<sub>2</sub>) and supplementation of FGF-2, both of which have been demonstrated to be beneficial for maintaining the chondrogenic potential of expanded bone marrow-derived MSCs [15]. Colony formation was evident in all donor SF-MSCs tested in this study. The SF-MSCs, including those isolated from an osteoarthritic donor joint, proliferated well under HYP and in the presence of FGF-2. Although Kurose *et al* showed that 19 out of 26 donors with osteoarthritis had SF-MSCs that expanded well under normoxia but in the absence of growth factors [313]. Conventionally used cell surface marker panel for the

characterization of MSCs was implemented using flow cytometry [112]. The isolated SF-MSCs were positive for the panel of MSC surface markers at the end of P2, suggesting that the conditions of cell isolation supported the proliferation and retention of the MSC-related phenotype of human SF-MSCs. However, there were notable donor-specific cell proliferation differences. Relative to the other three donors (male,  $26.3 \pm 6.0$  years) of SF-MSCs who suffered from acute injuries, the SF-MSCs from the older and osteoarthritic donor (male, 57 years) required more time to become confluent (36 days vs  $19 \pm 2.8$  days) and had the least number of colonies formed (10 vs  $45.4 \pm 17.2$ ), but the largest diameter of colonies ( $1.37 \pm 0.26$  cm vs  $1.1 \pm 0.2$  cm) at the end of passage 0 and beginning of passage 1. Our findings here are somewhat consistent with reports that the number of colonies of SF-MSCs positively correlates with post-injury time and with increased severity of osteoarthritis [180, 303]. Another factor that may have influenced the notable difference may be the age difference. Increased age has been reported to negatively impact the Cfu-f potential of MSCs [314]. But looking at our Cfu-f data (Fig.5-2A), age does not appear to have been a negative factor given the age range of the SF-MSCs donors; 18-57 years. It is probable that the use of HYP during isolation and expansion culture of SF-MSCs in this study may have mitigated the effect of age and contributed positively to the Cfu-f potential [15, 315]. However, the long doubling time for the human SF-MSCs to reach confluence from P0 to P2 ( $39.8 \pm 13.1$  days) is of concern for a timely generation of large cell numbers for tissue engineering and

regenerative medicine purposes.

We proceeded to investigate the potential of pure IGF-1 (+IGF-1), pure TGF- $\beta_3$  (+TGF $\beta_3$ ) and in combination (+TGF $\beta_3$ /IGF-1) to differentiate SF-MSCs towards a fibrochondrogenic phenotype using an *in vitro* pellet model. Moreover, the differentiation was implemented under hypoxic conditions to augment the chondrogenic differentiation [15]. In the presence of TGF- $\beta_3$  (i.e. +TGF $\beta_3$ ) induced SF-MSCs towards a fibrochondrogenic phenotype with deposition of collagens I and II protein, and sulphated proteoglycans. In contrast, +IGF-1 did not induce fibrochondrogenesis. This finding was surprising in view of a recent report that IGF-1 regulated embryonic development of mouse meniscus [305]. It is probable that the presence of insulin in our differentiation protocol abrogated the potential of IGF-1 to induce fibrochondrogenesis of SF-MSCs; insulin has been reported to inhibit the binding of IGF-1 to the IGF-1-receptor and reduce the stimulatory effects of IGF-1 [316]. Moreover, our data is consistent with several reports that IGF-1 had limited effects on the chondrogenesis of human/porcine SM-MSCs or human BM-MSCs [317-319]. The potential of IGF-1 in the absence of insulin to induce fibrochondrogenesis of SF-MSCs remains to be investigated. Although there was no gene expression differences between +TGF $\beta_3$  and +TGF $\beta_3$ /IGF-1, collagen II immunofluorescence seemed more intense in +TGF $\beta_3$ /IGF-1 suggesting a possible added benefit of the combined treatment over +TGF $\beta_3$  alone. Previous evidence suggests the two growth factors may work synergistically on chondrogenesis of MSCs [317-321].

Taken together, the combination of TGF- $\beta_3$  and IGF-1 appears to enhance the fibrochondrogenic differentiation of human SF-MSCs compared to pure +IGF-1, although future studies need to be done to clarify the role of IGF-1 when combined with TGF- $\beta_3$ .

Finally, we investigated whether human meniscus DCM scaffold has the capacity to induce fibrochondrogenesis of human SF-MSCs with or without combined TGF- $\beta_3$  and IGF-1 *in vitro*. To maximize the use of the limited number of fabricated DCM scaffolds used in this study, we investigated the combined treatment of +TGF $\beta_3$ /IGF-1 rather than +TGF $\beta_3$  or +IGF-1. The rationale for this is further supported by the most intense deposition of collagen II as observed in the +TGF $\beta_3$ /IGF-1 in the pellet study. The test of only +TGF $\beta_3$ /IGF-1 is recognized as a limitation of our investigation. Physical methods of homogenization and freeze-drying were used to generate our DCM scaffold [254]. SEM revealed that the DCM scaffold exhibited an interconnected porous structure for cell infiltration. Most of the collagen components of the meniscus (mainly collagen I/little collagen II) were retained while no cell or Safranin-O positive ECM content was detected in the scaffolds prepared by these methods. Interestingly, collagen X was weakly detected in the empty DCM (Fig.5-8B). Although we do not know the detailed medical history of the cadaver meniscus donor (male 46), it has previously been shown that small amounts of collagen X may be present in native human meniscus especially in degenerative cases [322].

Our findings in this study demonstrated that DCM scaffolds supported SF-MSCs differentiation towards a fibrochondrogenic phenotype but only in the presence of growth factors (i.e. TGF- $\beta_3$  and IGF-1) *in vitro*. This was consistent with previous studies that used soluble extracts of DCM of bovine meniscus but with TGF- $\beta_3$  supplementation to induce fibrochondrogenesis of human BM-MSCs [142, 310]. The DCM scaffold tended to support the proliferation of SF-MSCs in +TGF $\beta_3$ /IGF-1 based on the DNA content comparison to the day 0 control. Moreover, in the DCM groups +TGF $\beta_3$ /IGF-1 promoted a chondrocyte-like round morphology. An abundance of Safranin-O positive ECM, as well as collagen II ECM, was deposited by the SF-MSCs in the DCM scaffold in +TGF $\beta_3$ /IGF-1. However, examination of gene expression levels and protein production indicated the DCM scaffold alone did not induce fibrochondrogenesis of the SF-MSCs.

SEM revealed that human SF-MSCs had a flat fibroblast-like morphology on the DCM scaffold without growth factors, which is similar to *in vitro* monolayer-expanded, dedifferentiated meniscus fibrochondrocytes (MFCs) or MFCs residing in the outer region of the meniscus that mainly synthesize collagen I [12, 323]. Consistent with a fibroblast-like morphology, there was limited to no Safranin-O positive ECM and deposition of collagen II. However, collagen I was evident within the ECM, indicating that the pure DCM scaffold did not drive fibrochondrogenic differentiation of the SF-MSCs. These results were inconsistent with Cheng *et al* who showed that pure decellularized matrix scaffold derived from porcine articular cartilage promoted

fibrochondrogenesis of human adipose-derived MSCs [254]. The source of MSCs, cell expansion culture conditions and preparation methods of DCM may contribute to this disparity in outcomes. For example, a combination of TGF- $\beta_1$ , epidermal growth factor, and FGF-2 was used during AD-MSCs expansion in the study of Cheng *et al* [254], while we used FGF-2 in our study. The supplementation of different growth factors during cell expansion has been shown to regulate different chondrogenic differentiation capacities of articular chondrocytes [224]. Additionally, the use of serum during chondrogenic differentiation by Cheng *et al* [254] may have impacted the behavior of AD-MSCs. In another study, using DCM from porcine articular cartilage, the negligible inductive effect on chondrogenesis of human BM-MSCs and AD-ASCs was observed when no serum and growth factors were added [324], which is similar to our study. Another possibility may be the absence or reduced amounts of ECM components like Safranin-O positive ECM and collagen II in the empty scaffold. Our decellularization process using physical forces and multiple PBS washes may have led to the loss of binding and storage sites of growth factors, such as TGF- $\beta$ s and IGF-1 within the DCM [266], when compared to other decellularization methodologies using acidic treatments. Acidic method of decellularization has been shown to maintain ECM components such as proteoglycans and collagen II in porcine meniscus [256]. The lack of detailed characterization of biochemical contents, such as proteomic analysis via mass spectrometry, in our DCM compared to the native human meniscus is a limitation of our study. Further studies are

also needed to test the effect of other decellularized methods on the ECM components of the human meniscus. However, the novelty of our study is noteworthy in the context of the low oxygen tension culture conditions used. Synovial fluid exists in a hypoxic microenvironment [226] and Marsano *et al* had demonstrated that pure 2% oxygen tension induced spontaneous chondrogenesis of human BM-MSCs by triggering that was associated with upregulation of the TGF $\beta$  pathway [293]. Our data revealed no such inductive effect by pure low oxygen tension although we used 3% oxygen tension instead of the 2% by Marsano *et al* [293].

Hypertrophic differentiation of MSCs remains a significant challenge. In our study, negligible deposition of collagen X by SF-MSCs was observed in both the pellet and DCM-based models compared to the positive control pellet derived from human BM-MSCs *in vitro*. Peltari *et al.* had shown that the addition of TGF $\beta$ 3 during *in vitro* chondrogenesis can induce hypertrophic differentiation of human BM-MSCs, resulting in calcified matrix formation post subcutaneous implantation severe combined immunodeficient (SCID) mice [121]. Although Jones *et al* was the first to show that SF-MSCs may pose similar phenotypes to BM-MSCs [325], further studies found that human SF-MSCs may be more similar to the synovial membrane (SM-MSCs) [180, 181] and have better chondrogenic capacity and less osteogenic phenotype than BM-MSCs [302, 304]. Our findings were consistent with previous studies showing that porcine or human articular cartilage DCM can suppress the hypertrophic differentiation during

chondrogenesis of human adipose and synovium-derived MSCs, respectively [254, 324, 326]. The hypoxic conditions during the chondrogenic culture of our SF-MSCs is another possible factor for the noted but reduced hypertrophic differentiation as evidenced by the little to no deposition of collagen X. Our previous study [15] and Sheehy *et al* [327] have shown that low oxygen tension (3% or 5% O<sub>2</sub>) during chondrogenic culture of human BM-MSCs suppressed hypertrophic marker expression of collagen X (*COL10A1*). The mechanism underlying the suppression of *COL10A1* was deemed to be associated with the downregulation of *RUNX2* activity through Smad suppression and histone deacetylase 4 activation [327].

## 5.5 Conclusions

Human SF-MSCs exhibited advantageous characteristics for meniscus tissue engineering applications by undergoing fibrochondrogenesis with a reduced tendency for hypertrophic differentiation after growth factor induction *in vitro*. Our results were consistent with previous human and porcine studies, which demonstrated the superior fibrochondrogenic capacity of SF-MSCs compared to other MSCs. Our data also revealed that combined TGF- $\beta_3$  and IGF-1 had a beneficial effect on the fibrochondrogenesis of human SF-MSCs, while pure IGF-1 had no effects in our small-scale cell pellet model. Larger-scale fibrocartilaginous matrix was generated by human SF-MSCs seeded upon a decellularized ECM scaffold derived from normal human meniscus tissue with combined TGF- $\beta_3$  and IGF-1 supplementation *in vitro*, suggesting the promising use of

decellularized ECM scaffold as a natural supporting material for fibrochondrogenesis of SF-MSCs. Future studies hold merit to assess the phenotypic stability and efficacy of the newly-formed fibrocartilaginous matrix *in vivo*, as well as potential exogenous growth factor-free differentiation of SF-MSCs seeded on the DCM in the complex joint environment to repair meniscus defects.

**Chapter 6 Chondrogenically differentiated human synovial fluid-derived mesenchymal stem cells yield a vascularized and calcification-resistant matrix in immunodeficient mouse model**

**Yan Liang, Clayton Molter, Alexander R.A. Szojka, Enaam Idrees, Lynn Williams,**

**Melanie Kunze, Aillette Mulet-Sierra, Nadr M. Jomha, and Adetola B. Adesida**

This chapter has been submitted for publication.

## 6.1 Introduction

Adult inner meniscus injuries do not heal and may require surgical interventions that cause early onset of knee osteoarthritis (OA) [3]. Mesenchymal stem cells (MSCs) have been investigated to generate functional inner meniscus like-extracellular matrix (IM-ECM) composed primarily of type I & II collagen and proteoglycans for meniscus repair [9]. Compared to MSCs derived from bone marrow, synovial membrane, and infrapatellar fat pad, synovial fluid-derived MSCs (SF-MSCs) exhibit similar or higher chondrogenic differentiation capacity and reduced hypertrophic tendencies to form bone matrix *in vitro* [185, 304]. Previously, we demonstrated that human SF-MSCs (hSF-MSCs) can form IM-ECM after TGF- $\beta$ 3 induction under hypoxic incubator conditions (HYP, 3% O<sub>2</sub>) using a human meniscus-derived decellularized matrix scaffold *in vitro* (Chapter 5) [255]. HYP compared to normoxia (NRX) has been shown to promote chondrogenic differentiation of BM-MSCs, leading to superior IM-ECM formation [13, 15]. However, *in vitro*-generated bioengineered cartilaginous tissues from MSCs are not always stable in *in vivo* models. For example, *in vitro*-generated human SM-MSC [120] and BM-MSC [121]-derived cartilaginous tissues respectively failed to maintain the chondrogenic phenotype and underwent calcification when implanted in the commonly-used subcutaneous nude mouse model. Thus, despite the reduced hypertrophic tendencies of hSF-MSCs their *in vivo* performance needs to be investigated.

In adults, the peripheral meniscus regions are vascularized whereas the inner regions

are avascular. The inability of these inner regions to heal has been tied to this avascular nature [7] and the presence of anti-angiogenic factors like chondromodulin-1 produced by meniscus fibrochondrocytes (MFCs) [328]. Accordingly, one strategy to enhance the healing potential of bioengineered inner meniscus replacements may be to pre-enrich them with angiogenic factors that stimulate angiogenesis from the peripheral vascular meniscus regions. Previously, bovine calf MFCs transfected with an angiogenic factor-encoding gene produced stable IM-ECM that became vascularized in the subcutaneous nude mouse model [102]. Hypoxia promotes angiogenesis in tumors by expression of the angiogenic factor vascular endothelial growth factor (VEGF) [329]. *In vitro* hypoxia-pre-culture strategies can enhance the secretion of VEGF by MSCs which in turn enhanced angiogenesis and tissue repair [330, 331]. Hypoxia can also co-induce the expression of VEGF and stromal cell-derived factor-1 (SDF-1) [278], a stem cell homing factor [332], in synovial fibroblasts. SDF-1 promoted neovascularization and meniscus repair by recruiting endothelial progenitor cells [333] and injected MSCs [106], respectively. Thus, we speculated that hypoxia may similarly induce VEGF and SDF-1 expression in hSF-MSC-based IM-ECM.

Herein, we evaluated: (1) the effects of HYP (2% O<sub>2</sub>) relative to normoxia (NRX, ~20% O<sub>2</sub>) during pre-culture of hSF-MSCs in porous collagen scaffolds on IM-ECM formation and accumulation of angiogenic factors VEGF and SDF-1; (2) the *in vivo* stability in terms of ECM maintenance and calcification as well as the vascularization

tendencies of hSF-MSC-based IM-ECM in the subcutaneous nude mouse model after HYP and NRX pre-culture. Given the unique proclivity of hSF-MSCs for chondrogenic commitment and beneficial effects of HYP in terms of IM-ECM formation [15] and induction of angiogenic factors [330], we hypothesized that HYP would result in superior IM-ECM formation and angiogenesis without hypertrophic differentiation and resultant calcification *in vivo*.

## **6.2 Methods**

### **6.2.1 Ethics statement**

The synovial fluid aspirates were collected with the approval of the University of Alberta's Health Research Ethics Board- Biomedical Panel (Study ID: Pro00018778).

Work involving research animals was conducted in accordance with protocols approved by the University of Alberta Animal Care Committee (AUP00001363).

### **6.2.2 Isolation and monolayer expansion culture of human synovial fluid-derived mesenchymal stem cells (hSF-MSCs)**

Human synovial fluid was acquired from five male donors (Table 6-1). The isolation, monolayer expansion, and colony-forming unit fibroblast (Cfu-f) assay of hSF-MSCs were performed as previously described [255]. Briefly, the hSF-MSCs were cultured in standard  $\alpha$ -MEM with 10% fetal bovine serum (Sigma Aldrich) and 5 ng/mL FGF-2 in a regular hypoxic (37°C, 3% O<sub>2</sub>, 5% CO<sub>2</sub>) humidified incubator. Medium changes were performed twice a week. When the hSF-MSCs reached 80-90% confluence (defined in

this study as passage 0), they were detached and replated in new flasks at a 1:2 ratio for subsequent expansion. At the same time, the Cfu-f assay petri dishes were stained with crystal violet for colony counting. hSF-MSCs were split once more as before and were used at P2 for scaffold seeding and chondrogenic culture.

**Table 6-1:** Synovial fluid donor information

	Age	Medical History	Anatomic Sites	Volume
Donor 1	17y	Meniscus tears, healthy	Knee SF	5 mL
Donor 2	58y	Knee OA, high cholesterol, HTN	SF from both knees	3 mL
Donor 3	34y	Nonsmoker, healthy	Knee SF	10 mL
Donor 4	53y	Meniscus tears, smoker, healthy	Knee SF	2 mL
Donor 5	30y	Right knee meniscus tears, nonsmoker	Right knee SF	10 mL

### 6.2.3 Type I collagen scaffold seeding and experimental conditions

Human SF-MSCs from the end of P2 were seeded onto cylinder-shaped type I collagen scaffolds (3.5 mm in height and 6 mm in diameter) (Integra Lifesciences Corp., Plainsboro Township, NJ, USA) at a density of  $5 \times 10^6$  cells/cm<sup>3</sup> as previously described [13, 255]. Cell-seeded scaffolds were cultured in a defined serum-free medium (SFM) with 10 ng/mL of TGF- $\beta$ 3, dexamethasone, ascorbic acid 2-phosphate and L-proline (1 mL per construct) [255] under a regular normoxic (NRX, 37°C, 5% CO<sub>2</sub>) incubator or hypoxia (HYP, 37°C, 2% O<sub>2</sub>, 5% CO<sub>2</sub>) within an Xvivo X3 incubator system (Biospherix,

Parish, NY, USA) for 2 weeks. Medium changes were performed twice a week. For HYP, the fresh medium was equilibrated to HYP conditions for 2h before changing. Medium changes for the HYP group were under conditions of continuous HYP within the Xvivo X3 to avoid reoxygenation.

After two weeks of chondrogenic culture, constructs from the *in vitro* baseline (TGF- $\beta$ 3/2wks *in vitro*) were harvested. For donor 1 (M/17y, meniscus tears) and 2 (M/58y, osteoarthritis), constructs from NRX and HYP were either: 1) implanted subcutaneously in the back of athymic CD-1 nude mice (n=9, 7 weeks old, Charles River, Wilmington, USA) for an additional 5 weeks (Implantation/7wks) as previously described [280], and 2) cultured in a high glucose DMEM supplemented with 10% FBS (Sigma-Aldrich, St. Louis, MO, USA) for 5 weeks (DMEM/7wks *in vitro*) as controls for the *in vivo* groups under the same oxygen tensions.

#### **6.2.4 Assessment of inner meniscus-like extracellular matrix (IM-ECM) formation**

Constructs from each group were imaged to capture their gross morphology. They were then processed for biochemical analysis of glycosaminoglycan (GAG) and DNA content, histological analysis via Safranin-O staining, immunofluorescence analysis of type I & II collagen and CD31 (blood vessel invasion), Alizarin Red S staining of calcium deposition, and quantitative real-time polymerase chain reaction analysis of gene expression (Table 6-2: primer sequences) as previously described [255, 280]. mRNA

expression levels for each primer set were normalized to the mean expression level of three housekeeping genes: *β-actin*, Ribosomal Protein L13a (*RPL13A*) and Tyrosine 3-Monooxygenase/Tryptophan 5-Monooxygenase Activation Protein Zeta (*YWHAZ*), using the  $2^{-\Delta C_t}$  method [219]. Primary antibody-free controls were set up using only secondary antibodies to assess any non-specific binding for immunofluorescence.

Immunofluorescence and enzyme-linked immunosorbent assay (ELISA) analysis of VEGF and SDF-1 protein contents were also performed and described below. The homology of VEGF and SDF-1 between mouse and human are ~84% and ~92%, respectively (Sequence homology resource tool: <https://www.uniprot.org/align>).

**Table 6-2: Primer sequences**

Gene	Sequences		GenBank Accession
<i>β-actin</i>	5'AAGCCACCCCACTTCTCTCTAA-3'	Forward	NM_001101.4
	5'AATGCTATCACCTCCCCTGTGT-3'	Reverse	
<i>RPL13A</i>	5'-CCTGGAGGAGAAGAGGAAAGAGA-3'	Forward	NM_012423.4
	5'-TTGAGGACCTCTGTGTATTTGTCAA-3'	Reverse	
<i>YWHAZ</i>	5'-TCTGTCTTGTCCACCAACCATTCTT-3'	Forward	NM_003406.3
<i>COL1A2</i>	5'-GCTACCCAACTTGCCCTCATG-3'	Forward	NM_000089.3
	5'-GCAGTGGTAGGTGATGTTCTGAGA-3'	Reverse	
<i>COL2A1</i>	5'-CTGCAAAATAAAATCTCGGTGTTCT-3'	Forward	NM_001844.5
	5'-GGGCATTGACTCACACCAAGT-3'	Reverse	
<i>COL10A1</i>	5'-GAAGTTATAATTTACTGAGGGTTTCAA-3'	Forward	NM_000493.3
	5'-GAGGCACAGCTTAAAAGTTTTAAACA-3'	Reverse	
<i>SOX9</i>	5'-CTTTGGTTTGTGTTTCGTGTTTTG-3'	Forward	NM_000346.3
	5'-AGAGAAAGAAAAGGGAAAGGTAAGTTT-3'	Reverse	
<i>LOXL2</i>	5'-ACGGCCACCGCATCTG-3'	Forward	NM_002318.2
	5'-TCCGTCTCTTCGCTGAAGGA-3'	Reverse	
<i>HIF1α</i>	5'-GTAGTTGTGGAAGTTTATGCTAATATTGTGT-3'	Forward	NM_001530.4
	5'-TCTTGTTTACAGTCTGCTCAAAATATCTT-3'	Reverse	
<i>HIF2α</i>	5'-GGTGGCAGAAGTTGAAGGGTTA-3'	Forward	NM_001430.5
	5'-GGGCAACACACACAGGAAATC-3'	Reverse	
<i>VEGFA</i>	5'-GCACGGTCCCTCTTGGA-3'	Forward	NM_001025366.2
	5'-CGGTGATTTAGCAGCAAGAAAA-3'	Reverse	
<i>SDF-1α</i>	5'-TGCACCTCCCCAACCT-3'	Forward	NM_000609.6
	5'-GGAAGGGTCCAATGAGATCCA-3'	Reverse	
<i>CNMD</i>	5'-GCGCAAGTGAAGGCTCGTAT-3'	Forward	NM_007015.3
	5'-GTTTGGAGGAGATGCTCTGTTT-3'	Reverse	

### 6.2.5 Immunofluorescence (IF)

VEGF and SDF-1 IF was performed for both *in vitro* and *in vivo* constructs from the two implanted donors. Paraffin-embedded sections 5 μm thick were treated with citrate buffer in a steamer (IHC-Tek™) for 30 minutes after deparaffinization and rehydration. After being cooled down for 20 minutes at room temperature, the sections were incubated with two primary antibodies: rabbit anti-VEGF (biotin, ab83132) and rabbit anti-SDF-1

(ab18919) using a 1:100 and 1:50 dilution, respectively overnight at 4°C. The sections were incubated with the secondary antibodies: streptavidin-Alexa 488 (cat#S32354, ThermoFisher, Waltham, MA) for VEGF and goat anti-rabbit IgG (Alexa Flour®594, ab150080, Abcam) for SDF-1 using a 1:200 dilution for 45 minutes. Sections were mounted using the Biotium Everbrite Mounting Medium with DAPI. Images were taken using an Eclipse Ti-S microscope (Nikon, Japan).

### **6.2.6 Enzyme-linked immunosorbent assay (ELISA)**

ELISA was performed to quantify VEGF and SDF-1 (SDF-1 $\alpha$ ) proteins within the hSF-MS-C-based constructs after chondrogenic culture for two weeks, i.e. just before implantation (n=2, donor 1 and 2). The analysis was performed according to the manufacturer's protocol for VEGF (ab100663, Abcam, Cambridge, MA, USA) and SDF-1 $\alpha$  (ab100637, Abcam, Cambridge, MA, USA). For each group, 2 independent cell-seeded scaffolds per donor were used for analysis.

### **6.2.7 Statistical analysis**

Statistical analyses were performed using Excel (Microsoft Office 365). Data were presented as individual donors with overall mean  $\pm$  standard deviation (SD). For the comparison between oxygen tensions, a paired t-test was used except in cases of deviation of differences from normality by Shapiro-Wilks' test, in which cases the Wilcoxon signed rank test was used instead. For gene expression analysis, tests were performed on  $\Delta$ Ct values calculated as gene of interest minus the-mean of 3

housekeeping genes). The gene expression data is presented in figures as  $2^{-\Delta Ct}$  on a  $\log_{10}$  scale. Significance was concluded when  $p < 0.05$ .

### 6.3 Results

#### 6.3.1 Isolation and monolayer expansion culture of hSF-MSCs under hypoxia

##### (HYP) *in vitro*

All donors formed colonies, two of which are shown (Fig. 6-1A/B). Colony morphology was observed at the centre and perimeter of the colonies by crystal violet staining. Cells were predominantly spindle-shaped with some being polygonal (Fig. 6-1E/F). These morphologies were also observed for hSF-MSCs during expansion via light microscopy at the end of P0 and P2 at 80-90% confluency in hypoxic culture (Fig. 6-1C/D).

Quantitative metrics of the Cfu-f assay at the end of P0 showed great variability between donors, with gross mean colony numbers of triplicate petri dishes of the 17-year-old donor far exceeding that of the older donor (48 vs 3), despite colony diameters being comparable. The mean number of colonies ranged from 2.0 to 48 and the mean diameter of the cell colonies ranged from 3 to 11 mm. Variability between donors for quantitative expansion metrics was less pronounced than those in the Cfu-f assay. The mean total expansion time was  $45.6 \pm 10.3$  days, mean cumulative population doublings (PD) across all donors at the end of P2 was  $14.4 \pm 1.9$ , and PD per day was  $0.32 \pm 0.05$ .

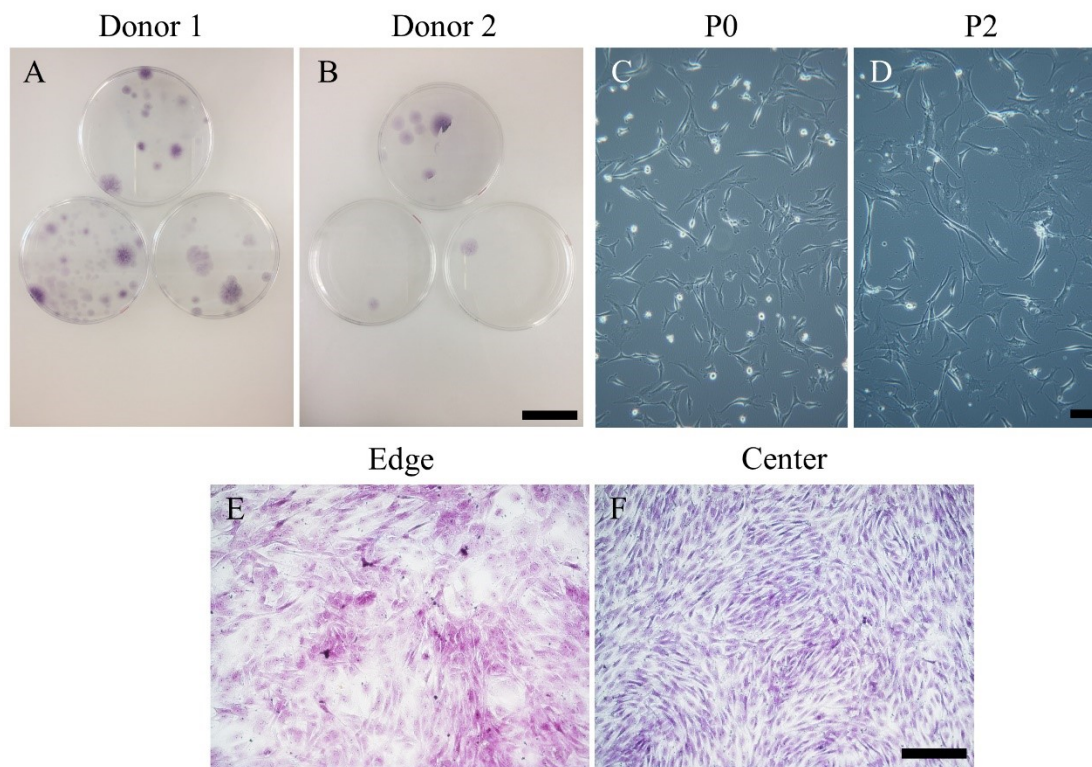


**Figure 6-1:** Colony-forming unit fibroblastic (Cfu-f) assay of human synovial fluid mesenchymal stem cells (hSF-MSCs) expanded with FGF-2 (5 ng/mL) under hypoxia (n=5). (A/B) Colony formation for two age-representative donors (17y/58y); (C/D) Morphology of expanded cells at the end of P0 and P2 as visualized under a light microscope; (E/F) Colony morphology of adherent cells from donor 1 as visualized by crystal violet staining on the colony edge and center. Scale bar: (B): 4 mm; (D): 100  $\mu$ m; (F): 200  $\mu$ m.

### **6.3.2 Analysis of inner meniscus-like extracellular matrix (IM-ECM) formation under HYP and NRX**

#### **6.3.2.1 Biochemical analysis of glycosaminoglycan (GAG) and DNA content**

GAG and DNA assays were only performed for the constructs after chondrogenic culture for two weeks *in vitro* (TGF- $\beta$ 3/2wks) under NRX or HYP. DNA content was used as a metric to estimate how many cells were present in each construct. One donor's construct (Donor 4, 53y) was found to have a low amount of DNA under NRX that led to a very high GAG/DNA ratio. Statistical computations were thus carried out with and without this value included. We observed the cells of this donor seemed to detach from the scaffold during 2 weeks' chondrogenic culture under NRX, but it was unclear why (Fig.6-2). HYP promoted a significant increase in the mean total GAG accumulation compared to NRX ( $p=0.013$ ), even upon including the Donor 4 ( $p=0.031$ ) (Fig.6-2A). A hypoxia-induced enhancement in GAG production could be observed for all five donors (Fig.6-2A). No significant difference in the mean total DNA content was found between HYP and NRX ( $p=0.19$ ) (Fig.6-2B). Upon normalizing the GAG to the DNA content, a significant enhancement in GAG was observed when donor 4 was excluded but not upon its inclusion (Fig.6-2C,  $p=0.006$  or  $p=0.35$ ). This result demonstrates that the increase in GAG may be attributed to HYP as opposed to a greater number of cells.

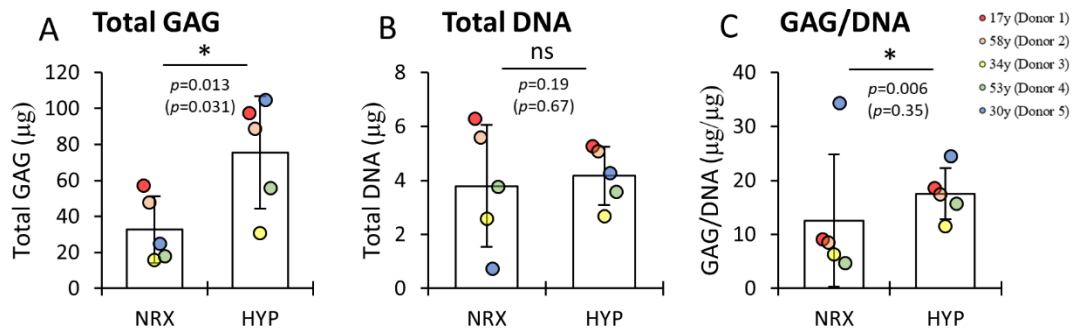


**Figure 6-2:** Biochemical analysis of hSF-MSCs-seeded constructs after 2 weeks of *in vitro* chondrogenic culture under normoxia (NRX) and hypoxia (HYP). (A) GAG content; (B) DNA content; and (C) GAG content normalized by total DNA content. \* indicates significant differences ( $p < 0.05$ ) between NRX and HYP groups, and ns indicates non-significant results. Donor 4 was deemed to be an outlier in this analysis because of its abnormally low DNA content measurement for the normoxia group, leading to a large skew in the GAG/DNA distribution. Error bars and p-values were calculated with the remaining four donors. Parenthesized values show the unadjusted p-values and each colour represent different donor (n=5).

### 6.3.2.2 Gross morphology and Safranin-O Staining

Gross morphologies of the constructs of donors 1 and 2 for all treatment groups including two empty scaffolds of both *in vitro* and *in vivo* groups were presented (Fig.6-3). The morphology of an implanted construct with blood vessel penetration at the time of harvest can be seen (Fig.6-3H1-2). Safranin-O staining was conducted on the same constructs to visualize the deposition of sulfated proteoglycans. Relative to the empty

scaffold *in vitro* (Fig.6-3G1), the constructs in TGF- $\beta$ 3/2wks *in vitro* (Fig.6-3A1-2/B1-2) appeared dense, contracted, and filled with white newly formed tissue. The overall sizes appeared larger in HYP (Fig.6-3B1-2) compared to NRX (Fig.6-3A1-2) for this group. In control groups where chondrogenic medium containing TGF- $\beta$ 3 was replaced by DMEM with 10% FBS (DMEM/7wks *in vitro*), the sizes of all constructs decreased dramatically (Fig.6-3C1-2/D1-2). The pre-formed IM-ECM in this group seemed to degrade, leaving only dense yellow cell aggregates behind. The implanted constructs (Fig.6-3E1-2/F1-2) were smaller than the empty scaffold *in vivo* (Fig.6-3G2). All the implanted constructs were surrounded by connective tissue and blood vessels from the mouse at the time of harvest (Fig.6-3E1-2/F1-2/G2).

Safranin-O positive staining for sulphated proteoglycans was observed in all the TGF- $\beta$ 3/2wks *in vitro* constructs (Fig.6-3A3-4/B3-4) when compared to the empty scaffold *in vitro*, confirming IM-ECM formation (Fig.6-3G3). Cells were well dispersed although the scaffold material was not entirely filled with dense matrix except for the Donor 2 construct in HYP (Fig.6-3B4). Safranin-O positive ECM was distinctly more abundant in HYP than NRX (Fig.6-3A4-B4), corroborating the findings of the GAG assay and gross morphologies. Only cell aggregates without Safranin-O staining and little matrix can be observed in NRX and HYP in DMEM/7wks *in vitro* controls (Fig.6-3C3-4/D3-4), suggesting that the previously-formed pre-culture matrix had degraded. In the Implantation/7wks groups, cells were dispersed throughout the construct cross-sections

and previously established matrix remained dense (Fig.6-3E3-4/F3-4) relative to the empty scaffold *in vivo* (Fig.6-3G4), indicating much of the matrix established during the *in vitro* pre-culture was sustained *in vivo*. The intensity of Safranin-O staining decreased *in vivo* compared to TGF- $\beta$ 3/2wks *in vitro*, but could still be faintly detected especially in the construct of donor 2 in HYP (Fig.6-3F4)

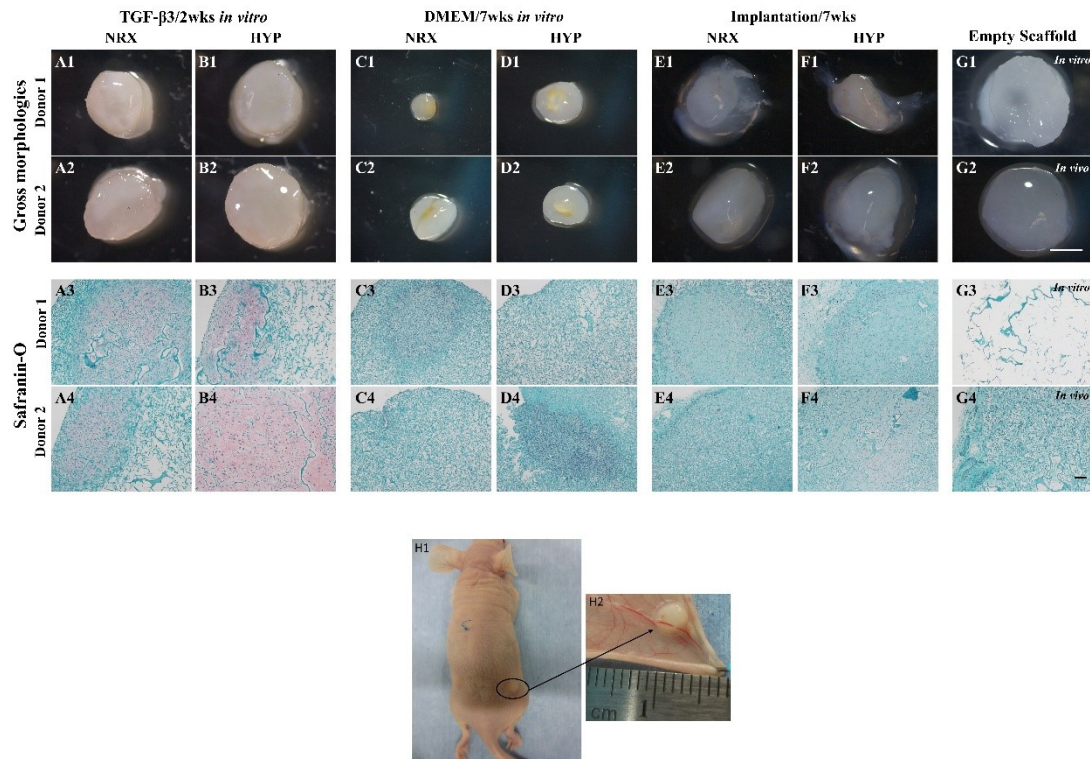


**Figure 6-3:** Gross morphologies and Safranin-O staining analysis for proteoglycan deposition in hSF-MSCs-seeded constructs following different culture conditions and oxygen tensions. The series of images labeled as A1-4 and B1-4 represent 2 weeks of *in vitro* chondrogenic cultured with TGF- $\beta$ 3 (T3/2wks *in vitro*) in NRX or HYP; images labeled as C1-4 and D1-4 represent 5 weeks of additional *in vitro* culture under NRX or

HYP in DMEM with 10% FBS (DMEM/7wks *in vitro*); images labeled as E1-E4 and F1-F4 represent 5 weeks of additional *in vivo* implantation at a subcutaneous ectopic site using a nude SCID mouse model (Implantation/7wks), where NRX and HYP indicate the oxygen tensions from which the implanted constructs were sourced; images labeled as H1-2 represent subcutaneous implantation of chondrogenically-induced SF-MSC-seeded constructs before harvest. This analysis was completed on Donor 1 (17 years old male, meniscus tear) and Donor 2 (53 years old, osteoarthritis). Empty collagen scaffolds were either cultured *in vitro* (G1 and G3) or implanted *in vivo* (G2 and G4) as controls. Scale bar: (G2): 2 mm; (G4): 100  $\mu$ m.

### **6.3.2.3 Immunofluorescence (IF) analysis of ECM molecules**

The deposition of extracellular matrix components: type I/II collagen, and cells (DAPI) in both *in vitro* and *in vivo* constructs was detected by IF. Since the matrix had clearly degraded in the DMEM/7wks *in vitro* group based on the Safranin-O staining, IF results for this group were not presented. Cells visualized via DAPI were evenly distributed through the constructs in all conditions (Fig.6-4A1-6/E1-6) including the empty scaffold *in vivo* (Fig.6-4E6). Types I/II collagen were detected in all hSF-MSC-based constructs. However, their deposition differed between both Donors 1 with meniscus injuries and Donor 2 with OA and between NRX and HYP.

For both *in vitro* and implanted constructs, HYP promoted the deposition of type II collagen in both donors (Fig.6-4G1-2, Fig.6-4G3-4) compared to NRX (Fig.6-4C1-2,

Fig.6-4G3-4). These observations were more obvious in the OA donor compared to donor 1 with meniscus injuries and were consistent with the Safranin-O staining.

For constructs *in vitro* under NRX, a homogenous distribution of type I collagen was observed for both donors (Fig.6-4B1-2) while in HYP, the OA Donor 2 produced less type I collagen (Fig.6-4F2) than donor 1 (Fig.6-4F1). For donor 2, this trend was also observed *in vivo* when comparing the construct pre-cultured in HYP (Fig.6-4F4) to the construct pre-cultured in NRX (Fig.6-4B4). Conversely, the opposite effect was observed for the *in vivo* Donor 1 groups. Donor 1's NRX-pre-cultured *in vivo* construct had only faint type I collagen deposition around the perimeter (Fig.6-4B3), whereas dense, homogeneous deposition of type I collagen was observed in the *in vivo* HYP group (Fig.6-4F3). No non-specific binding was observed on the primary antibody-free controls (Fig.6-4A5-H5). Marginal type collagen I but not type II collagen immunofluorescence was observed in the empty scaffold in both *in vitro* (Fig.6-4B6) and *in vivo* (Fig.6-4F6) groups.

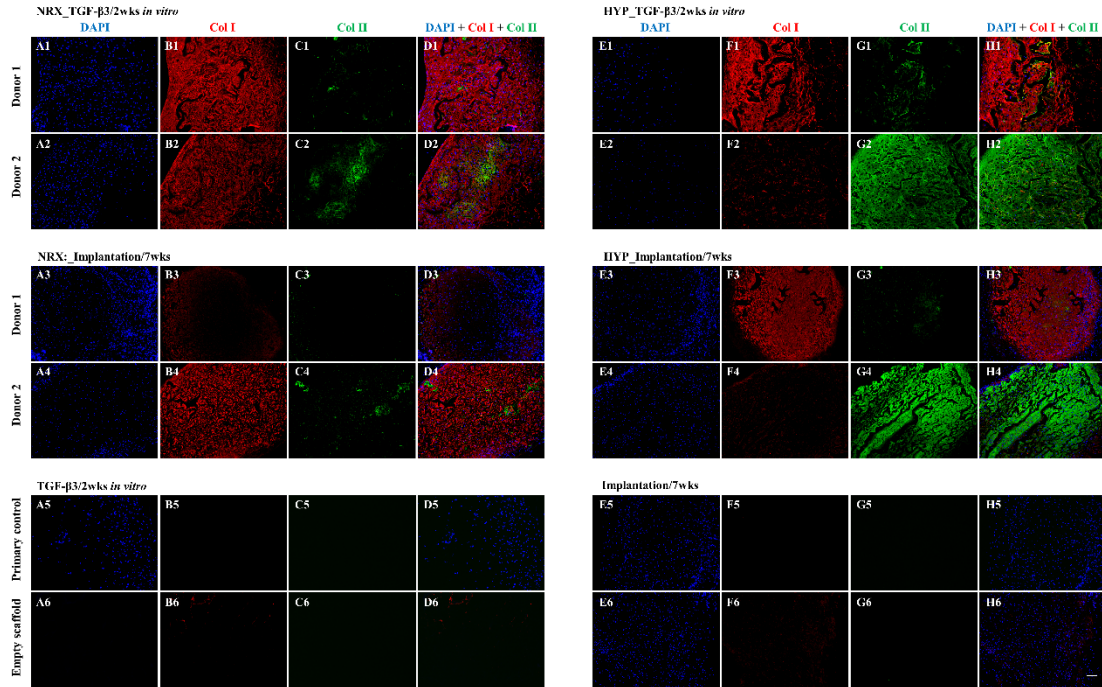


**Figure 6-4:** Immunofluorescent analysis of type I and II collagen I in hSF-MSCs-seeded constructs in groups of T3/2wks *in vitro* and Implantation/7wks under NRX and HYP.

Donor 1 and Donor 2 were used as representative samples. Analyses were also performed on constructs without primary antibody to characterize non-specific binding and empty scaffold controls *in vitro* and *in vivo*. Images labeled as A1-6 and E1-6 represent DAPI 4',6-diamidino-2-phenylindole for cells (blue); images labeled as B1-6 and F1-6 represent Alexa Fluor 594 for type I collagen (red); images labeled as C1-6 and G1-6 represent Alexa Fluor 488 for type II Collagen (Green); images labeled as D1-6 and H1-6 represent the overlap images of DAPI, type I and II collagen. Scale bar (H6): 200  $\mu$ m.

### 6.3.3 Alizarin Red S staining for calcium deposition

The hypertrophic differentiation potential of hSF-MSCs constructs was evaluated using Alizarin Red S staining to detect calcium deposition. Constructs of Donors 1 and 2 in all

groups were presented. Human BM-MSC constructs, pre-cultured on the same collagen scaffolds using the same chondrogenic factors but with 3% O<sub>2</sub> for 3 weeks (rather than 2% O<sub>2</sub> and two weeks in the present study) followed by subcutaneous implantation into mice for five weeks were used as positive *in vivo* controls (Fig.6-5A3). Among all *in vitro* groups there was no positive staining for Alizarin Red S, indicating no calcification (Fig.6-5A1-2/B1-2/C1-2/D1-2). Most interestingly, among the *in vivo* groups there was also no calcification (Fig.6-5E1-2/F1-2), matching the negative empty scaffold control implanted *in vivo*. This result suggests that hSF-MSCs can generate non-calcifying IM-ECM in the subcutaneous nude mouse model, in stark contrast to the intense staining observed in the BM-MSC positive control group (Fig.6-5A3).

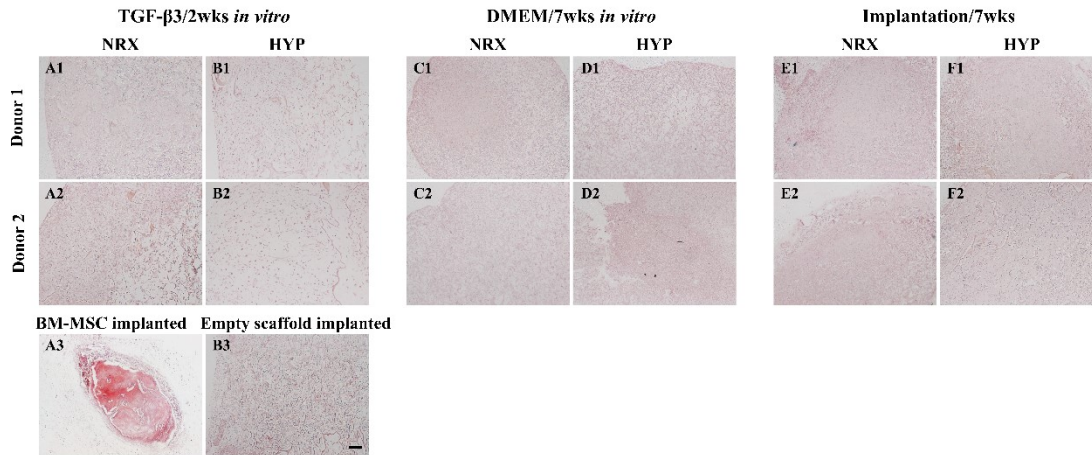


**Figure 6-5:** Alizarin Red S staining of hSF-MSCs-seeded constructs to assess calcium deposition in implantation/7wks (images E1-2 and F1-2). The groups of T3/2wks *in vitro* (images A1-2 and B1-2), DMEM/7wks *in vitro* (images C1-2 and D1-2) and empty collagen scaffold *in vivo* (image B3) were served as a negative control. Human BM-

MSCs-derived matrix on the same collagen scaffold was implanted for 5 weeks as a positive control (image A3). Orange-red staining indicates calcium deposition. Scale bar: 200  $\mu\text{m}$ .

### **6.3.4 Analysis of angiogenic potential of pre-formed constructs**

#### **6.3.4.1 ELISA and immunofluorescence analysis of VEGF and SDF-1**

The production of angiogenic factors: VEGF and SDF-1 (SDF-1 $\alpha$ ) of donor 1 and donor 2 after chondrogenic culture for two weeks *in vitro* were measured by ELISA (Table 6-3).

There was a consistent upregulation trend in HYP for VEGF compared to NRX across both donors. HYP-pre-cultured constructs of the OA donor 2 produced 4.1-fold more VEGF protein than NRX. By comparison, although the VEGF levels under HYP were comparable between Donor 1 and Donor 2, the non-OA donor 1 produced markedly higher levels of baseline VEGF under NRX relative to Donor 2, and although HYP enhanced the accumulation of VEGF, it was only by a factor of 1.2-fold. Overall, these results demonstrate that culturing hSF-MSCs under HYP promoted VEGF production; this is consistent with the gene expression analysis described below. There was no consistent trend across donors of oxygen tension affecting SDF-1 $\alpha$  production from either donor investigated; this was also consistent with the gene expression analysis.

The ELISA results were consistent with the immunofluorescence (IF) *in vitro*, which showed SDF-1 IF remain relatively constant between donors and between HYP (Fig.6-6H1-2) and NRX (Fig.6-6C1-2). VEGF IF increased dramatically in the hypoxia group

(Fig.6-6I1-2), although the variation in VEGF quantity between Donor 1 and 2 under normoxia (Fig.6-6D1-2) was less apparent. After implantation for five weeks, VEGF detection by IF fell off for both oxygen treatment groups (Fig.6-6D3-4 and Fig.6-6I3-4) compared to the TGF- $\beta$ 3/2wks groups. VEGF deposition in HYP-pre-culture groups (Fig.6-6I3-4) was more comparable to NRX-pre-culture (Fig.6-6D3-4) groups after the 5-week implantation in both donors. No non-specific binding was observed on the primary antibody-free controls for SDF-1 and VEGF *in vitro* (Fig.6-6C5/D5) and *in vivo* (Fig.6-6H5/I5). No IF of SDF-1 and VEGF was detected in the empty collagen scaffold *in vitro* (Fig.6-6C6/D6) while the implanted empty collagen scaffold had intense SDF-1 (Fig.6-6H6) and faint VEGF (Fig.6-6I6) immunofluorescence.

**Table 6-3:** Quantification of SDF-1 $\alpha$  and VEGF by ELISA

Protein	Donor	NRX	HYP
SDF-1 $\alpha$ (pg)	Donor 1 (17y)	5.9	5.0
	Donor 2 (58y)	4.4	6.2
VEGF (pg)	Donor 1 (17y)	78.6	96.7
	Donor 2 (58y)	25.5	105.4

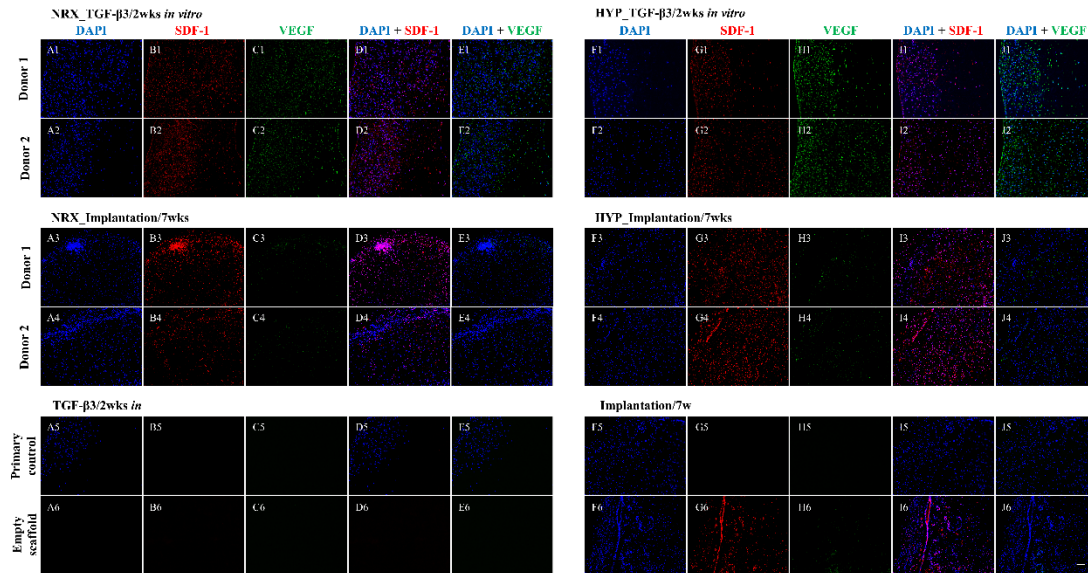


**Figure 6-6:** Analysis of angiogenic factors: VEGF and SDF-1 in hSF-MSC-seeded constructs by immunofluorescence in donor 1 and 2. SDF-1 and VEGF immunofluorescence was performed in TGF- $\beta$ 3/2wks *in vitro* group and implanted/7wks of the same donors where NRX and HYP indicate the preculture oxygen tensions from which the implanted constructs were sourced. Analyses were also performed on constructs without primary antibody to characterize non-specific binding and empty scaffold controls *in vitro* and *in vivo*. Images labeled as A1-6 and F1-6 represent DAPI for cells (blue); images labeled as B1-6 and G1-6 represent Alexa Fluor 594 for SDF-1 $\alpha$  (red); images labeled as C1-6 and H1-6 represent Alexa Fluor 488 for VEGF-A (Green); images labeled as D1-6 and I1-6 represent the overlap images of DAPI and SDF-1 $\alpha$ ; images labeled as E1-6 and J1-6 represent the overlap images of DAPI and VEGF-A. Scale bar: 200  $\mu$ m.

#### 6.3.4.2 IF analysis of CD31 for vascular invasion in vivo

IF was used to detect CD31 as an indicator of angiogenesis in implanted constructs of donors 1 and 2. Among the *in vitro* constructs, as expected no CD31 IF was identified in either hypoxic or normoxic constructs following chondrogenic culture for 2 weeks (data not shown). Among implanted constructs, both oxygen tension groups demonstrated CD31 IF mostly around the construct perimeters (Fig.6-7B1-2 and Fig.6-7F1-2), which may be attributed to the host-generated vascularized connective tissue surrounding the constructs at the ectopic site after implantation. This is consistent with the cell density indicated by the DAPI staining (Fig.6-7A1-2 and Fig.6-7E1-2) which shows a relatively high density of what are likely host cells surrounding the constructs, and a relatively low density of dispersed cells within the construct. In the middle of the constructs where the pre-formed IM-ECM was maintained, some CD31 IF was observed in both oxygen tension-pre-cultured constructs of both donors (Fig.6-7C1-2/G1-2). There seemed to be more CD31 detection overall in NRX-pre-cultured constructs, which was unexpected given the greater VEGF expression in HYP-pre-cultured constructs demonstrated by the ELISA and IF (table 6-2 and Fig.6-6). A greater degree of CD31 IF relative to either pre-cultured group was identified at the interior of the implanted empty scaffold (Fig.6-7B3/C3) indicating that the pure scaffold material supported vascularization from the host.

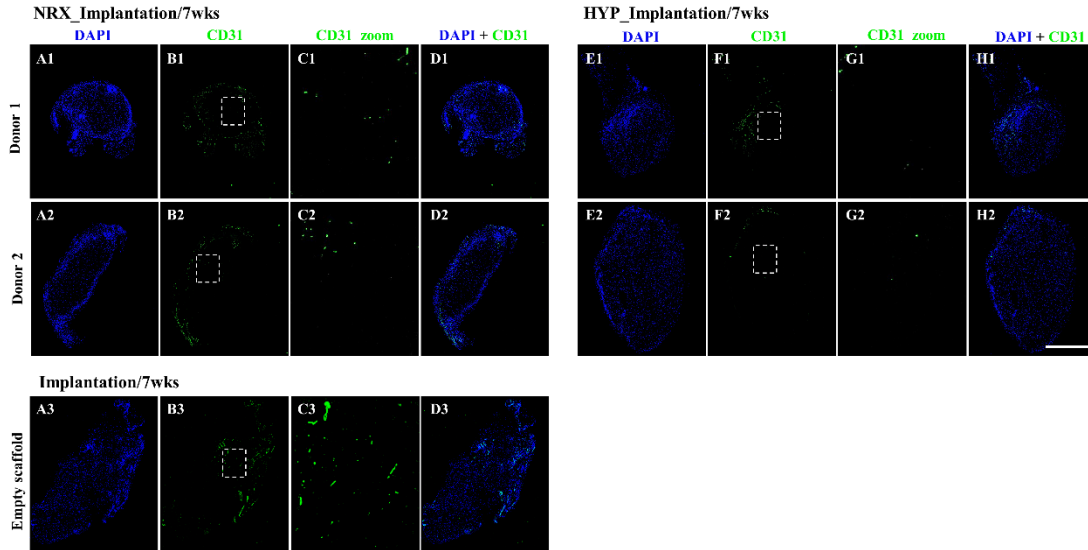


**Figure 6-7:** Immunofluorescence analysis of CD31 for blood vessel invasion in hSF-MSCs-seeded constructs of implantation/7wks of donor 1 and donor 2. Analysis was also performed in empty collagen scaffold *in vivo*. No fluorescence was observed on primary antibody controls or on *in vitro* scaffolds and were therefore omitted. Images labeled as A1-3 and E1-3 represent DAPI for cells (blue); images labeled as B1-3 and F1-2 represent Alexa Fluor 488 for CD31 (Green); images labeled as C1-3 and G1-2 the zoom images of the interior matrix regions; images labeled as D1-3 and H1-2 represent the overlap images of DAPI and CD31. Scale bar: 1mm.

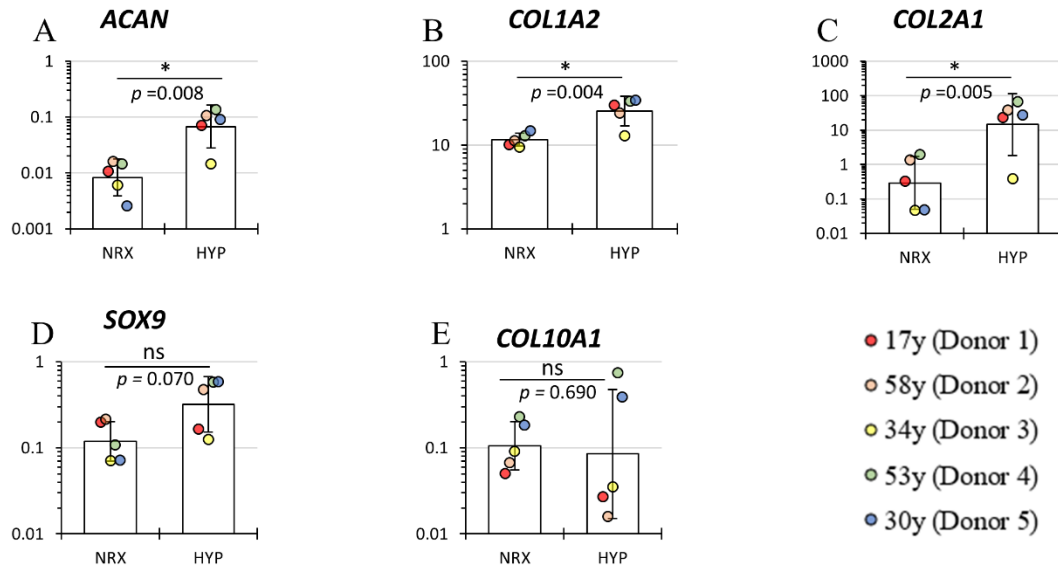
### 6.3.5 *In vitro* gene expression analysis

For *in vitro*-cultured constructs only, gene expression analysis was carried out to characterize the IM-ECM-forming phenotype and assess expression of hypoxia and angiogenesis-related genes. The mean relative gene expression levels of IM-ECM macromolecules aggrecan (*ACAN*), type I collagen (*COL1A2*), type II collagen

(*COL2A1*), chondrogenic regulator *SOX9*, and hypertrophic marker collagen X (*COL10A1*) were analyzed. Additionally, the hypoxia response-related factors *HIF-1 $\alpha$*  and *HIF-2 $\alpha$* , and angiogenic factors: VEGF (*VEGF-A*) and SDF-1 (*SDF-1 $\alpha$* ) were also assessed, in addition to matrix cross-linker *LOXL2* and anti-angiogenic factor chondromodulin-1 (*CNMD*). All results are shown in Figure.6-8.

HYP upregulated the IM-ECM-related gene expression levels with significant differences observed in *ACAN*, *COL1A2*, *COL2A1* (Fig.6-8A/B/C). The expression level of chondrogenic differentiation regulator *SOX9* was also increased by HYP to an extent approaching significance ( $p=0.07$ ) (Fig.6-8D). No significant difference was observed for the hypertrophic marker *COL10A1* between HYP and NRX (Fig.6-8E). The gene expression levels of *HIF-1 $\alpha$*  (Fig.6-8F) and *HIF-2 $\alpha$*  (Fig.6-8G) both appeared upregulated in HYP ( $p=0.06$  and  $p<0.05$ , respectively). *LOXL2* (Fig.6-8H) and *VEGF-A* (Fig.6-8I) were significantly increased by HYP, whereas with no significant difference and very low expression observed in *SDF-1 $\alpha$*  (Fig.6-8J). The anti-angiogenic factor *CNMD* was also significantly upregulated by HYP (Fig.6-8K).

### Inner meniscus matrix-related genes



### Hypoxia and angiogenesis-related genes

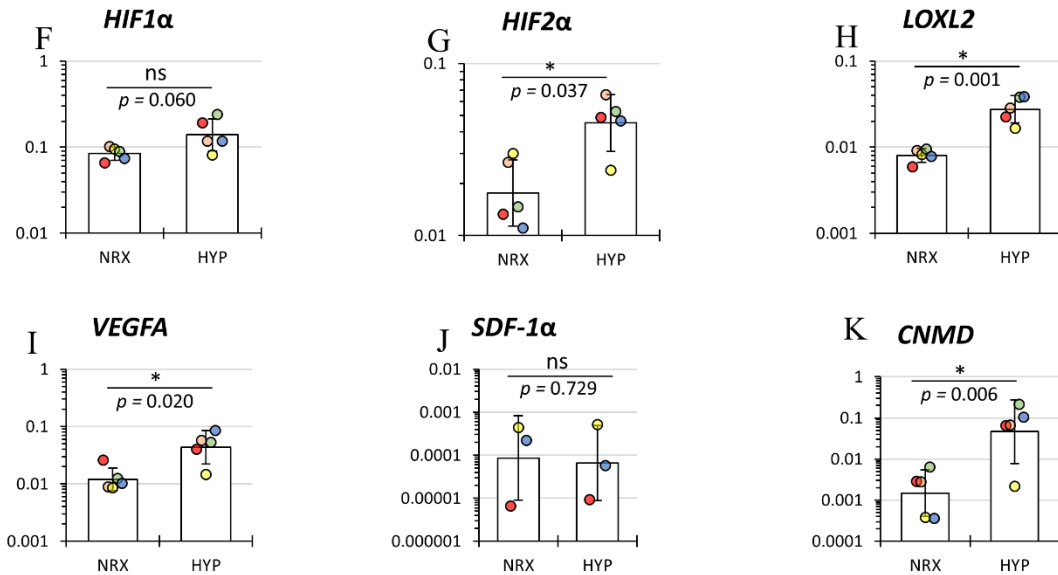


**Figure 6-8:** Real-time PCR analysis of gene expression levels of hSF-MSCs-seeded constructs in TGF- $\beta$ 3/2wks *in vitro* under NRX and HYP (n=5). Each gene expression level was normalized to the mean expression levels of 3 housekeeping genes:  *$\beta$ -actin*, *RPL13A* and *YWHAZ*. A-E represent inner meniscus matrix-related genes and F-K

represent hypoxia and angiogenesis-related genes. \* indicates significant differences ( $p < 0.05$ ) between NRX and HYP groups, and ns indicates non-significant results.

#### 6.4 Discussion

The aims of this study were to first evaluate the *in vitro* IM-ECM formation of hSF-MSCs cultured in porous collagen scaffolds with chondrogenic growth factor TGF- $\beta$ 3 in hypoxia (HYP) versus normoxia (NRX), and then to assess whether hSF-MSCs are a suitable stem cell source for engineering stable IM-ECM that invites vascularization using a nude mouse model.

To address these aims, human knee joint hSF-MSCs were isolated and expanded using HYP (3% O<sub>2</sub>) and FGF-2 to maintain the chondrogenic potential of expanded cells [16, 22]. The findings of the Cfu-f assay in this study were consistent with our previous result [255] in that all donors exhibited colony-forming and proliferation capacity under HYP-mediated isolation and expansion. As well, the result that the younger donor (17-year-old) seemed to have better Cfu-f potential compared to the 58-year-old donor with OA is also consistent with previous work showing the Cfu-f potential for MSCs is negatively related to donor age [314].

The effects of HYP (2% O<sub>2</sub>) on the *in vitro* IM-ECM formation of hSF-MSCs within a type I collagen scaffold were first examined. The results supported our initial hypothesis that HYP pre-chondrogenic culture for 2 weeks enhanced IM-ECM formation *in vitro* compared to NRX based on accumulation of GAG, type II collagen, and

proteoglycans. This is consistent with previous demonstrations of enhanced chondrogenic differentiation of BM-MSCs by HYP [13, 15]. However, our *in vitro* results are in partial contrast to those presented by Neybecker *et al.* [188]. Although both studies found chondrogenic-related genes (*ACAN*, *COL2A1*, and *SOX9*) were upregulated in hSF-MSC-seeded collagen scaffolds under HYP, Neybecker *et al.* found that HYP did not enhance ECM synthesis by OA-derived hSF-MSCs during *in vitro* chondrogenic culture using TGF- $\beta$ 1 and BMP-2 within a type I/III collagen scaffold [188]. However, it should be noted that HYP (3% O<sub>2</sub>) was applied during hSF-MSCs isolation and expansion in our current study, while Neybecker used NRX. The knee joint SF-MSCs reside under a low oxygen tension environment physiologically [226] and HYP-expanded BM-MSCs have been shown to exhibit superior chondrogenic potential relative to those expanded under NRX, regardless of the oxygen tension during chondrogenic culture [13, 15]. Moreover, during *in vitro* chondrogenic culture our current study used 2% oxygen tension whereas Neybecker used 5% O<sub>2</sub>.

The enhanced IM-ECM formation in the 58-year-old donor (donor 2) with OA compared to the 17-year-old donor (donor 1) with meniscus injury under both oxygen tensions was an unexpected finding, even though the Cfu-f potential regarding the colony numbers was better in the younger donor. The results of these two donors are inconsistent with previous findings that the chondrogenic potential of BM-MSCs [334] and synovial membrane-derived MSCs (SM-MSCs) [335, 336] were independent of age, despite it

being generally accepted that SF-MSCs are derived from the synovium, as the chondrogenic potential between SF-MSCs and SM-MSCs are typically comparable [181, 302, 337, 338]. Previous scaffold-based hSF-MSC studies have not focused on donors with meniscus tears [188, 255]. However, previous findings did show that the pathology state of the synovial fluid (SF) where the SF-MSCs reside can be detrimental to or promote the chondrogenic differentiation capacity of human articular chondrocytes [339] and equine BM-MSC [340], respectively. The density of hSF-MSCs isolated from knee joint synovial fluid from OA was found to be higher compared to rheumatoid arthritis [325]. Such findings emphasize the need for well-designed studies to characterize how patient characteristics and knee joint pathologies may influence the chondrogenic capacity of hSF-MSCs for tissue engineering applications.

In terms of angiogenic potential of the bioengineered IM-ECM, HYP significantly upregulated the production of VEGF but not SDF-1 compared to NRX at both gene expression and protein production levels *in vitro*. The upregulation of VEGF in hSF-MSC by HYP was consistent with previous findings in MSCs [330, 331]. The HYP-mediated upregulation of VEGF was correlated with the evaluated gene expression levels of *HIF-1 $\alpha$*  and *HIF-2 $\alpha$*  (Fig.8F/G). This result is consistent with established knowledge that VEGF is upregulated under HYP by the action of the HIF-1 signaling system [341]. The lack of HYP-mediated SDF-1 regulation may be caused by a downregulatory effect induced by TGF- $\beta$ 3 supplementation, as members of the TGF- $\beta$  family have been shown

to inhibit SDF-1 production in MSCs [342].

Next, an *in vivo* subcutaneous nude mouse model was employed to evaluate the stability and angiogenic capacity of the hSF-MSC-based bioengineered IM-ECM [102, 120, 343]. Histological findings demonstrated that in both oxygen tensions the IM-ECM was partially maintained, did not calcify, and underwent angiogenesis. The partial loss of matrix may be attributed to removal from the growth factor-supplemented *in vitro* culture environment into an ectopic site in an animal model, causing potential death of human cells [120]. One reason for the non-calcified IM-ECM may be due to the negligible deposition of type X collagen by hSF-MSCs *in vitro* compared to BM-MSCs, as demonstrated previously on decellularized matrix and pellet models [255]. Our findings here further support other studies' findings that porcine- and bovine-derived SF-MSCs were more committed toward a chondrogenic phenotype compared to BM-MSCs *in vitro* [302, 304].

Despite the upregulated production of VEGF by HYP *in vitro*, angiogenesis assessed by CD31 expression was lower in the hypoxic group (Fig.6-7G1-2) compared to NRX for both implanted donors. This could perhaps be explained by the hypoxia-enhanced expression of collagen cross-linker *LOXL2* (Fig.6-8H). Makris *et al.* found that hypoxic culture (oxygen tension; 2% O<sub>2</sub>) induced a 6.4-fold increase in crosslinking in engineered tissues by the action of LOX, concomitantly increasing stiffness [273]. An increase in hypoxia-induced cross-linking could potentially impede vascularization of engineered

tissues.

The reduced vascular invasion in the HYP-derived engineered constructs may be associated with the upregulation of chondromodulin-1 (gene: *CNMD*), an anti-angiogenic factor expressed meniscal in fibrocartilage and articular cartilage [328, 344]. The upregulation of *CNMD* under HYP relative to NRX after 2 weeks of chondrogenic culture was consistent with previous findings in human articular chondrocytes [345]. Chondromodulin-1 has been shown to be increased by HYP in human articular chondrocytes via HIF-2 $\alpha$ -mediated upregulation of SOX9 pathway [287, 345]. The upregulated gene expression of *CNMD* by HYP observed in the SF-MSCs may have followed this pathway, given gene expression levels of *CNMD* and *HIF-2 $\alpha$*  were significantly upregulated and *SOX9* tended to be increased in HYP compared to NRX. However, the role of HIF-1 $\alpha$  cannot be ruled out since the gene expression level of HIF-1 was also approaching significant upregulation by HYP. In addition, when *CNMD* was adenovirally transduced into rabbit BM-MSCs, it was shown to prevent calcification and reduce angiogenesis in the BM-MSC-derived matrix compared to naïve BM-MSCs when implanted in nude mouse using a coral scaffold model [346]. Even though the decreased expression of chondromodulin-1 was shown to be negatively related with upregulation of VEGF and induction of neovascularization in articular cartilage during the progression of OA in a rat knee joint model [347], the upregulated gene expression levels of *CNMD* in the current study were positively correlated with the gene expression and protein

production of VEGF in hSF-MSCs HYP *in vitro*. Previously, overexpression of *CNMD* in human osteochondral progenitor cells did not influence the mRNA levels of *VEGF in vitro* and decreased mRNA levels of *COL10A1*, indicating potential suppression of hypertrophic differentiation [348]. Interestingly, even though HYP [15, 327] and chondromodulin-1 [348, 349] were reported to suppress gene expression levels of *COL10A1*, this effect was not observed in hSF-MSCs as similar *COL10A1* gene expression was observed between oxygen tensions *in vitro*. It may suggest that the lack of hypertrophic differentiation to form bone matrix in hSF-MSCs may be due to a complex interaction of these agents.

However, even though the NRX-cultured constructs showed inferior matrix and less VEGF protein compared to HYP *in vitro* and *in vivo*, they showed more angiogenic potential (i.e. less *CDMN* expression and more CD31 IF). Thus, due to this tradeoff of matrix quality and angiogenic potential it remains undetermined what pre-culture oxygen tension is preferred for generation of constructs for the purpose of inducing blood vessels to repair inner meniscus injury. It would be interesting to investigate the performance of constructs with regards to inducing vascularization and stem cell homing within a knee joint environment, provided they have adequate mechanical properties to withstand loading. As well, it would be interesting to inhibit expression of chondromodulin-1 in the SF-MSCs cultured under HYP to promote neovascularization while providing inner meniscus-like extracellular matrix for the meniscus defects.

## **6.5 Conclusions**

This study demonstrates for the first time that pre-culture of hSF-MSCs on type I collagen scaffolds produce IM-ECM that is partially retained and non-calcifying with concomitant vascularization *in vivo* using the subcutaneous nude mouse model.

## Chapter 7 General discussion and conclusions

Yan Liang

### 7.1 General discussion

Various strategies have been used towards generating engineered tissues that resemble the native meniscus. Regeneration of meniscus-like tissues with extracellular matrix (ECM) containing proteoglycan, type I and II collagen have been demonstrated *in vitro* and in animal studies to some extent. However, limited success has been shown in human studies. Human meniscus tissue engineering is still in its early stages with inconsistent results in tissue quality and clinical scores. There are gaps regarding the variables of appropriate cell types, isolation, expansion protocols and culture conditions, and inductive stimuli towards a robust meniscus-ECM-forming phenotype prior to clinical application. Based on the literature, human meniscus fibrochondrocytes (MFCs) and synovial fluid-derived mesenchymal stem cells (SFMSCs) were two promising cell types given their tendency towards chondrogenic differentiation and resistance to osteogenic differentiation. Thus, investigating these variables using these two cell types could advance the field of human cell-based meniscus tissue engineering.

The first study in Chapter 2 aimed to assess the effects of mitotic division in human MFCs on their subsequent trilineage differentiation capacity under different oxygen tensions, especially the chondrogenic differentiation to form meniscus-like extracellular matrix (ECM) using a cell pellet model. The reasons for these objectives are because of

the low cell yields that are isolated from the surgical discard meniscus tissue and the loss of ability to form inner meniscus-like ECM containing aggrecan and type II collagen after monolayer expansion [12] have limited the use of human autologous MFCs for meniscus tissue engineering. In the current study, it was clearly shown that TGF- $\beta$ 1 and FGF-2 (T1F2) supplementation during monolayer expansion increased proliferation rates of human MFCs compared to our previous studies using no growth factors or pure FGF-2 [11]. The dedifferentiation status of monolayer expanded human MFCs seemed to be alleviated based on the mRNA expression levels of ECM-related aggrecan (*ACAN*) and type II collagen (*COL2A1*) which did not show significant decrease up to 13 population doublings (PD). Consequently, large amounts of human MFCs can be obtained by monolayer expansion within a short period of time. For example, it was an average of  $\sim 0.5$  population doublings (PD)/day in passage 1 to reach  $\sim 3.43$  PD after 7 days. Based on the average primary MFCs numbers that can be isolated from meniscus tissue in our study ( $\sim 3.14$  millions per gram meniscus tissue), more than 27 million MFCs can be obtained. Importantly, the resulting 27 million human MFCs with 3.43 PD formed inner meniscus-like ECM especially under hypoxia in the cell pellet model when exposed to chondrogenic factors. These findings have significant implications for future clinical study using 3-dimensional scaffold to generate meniscus-like tissue for meniscus repair or replacement. The volume of human medial and lateral meniscus were reported to be about  $4.50 \text{ cm}^3$  and  $4.59 \text{ cm}^3$ , respectively [238] and a potential optimal seeding cell

density for cartilaginous tissue formation within collagen scaffold was  $5 \times 10^6$  per  $\text{cm}^3$  [239], which indicates that 22.5-25 millions human MFCs will be required to generate a whole meniscus. In addition, compared to a previous study that non-growth factor expanded human MFCs showed osteogenic differentiation *in vitro* [235], it was the first time that the human MFCs expanded with T1F2 was shown to have low expression of hypertrophic marker type X collagen and lack of calcium deposition after *in vitro* osteogenic induction. It further confirmed that the T1F2-expanded human MFCs may be an promising cell sources to produce meniscus tissue instead of bone.

The results of this study are essential for the cell-based meniscus tissue engineering by demonstrating how to achieve sufficient cells with the demonstrated capacity to form meniscus-like ECM through growth factor supplementation and to enhance the quality of new ECM through manipulation of oxygen tension within the culture environment. The identified PD may be used as a parameter to estimate the production of cell numbers with desired tissue quality, especially under HYP for future clinical studies.

In chapter 3 and 5, we were able to generate porous 3-dimensional human cadaveric meniscus-derived decellularized matrix (DCM) scaffold using physical homogenization methods and freeze drying. Two studies were performed to investigate the potential inductive capacity of human meniscus-derived DCM on ECM formation of T1F2-expanded human MFCs and knee joint SFMSCs cultured without exogenous chondrogenic factors under hypoxia. Previous studies have shown the ability of porcine

articular cartilage or meniscus-derived DCM to induce chondrogenic differentiation of MSCs or re-differentiate articular chondrocytes without exogenous chondrogenic factors [254, 256]. These two studies had the potential to discover the existence of previously unidentified inductive factors embedded within the human native meniscus matrix for the first time to redifferentiate T1F2-expanded human MFCs to form ECM or differentiate human SFMSCs towards an MFC phenotype. However, it was obvious that the human meniscus-derived DCM alone prepared by physical methods did not support appreciable meniscus-like ECM formation of both cell types. The possible reasons for these may be the loss of ECM components such as proteoglycans that can sequester the inductive factors [266] during DCM processing. Future studies may need to improve the manufacturing process using chemical treatments which was reported to maintain most the glycosaminoglycan content compared to native porcine meniscus [256]. Nevertheless, both cell types on the DCM scaffold exhibited advantageous characteristics for meniscus tissue engineering applications under chondrogenic induction, producing meniscus-like ECM with a reduced tendency for hypertrophic differentiation to form bone. These results provide the basis to support the potential use of the two cell types to form meniscus-like ECM within large-scale scaffold models.

With the goals to further determine the implantation potential and phenotype stability of the *in vitro* generated meniscus-like ECM by human MFCs and SFMSCs under hypoxia, a subcutaneous nude mouse model was used. Based on our *in vitro* results

showing little evidence of type X collagen, we did not expect to see calcification after implantation. A previous study has shown that negligible meniscus-like ECM can be formed by human MFCs expanded with growth factors: TGF- $\beta$ 1, FGF2 and PDGF-bb followed by normoxic chondrogenic culture both *in vitro* and *in vivo* using the subcutaneous nude mouse [94]. In addition, *in vitro*-generated human SM-MSC and BM-MSC-derived cartilaginous tissues under normoxia respectively failed to maintain the chondrogenic phenotype and underwent calcification after subcutaneous implantation in nude mouse [120, 121]. The two studies in chapter 4 and 6 were the first time to demonstrate the beneficial effects of hypoxia on meniscus-like ECM formation of both cell types within the collagen scaffold both *in vitro* and *in vivo*, even though partial degradation of the ECM over time after implantation was observed. Further investigations to improve the resilience of the ECM after *in vivo* implantation may be necessary. A possible strategy would be longer preculture durations to allow formation of more mature ECM before ectopic implantation like that demonstrated after 8-weeks preculture by MFCs.

With regards to the angiogenic potential of these two cell types, we first demonstrated that hypoxia chondrogenic culture upregulated expression of pro-angiogenic factor VEGF *in vitro*. Interestingly, both oxygen tensions-derived ECM showed the capacity to support blood vessel invasion after implantation. However, the contribution of the HYP-derived endogenous VEGF to promote meniscus healing or

repair by inducing angiogenesis from the peripheral aspects of the menisci remains to be investigated in the knee joint environment.

In summary, the studies in this thesis have broadened our knowledge by showing the potential strategies to improve the quality of meniscus-like ECM for the purpose of autologous cell-based human meniscus tissue engineering.

We identified a human MFC expansion protocol *in vitro* using the supplementation of growth factors: TGF $\beta$ 1 and FGF2 for the first time. This protocol may provide a solution to the cell shortage problem for MFC-based meniscus tissue engineering by obtaining large number of MFCs in a short period of time. The expanded MFCs can form inner meniscus-like ECM after chondrogenic induction *in vitro*. We also showed that the human meniscus-derived DCM prepared by physical methods supports inner meniscus-like ECM formation by human MFCs and SFMSCs but only with exogenous growth factor supplementation for the first time. Lastly, we showed that hypoxia promotes inner meniscus-like ECM formation within the collagen scaffold by both cell types in the subcutaneous nude mouse model. Even though the pre-formed ECM underwent partial degradation, the remaining ECM did not calcify and was vascularized, which are promising for avascular meniscus repair and replacement.

However, several questions remain to be investigated. Even though hypoxic chondrogenic culture has consistently improved the meniscus-like ECM formation in pellet (chapter 2), collagen scaffold (chapter 4 and 6), and after subcutaneous

implantation in nude mouse (chapter 4 and 6), the maintenance of cell phenotype and the efficacy of hypoxia-derived ECM in the knee joint environment is still unclear. Further investigation using large animal models such as sheep to examine the performance of the ECM is required.

In the current clinical setting, meniscus allograft replacement has been considered the only option for carefully selected patients after total or subtotal meniscectomy [81]. A comprehensive meta-analysis has shown that the most commonly used allograft is prepared by cryopreservation [350]. The cryopreservation technique allows long-term meniscus allograft storage with viable cells and did not seem to alter the meniscus ultrastructure [351]. However, the cryopreservation is complex and difficult (4% to 50% cell viability [351, 352]) with potential disease transmission such as HIV [353]. Nevertheless, the experiences of its application may provide us valuable information when implanting autologous cell-derived meniscus-like constructs (autograft) in the future.

Compared to meniscus allograft, the first advantage of autografts may be the lack of immunogenic rejection risk and potential disease transmission [354].

Second, the sizing of the autograft should match the dissected native meniscus since it has been demonstrated as an important factor for tissue healing [355] and preservation of knee biomechanics [356] when using allograft. It was reported that 10% larger or smaller than the original size of the original meniscus may be acceptable [356] otherwise

the grafts may not restore the joint congruence or be prone to extrusion [357]. Nowadays, preoperative sizing of meniscus allograft using plain radiographs, CT [358] and MRI [359] are frequently used. However, perfect sizing of allograft remains difficult to achieve. On the other hand, with the combination of 3D printing techniques, CT or/and MRI, anatomical shape and structure of autograft similar to native meniscus may be achieved in the clinical setting [360]. However, to create patient-specific whole meniscus autografts, not only is the shape and sizing important, but also the regional distribution of cells, ECM, and vascular structure need to be addressed. Several recent studies have shown the potential to achieve these. Circumferentially and radially oriented structures resembling native meniscus collagen can be 3D-printed using PCL and can provide a potential biomimetic template for ECM formation [360]. Furthermore, Lee *et al.* showed that 3D-printed protein-releasing meniscus-shaped scaffolds can induce regional-specific type I and type II collagen deposition by endogenous cells in a sheep model with meniscectomy [240]. Perfusable vascular structure resembling mature native vasculature could be generated by 3D-printing bioink with encapsulated endothelial and stem cells [361], which may be potentially applied for the regeneration of outer vascular region or promoting healing process of inner avascular region by providing oxygen and nutrients.

Third, the viable cells in the meniscus allografts prepared by cryopreservation were shown to be critical for maintenance of ECM [362], which in turn may affect the mechanical integrity after implantation [362]. Similarly, the architecture of the 3D-

printed anatomical-shaped autograft should allow cell attachment, infiltration, proliferation and (re)differentiation to produce the region-specific ECM before and after implantation. More importantly, the autograft should possess appropriate mechanical properties and not undergo degradation, rupture or shrinkage as reported in the meniscus allograft.

The lack of characterization of mechanical properties of the newly-synthesized ECM is a limitation in this thesis. Now that we have demonstrated ways to: 1) overcome the cell availability barrier to meniscus tissue engineering, 2) synthesize the principal ECM components of the native meniscus without signs of calcification, the focus must shift towards achieving mechanically competent tissue. To achieve these, scaffolds possessing mechanical properties and appropriate degradation rates to allow the cell-derived ECM to become mature and mechanically competent could be applied. Then *in vitro* maturation of the ECM could also require complex culture condition modalities like oxygen tensions and longer culture periods. At the same time, the role of *in vivo* mechanobiology should be considered for ECM maturation. This may be achieved using mechanical loading such as in bioreactors that can apply forces and fluid dynamics resembling the native knee joint environment. It may help to investigate loading regimes that build up towards the loading that the autograft will experience following implantation.

Another limitation is that we did not investigate the influences of sex on ECM formation by human MFCs and SFMSCs. Only MFCs (except one female donor in

chapter 3) and SFMSCs isolated from male donors were used in this thesis. As well, all the nude mice used in implantation studies were male. Female sex is clearly a major risk factor for the development of knee osteoarthritis with more severe symptoms, especially after menopausal age [363]. The differences of knee anatomy [364], biomechanics [365], genetic polymorphisms [366] and hormones [367] between sexes may contribute to this phenomenon. With respect to meniscus, female sex was also reported to be a risk factor to develop knee osteoarthritis after meniscectomy [368]. Females were found to have higher MRI T2 signal in the posterior horn (a location that is most vulnerable to injury and degradation [369, 370]) of the medial meniscus compared to male regardless of ages [371], which may indicate different contents of collagen fiber network, proteoglycans, and water. With simultaneous anterior cruciate ligament injury, Kilcoyne *et al.* showed that there were no sex differences of meniscus tears incidences in a young athletic population [372] while Piasecki *et al.* showed that female high school athletes have less medial meniscus tears than male [373]. Stanley *et al.* also reported that meniscus injury incidences were significantly lower in female athletes than male in high school while no differences were found at college level [374]. Regarding the meniscus repair, it was mostly performed in the young patients age 10-19 years old and sexes seemed to affect the choice of meniscus repair (63% male vs 37% female) [375]. However, to our knowledge, there were no other clear evidence of sex difference in meniscus treatment.

Only one study has found that i) menisci from female rabbits yielded more MFCs

than male and ii) female MFCs produced larger amounts of sulfated proteoglycans than male at the age of 2 years [376]. For MSCs, recent studies have shown sex can modulate the differentiation potential of both animal and human MSCs especially in the context of osteogenesis [377-379]. Human BMSCs from males but not females showed decreased chondrogenic differentiation to form ECM with increasing age [380]. Muscle-derived MSCs from male vs. female mice were shown to produce better ECM after chondrogenic differentiation *in vitro* and enhanced cartilage regeneration *in vivo* in the nude mouse model [381]. However, another study also reported no differences in the osteogenic, adipogenic and chondrogenic differentiation potential of human BMSCs *in vitro* [382]. For angiogenic potential, BMSCs from female mice were reported to produce more VEGF and less tumor necrosis factor  $\alpha$  compared to male after exposure to hypoxia *in vitro* [383, 384]. In summary, tissue engineering strategies to address the meniscus repair or replacement should consider the sex differences. Well-designed studies including female donors and animals are essential for better understanding the gender-specific differences in modulating the meniscus-like ECM formation by human MFCs and SF-MSCs.

## 7.2 Conclusions

This thesis investigated the variables in human MFCs and SFMSCs-based meniscus tissue engineering. Sufficient cell numbers of human MFCs with meniscus-like ECM-

forming capacity within a short period can be obtained using a growth factors supplementation strategy during monolayer expansion *in vitro*. *In vitro* expanded human MFCs and SFMSCs were capable of producing meniscus-like ECM with limited evidence of hypertrophic differentiation within the human native meniscus-derived DCM scaffold after stimulation with chondrogenic factors. Chondrogenic culture under hypoxic conditions enhanced the synthesis and deposition of meniscus-like ECM by human MFCs and SFMSCs within collagen scaffolds *in vitro*. The formed meniscus-like ECM under hypoxia remained after ectopic implantation in nude mice in contrast to its normoxia counterpart. Moreover, increased amount of VEGF accompanied the enhanced meniscus-like ECM which may have contributed to the observed vascularisation of the engineered meniscus-like ECM. Thus, suggesting that hypoxia-inducible VEGF deposition in meniscus-like ECM may be strategic for the vascularisation and repair of avascular meniscus injuries.

## References

- [1] Proctor CS, Schmidt MB, Whipple RR, Kelly MA, Mow VC. Material properties of the normal medial bovine meniscus. *Journal of orthopaedic research : official publication of the Orthopaedic Research Society* 1989;7:771-82.
- [2] Makris EA, Hadidi P, Athanasiou KA. The knee meniscus: structure-function, pathophysiology, current repair techniques, and prospects for regeneration. *Biomaterials* 2011;32:7411-31.
- [3] McDermott I, Amis A. The consequences of meniscectomy. *Bone & Joint Journal* 2006;88:1549-56.
- [4] Bijlsma JW, Berenbaum F, Lafeber FP. Osteoarthritis: an update with relevance for clinical practice. *Lancet* 2011;377:2115-26.
- [5] Mitchell J, Graham W, Best TM, Collins C, Currie DW, Comstock RD, et al. Epidemiology of meniscal injuries in US high school athletes between 2007 and 2013. *Knee surgery, sports traumatology, arthroscopy* 2016;24:715-22.
- [6] Arnoczky SP, Warren RF. The microvasculature of the meniscus and its response to injury. An experimental study in the dog. *The American journal of sports medicine* 1983;11:131-41.
- [7] Arnoczky SP, Warren RF. Microvasculature of the human meniscus. *The American journal of sports medicine* 1982;10:90-5.
- [8] Arthritis Alliance of Canada. The impact of arthritis in Canada: today and over the next 30 years. 2011.
- [9] Yu H, Adesida AB, Jomha NM. Meniscus repair using mesenchymal stem cells - a comprehensive review. *Stem cell research & therapy* 2015;6:86.
- [10] Adesida AB, Grady LM, Khan WS, Millward-Sadler SJ, Salter DM, Hardingham TE. Human meniscus cells express hypoxia inducible factor-1alpha and increased SOX9 in response to low oxygen tension in cell aggregate culture. *Arthritis research & therapy* 2007;9:R69.
- [11] Adesida AB, Grady LM, Khan WS, Hardingham TE. The matrix-forming phenotype of cultured human meniscus cells is enhanced after culture with fibroblast growth factor 2 and is further stimulated by hypoxia. *Arthritis research & therapy* 2006;8:R61.
- [12] Nakata K, Shino K, Hamada M, Mae T, Miyama T, Shinjo H, et al. Human meniscus cell: characterization of the primary culture and use for tissue engineering. *Clin Orthop Relat Res* 2001:S208-18.
- [13] Bornes TD, Jomha NM, Mulet-Sierra A, Adesida AB. Hypoxic culture of bone marrow-derived mesenchymal stromal stem cells differentially enhances in vitro chondrogenesis within cell-seeded collagen and hyaluronic acid porous scaffolds. *Stem cell research & therapy* 2015;6:84.
- [14] Adesida AB, Mulet-Sierra A, Laouar L, Jomha NM. Oxygen tension is a determinant of the matrix-forming phenotype of cultured human meniscal fibrochondrocytes. *PloS one* 2012;7:e39339.
- [15] Adesida AB, Mulet-Sierra A, Jomha NM. Hypoxia mediated isolation and expansion enhances the chondrogenic capacity of bone marrow mesenchymal stromal cells. *Stem cell research & therapy* 2012;3:9.
- [16] Solchaga LA, Penick K, Goldberg VM, Caplan AI, Welter JF. Fibroblast growth factor-2 enhances proliferation and delays loss of chondrogenic potential in human adult bone-marrow-derived mesenchymal stem cells. *Tissue engineering Part A* 2010;16:1009-19.
- [17] Solchaga LA, Penick K, Porter JD, Goldberg VM, Caplan AI, Welter JF. FGF-2 enhances the mitotic and chondrogenic potentials of human adult bone marrow-derived mesenchymal stem cells. *Journal of*

cellular physiology 2005;203:398-409.

- [18] McKee C, Chaudhry GR. Advances and challenges in stem cell culture. *Colloids and surfaces B, Biointerfaces* 2017;159:62-77.
- [19] Deponti D, Giancamillo AD, Scotti C, Peretti GM, Martin I. Animal models for meniscus repair and regeneration. *Journal of tissue engineering and regenerative medicine* 2015;9:512-27.
- [20] Chew E, Prakash R, Khan W. Mesenchymal stem cells in human meniscal regeneration: A systematic review. *Annals of medicine and surgery (2012)* 2017;24:3-7.
- [21] Vangsness Jr CT, Jack Farr I, Boyd J, Dellaero DT, Mills CR, LeRoux-Williams M. Adult human mesenchymal stem cells delivered via intra-articular injection to the knee following partial medial meniscectomy: a randomized, double-blind, controlled study. *JBJS* 2014;96:90-8.
- [22] Gardner E, O'Rahilly R. The early development of the knee joint in staged human embryos. *Journal of anatomy* 1968;102:289-99.
- [23] Clark CR, Ogden JA. Development of the menisci of the human knee joint. Morphological changes and their potential role in childhood meniscal injury  
*The Journal of bone and joint surgery American volume* 1983;65:538-47.
- [24] Fox AJ, Wanivenhaus F, Burge AJ, Warren RF, Rodeo SA. The human meniscus: A review of anatomy, function, injury, and advances in treatment. *Clinical anatomy (New York, NY)* 2014.
- [25] Chivers MD, Howitt SD. Anatomy and physical examination of the knee menisci: a narrative review of the orthopedic literature. *The Journal of the Canadian Chiropractic Association* 2009;53:319-33.
- [26] Hasan J, Fisher J, Ingham E. Current strategies in meniscal regeneration. *Journal of biomedical materials research Part B, Applied biomaterials* 2014;102:619-34.
- [27] Messner K, Gao J. The menisci of the knee joint. Anatomical and functional characteristics, and a rationale for clinical treatment. *Journal of anatomy* 1998;193 ( Pt 2):161-78.
- [28] Rath E, Richmond JC. The menisci: basic science and advances in treatment. *British journal of sports medicine* 2000;34:252-7.
- [29] Petersen W, Tillmann B. Age-related blood and lymph supply of the knee menisci. A cadaver study. *Acta orthopaedica Scandinavica* 1995;66:308-12.
- [30] Myers E, Zhu W, Mow V. Viscoelastic properties of articular cartilage and meniscus. *Collagen: Chemistry, Biology and Biotechnology* Boca Raton, FL: CRC 1988.
- [31] Danzig L, Resnick D, Gonsalves M, Akeson WH. Blood supply to the normal and abnormal menisci of the human knee. *Clinical orthopaedics and related research* 1983:271-6.
- [32] Day B, Mackenzie WG, Shim SS, Leung G. The vascular and nerve supply of the human meniscus. *Arthroscopy : the journal of arthroscopic & related surgery : official publication of the Arthroscopy Association of North America and the International Arthroscopy Association* 1985;1:58-62.
- [33] Lee JM, Fu FH. The meniscus: basic science and clinical applications. *Operative Techniques in Orthopaedics* 2000;10:162-8.
- [34] Herwig J, Egner E, Buddecke E. Chemical changes of human knee joint menisci in various stages of degeneration. *Annals of the rheumatic diseases* 1984;43:635-40.
- [35] Sweigart MA, Athanasiou KA. Toward tissue engineering of the knee meniscus. *Tissue engineering*

2001;7:111-29.

- [36] McDevitt CA, Webber RJ. The ultrastructure and biochemistry of meniscal cartilage. *Clinical orthopaedics and related research* 1990;8-18.
- [37] Eyre DR, Wu JJ. Collagen of fibrocartilage: a distinctive molecular phenotype in bovine meniscus. *FEBS letters* 1983;158:265-70.
- [38] Cheung HS. Distribution of type I, II, III and V in the pepsin solubilized collagens in bovine menisci. *Connective tissue research* 1987;16:343-56.
- [39] Bullough PG, Munuera L, Murphy J, Weinstein AM. The strength of the menisci of the knee as it relates to their fine structure. *The Journal of bone and joint surgery British volume* 1970;52:564-7.
- [40] Aspden RM, Yarker YE, Hukins DW. Collagen orientations in the meniscus of the knee joint. *Journal of anatomy* 1985;140 ( Pt 3):371-80.
- [41] Petersen W, Tillmann B. Collagenous fibril texture of the human knee joint menisci. *Anatomy and embryology* 1998;197:317-24.
- [42] Adams ME, Muir H. The glycosaminoglycans of canine menisci. *The Biochemical journal* 1981;197:385-9.
- [43] Scott PG, Nakano T, Dodd CM. Isolation and characterization of small proteoglycans from different zones of the porcine knee meniscus. *Biochimica et biophysica acta* 1997;1336:254-62.
- [44] Tanaka T, Fujii K, Kumagae Y. Comparison of biochemical characteristics of cultured fibrochondrocytes isolated from the inner and outer regions of human meniscus. *Knee surgery, sports traumatology, arthroscopy : official journal of the ESSKA* 1999;7:75-80.
- [45] Collier S, Ghosh P. Effects of transforming growth factor beta on proteoglycan synthesis by cell and explant cultures derived from the knee joint meniscus. *Osteoarthritis and cartilage / OARS, Osteoarthritis Research Society* 1995;3:127-38.
- [46] Miller RR, McDevitt CA. Thrombospondin in ligament, meniscus and intervertebral disc. *Biochimica et biophysica acta* 1991;1115:85-8.
- [47] Marcelino J, McDevitt CA. Attachment of articular cartilage chondrocytes to the tissue form of type VI collagen. *Biochimica et biophysica acta* 1995;1249:180-8.
- [48] Hellio Le Graverand MP, Ou Y, Schield-Yee T, Barclay L, Hart D, Natsume T, et al. The cells of the rabbit meniscus: their arrangement, interrelationship, morphological variations and cytoarchitecture. *Journal of anatomy* 2001;198:525-35.
- [49] Crawford K, Briggs KK, Rodkey WG, Steadman JR. Reliability, validity, and responsiveness of the IKDC score for meniscus injuries of the knee. *Arthroscopy : the journal of arthroscopic & related surgery : official publication of the Arthroscopy Association of North America and the International Arthroscopy Association* 2007;23:839-44.
- [50] Anderson AF, Irrgang JJ, Dunn W, Beaufils P, Cohen M, Cole BJ, et al. Interobserver reliability of the International Society of Arthroscopy, Knee Surgery and Orthopaedic Sports Medicine (ISAKOS) classification of meniscal tears. *The American journal of sports medicine* 2011;39:926-32.
- [51] Jee WH, McCauley TR, Kim JM, Jun DJ, Lee YJ, Choi BG, et al. Meniscal tear configurations: categorization with MR imaging. *AJR American journal of roentgenology* 2003;180:93-7.

- [52] knee Mipodmiot, Singson RD, Feldman F, Staron R, Kiernan H. MR imaging of displaced bucket-handle tear of the medial meniscus. *AJR American journal of roentgenology* 1991;156:121-4.
- [53] Ruff C, Weingardt JP, Russ PD, Kilcoyne RF. MR imaging patterns of displaced meniscus injuries of the knee. *AJR American journal of roentgenology* 1998;170:63-7.
- [54] Ververidis AN, Verettas DA, Kazakos KJ, Tilkeridis CE, Chatzipapas CN. Meniscal bucket handle tears: a retrospective study of arthroscopy and the relation to MRI. *Knee surgery, sports traumatology, arthroscopy : official journal of the ESSKA* 2006;14:343-9.
- [55] Tuckman GA, Miller WJ, Remo JW, Fritts HM, Rozansky MI. Radial tears of the menisci: MR findings. *AJR American journal of roentgenology* 1994;163:395-400.
- [56] Magee T, Shapiro M, Williams D. MR accuracy and arthroscopic incidence of meniscal radial tears. *Skeletal radiology* 2002;31:686-9.
- [57] Harper KW, Helms CA, Lambert HS, 3rd, Higgins LD. Radial meniscal tears: significance, incidence, and MR appearance. *AJR American journal of roentgenology* 2005;185:1429-34.
- [58] Greis PE, Bardana DD, Holmstrom MC, Burks RT. Meniscal injury: I. Basic science and evaluation. *The Journal of the American Academy of Orthopaedic Surgeons* 2002;10:168-76.
- [59] Brindle T, Nyland J, Johnson DL. The meniscus: review of basic principles with application to surgery and rehabilitation. *Journal of athletic training* 2001;36:160-9.
- [60] Taylor SA, Rodeo SA. Augmentation techniques for isolated meniscal tears. *Current reviews in musculoskeletal medicine* 2013;6:95-101.
- [61] Laible C, Stein DA, Kiridly DN. Meniscal repair. *The Journal of the American Academy of Orthopaedic Surgeons* 2013;21:204-13.
- [62] Zhang ZN, Tu KY, Xu YK, Zhang WM, Liu ZT, Ou SH. Treatment of longitudinal injuries in avascular area of meniscus in dogs by trephination. *Arthroscopy : the journal of arthroscopic & related surgery : official publication of the Arthroscopy Association of North America and the International Arthroscopy Association* 1988;4:151-9.
- [63] Henning CE, Lynch MA, Yearout KM, Vequist SW, Stallbaumer RJ, Decker KA. Arthroscopic meniscal repair using an exogenous fibrin clot. *Clinical orthopaedics and related research* 1990:64-72.
- [64] Delos D, Rodeo SA. Enhancing meniscal repair through biology: platelet-rich plasma as an alternative strategy. *Instructional course lectures* 2011;60:453-60.
- [65] Kumar A, Malhan K, Roberts SN. Chondral injury from bioabsorbable screws after meniscal repair. *Arthroscopy : the journal of arthroscopic & related surgery : official publication of the Arthroscopy Association of North America and the International Arthroscopy Association* 2001;17:34.
- [66] Jarvela S, Sihvonen R, Sirkeoja H, Jarvela T. All-inside meniscal repair with bioabsorbable meniscal screws or with bioabsorbable meniscus arrows: a prospective, randomized clinical study with 2-year results. *The American journal of sports medicine* 2010;38:2211-7.
- [67] Arnoczky SP, Warren RF, Spivak JM. Meniscal repair using an exogenous fibrin clot. An experimental study in dogs. *The Journal of bone and joint surgery American volume* 1988;70:1209-17.
- [68] Eppley BL, Woodell JE, Higgins J. Platelet quantification and growth factor analysis from platelet-rich plasma: implications for wound healing. *Plastic and reconstructive surgery* 2004;114:1502-8.

- [69] Tumia NS, Johnstone AJ. Platelet derived growth factor-AB enhances knee meniscal cell activity in vitro. *The Knee* 2009;16:73-6.
- [70] Ishida K, Kuroda R, Miwa M, Tabata Y, Hokugo A, Kawamoto T, et al. The regenerative effects of platelet-rich plasma on meniscal cells in vitro and its in vivo application with biodegradable gelatin hydrogel. *Tissue engineering* 2007;13:1103-12.
- [71] Ghadially FN, Wedge JH, Lalonde JM. Experimental methods of repairing injured menisci. *The Journal of bone and joint surgery British volume* 1986;68:106-10.
- [72] Shirakura K, Niijima M, Kobuna Y, Kizuki S. Free synovium promotes meniscal healing. Synovium, muscle and synthetic mesh compared in dogs. *Acta orthopaedica Scandinavica* 1997;68:51-4.
- [73] Roeddecker K, Muennich U, Nagelschmidt M. Meniscal healing: a biomechanical study. *The Journal of surgical research* 1994;56:20-7.
- [74] Milachowski KA, Weismeier K, Wirth CJ. Homologous meniscus transplantation. Experimental and clinical results. *International orthopaedics* 1989;13:1-11.
- [75] Peters G, Wirth CJ. The current state of meniscal allograft transplantation and replacement. *The Knee* 2003;10:19-31.
- [76] Verdonk R, Almqvist KF, Huysse W, Verdonk PC. Meniscal allografts: indications and outcomes. *Sports medicine and arthroscopy review* 2007;15:121-5.
- [77] Verdonk R, Kohn D. Harvest and conservation of meniscal allografts. *Scandinavian journal of medicine & science in sports* 1999;9:158-9.
- [78] Jackson DW, McDevitt CA, Simon TM, Arnoczky SP, Atwell EA, Silvino NJ. Meniscal transplantation using fresh and cryopreserved allografts. An experimental study in goats. *The American journal of sports medicine* 1992;20:644-56.
- [79] Wirth CJ, Peters G, Milachowski KA, Weismeier KG, Kohn D. Long-term results of meniscal allograft transplantation. *The American journal of sports medicine* 2002;30:174-81.
- [80] Scotti C, Hirschmann MT, Antinolfi P, Martin I, Peretti GM. Meniscus repair and regeneration: review on current methods and research potential. *European cells & materials* 2013;26:150-70.
- [81] Verdonk R, Volpi P, Verdonk P, Van der Bracht H, Van Laer M, Almqvist KF, et al. Indications and limits of meniscal allografts. *Injury* 2013;44 Suppl 1:S21-7.
- [82] Bland-Sutton J. *Ligaments; Their Nature and Morphology*: Lewis; 1897.
- [83] Pery O. Follow-up results of meniscectomy with regard to the working capacity. *Acta orthopaedica Scandinavica* 1962;32:457-60.
- [84] Burks RT, Metcalf MH, Metcalf RW. Fifteen-year follow-up of arthroscopic partial meniscectomy. *Arthroscopy : the journal of arthroscopic & related surgery : official publication of the Arthroscopy Association of North America and the International Arthroscopy Association* 1997;13:673-9.
- [85] Fairbank TJ. Knee joint changes after meniscectomy. *The Journal of bone and joint surgery British volume* 1948;30B:664-70.
- [86] Newman AP, Anderson DR, Daniels AU, Jee KW. The effect of medial meniscectomy and coronal plane angulation on in vitro load transmission in the canine stifle joint. *Journal of orthopaedic research : official publication of the Orthopaedic Research Society* 1989;7:281-91.

- [87] Shelbourne KD, Dickens JF. Joint space narrowing after partial medial meniscectomy in the anterior cruciate ligament-intact knee. *The Journal of the American Academy of Orthopaedic Surgeons* 2007;15:519-24.
- [88] Cox JS, Nye CE, Schaefer WW, Woodstein IJ. The degenerative effects of partial and total resection of the medial meniscus in dogs' knees. *Clinical orthopaedics and related research* 1975:178-83.
- [89] Jeong HJ, Lee SH, Ko CS. Meniscectomy. *Knee surgery & related research* 2012;24:129-36.
- [90] Webber RJ, Harris MG, Hough AJ, Jr. Cell culture of rabbit meniscal fibrochondrocytes: proliferative and synthetic response to growth factors and ascorbate. *Journal of orthopaedic research : official publication of the Orthopaedic Research Society* 1985;3:36-42.
- [91] Furumatsu T, Kanazawa T, Yokoyama Y, Abe N, Ozaki T. Inner meniscus cells maintain higher chondrogenic phenotype compared with outer meniscus cells. *Connective tissue research* 2011;52:459-65.
- [92] Baker BM, Nathan AS, Huffman GR, Mauck RL. Tissue engineering with meniscus cells derived from surgical debris. *Osteoarthritis and cartilage / OARS, Osteoarthritis Research Society* 2009;17:336-45.
- [93] Freymann U, Endres M, Goldmann U, Sittinger M, Kaps C. Toward scaffold-based meniscus repair: effect of human serum, hyaluronic acid and TGF- $\beta$ 3 on cell recruitment and re-differentiation. *Osteoarthritis and cartilage / OARS, Osteoarthritis Research Society* 2013;21:773-81.
- [94] Marsano A, Millward-Sadler SJ, Salter DM, Adesida A, Hardingham T, Tognana E, et al. Differential cartilaginous tissue formation by human synovial membrane, fat pad, meniscus cells and articular chondrocytes. *Osteoarthritis and cartilage / OARS, Osteoarthritis Research Society* 2007;15:48-58.
- [95] Baker BM, Nathan AS, Gee AO, Mauck RL. The influence of an aligned nanofibrous topography on human mesenchymal stem cell fibrochondrogenesis. *Biomaterials* 2010;31:6190-200.
- [96] Croutze R, Jomha N, Uludag H, Adesida A. Matrix forming characteristics of inner and outer human meniscus cells on 3D collagen scaffolds under normal and low oxygen tensions. *BMC musculoskeletal disorders* 2013;14:353.
- [97] Chowdhury A, Bezuidenhout LW, Mulet-Sierra A, Jomha NM, Adesida AB. Effect of interleukin-1 $\beta$  treatment on co-cultures of human meniscus cells and bone marrow mesenchymal stromal cells. *BMC musculoskeletal disorders* 2013;14:216.
- [98] Saliken DJ, Mulet-Sierra A, Jomha NM, Adesida AB. Decreased hypertrophic differentiation accompanies enhanced matrix formation in co-cultures of outer meniscus cells with bone marrow mesenchymal stromal cells. *Arthritis research & therapy* 2012;14:R153.
- [99] Matthies NF, Mulet-Sierra A, Jomha NM, Adesida AB. Matrix formation is enhanced in co-cultures of human meniscus cells with bone marrow stromal cells. *J Tissue Eng Regen Med* 2012.
- [100] Paschos NK, Brown WE, Eswaramoorthy R, Hu JC, Athanasiou KA. Advances in tissue engineering through stem cell-based co-culture. *Journal of tissue engineering and regenerative medicine* 2015;9:488-503.
- [101] Ibarra C, Jannetta C, Vacanti CA, Cao Y, Kim TH, Upton J, et al. Tissue engineered meniscus: a potential new alternative to allogeneic meniscus transplantation. *Transplantation proceedings* 1997;29:986-8.
- [102] Hidaka C, Ibarra C, Hannafin JA, Torzilli PA, Quitoriano M, Jen SS, et al. Formation of vascularized

- meniscal tissue by combining gene therapy with tissue engineering. *Tissue engineering* 2002;8:93-105.
- [103] Schoenfeld AJ, Jacquet R, Lowder E, Doherty A, Leeson MC, Landis WJ. Histochemical analyses of tissue-engineered human menisci. *Connective tissue research* 2009;50:307-14.
- [104] Ding Z, Huang H. Mesenchymal stem cells in rabbit meniscus and bone marrow exhibit a similar feature but a heterogeneous multi-differentiation potential: superiority of meniscus as a cell source for meniscus repair. *BMC musculoskeletal disorders* 2015;16:65.
- [105] Osawa A, Harner CD, Gharaibeh B, Matsumoto T, Mifune Y, Kopf S, et al. The Use of Blood Vessel-Derived Stem Cells for Meniscal Regeneration and Repair. *Medicine and science in sports and exercise* 2013;45:813.
- [106] Shen W, Chen J, Zhu T, Chen L, Zhang W, Fang Z, et al. Intra-articular injection of human meniscus stem/progenitor cells promotes meniscus regeneration and ameliorates osteoarthritis through stromal cell-derived factor-1/CXCR4-mediated homing. *Stem cells translational medicine* 2014;3:387-94.
- [107] Shen W, Chen J, Zhu T, Yin Z, Chen X, Chen L, et al. Osteoarthritis prevention through meniscal regeneration induced by intra-articular injection of meniscus stem cells. *Stem cells and development* 2013;22:2071-82.
- [108] Kang SW, Son SM, Lee JS, Lee ES, Lee KY, Park SG, et al. Regeneration of whole meniscus using meniscal cells and polymer scaffolds in a rabbit total meniscectomy model. *Journal of biomedical materials research Part A* 2006;78:659-71.
- [109] Hua-ding L, Dao-zhang C, Kun W, De-hai S, Gang W, Gui-e L. Whole meniscus regeneration using polymer scaffolds loaded with fibrochondrocytes. *Chinese Journal of Traumatology* 2011;14:195-204.
- [110] Martinek V, Ueblacker P, Braun K, Nitschke S, Mannhardt R, Specht K, et al. Second generation of meniscus transplantation: in-vivo study with tissue engineered meniscus replacement. *Archives of orthopaedic and trauma surgery* 2006;126:228-34.
- [111] Esposito AR, Moda M, Cattani SMdM, de Santana GM, Barbieri JA, Munhoz MM, et al. PLDLA/PCL-T scaffold for meniscus tissue engineering. *BioResearch open access* 2013;2:138-47.
- [112] Dominici M, Le Blanc K, Mueller I, Slaper-Cortenbach I, Marini F, Krause D, et al. Minimal criteria for defining multipotent mesenchymal stromal cells. The International Society for Cellular Therapy position statement. *Cytotherapy* 2006;8:315-7.
- [113] Delorme B, Ringe J, Gallay N, Le Vern Y, Kerboeuf D, Jorgensen C, et al. Specific plasma membrane protein phenotype of culture-amplified and native human bone marrow mesenchymal stem cells. *Blood* 2008;111:2631-5.
- [114] Wright G, Jones M, Puklavec M, Brown M, Barclay A. The unusual distribution of the neuronal/lymphoid cell surface CD200 (OX2) glycoprotein is conserved in humans. *Immunology* 2001;102:173-9.
- [115] Gronthos S, Zannettino AC, Hay SJ, Shi S, Graves SE, Kortessidis A, et al. Molecular and cellular characterisation of highly purified stromal stem cells derived from human bone marrow. *Journal of cell science* 2003;116:1827-35.
- [116] Gharibi B, Hughes FJ. Effects of medium supplements on proliferation, differentiation potential, and in vitro expansion of mesenchymal stem cells. *Stem cells translational medicine* 2012;1:771-82.

- [117] Rada T, Reis RL, Gomes ME. Distinct stem cells subpopulations isolated from human adipose tissue exhibit different chondrogenic and osteogenic differentiation potential. *Stem Cell Reviews and Reports* 2011;7:64-76.
- [118] Arufe MC, De la Fuente A, Fuentes I, De Toro F, Blanco F. Chondrogenic potential of subpopulations of cells expressing mesenchymal stem cell markers derived from human synovial membranes. *Journal of cellular biochemistry* 2010;111:834-45.
- [119] Di Maggio N, Mehrkens A, Papadimitropoulos A, Schaeren S, Heberer M, Banfi A, et al. Fibroblast growth factor-2 maintains a niche-dependent population of self-renewing highly potent non-adherent mesenchymal progenitors through FGFR2c. *Stem cells (Dayton, Ohio)* 2012;30:1455-64.
- [120] De Bari C, Dell'Accio F, Luyten FP. Failure of in vitro-differentiated mesenchymal stem cells from the synovial membrane to form ectopic stable cartilage in vivo. *Arthritis and rheumatism* 2004;50:142-50.
- [121] Pelttari K, Winter A, Steck E, Goetzke K, Hennig T, Ochs BG, et al. Premature induction of hypertrophy during in vitro chondrogenesis of human mesenchymal stem cells correlates with calcification and vascular invasion after ectopic transplantation in SCID mice. *Arthritis and rheumatism* 2006;54:3254-66.
- [122] Abdel-Hamid M, Hussein MR, Ahmad AF, Elgezawi EM. Enhancement of the repair of meniscal wounds in the red-white zone (middle third) by the injection of bone marrow cells in canine animal model. *International journal of experimental pathology* 2005;86:117-23.
- [123] Zellner J, Hierl K, Mueller M, Pfeifer C, Berner A, Dienstknecht T, et al. Stem cell-based tissue-engineering for treatment of meniscal tears in the avascular zone. *Journal of Biomedical Materials Research Part B: Applied Biomaterials* 2013;101:1133-42.
- [124] Koch M, Hammer S, Fuellerer J, Lang S, Pfeifer CG, Pattappa G, et al. Bone Marrow Aspirate Concentrate for the Treatment of Avascular Meniscus Tears in a One-Step Procedure-Evaluation of an In Vivo Model. *International journal of molecular sciences* 2019;20.
- [125] Ruiz-Ibán MÁ, Díaz-Heredia J, García-Gómez I, Gonzalez-Lizá F, Elías-Martín E, Abreira V. The effect of the addition of adipose-derived mesenchymal stem cells to a meniscal repair in the avascular zone: an experimental study in rabbits Arthroscopy, *J Arthroscop Related Surg* 2011;27:1688-96.
- [126] Nakagawa Y, Muneta T, Kondo S, Mizuno M, Takakuda K, Ichinose S, et al. Synovial mesenchymal stem cells promote healing after meniscal repair in microminipigs. *Osteoarthritis and cartilage / OARS, Osteoarthritis Research Society* 2015;23:1007-17.
- [127] Dutton A, Choong P, Goh JC, Lee E, Hui J. Enhancement of meniscal repair in the avascular zone using mesenchymal stem cells in a porcine model. *The Journal of bone and joint surgery British volume* 2010;92:169-75.
- [128] Caminal M, Fonseca C, Peris D, Moll X, Rabanal RM, Barrachina J, et al. Use of a chronic model of articular cartilage and meniscal injury for the assessment of long-term effects after autologous mesenchymal stromal cell treatment in sheep. *New biotechnology* 2014;31:492-8.
- [129] Ishimura M, Ohgushi H, Habata T, Tamai S, Fujisawa Y. Arthroscopic meniscal repair using fibrin glue. Part I: Experimental study. *Arthroscopy: The Journal of Arthroscopic & Related Surgery* 1997;13:551-7.

- [130] Liu F, Xu H, Huang H. A novel kartogenin-platelet-rich plasma gel enhances chondrogenesis of bone marrow mesenchymal stem cells in vitro and promotes wounded meniscus healing in vivo. *Stem cell research & therapy* 2019;10:201.
- [131] Mizuno K, Muneta T, Morito T, Ichinose S, Koga H, Nimura A, et al. Exogenous synovial stem cells adhere to defect of meniscus and differentiate into cartilage cells. *Journal of medical and dental sciences* 2008;55:101-11.
- [132] Moriguchi Y, Tateishi K, Ando W, Shimomura K, Yonetani Y, Tanaka Y, et al. Repair of meniscal lesions using a scaffold-free tissue-engineered construct derived from allogenic synovial MSCs in a miniature swine model. *Biomaterials* 2013;34:2185-93.
- [133] Port J, Jackson DW, Lee TQ, Simon TM. Meniscal repair supplemented with exogenous fibrin clot and autogenous cultured marrow cells in the goat model. *The American journal of sports medicine* 1996;24:547-55.
- [134] Angele P, Johnstone B, Kujat R, Zellner J, Nerlich M, Goldberg V, et al. Stem cell based tissue engineering for meniscus repair. *Journal of biomedical materials research Part A* 2008;85:445-55.
- [135] Horie M, Choi H, Lee RH, Reger RL, Ylostalo J, Muneta T, et al. Intra-articular injection of human mesenchymal stem cells (MSCs) promote rat meniscal regeneration by being activated to express Indian hedgehog that enhances expression of type II collagen. *Osteoarthritis and cartilage / OARS, Osteoarthritis Research Society* 2012;20:1197-207.
- [136] Desando G, Giavaresi G, Cavallo C, Bartolotti I, Sartoni F, Nicoli Aldini N, et al. Autologous Bone Marrow Concentrate in a Sheep Model of Osteoarthritis: New Perspectives for Cartilage and Meniscus Repair. *Tissue engineering Part C, Methods* 2016;22:608-19.
- [137] Hatsushika D, Muneta T, Nakamura T, Horie M, Koga H, Nakagawa Y, et al. Repetitive allogeneic intraarticular injections of synovial mesenchymal stem cells promote meniscus regeneration in a porcine massive meniscus defect model. *Osteoarthritis and cartilage / OARS, Osteoarthritis Research Society* 2014;22:941-50.
- [138] Gonzalez-Fernandez ML, Perez-Castrillo S, Sanchez-Lazaro JA, Prieto-Fernandez JG, Lopez-Gonzalez ME, Lobato-Perez S, et al. Assessment of regeneration in meniscal lesions by use of mesenchymal stem cells derived from equine bone marrow and adipose tissue. *American journal of veterinary research* 2016;77:779-88.
- [139] Zhang ZZ, Wang SJ, Zhang JY, Jiang WB, Huang AB, Qi YS, et al. 3D-Printed Poly(epsilon-caprolactone) Scaffold Augmented With Mesenchymal Stem Cells for Total Meniscal Substitution: A 12- and 24-Week Animal Study in a Rabbit Model. *The American journal of sports medicine* 2017;45:1497-511.
- [140] Ying XZ, Qian JJ, Peng L, Zheng Q, Zhu B, Jin YH. Model research on repairing meniscus injury in rabbits using bone marrow mesenchymal stem cells and silk fibroin meniscus porous scaffold. *European review for medical and pharmacological sciences* 2018;22:3689-93.
- [141] Walsh CJ, Goodman D, Caplan AI, Goldberg VM. Meniscus regeneration in a rabbit partial meniscectomy model. *Tissue engineering* 1999;5:327-37.
- [142] Rothrauff BB, Shimomura K, Gottardi R, Alexander PG, Tuan RS. Anatomical region-dependent

- enhancement of 3-dimensional chondrogenic differentiation of human mesenchymal stem cells by soluble meniscus extracellular matrix. *Acta biomaterialia* 2017;49:140-51.
- [143] Shimomura K, Rothrauff BB, Tuan RS. Region-Specific Effect of the Decellularized Meniscus Extracellular Matrix on Mesenchymal Stem Cell-Based Meniscus Tissue Engineering. *The American journal of sports medicine* 2017;45:604-11.
- [144] Yamasaki T, Deie M, Shinomiya R, Izuta Y, Yasunaga Y, Yanada S, et al. Meniscal regeneration using tissue engineering with a scaffold derived from a rat meniscus and mesenchymal stromal cells derived from rat bone marrow. *Journal of biomedical materials research Part A* 2005;75:23-30.
- [145] Fisher MB, Henning EA, Soegaard N, Bostrom M, Esterhai JL, Mauck RL. Engineering meniscus structure and function via multi-layered mesenchymal stem cell-seeded nanofibrous scaffolds. *Journal of biomechanics* 2015;48:1412-9.
- [146] Baker BM, Mauck RL. The effect of nanofiber alignment on the maturation of engineered meniscus constructs. *Biomaterials* 2007;28:1967-77.
- [147] Baker BM, Shah RP, Huang AH, Mauck RL. Dynamic tensile loading improves the functional properties of mesenchymal stem cell-laden nanofiber-based fibrocartilage. *Tissue engineering Part A* 2011;17:1445-55.
- [148] Driscoll TP, Nerurkar NL, Jacobs NT, Elliott DM, Mauck RL. Fiber angle and aspect ratio influence the shear mechanics of oriented electrospun nanofibrous scaffolds. *Journal of the mechanical behavior of biomedical materials* 2011;4:1627-36.
- [149] Nerurkar NL, Han W, Mauck RL, Elliott DM. Homologous structure-function relationships between native fibrocartilage and tissue engineered from MSC-seeded nanofibrous scaffolds. *Biomaterials* 2011;32:461-8.
- [150] Nerurkar NL, Sen S, Baker BM, Elliott DM, Mauck RL. Dynamic culture enhances stem cell infiltration and modulates extracellular matrix production on aligned electrospun nanofibrous scaffolds. *Acta biomaterialia* 2011;7:485-91.
- [151] Liu C, Abedian R, Meister R, Haasper C, Hurschler C, Krettek C, et al. Influence of perfusion and compression on the proliferation and differentiation of bone mesenchymal stromal cells seeded on polyurethane scaffolds. *Biomaterials* 2012;33:1052-64.
- [152] Petri M, Ufer K, Toma I, Becher C, Lioudakis E, Brand S, et al. Effects of perfusion and cyclic compression on in vitro tissue engineered meniscus implants. *Knee Surgery, Sports Traumatology, Arthroscopy* 2012;20:223-31.
- [153] McCorry MC, Bonassar LJ. Fiber development and matrix production in tissue-engineered menisci using bovine mesenchymal stem cells and fibrochondrocytes. *Connective tissue research* 2017;58:329-41.
- [154] Ferris DJ, Frisbie DD, Kisiday JD, McIlwraith CW, Hague BA, Major MD, et al. Clinical outcome after intra-articular administration of bone marrow derived mesenchymal stem cells in 33 horses with stifle injury. *Veterinary Surgery* 2014;43:255-65.
- [155] Yuan X, Wei Y, Villasante A, Ng JJD, Arkonac DE, Chao PG, et al. Stem cell delivery in tissue-specific hydrogel enabled meniscal repair in an orthotopic rat model. *Biomaterials* 2017;132:59-71.
- [156] Yamasaki T, Deie M, Shinomiya R, Yasunaga Y, Yanada S, Ochi M. Transplantation of meniscus

- regenerated by tissue engineering with a scaffold derived from a rat meniscus and mesenchymal stromal cells derived from rat bone marrow. *Artificial organs* 2008;32:519-24.
- [157] Agung M, Ochi M, Yanada S, Adachi N, Izuta Y, Yamasaki T, et al. Mobilization of bone marrow-derived mesenchymal stem cells into the injured tissues after intraarticular injection and their contribution to tissue regeneration. *Knee Surgery, Sports Traumatology, Arthroscopy* 2006;14:1307-14.
- [158] Sakaguchi Y, Sekiya I, Yagishita K, Muneta T. Comparison of human stem cells derived from various mesenchymal tissues: superiority of synovium as a cell source. *Arthritis and rheumatism* 2005;52:2521-9.
- [159] Horie M, Driscoll MD, Sampson HW, Sekiya I, Caroom CT, Prockop DJ, et al. Implantation of allogenic synovial stem cells promotes meniscal regeneration in a rabbit meniscal defect model. *The Journal of Bone and Joint Surgery American volume* 2012;94:701.
- [160] Yoshimura H, Muneta T, Nimura A, Yokoyama A, Koga H, Sekiya I. Comparison of rat mesenchymal stem cells derived from bone marrow, synovium, periosteum, adipose tissue, and muscle. *Cell and tissue research* 2007;327:449-62.
- [161] Nimura A, Muneta T, Koga H, Mochizuki T, Suzuki K, Makino H, et al. Increased proliferation of human synovial mesenchymal stem cells with autologous human serum: comparisons with bone marrow mesenchymal stem cells and with fetal bovine serum. *Arthritis & Rheumatism: Official Journal of the American College of Rheumatology* 2008;58:501-10.
- [162] Tan Y, Zhang Y, Pei M. Meniscus reconstruction through coculturing meniscus cells with synovium-derived stem cells on small intestine submucosa--a pilot study to engineer meniscus tissue constructs. *Tissue engineering Part A* 2010;16:67-79.
- [163] Xie X, Zhu J, Hu X, Dai L, Fu X, Zhang J, et al. A co-culture system of rat synovial stem cells and meniscus cells promotes cell proliferation and differentiation as compared to mono-culture. *Scientific reports* 2018;8:7693.
- [164] Song X, Xie Y, Liu Y, Shao M, Wang W. Beneficial effects of coculturing synovial derived mesenchymal stem cells with meniscus fibrochondrocytes are mediated by fibroblast growth factor 1: increased proliferation and collagen synthesis. *Stem cells international* 2015;2015:926325.
- [165] Horie M, Sekiya I, Muneta T, Ichinose S, Matsumoto K, Saito H, et al. Intra-articular Injected synovial stem cells differentiate into meniscal cells directly and promote meniscal regeneration without mobilization to distant organs in rat massive meniscal defect. *Stem cells (Dayton, Ohio)* 2009;27:878-87.
- [166] Katagiri H, Muneta T, Tsuji K, Horie M, Koga H, Ozeki N, et al. Transplantation of aggregates of synovial mesenchymal stem cells regenerates meniscus more effectively in a rat massive meniscal defect. *Biochemical and biophysical research communications* 2013;435:603-9.
- [167] Ozeki N, Muneta T, Matsuta S, Koga H, Nakagawa Y, Mizuno M, et al. Synovial mesenchymal stem cells promote meniscus regeneration augmented by an autologous Achilles tendon graft in a rat partial meniscus defect model. *Stem cells (Dayton, Ohio)* 2015;33:1927-38.
- [168] Kondo S, Muneta T, Nakagawa Y, Koga H, Watanabe T, Tsuji K, et al. Transplantation of autologous synovial mesenchymal stem cells promotes meniscus regeneration in aged primates. *Journal of orthopaedic research : official publication of the Orthopaedic Research Society* 2017;35:1274-82.
- [169] Perdisa F, Gostyńska N, Roffi A, Filardo G, Marcacci M, Kon E. Adipose-derived mesenchymal stem

cells for the treatment of articular cartilage: a systematic review on preclinical and clinical evidence. *Stem cells international* 2015;2015.

[170] Segawa Y, Muneta T, Makino H, Nimura A, Mochizuki T, Ju YJ, et al. Mesenchymal stem cells derived from synovium, meniscus, anterior cruciate ligament, and articular chondrocytes share similar gene expression profiles. *Journal of orthopaedic research : official publication of the Orthopaedic Research Society* 2009;27:435-41.

[171] Meier EM, Wu B, Siddiqui A, Tepper DG, Longaker MT, Lam MT. Mechanical Stimulation Increases Knee Meniscus Gene RNA-level Expression in Adipose-derived Stromal Cells. *Plastic and reconstructive surgery Global open* 2016;4:e864.

[172] Baek J, Sovani S, Choi W, Jin S, Grogan SP, D'Lima DD. Meniscal Tissue Engineering Using Aligned Collagen Fibrous Scaffolds: Comparison of Different Human Cell Sources. *Tissue engineering Part A* 2018;24:81-93.

[173] Romanazzo S, Vedicherla S, Moran C, Kelly DJ. Meniscus ECM-functionalised hydrogels containing infrapatellar fat pad-derived stem cells for bioprinting of regionally defined meniscal tissue. *Journal of tissue engineering and regenerative medicine* 2018;12:e1826-e35.

[174] Weiss WM, Mulet-Sierra A, Kunze M, Jomha NM, Adesida AB. Coculture of meniscus cells and mesenchymal stem cells in simulated microgravity. *npj Microgravity* 2017;3:28.

[175] Sasaki H, Rothrauff BB, Alexander PG, Lin H, Gottardi R, Fu FH, et al. In Vitro Repair of Meniscal Radial Tear With Hydrogels Seeded With Adipose Stem Cells and TGF-beta3. *The American journal of sports medicine* 2018;46:2402-13.

[176] Qi Y, Yang Z, Ding Q, Zhao T, Huang Z, Feng G. Targeted transplantation of iron oxide-labeled, adipose-derived mesenchymal stem cells in promoting meniscus regeneration following a rabbit massive meniscal defect. *Experimental and therapeutic medicine* 2016;11:458-66.

[177] Toratani T, Nakase J, Numata H, Oshima T, Takata Y, Nakayama K, et al. Scaffold-Free Tissue-Engineered Allogenic Adipose-Derived Stem Cells Promote Meniscus Healing. *Arthroscopy : the journal of arthroscopic & related surgery : official publication of the Arthroscopy Association of North America and the International Arthroscopy Association* 2017;33:346-54.

[178] Jones EA, English A, Henshaw K, Kinsey SE, Markham AF, Emery P, et al. Enumeration and phenotypic characterization of synovial fluid multipotential mesenchymal progenitor cells in inflammatory and degenerative arthritis. *Arthritis and rheumatism* 2004;50:817-27.

[179] Jones EA, Crawford A, English A, Henshaw K, Mundy J, Corscadden D, et al. Synovial fluid mesenchymal stem cells in health and early osteoarthritis: detection and functional evaluation at the single-cell level. *Arthritis and rheumatism* 2008;58:1731-40.

[180] Morito T, Muneta T, Hara K, Ju Y-J, Mochizuki T, Makino H, et al. Synovial fluid-derived mesenchymal stem cells increase after intra-articular ligament injury in humans. *Rheumatology* 2008;47:1137-43.

[181] Sekiya I, Ojima M, Suzuki S, Yamaga M, Horie M, Koga H, et al. Human mesenchymal stem cells in synovial fluid increase in the knee with degenerated cartilage and osteoarthritis. *Journal of Orthopaedic Research* 2012;30:943-9.

- [182] Zayed M, Caniglia C, Misk N, Dhar MS. Donor-Matched Comparison of Chondrogenic Potential of Equine Bone Marrow- and Synovial Fluid-Derived Mesenchymal Stem Cells: Implications for Cartilage Tissue Regeneration. *Frontiers in veterinary science* 2016;3:121.
- [183] Ando W, Kutcher JJ, Krawetz R, Sen A, Nakamura N, Frank CB, et al. Clonal analysis of synovial fluid stem cells to characterize and identify stable mesenchymal stromal cell/mesenchymal progenitor cell phenotypes in a porcine model: a cell source with enhanced commitment to the chondrogenic lineage. *Cytotherapy* 2014;16:776-88.
- [184] Lee WJ, Hah YS, Ock SA, Lee JH, Jeon RH, Park JS, et al. Cell source-dependent in vivo immunosuppressive properties of mesenchymal stem cells derived from the bone marrow and synovial fluid of minipigs. *Experimental cell research* 2015;333:273-88.
- [185] Garcia J, Wright K, Roberts S, Kuiper JH, Mangham C, Richardson J, et al. Characterisation of synovial fluid and infrapatellar fat pad derived mesenchymal stromal cells: the influence of tissue source and inflammatory stimulus. *Scientific reports* 2016;6.
- [186] Krawetz RJ, Wu YE, Martin L, Rattner JB, Matyas JR, Hart DA. Synovial fluid progenitors expressing CD90+ from normal but not osteoarthritic joints undergo chondrogenic differentiation without micro-mass culture. *PloS one* 2012;7:e43616.
- [187] Bianchessi M, Chen Y, Durgam S, Pondenis H, Stewart M. Effect of Fibroblast Growth Factor 2 on Equine Synovial Fluid Chondroprogenitor Expansion and Chondrogenesis. *Stem cells international* 2016;2016:9364974.
- [188] Neybecker P, Henrionnet C, Pape E, Mainard D, Galois L, Loeuille D, et al. In vitro and in vivo potentialities for cartilage repair from human advanced knee osteoarthritis synovial fluid-derived mesenchymal stem cells. *Stem cell research & therapy* 2018;9:329.
- [189] Zhang Z-Z, Zhou Y-F, Li W-P, Jiang C, Chen Z, Luo H, et al. Local Administration of Magnesium Promotes Meniscal Healing Through Homing of Endogenous Stem Cells: A Proof-of-Concept Study. *The American journal of sports medicine* 2019;47:954-67.
- [190] Westminster C, Westminster C, Vail C, Busse D. Increased knee cartilage volume in degenerative joint disease using percutaneously implanted, autologous mesenchymal stem cells. *Pain physician* 2008;11:343-53.
- [191] Whitehouse MR, Howells NR, Parry MC, Austin E, Kafienah W, Brady K, et al. Repair of torn avascular meniscal cartilage using undifferentiated autologous mesenchymal stem cells: from in vitro optimization to a first-in-human study. *Stem cells translational medicine* 2017;6:1237-48.
- [192] Sekiya I, Koga H, Otabe K, Nakagawa Y, Katano H, Ozeki N, et al. Additional Use of Synovial Mesenchymal Stem Cell Transplantation Following Surgical Repair of a Complex Degenerative Tear of the Medial Meniscus of the Knee: A Case Report. *Cell transplantation* 2019;963689719863793.
- [193] Pak J. Regeneration of human bones in hip osteonecrosis and human cartilage in knee osteoarthritis with autologous adipose-tissue-derived stem cells: a case series. *Journal of medical case reports* 2011;5:296.
- [194] Pak J, Lee JH, Lee SH. Regenerative repair of damaged meniscus with autologous adipose tissue-derived stem cells. *BioMed research international* 2014;2014.

- [195] Woolf AD. Global burden of osteoarthritis and musculoskeletal diseases. *BMC musculoskeletal disorders* 2015;16:S3.
- [196] Zhang Y, Jordan JM. Epidemiology of osteoarthritis. *Clinics in geriatric medicine* 2010;26:355-69.
- [197] Roos H, Adalberth T, Dahlberg L, Lohmander LS. Osteoarthritis of the knee after injury to the anterior cruciate ligament or meniscus: the influence of time and age. *Osteoarthritis and cartilage / OARS, Osteoarthritis Research Society* 1995;3:261-7.
- [198] Shrive NG, O'Connor JJ, Goodfellow JW. Load-bearing in the knee joint. *Clinical orthopaedics and related research* 1978:279-87.
- [199] Jaspers P, De Lange A, Huijskes R. The mechanical function of the meniscus, experiments on cadaveric pig knee-joints. 1980.
- [200] Schumacher BL, Schmidt TA, Voegtline MS, Chen AC, Sah RL. Proteoglycan 4 (PRG4) synthesis and immunolocalization in bovine meniscus. *Journal of orthopaedic research* 2005;23:562-8.
- [201] Verdonk PC, Forsyth RG, Wang J, Almqvist KF, Verdonk R, Veys EM, et al. Characterisation of human knee meniscus cell phenotype. *Osteoarthritis Cartilage* 2005;13:548-60.
- [202] Melrose J, Smith S, Croke M, Read R, Whitelock J. Comparative spatial and temporal localisation of perlecan, aggrecan and type I, II and IV collagen in the ovine meniscus: an ageing study. *Histochemistry and cell biology* 2005;124:225-35.
- [203] Kambic HE, McDevitt CA. Spatial organization of types I and II collagen in the canine meniscus. *Journal of Orthopaedic Research* 2005;23:142-9.
- [204] Eyre DR, Wu J-J. Collagen of fibrocartilage: a distinctive molecular phenotype in bovine meniscus. *FEBS letters* 1983;158:265-70.
- [205] McDermott ID, Amis AA. The consequences of meniscectomy. *J Bone Joint Surg Br* 2006;88:1549-56.
- [206] Niu W, Guo W, Han S, Zhu Y, Liu S, Guo Q. Cell-Based Strategies for Meniscus Tissue Engineering. *Stem cells international* 2016;2016.
- [207] Marsano A, Wendt D, Raiteri R, Gottardi R, Stolz M, Wirz D, et al. Use of hydrodynamic forces to engineer cartilaginous tissues resembling the non-uniform structure and function of meniscus. *Biomaterials* 2006;27:5927-34.
- [208] Pabbruwe MB, Kafienah W, Tarlton JF, Mistry S, Fox DJ, Hollander AP. Repair of meniscal cartilage white zone tears using a stem cell/collagen-scaffold implant. *Biomaterials* 2010;31:2583-91.
- [209] Horie M, Driscoll MD, Sampson HW, Sekiya I, Caroom CT, Prockop DJ, et al. Implantation of allogenic synovial stem cells promotes meniscal regeneration in a rabbit meniscal defect model. *The Journal of bone and joint surgery American volume* 2012;94:701-12.
- [210] Ruiz-Ibán MÁ, Díaz-Heredía J, García-Gómez I, Gonzalez-Lizán F, Elías-Martín E, Abaira V. The effect of the addition of adipose-derived mesenchymal stem cells to a meniscal repair in the avascular zone: an experimental study in rabbits. *Arthroscopy: The Journal of Arthroscopic & Related Surgery* 2011;27:1688-96.
- [211] Herwig J, Egnér E, Buddecke E. Chemical changes of human knee joint menisci in various stages of degeneration. *Annals of the rheumatic diseases* 1984;43:635-40.

- [212] Gunja NJ, Athanasiou KA. Passage and reversal effects on gene expression of bovine meniscal fibrochondrocytes. *Arthritis Res Ther* 2007;9:R93.
- [213] Son MS, Levenston ME. Quantitative tracking of passage and 3D culture effects on chondrocyte and fibrochondrocyte gene expression. *Journal of tissue engineering and regenerative medicine* 2015.
- [214] Stevens MM, Marini RP, Martin I, Langer R, Shastri VP. FGF-2 enhances TGF- $\beta$ 1-induced periosteal chondrogenesis. *Journal of orthopaedic research* 2004;22:1114-9.
- [215] Cui X, Breitenkamp K, Lotz M, D'Lima D. Synergistic action of fibroblast growth factor-2 and transforming growth factor-beta1 enhances bioprinted human neocartilage formation. *Biotechnology and bioengineering* 2012;109:2357-68.
- [216] Jakob M, Demarteau O, Schafer D, Hintermann B, Dick W, Heberer M, et al. Specific growth factors during the expansion and redifferentiation of adult human articular chondrocytes enhance chondrogenesis and cartilaginous tissue formation in vitro. *J Cell Biochem* 2001;81:368-77.
- [217] Martin I, Vunjak-Novakovic G, Yang J, Langer R, Freed LE. Mammalian chondrocytes expanded in the presence of fibroblast growth factor 2 maintain the ability to differentiate and regenerate three-dimensional cartilaginous tissue. *Experimental cell research* 1999;253:681-8.
- [218] Farndale RW, Buttle DJ, Barrett AJ. Improved quantitation and discrimination of sulphated glycosaminoglycans by use of dimethylmethylene blue. *Biochimica et biophysica acta* 1986;883:173-7.
- [219] Livak KJ, Schmittgen TD. Analysis of relative gene expression data using real-time quantitative PCR and the 2<sup>-</sup> $\Delta\Delta$ CT method. *methods* 2001;25:402-8.
- [220] Son MS, Levenston ME. Quantitative tracking of passage and 3D culture effects on chondrocyte and fibrochondrocyte gene expression. *Journal of tissue engineering and regenerative medicine* 2015.
- [221] Martin I, Vunjak-Novakovic G, Yang J, Langer R, Freed L. Mammalian chondrocytes expanded in the presence of fibroblast growth factor 2 maintain the ability to differentiate and regenerate three-dimensional cartilaginous tissue. *Experimental cell research* 1999;253:681-8.
- [222] Barbero A, Ploegert S, Heberer M, Martin I. Plasticity of clonal populations of dedifferentiated adult human articular chondrocytes. *Arthritis & Rheumatism* 2003;48:1315-25.
- [223] Guerne PA, Sublet A, Lotz M. Growth factor responsiveness of human articular chondrocytes: distinct profiles in primary chondrocytes, subcultured chondrocytes, and fibroblasts. *Journal of cellular physiology* 1994;158:476-84.
- [224] Jakob M, Demarteau O, Schäfer D, Hintermann B, Dick W, Heberer M, et al. Specific growth factors during the expansion and redifferentiation of adult human articular chondrocytes enhance chondrogenesis and cartilaginous tissue formation in vitro. *Journal of cellular biochemistry* 2001;81:368-77.
- [225] Pennathur-Das R, Levitt L. Augmentation of in vitro human marrow erythropoiesis under physiological oxygen tensions is mediated by monocytes and T lymphocytes. *Blood* 1987;69:899-907.
- [226] Lund-Olesen K. Oxygen tension in synovial fluids. *Arthritis & Rheumatism* 1970;13:769-76.
- [227] Bornes TD, Adesida AB, Jomha NM. Mesenchymal stem cells in the treatment of traumatic articular cartilage defects: a comprehensive review. *Arthritis research & therapy* 2014;16:432.
- [228] Leijten J, Georgi N, Teixeira LM, van Blitterswijk CA, Post JN, Karperien M. Metabolic programming of mesenchymal stromal cells by oxygen tension directs chondrogenic cell fate. *Proceedings*

- of the National Academy of Sciences 2014;111:13954-9.
- [229] Falanga V, Zhou L, Yufit T. Low oxygen tension stimulates collagen synthesis and COL1A1 transcription through the action of TGF-beta1. *J Cell Physiol* 2002;191:42-50.
- [230] Sophia Fox AJ, Bedi A, Rodeo SA. The basic science of articular cartilage: structure, composition, and function. *Sports Health* 2009;1:461-8.
- [231] Mauck RL, Martinez-Diaz GJ, Yuan X, Tuan RS. Regional multilineage differentiation potential of meniscal fibrochondrocytes: implications for meniscus repair. *The Anatomical record* 2007;290:48-58.
- [232] Crisan M, Yap S, Casteilla L, Chen C-W, Corselli M, Park TS, et al. A perivascular origin for mesenchymal stem cells in multiple human organs. *Cell stem cell* 2008;3:301-13.
- [233] Segawa Y, Muneta T, Makino H, Nimura A, Mochizuki T, Ju YJ, et al. Mesenchymal stem cells derived from synovium, meniscus, anterior cruciate ligament, and articular chondrocytes share similar gene expression profiles. *Journal of Orthopaedic Research* 2009;27:435-41.
- [234] Seol D, Zhou C, Brouillette MJ, Song I, Yu Y, Choe HH, et al. Characteristics of meniscus progenitor cells migrated from injured meniscus. *Journal of Orthopaedic Research* 2016.
- [235] Fu W, Xie X, Li Q, Chen G, Zhang C, Tang X, et al. Isolation, Characterization, and Multipotent Differentiation of Mesenchymal Stem Cells Derived from Meniscal Debris. *Stem cells international* 2016;2016.
- [236] Sun Y, Mauerhan DR, Honeycutt PR, Kneisl JS, Norton JH, Hanley EN, et al. Analysis of meniscal degeneration and meniscal gene expression. *BMC musculoskeletal disorders* 2010;11:1.
- [237] Barbero A, Grogan S, Schäfer D, Heberer M, Mainil-Varlet P, Martin I. Age related changes in human articular chondrocyte yield, proliferation and post-expansion chondrogenic capacity. *Osteoarthritis and cartilage* 2004;12:476-84.
- [238] Takroni T, Laouar L, Adesida A, Elliott JA, Jomha NM. Anatomical study: comparing the human, sheep and pig knee meniscus. *Journal of Experimental Orthopaedics* 2016;3:35.
- [239] Bornes TD, Jomha NM, Mulet-Sierra A, Adesida AB. Optimal Seeding Densities for In Vitro Chondrogenesis of Two- and Three-Dimensional-Isolated and -Expanded Bone Marrow-Derived Mesenchymal Stromal Stem Cells Within a Porous Collagen Scaffold. *Tissue engineering Part C, Methods* 2016;22:208-20.
- [240] Lee CH, Rodeo SA, Fortier LA, Lu C, Eriskin C, Mao JJ. Protein-releasing polymeric scaffolds induce fibrochondrocytic differentiation of endogenous cells for knee meniscus regeneration in sheep. *Science translational medicine* 2014;6:266ra171-266ra171.
- [241] Lund-Olesen K. Oxygen tension in synovial fluids. *Arthritis Rheum* 1970;13:769-76.
- [242] Szojka ARA, Lyons BD, Moore CN, Liang Y, Kunze M, Idrees E, et al. Hypoxia and TGF-beta3 Synergistically Mediate Inner Meniscus-Like Matrix Formation by Fibrochondrocytes. *Tissue engineering Part A* 2019;25:446-56.
- [243] McDermott I, Amis A. The consequences of meniscectomy. *Journal of Bone & Joint Surgery, British Volume* 2006;88:1549-56.
- [244] Cheung HS. Distribution of type I, II, III and V in the pepsin solubilized collagens in bovine menisci. *Connective tissue research* 1987;16:343-56.

- [245] Scott PG, Nakano T, Dodd CM. Isolation and characterization of small proteoglycans from different zones of the porcine knee meniscus. *Biochimica et Biophysica Acta (BBA)-General Subjects* 1997;1336:254-62.
- [246] Liang Y, Idrees E, Andrews SHJ, Labib K, Szojka A, Kunze M, et al. Plasticity of Human Meniscus Fibrochondrocytes: A Study on Effects of Mitotic Divisions and Oxygen Tension. *Scientific reports* 2017;7:12148.
- [247] Hoshiba T, Chen G, Endo C, Maruyama H, Wakui M, Nemoto E, et al. Decellularized extracellular matrix as an in vitro model to study the comprehensive roles of the ECM in stem cell differentiation. *Stem cells international* 2015;2016.
- [248] Monibi FA, Cook JL. Tissue-Derived Extracellular Matrix Bioscaffolds: Emerging Applications in Cartilage and Meniscus Repair. *Tissue engineering Part B, Reviews* 2017;23:386-98.
- [249] Chen YC, Chen RN, Jhan HJ, Liu DZ, Ho HO, Mao Y, et al. Development and Characterization of Acellular Extracellular Matrix Scaffolds from Porcine Menisci for Use in Cartilage Tissue Engineering. *Tissue engineering Part C, Methods* 2015;21:971-86.
- [250] Monibi FA, Bozynski CC, Kuroki K, Stoker AM, Pfeiffer FM, Sherman SL, et al. Development of a Micronized Meniscus Extracellular Matrix Scaffold for Potential Augmentation of Meniscal Repair and Regeneration. *Tissue Engineering Part C: Methods* 2016;22:1059-70.
- [251] Maier D, Braeun K, Steinhauser E, Ueblacker P, Oberst M, Kreuz PC, et al. In vitro analysis of an allogenic scaffold for tissue-engineered meniscus replacement. *Journal of Orthopaedic Research* 2007;25:1598-608.
- [252] Gao S, Guo W, Chen M, Yuan Z, Wang M, Zhang Y, et al. Fabrication and characterization of electrospun nanofibers composed of decellularized meniscus extracellular matrix and polycaprolactone for meniscus tissue engineering. *Journal of Materials Chemistry B* 2017;5:2273-85.
- [253] Sandmann G, Eichhorn S, Vogt S, Adamczyk C, Aryee S, Hoberg M, et al. Generation and characterization of a human acellular meniscus scaffold for tissue engineering. *Journal of Biomedical Materials Research Part A: An Official Journal of The Society for Biomaterials, The Japanese Society for Biomaterials, and The Australian Society for Biomaterials and the Korean Society for Biomaterials* 2009;91:567-74.
- [254] Cheng NC, Estes BT, Awad HA, Guilak F. Chondrogenic differentiation of adipose-derived adult stem cells by a porous scaffold derived from native articular cartilage extracellular matrix. *Tissue engineering Part A* 2009;15:231-41.
- [255] Liang Y, Idrees E, Szojka ARA, Andrews SHJ, Kunze M, Mulet-Sierra A, et al. Chondrogenic differentiation of synovial fluid mesenchymal stem cells on human meniscus-derived decellularized matrix requires exogenous growth factors. *Acta Biomater* 2018;80:131-43.
- [256] Chen YC, Chen RN, Jhan HJ, Liu DZ, Ho HO, Mao Y, et al. Development and Characterization of Acellular Extracellular Matrix Scaffolds from Porcine Menisci for Use in Cartilage Tissue Engineering. *Tissue engineering Part C, Methods* 2015.
- [257] Crapo PM, Gilbert TW, Badylak SF. An overview of tissue and whole organ decellularization processes. *Biomaterials* 2011;32:3233-43.

- [258] Marsano A, Medeiros da Cunha CM, Ghanaati S, Gueven S, Centola M, Tsaryk R, et al. Spontaneous In Vivo Chondrogenesis of Bone Marrow-Derived Mesenchymal Progenitor Cells by Blocking Vascular Endothelial Growth Factor Signaling. *Stem cells translational medicine* 2016;5:1730-8.
- [259] Wei F, Zhou J, Wei X, Zhang J, Fleming BC, Terek R, et al. Activation of Indian hedgehog promotes chondrocyte hypertrophy and upregulation of MMP-13 in human osteoarthritic cartilage. *Osteoarthritis and cartilage* 2012;20:755-63.
- [260] Mauck RL, Wang CC, Oswald ES, Ateshian GA, Hung CT. The role of cell seeding density and nutrient supply for articular cartilage tissue engineering with deformational loading. *Osteoarthritis and cartilage / OARS, Osteoarthritis Research Society* 2003;11:879-90.
- [261] Oberlender SA, Tuan RS. Expression and functional involvement of N-cadherin in embryonic limb chondrogenesis. *Development* 1994;120:177-87.
- [262] Hall BK, Miyake T. Divide, accumulate, differentiate: cell condensation in skeletal development revisited. *International Journal of Developmental Biology* 2004;39:881-93.
- [263] Bornes TD, Jomha NM, Mulet-Sierra A, Adesida AB. Optimal seeding densities for in vitro chondrogenesis of two-and three-dimensional-isolated and-expanded bone marrow-derived mesenchymal stromal stem cells within a porous collagen scaffold. *Tissue Engineering Part C: Methods* 2016;22:208-20.
- [264] Lim Y-B, Kang S-S, Park TK, Lee Y-S, Chun J-S, Sonn JK. Disruption of actin cytoskeleton induces chondrogenesis of mesenchymal cells by activating protein kinase C- $\alpha$  signaling. *Biochemical and biophysical research communications* 2000;273:609-13.
- [265] Urist MR. Bone: formation by autoinduction. *Science (New York, NY)* 1965;150:893-9.
- [266] Van der Kraan P, Buma P, Van Kuppevelt T, Van Den Berg W. Interaction of chondrocytes, extracellular matrix and growth factors: relevance for articular cartilage tissue engineering. *Osteoarthritis and Cartilage* 2002;10:631-7.
- [267] Stapleton TW, Ingram J, Katta J, Knight R, Korossis S, Fisher J, et al. Development and characterization of an acellular porcine medial meniscus for use in tissue engineering. *Tissue Engineering Part A* 2008;14:505-18.
- [268] Azhim A, Ono T, Fukui Y, Morimoto Y, Furukawa K, Ushida T. Preparation of decellularized meniscal scaffolds using sonication treatment for tissue engineering. *Engineering in Medicine and Biology Society (EMBC), 2013 35th Annual International Conference of the IEEE: IEEE; 2013. p. 6953-6.*
- [269] Abdelgaied A, Stanley M, Galfe M, Berry H, Ingham E, Fisher J. Comparison of the biomechanical tensile and compressive properties of decellularised and natural porcine meniscus. *Journal of biomechanics* 2015;48:1389-96.
- [270] Marsano A, Medeiros da Cunha CM, Ghanaati S, Gueven S, Centola M, Tsaryk R, et al. Spontaneous In Vivo Chondrogenesis of Bone Marrow-Derived Mesenchymal Progenitor Cells by Blocking Vascular Endothelial Growth Factor Signaling. *Stem cells translational medicine* 2016;5:1730-8.
- [271] Mauck R, Yuan X, Tuan R. Chondrogenic differentiation and functional maturation of bovine mesenchymal stem cells in long-term agarose culture. *Osteoarthritis and cartilage* 2006;14:179-89.
- [272] Erickson IE, Huang AH, Chung C, Li RT, Burdick JA, Mauck RL. Differential maturation and structure–function relationships in mesenchymal stem cell-and chondrocyte-seeded hydrogels. *Tissue*

Engineering Part A 2008;15:1041-52.

[273] Makris EA, Responde DJ, Paschos NK, Hu JC, Athanasiou KA. Developing functional musculoskeletal tissues through hypoxia and lysyl oxidase-induced collagen cross-linking. *Proceedings of the National Academy of Sciences* 2014;111:E4832-E41.

[274] Lima EG, Bian L, Ng KW, Mauck RL, Byers BA, Tuan RS, et al. The beneficial effect of delayed compressive loading on tissue-engineered cartilage constructs cultured with TGF- $\beta$ 3. *Osteoarthritis and cartilage* 2007;15:1025-33.

[275] Huang AH, Stein A, Tuan RS, Mauck RL. Transient exposure to transforming growth factor beta 3 improves the mechanical properties of mesenchymal stem cell-laden cartilage constructs in a density-dependent manner. *Tissue engineering Part A* 2009;15:3461-72.

[276] Byers BA, Mauck RL, Chiang IE, Tuan RS. Transient exposure to transforming growth factor beta 3 under serum-free conditions enhances the biomechanical and biochemical maturation of tissue-engineered cartilage. *Tissue engineering Part A* 2008;14:1821-34.

[277] Liang Y, Szojka ARA, Idrees E, Kunze M, Mulet-Sierra A, Adesida AB. Re-Differentiation of Human Meniscus Fibrochondrocytes Differs in Three-Dimensional Cell Aggregates and Decellularized Human Meniscus Matrix Scaffolds. *Annals of biomedical engineering* 2019.

[278] Hitchon C, Wong K, Ma G, Reed J, Lyttle D, El-Gabalawy H. Hypoxia-induced production of stromal cell-derived factor 1 (CXCL12) and vascular endothelial growth factor by synovial fibroblasts. *Arthritis & Rheumatism* 2002;46:2587-97.

[279] Williams LB, Adesida AB. Angiogenic approaches to meniscal healing. *Injury* 2018;49:467-72.

[280] Andrews SH, Kunze M, Mulet-Sierra A, Williams L, Ansari K, Osswald M, et al. Strategies to Mitigate Variability in Engineering Human Nasal Cartilage. *Scientific reports* 2017;7.

[281] Gonda K, Shigeura T, Sato T, Matsumoto D, Suga H, Inoue K, et al. Preserved proliferative capacity and multipotency of human adipose-derived stem cells after long-term cryopreservation. *Plastic and reconstructive surgery* 2008;121:401-10.

[282] Almici C, Carlo-Stella C, Wagner J, Mangoni L, Garau D, Re A, et al. Clonogenic capacity and ex vivo expansion potential of umbilical cord blood progenitor cells are not impaired by cryopreservation. *Bone marrow transplantation* 1997;19:1079.

[283] Chiari C, Koller U, Kapeller B, Dorotka R, Bindreiter U, Nehrer S. Different behavior of meniscal cells in collagen II/I,III and Hyaff-11 scaffolds in vitro. *Tissue engineering Part A* 2008;14:1295-304.

[284] Gavénis K, Schmidt-Rohlfing B, Mueller-Rath R, Andereya S, Schneider U. In vitro comparison of six different matrix systems for the cultivation of human chondrocytes. *In Vitro Cellular & Developmental Biology-Animal* 2006;42:159-67.

[285] Murphy CL, Thoms BL, Vaghjiani RJ, Lafont JE. Hypoxia. HIF-mediated articular chondrocyte function: prospects for cartilage repair. *Arthritis research & therapy* 2009;11:213.

[286] Loboda A, Jozkowicz A, Dulak J. HIF-1 and HIF-2 transcription factors—similar but not identical. *Molecules and cells* 2010;29:435-42.

[287] Lafont JE, Talma S, Murphy CL. Hypoxia-inducible factor 2 $\alpha$  is essential for hypoxic induction of the human articular chondrocyte phenotype. *Arthritis & Rheumatism: Official Journal of the American*

College of Rheumatology 2007;56:3297-306.

- [288] Khan WS, Adesida AB, Hardingham TE. Hypoxic conditions increase hypoxia-inducible transcription factor 2alpha and enhance chondrogenesis in stem cells from the infrapatellar fat pad of osteoarthritis patients. *Arthritis research & therapy* 2007;9:R55.
- [289] Hu C-J, Wang L-Y, Chodosh LA, Keith B, Simon MC. Differential roles of hypoxia-inducible factor 1 $\alpha$  (HIF-1 $\alpha$ ) and HIF-2 $\alpha$  in hypoxic gene regulation. *Molecular and cellular biology* 2003;23:9361-74.
- [290] Hu C-J, Iyer S, Sataur A, Covelto KL, Chodosh LA, Simon MC. Differential regulation of the transcriptional activities of hypoxia-inducible factor 1 alpha (HIF-1 $\alpha$ ) and HIF-2 $\alpha$  in stem cells. *Molecular and cellular biology* 2006;26:3514-26.
- [291] Amarilio R, Viukov SV, Sharir A, Eshkar-Oren I, Johnson RS, Zelzer E. HIF1alpha regulation of Sox9 is necessary to maintain differentiation of hypoxic prechondrogenic cells during early skeletogenesis. *Development* 2007;134:3917-28.
- [292] Puetzer JL, Petite JN, Lobo EG. Comparative review of growth factors for induction of three-dimensional in vitro chondrogenesis in human mesenchymal stem cells isolated from bone marrow and adipose tissue. *Tissue engineering Part B, Reviews* 2010;16:435-44.
- [293] Marsano A, Medeiros da Cunha CM, Ghanaati S, Gueven S, Centola M, Tsaryk R, et al. Spontaneous In Vivo Chondrogenesis of Bone Marrow-Derived Mesenchymal Progenitor Cells by Blocking Vascular Endothelial Growth Factor Signaling. *Stem cells translational medicine* 2016.
- [294] Barry F, Boynton RE, Liu B, Murphy JM. Chondrogenic differentiation of mesenchymal stem cells from bone marrow: differentiation-dependent gene expression of matrix components. *Experimental cell research* 2001;268:189-200.
- [295] Sun Y, Mauerhan DR, Honeycutt PR, Kneisl JS, Norton HJ, Zinchenko N, et al. Calcium deposition in osteoarthritic meniscus and meniscal cell culture. *Arthritis research & therapy* 2010;12:R56.
- [296] Becker R, Pufe T, Kulow S, Giessmann N, Neumann W, Mentlein R, et al. Expression of vascular endothelial growth factor during healing of the meniscus in a rabbit model. *The Journal of bone and joint surgery British volume* 2004;86:1082-7.
- [297] Petersen W, Pufe T, Stärke C, Fuchs T, Kopf S, Raschke M, et al. Locally applied angiogenic factors—a new therapeutic tool for meniscal repair. *Annals of Anatomy-Anatomischer Anzeiger* 2005;187:509-19.
- [298] Phillips GD, Stone AM, Jones BD, Schultz JC, Whitehead RA, Knighton DR. Vascular endothelial growth factor (rhVEGF165) stimulates direct angiogenesis in the rabbit cornea. *In vivo* 1994;8:961-5.
- [299] Proctor C, Schmidt M, Whipple R, Kelly M, Mow V. Material properties of the normal medial bovine meniscus. *Journal of Orthopaedic Research* 1989;7:771-82.
- [300] Chevrier A, Nelea M, Hurtig MB, Hoemann CD, Buschmann MD. Meniscus structure in human, sheep, and rabbit for animal models of meniscus repair. *Journal of orthopaedic research : official publication of the Orthopaedic Research Society* 2009;27:1197-203.
- [301] Liang Y, Idrees E, Andrews SHJ, Labib K, Szojka A, Kunze M, et al. Plasticity of Human Meniscus Fibrochondrocytes: A Study on Effects of Mitotic Divisions and Oxygen Tension. *Scientific Reports* 2017;7:12148.
- [302] Jones EA, Crawford A, English A, Henshaw K, Mundy J, Corscadden D, et al. Synovial fluid

mesenchymal stem cells in health and early osteoarthritis: Detection and functional evaluation at the single-cell level. *Arthritis & Rheumatism* 2008;58:1731-40.

- [303] Matsukura Y, Muneta T, Tsuji K, Koga H, Sekiya I. Mesenchymal stem cells in synovial fluid increase after meniscus injury. *Clinical Orthopaedics and Related Research*® 2014;472:1357-64.
- [304] Ando W, Kutcher JJ, Krawetz R, Sen A, Nakamura N, Frank CB, et al. Clonal analysis of synovial fluid stem cells to characterize and identify stable mesenchymal stromal cell/mesenchymal progenitor cell phenotypes in a porcine model: a cell source with enhanced commitment to the chondrogenic lineage. *Cytotherapy* 2014;16:776-88.
- [305] Pazin DE, Gamer LW, Capelo LP, Cox KA, Rosen V. Gene signature of the embryonic meniscus. *J Orthop Res* 2014;32:46-53.
- [306] Ibán MÁR, Melero NC, Martínez-Botas J, Ortiz A, Heredia JD. Growth factor expression after lesion creation in the avascular zone of the meniscus: A quantitative PCR study in rabbits. *Arthroscopy: The Journal of Arthroscopic & Related Surgery* 2014;30:1131-8.
- [307] Zhang H, Leng P, Zhang J. Enhanced meniscal repair by overexpression of hIGF-1 in a full-thickness model. *Clinical Orthopaedics and Related Research*® 2009;467:3165-74.
- [308] van Osch GJ, van den Berg WB, Hunziker EB, Häusselmann HJ. Differential effects of IGF-1 and TGF $\beta$ -2 on the assembly of proteoglycans in pericellular and territorial matrix by cultured bovine articular chondrocytes. *Osteoarthritis and Cartilage* 1998;6:187-95.
- [309] Urist MR. Bone: formation by autoinduction. *Science* 1965;150:893-9.
- [310] Shimomura K, Rothrauff BB, Tuan RS. Region-Specific Effect of the Decellularized Meniscus Extracellular Matrix on Mesenchymal Stem Cell-Based Meniscus Tissue Engineering. *The American journal of sports medicine* 2016:0363546516674184.
- [311] Buravkova L, Andreeva E, Gogvadze V, Zhivotovsky B. Mesenchymal stem cells and hypoxia: where are we? *Mitochondrion* 2014;19:105-12.
- [312] Kelly DJ, Jacobs CR. The role of mechanical signals in regulating chondrogenesis and osteogenesis of mesenchymal stem cells. *Birth Defects Research Part C: Embryo Today: Reviews* 2010;90:75-85.
- [313] Kurose R, Ichinohe S, Tajima G, Horiuchi S, Kurose A, Sawai T, et al. Characterization of human synovial fluid cells of 26 patients with osteoarthritis knee for cartilage repair therapy. *International journal of rheumatic diseases* 2010;13:68-74.
- [314] Sethe S, Scutt A, Stolzing A. Aging of mesenchymal stem cells. *Ageing research reviews* 2006;5:91-116.
- [315] Tsai CC, Chen YJ, Yew TL, Chen LL, Wang JY, Chiu CH, et al. Hypoxia inhibits senescence and maintains mesenchymal stem cell properties through down-regulation of E2A-p21 by HIF-TWIST. *Blood* 2011;117:459-69.
- [316] Longobardi L, O'Rear L, Aakula S, Johnstone B, Shimer K, Chytil A, et al. Effect of IGF-I in the chondrogenesis of bone marrow mesenchymal stem cells in the presence or absence of TGF- $\beta$  signaling. *Journal of Bone and Mineral Research* 2006;21:626-36.
- [317] Sakimura K, Matsumoto T, Miyamoto C, Osaki M, Shindo H. Effects of insulin-like growth factor I on transforming growth factor beta1 induced chondrogenesis of synovium-derived mesenchymal stem cells

- cultured in a polyglycolic acid scaffold. *Cells, tissues, organs* 2006;183:55-61.
- [318] Bilgen B, Ren Y, Pei M, Aaron RK, Ciombor DM. CD14-negative isolation enhances chondrogenesis in synovial fibroblasts. *Tissue Engineering Part A* 2009;15:3261-70.
- [319] Indrawattana N, Chen G, Tadokoro M, Shann LH, Ohgushi H, Tateishi T, et al. Growth factor combination for chondrogenic induction from human mesenchymal stem cell. *Biochemical and biophysical research communications* 2004;320:914-9.
- [320] Fukumoto T, Sperling JW, Sanyal A, Fitzsimmons JS, Reinholz GG, Conover CA, et al. Combined effects of insulin-like growth factor-1 and transforming growth factor-beta1 on periosteal mesenchymal cells during chondrogenesis in vitro. *Osteoarthritis and cartilage / OARS, Osteoarthritis Research Society* 2003;11:55-64.
- [321] Pei M, Aaron R, Ciombor D. Modulation of chondrogenesis in synovial fibroblast engineered cartilage by sequential growth factors. *Transactions of the Orthopaedic Research Society* 2005;30:0720.
- [322] Bluteau G, Labourdette L, Ronzière M-C, Conrozier T, Mathieu P, Herbage D, et al. Type X collagen in rabbit and human meniscus. *Osteoarthritis and cartilage* 1999;7:498-501.
- [323] Hellio Le Graverand M-P, Ou Y, Schield-Yee T, Barclay L, Hart D, Natsume T, et al. The cells of the rabbit meniscus: their arrangement, interrelationship, morphological variations and cytoarchitecture. *J Anat* 2000;198:525-35.
- [324] Diekman BO, Rowland CR, Lennon DP, Caplan AI, Guilak F. Chondrogenesis of adult stem cells from adipose tissue and bone marrow: induction by growth factors and cartilage-derived matrix. *Tissue Engineering Part A* 2009;16:523-33.
- [325] Jones EA, English A, Henshaw K, Kinsey SE, Markham AF, Emery P, et al. Enumeration and phenotypic characterization of synovial fluid multipotential mesenchymal progenitor cells in inflammatory and degenerative arthritis. *Arthritis & Rheumatology* 2004;50:817-27.
- [326] Chang CH, Chen CC, Liao CH, Lin FH, Hsu YM, Fang HW. Human acellular cartilage matrix powders as a biological scaffold for cartilage tissue engineering with synovium-derived mesenchymal stem cells. *Journal of Biomedical Materials Research Part A* 2014;102:2248-57.
- [327] Sheehy EJ, Buckley CT, Kelly DJ. Oxygen tension regulates the osteogenic, chondrogenic and endochondral phenotype of bone marrow derived mesenchymal stem cells. *Biochemical and biophysical research communications* 2012;417:305-10.
- [328] Fujii M, Furumatsu T, Yokoyama Y, Kanazawa T, Kajiki Y, Abe N, et al. Chondromodulin-I derived from the inner meniscus prevents endothelial cell proliferation. *Journal of Orthopaedic Research* 2013;31:538-43.
- [329] Richard DE, Berra E, Pouysségur J. Angiogenesis: how a tumor adapts to hypoxia. *Biochemical and biophysical research communications* 1999;266:718-22.
- [330] Hu X, Yu SP, Fraser JL, Lu Z, Ogle ME, Wang J-A, et al. Transplantation of hypoxia-preconditioned mesenchymal stem cells improves infarcted heart function via enhanced survival of implanted cells and angiogenesis. *The Journal of thoracic and cardiovascular surgery* 2008;135:799-808.
- [331] Lee EY, Xia Y, Kim WS, Kim MH, Kim TH, Kim KJ, et al. Hypoxia-enhanced wound-healing function of adipose-derived stem cells: Increase in stem cell proliferation and up-regulation of VEGF and

- bFGF. *Wound Repair and Regeneration* 2009;17:540-7.
- [332] Askari AT, Unzek S, Popovic ZB, Goldman CK, Forudi F, Kiedrowski M, et al. Effect of stromal-cell-derived factor 1 on stem-cell homing and tissue regeneration in ischaemic cardiomyopathy. *The Lancet* 2003;362:697-703.
- [333] Yamaguchi J-i, Kusano KF, Masuo O, Kawamoto A, Silver M, Murasawa S, et al. Stromal cell-derived factor-1 effects on ex vivo expanded endothelial progenitor cell recruitment for ischemic neovascularization. *Circulation* 2003;107:1322-8.
- [334] Murphy JM, Dixon K, Beck S, Fabian D, Feldman A, Barry F. Reduced chondrogenic and adipogenic activity of mesenchymal stem cells from patients with advanced osteoarthritis *Arthritis & Rheumatism* 2002;46:704-13.
- [335] De Bari C, Dell'Accio F, Tylzanowski P, Luyten FP. Multipotent mesenchymal stem cells from adult human synovial membrane. *Arthritis and rheumatism* 2001;44:1928-42.
- [336] Mochizuki T, Muneta T, Sakaguchi Y, Nimura A, Yokoyama A, Koga H, et al. Higher chondrogenic potential of fibrous synovium- and adipose synovium-derived cells compared with subcutaneous fat-derived cells: Distinguishing properties of mesenchymal stem cells in humans. *Arthritis & Rheumatism* 2006;54:843-53.
- [337] Amemiya M, Tsuiji K, Sekiya I, Muneta T, Koga H. Characteristics and usefulness of synovial fluid-derived stem cells compared with synovium-derived stem cells. *Osteoarthritis and Cartilage* 2018;26:S23-S4.
- [338] de Sousa EB, Casado PL, Moura Neto V, Duarte ME, Aguiar DP. Synovial fluid and synovial membrane mesenchymal stem cells: latest discoveries and therapeutic perspectives. *Stem Cell Res Ther* 2014;5:112.
- [339] Yang KA, Saris D, Verbout A, Creemers L, Dhert W. The effect of synovial fluid from injured knee joints on in vitro chondrogenesis. *Tissue engineering* 2006;12:2957-64.
- [340] Hegewald AA, Ringe J, Bartel J, Kruger I, Notter M, Barnewitz D, et al. Hyaluronic acid and autologous synovial fluid induce chondrogenic differentiation of equine mesenchymal stem cells: a preliminary study. *Tissue & cell* 2004;36:431-8.
- [341] Pugh CW, Ratcliffe PJ. Regulation of angiogenesis by hypoxia: role of the HIF system. *Nature medicine* 2003;9:677.
- [342] Yu P, Huang Y, Xu C, Lin L, Han Y, Sun W, et al. Downregulation of CXCL12 in mesenchymal stromal cells by TGF $\beta$  promotes breast cancer metastasis. *Oncogene* 2017;36:840.
- [343] Pelttari K, Winter A, Steck E, Goetzke K, Hennig T, Ochs BG. Premature induction of hypertrophy during in vitro chondrogenesis of human mesenchymal stem cells correlates with calcification and vascular invasion after ectopic transplantation in SCID mice. *Arthritis Rheum* 2006;54.
- [344] Shukunami C, Hiraki Y. Role of cartilage-derived anti-angiogenic factor, chondromodulin-I, during endochondral bone formation. *Osteoarthritis and cartilage* 2001;9:S91-S101.
- [345] Lafont JE, Talma S, Hopfgarten C, Murphy CL. Hypoxia promotes the differentiated human articular chondrocyte phenotype through SOX9-dependent and-independent pathways. *Journal of Biological Chemistry* 2008;283:4778-86.

- [346] Chen Z, Wei J, Zhu J, Liu W, Cui J, Li H, et al. Chm-1 gene-modified bone marrow mesenchymal stem cells maintain the chondrogenic phenotype of tissue-engineered cartilage. *Stem cell research & therapy* 2016;7:70.
- [347] Hayami T, Funaki H, Yaoeda K, Mitui K, Yamagiwa H, Tokunaga K, et al. Expression of the cartilage derived anti-angiogenic factor chondromodulin-I decreases in the early stage of experimental osteoarthritis. *The Journal of rheumatology* 2003;30:2207-17.
- [348] Klinger P, Surmann-Schmitt C, Brem M, Swoboda B, Distler JH, Carl HD, et al. Chondromodulin 1 stabilizes the chondrocyte phenotype and inhibits endochondral ossification of porcine cartilage repair tissue. *Arthritis & Rheumatism* 2011;63:2721-31.
- [349] Zhang X, Prasad I, Fang W, Crawford R, Xiao Y. Chondromodulin-1 ameliorates osteoarthritis progression by inhibiting HIF-2 $\alpha$  activity. *Osteoarthritis and cartilage* 2016;24:1970-80.
- [350] ElAttar M, Dhollander A, Verdonk R, Almqvist KF, Verdonk P. Twenty-six years of meniscal allograft transplantation: is it still experimental? A meta-analysis of 44 trials. *Knee Surgery, Sports Traumatology, Arthroscopy* 2011;19:147-57.
- [351] Gelber PE, Gonzalez G, Torres R, Giralt NG, Caceres E, Monllau JC. Cryopreservation does not alter the ultrastructure of the meniscus. *Knee surgery, sports traumatology, arthroscopy* 2009;17:639-44.
- [352] Verdonk R, Kohn D. Harvest and conservation of meniscal allografts. *Scandinavian journal of medicine & science in sports* 1999;9:158-9.
- [353] Buck B, Resnick L, Shah S, Malinin T. Human immunodeficiency virus cultured from bone. Implications for transplantation. *Clinical orthopaedics and related research* 1990:249-53.
- [354] Hamlet W, Liu SH, Yang R. Destruction of a cryopreserved meniscal allograft: a case for acute rejection. *Arthroscopy: The Journal of Arthroscopic & Related Surgery* 1997;13:517-21.
- [355] Lee SR, Kim JG, Nam SW. The tips and pitfalls of meniscus allograft transplantation. *Knee surgery & related research* 2012;24:137.
- [356] Dienst M, Greis PE, Ellis BJ, Bachus KN, Burks RT. Effect of lateral meniscal allograft sizing on contact mechanics of the lateral tibial plateau: an experimental study in human cadaveric knee joints. *The American journal of sports medicine* 2007;35:34-42.
- [357] Hutchinson ID, Moran CJ, Potter HG, Warren RF, Rodeo SA. Restoration of the meniscus: form and function. *The American journal of sports medicine* 2014;42:987-98.
- [358] McConkey M, Lyon C, Bennett DL, Schoch B, Britton C, Amendola A, et al. Radiographic sizing for meniscal transplantation using 3-D CT reconstruction. *The journal of knee surgery* 2012;25:221-6.
- [359] Lee D-H, Kim T-H, Lee S-H, Kim C-W, Kim J-M, Bin S-I. Evaluation of meniscus allograft transplantation with serial magnetic resonance imaging during the first postoperative year: focus on graft extrusion. *Arthroscopy: The Journal of Arthroscopic & Related Surgery* 2008;24:1115-21.
- [360] Szojka A, Lahl K, Andrews SH, Jomha NM, Osswald M, Adesida AB. Biomimetic 3D Printed Scaffolds for Meniscus Tissue Engineering. *Bioprinting* 2017.
- [361] Jia W, Gungor-Ozkerim PS, Zhang YS, Yue K, Zhu K, Liu W, et al. Direct 3D bioprinting of perfusable vascular constructs using a blend bioink. *Biomaterials* 2016;106:58-68.
- [362] Lubowitz JH, Verdonk PC, Reid JB, Verdonk R. Meniscus allograft transplantation: a current

- concepts review. *Knee Surgery, Sports Traumatology, Arthroscopy* 2007;15:476-92.
- [363] Srikanth VK, Fryer JL, Zhai G, Winzenberg TM, Hosmer D, Jones G. A meta-analysis of sex differences prevalence, incidence and severity of osteoarthritis. *Osteoarthritis and cartilage* 2005;13:769-81.
- [364] O'Connor MI. Sex differences in osteoarthritis of the hip and knee. *JAAOS-Journal of the American Academy of Orthopaedic Surgeons* 2007;15:S22-S5.
- [365] Kerrigan DC, Todd MK, Della UC. Gender differences in joint biomechanics during walking: normative study in young adults. *American journal of physical medicine & rehabilitation* 1998;77:2-7.
- [366] Valdes AM, Loughlin J, Oene MV, Chapman K, Surdulescu GL, Doherty M, et al. Sex and ethnic differences in the association of ASPN, CALM1, COL2A1, COMP, and FRZB with genetic susceptibility to osteoarthritis of the knee. *Arthritis & Rheumatism* 2007;56:137-46.
- [367] Richette P, Corvol M, Bardin T. Estrogens, cartilage, and osteoarthritis. *Joint, bone, spine : revue du rhumatisme* 2003;70:257-62.
- [368] Englund M, Lohmander L. Risk factors for symptomatic knee osteoarthritis fifteen to twenty-two years after meniscectomy. *Arthritis & Rheumatism: Official Journal of the American College of Rheumatology* 2004;50:2811-9.
- [369] Fukuta S, Masaki K, Korai F. Prevalence of abnormal findings in magnetic resonance images of asymptomatic knees. *Journal of orthopaedic science* 2002;7:287-91.
- [370] Kornick J, Trefelner E, McCarthy S, Lange R, Lynch K, Jokl P. Meniscal abnormalities in the asymptomatic population at MR imaging. *Radiology* 1990;177:463-5.
- [371] Chiang S-W, Tsai P-H, Chang Y-C, Wang C-Y, Chung H-W, Lee H-S, et al. T2 values of posterior horns of knee menisci in asymptomatic subjects. *PloS one* 2013;8:e59769.
- [372] Kilcoyne KG, Dickens JF, Haniuk E, Cameron KL, Owens BD. Epidemiology of meniscal injury associated with ACL tears in young athletes. *Orthopedics* 2012;35:208-12.
- [373] Piasecki DP, Spindler KP, Warren TA, Andrish JT, Parker RD. Intraarticular injuries associated with anterior cruciate ligament tear: findings at ligament reconstruction in high school and recreational athletes: an analysis of sex-based differences. *The American journal of sports medicine* 2003;31:601-5.
- [374] Stanley LE, Kerr ZY, Dompier TP, Padua DA. Sex differences in the incidence of anterior cruciate ligament, medial collateral ligament, and meniscal injuries in collegiate and high school sports: 2009-2010 through 2013-2014. *The American journal of sports medicine* 2016;44:1565-72.
- [375] Montgomery SR, Zhang A, Ngo SS, Wang JC, Hame SL. Cross-sectional analysis of trends in meniscectomy and meniscus repair. *Orthopedics* 2013;36:e1007-e13.
- [376] Webber RJ, Zitaglio T, Hough Jr AJ. In vitro cell proliferation and proteoglycan synthesis of rabbit meniscal fibrochondrocytes as a function of age and sex. *Arthritis & Rheumatism: Official Journal of the American College of Rheumatology* 1986;29:1010-6.
- [377] Aksu AE, Rubin JP, Dudas JR, Marra KG. Role of gender and anatomical region on induction of osteogenic differentiation of human adipose-derived stem cells. *Annals of plastic surgery* 2008;60:306-22.
- [378] Corsi KA, Pollett JB, Phillippi JA, Usas A, Li G, Huard J. Osteogenic potential of postnatal skeletal muscle-derived stem cells is influenced by donor sex. *Journal of Bone and Mineral Research*

2007;22:1592-602.

[379] Deasy BM, Lu A, Tebbets JC, Feduska JM, Schugar RC, Pollett JB, et al. A role for cell sex in stem cell-mediated skeletal muscle regeneration: female cells have higher muscle regeneration efficiency. *The Journal of cell biology* 2007;177:73-86.

[380] Payne KA, Didiano DM, Chu CR. Donor sex and age influence the chondrogenic potential of human femoral bone marrow stem cells. *Osteoarthritis and cartilage* 2010;18:705-13.

[381] Matsumoto T, Kubo S, Meszaros LB, Corsi KA, Cooper GM, Li G, et al. The influence of sex on the chondrogenic potential of muscle-derived stem cells: Implications for cartilage regeneration and repair. *Arthritis & Rheumatism: Official Journal of the American College of Rheumatology* 2008;58:3809-19.

[382] Siegel G, Kluba T, Hermanutz-Klein U, Bieback K, Northoff H, Schäfer R. Phenotype, donor age and gender affect function of human bone marrow-derived mesenchymal stromal cells. *BMC medicine* 2013;11:146.

[383] Crisostomo PR, Wang M, Herring CM, Morrell ED, Seshadri P, Meldrum KK, et al. Sex dimorphisms in activated mesenchymal stem cell function. *Shock* 2006;26:571-4.

[384] Crisostomo PR, Markel TA, Wang M, Lahm T, Lillemoe KD, Meldrum DR. In the adult mesenchymal stem cell population, source gender is a biologically relevant aspect of protective power. *Surgery* 2007;142:215-21.